MACCS VERIFICATION REPORT

REVISION 1

Prepared for

U.S. Nuclear Regulatory Commission
Contract 31310018D0002
Task Order No. 31310020F0081

Prepared by

Osvaldo Pensado

Southwest Research Institute®
Center for Nuclear Waste Regulatory Analyses
San Antonio, Texas

August 2022

ABSTRACT

This report documents systematic testing of the MELCOR Accident Consequence Code System (MACCS) functions by a third party (the Center for Nuclear Waste Regulatory Analyses at the Southwest Research Institute®) not involved in MACCS software development. Testing focused on verifying equations and algorithms of the MACCS code, as described in the MACCS Theory Manual. It is not practical to generate independent benchmarks that reproduce details of the MACCS code, given that MACCS has been developed over decades. Instead, simplified systems were examined that allowed for direct comparison to closed-form equations. Other tests were designed by predicting non-trivial trends and relationships of different outputs of the MACCS code. It was verified that MACCS outputs mostly satisfied those predicted relationships.

The project began with testing MACCS Version 4.0. A small number of issues were identified through that testing, which were addressed in MACCS Version 4.1. Examples of changes in Version 4.1 to address issues include expanding the domain of the independent variables (related to the effective plume size and receptor distance) in the lookup table used to compute the cloudshine factor, and imposing constraints on the extent of the lateral spread of simulated plumes. This report documents only tests applied to MACCS Version 4.1. The MACCS 4.1 code successfully satisfied most of the designed benchmarks and tests.

This report is structured in a modular manner, with tests of specific features documented in independent and stand-alone sections, thus allowing new tests to be incorporated later. For example, the current Revision 1 report includes all tests of the Revision 0 report (dated October 2021, ADAMS Accession Number ML22026A461) plus new tests in additional sections. Testing covered a broad range of features and functions of the MACCS code. Results are organized according to the three basic modules of the MACCS code: ATMOS, EARLY, and CHRONC.

This report supplements information provided in the MACCS Theory Manual. The user is referred to the MACCS Theory Manual for a detailed discussion of models and solution algorithms; however, key equations of the MACCS Theory Manual are replicated in this report, with minor modifications for the sake of clarity, to serve as a stand-alone document. The graphic display of results and the designed benchmarks provide insights into models, equations, algorithms, and methods of the MACCS code as described in the Theory Manual.

CONTENTS

LIST OF FIGURES

LIST OF TABLES

Page

ACKNOWLEDGMENTS

This report was prepared to document work performed by the Center for Nuclear Waste Regulatory Analyses (CNWRA®) for the U.S. Nuclear Regulatory Commission (NRC) under Contract No. 31310018D0002, for Task Order No. 31310020F0081. The activities reported here were performed on behalf of the NRC Office of Nuclear Regulatory Research, Division of Systems Analysis. The author benefited from multiple discussions on MACCS algorithms with A.J. Nosek, K. Compton, and S. Haq of NRC, and with D. Clayton and J. Leute, MACCS software developers affiliated with Sandia National Laboratories. The author recognizes the technical review by G. Adams and the editorial and programmatic review by W. Patrick. Appreciation is extended to L. Neill and A. Ramos for assistance in preparation of the report.

QUALITY OF DATA, ANALYSES, AND CODE DEVELOPMENT

DATA: All CNWRA-generated original data contained in this report meet the quality assurance (QA) requirements described in the CNWRA QA Manual.

ANALYSES AND CODES: The Windows version of the MACCS code (SNL, 2021), WinMACCS Version 4.1, was used to compute consequences of postulated accidents. Consequence outputs and input values were extracted from WinMACCS output files. Python 3 was used to translate MACCS outputs to Excel® files. Mathematica® 12 (Wolfram Research, 2021) was used to import values from WinMACCS output files, to plot results, and to compute expected results. Mathematica 12, Python 3, and Excel are general use software classified as “exempt from control” by TOP–018. Relevant electronic files and scripts were archived in the CNWRA QA records system.

References

SNL. “MELCOR Accident Consequence Code System (MACCS).” Albuquerque, New Mexico: Sandia National Laboratories. 2021. <https://maccs.sandia.gov/maccs.aspx> (Accessed date 12 July 2022).

Wolfram Research. “Wolfram Mathematica 12.” Champaign, Illinois: Wolfram Research. 2021. <https://www.wolfram.com/mathematica/?source=nav> (Accessed date 21 September 2021).

1 INTRODUCTION

MACCS is a short name for MELCOR Accident Consequence Code System (SNL, 2021). The MACCS code is aimed at modeling the impact of severe accidents at nuclear power plants on the surrounding environment. Impacts are quantified as radiological doses and health effects (e.g., the number of people with immediate injury due to exposure to a cloud of radiation, or affected by cancer developed after a long-term), as well as measured in economic terms from loss of productivity and compromised land. The consequence analysis is a tool to inform adequate levels protection to the public, emergency planning, and gain insights on hazards posed by nuclear installations including nuclear power plants. Consequence analyses have been used, for example, in environmental assessments, regulatory cost-benefit analyses, and the State-of-the-Art Reactor Consequence Analyses (SOARCA) project (SNL, 2017a; SNL, 2019; Chang, et al., 2012).

MACCS has been developed by Sandia National Laboratories (SNL) for the U.S. Nuclear Regulatory Commission (NRC), over a span of more than two decades. Version 1.12 of MACCS was released in 1997 (Bixler, Walton, Eubanks, Haaker, & McFadden, 2017; SNL, 2015a), and the Windows-interface version of MACCS (WinMACCS) was released in 2008 (SNL, 2015b). MACCS has been produced under a software quality assurance program (SNL, 2017b), which calls for verification testing of its functions. However, there are only limited benchmark studies on MACCS functions by independent parties (Thoman, Brotherton, & Davis, 2009; Molenkamp, Bixler, Morrow, Ramsdell, & Mitchell, 2004). This report documents systematic testing of MACCS functions implemented by a third party, Center for Nuclear Waste Regulatory Analyses, not involved in MACCS software development. This project initiated with testing MACCS Version 4.0, released on June 5, 2020. A small number of issues were identified as part of that initial testing and communicated to the SNL software developer. Those issues were addressed in the latest version of the MACCS code, Version 4.1, released on July 30, 2021 (SNL, 2021). The initial set of tests were repeated with the MACCS Version 4.1 to verify those issues were addressed, as documented in this report.

The MACCS is organized into three basic modules: ATMOS, EARLY, and CHRONC. The ATMOS module includes a model for the release of radionuclides from a source, a model for propagation of the plume (or finite plume segments) based on steady-state Gaussian dispersion plume functions or the HYSPLIT model, and a description of dynamic weather patterns (e.g., windspeed and direction, atmospheric stability index, rain rate). The EARLY module simulates the early phase of the accident with a duration of up to 40 days. During this time, people could be exposed to radionuclides in the plume cloud and to ground contamination. Several protective actions in the early phase are accounted for in the EARLY module, including sheltering, evacuation, dose-dependent early relocation, and ingestion of potassium iodide pills to mitigate effects of inhalation of radio-iodine. The CHRONC module models consequences in the intermediate and long-term phase. The intermediate phase is modeled as an optional phase (i.e., it can be bypassed or disabled) and it can last up to one year after the end of the EARLY phase; the exposure pathways are associated with ground contamination, and the only protective action is relocation. CHRONC also simulates the long-term phase, including exposure pathways arising from ground contamination (which could contaminate farm food products and water, which then become indirect exposure pathways). The long-term phase accounts for protective actions such as habitation and farming restrictions (including interdiction and condemnation of property), and land decontamination. Those protective actions constrain radiological doses but at an economic cost, also quantified by the CHRONC module. The duration of the long-term phase is limited to 50 years. Tests in this report were aimed at checking features and functions of the ATMOS, EARLY, and CHROC modules, and the testing

is organized into three main sections separately addressing these three modules (ATMOS tests are included in Section 2, EARLY tests in Section 3, and CHRONC tests in Section 3.7).

The MACCS software quality assurance plan (SNL, 2017b) defines *validation testing* as the process to ensure that the algorithms and models used in the program correctly describe the physical events that are being modeled. On the other hand, *verification testing* is defined as the process to ensure that the program/code correctly solves equations as intended. In this report, the focus is on verification testing; however, by examining assumptions and technical bases of those assumptions model confidence is gained, which relates to validation testing. This is a reason why this report is titled MACCS *Verification* Report, although it indirectly covered a level of model validation testing by the examination of the underlying models including discussion of those models with peers and technical counterparts at the NRC.

Given the more than two decades of development of the MACCS code, it is impractical to reproduce the functionality and complexity of the MACCS code by independent means. Instead, the main verification strategy adopted in this project was to examine very simple systems (e.g., constant wind speed and direction, one plume segment, one cohort, one single long-lived radionuclide, no mitigation actions, no evacuation, no relocation) where analytical equations can be used to compute radionuclide concentrations in air and on the ground, as well as dose consequences and health effects. Only a sample of the MACCS functions were tested but covering a broad range of features of the ATMOS, EARLY, and CHRONC modules. The emphasis of the testing was on radionuclide concentrations, dose computations, and health effects. MACCS functions to model protective actions and socioeconomic impacts and costs were not included in tests in this report. Complexities of the MACCS model such as plumes specified in multiple discrete segments, weather patterns, multiple cohorts, evacuation paths, and sampling of input parameters from distribution functions were also not included in tests in this report.

The MACCS Theory Manual (Nosek & Bixler, 2021) was the document consulted to guide the development of tests. Equations of the MACCS Theory Manual used in the tests are reproduced in this report to add specificity on the MACCS functions tested and numerical approaches adopted. A table in Section 5 compares the table of contents of the MACCS Theory Manual to tests documented in this report. This report covered a broad range of features of the MACCS code but keeping in mind that the systems modeled in the MACCS runs represented simple systems.

The tests in this report refer to multiple outputs of the MACCS code, such as Type A, Type C, Type 1, etcetera. Effort is made in the test documentation to add a description to the output such as Type A maximum dose, Type C sector average dose, Type 6 centerline dose. Those outputs are printed in blocks in three MACCS output files, Model1.out, Summary.txt, and tbl_outStat.txt. Scripts were prepared to extract information from those blocks of text into multi-worksheet Excel files or CSV files that are much easier to read and query. Those Excel® and CSV files were archived with the quality assurance records of this report, as well as the original MACCS output files. The reader is referred to the MACCS Theory Manual (Nosek & Bixler, 2021), Sections 2.9, 3.5, and 6.3 for a detailed description of the MACCS model outputs.

The food chain model of the CHRONC module was not tested. However, the reader is referred to another independent report (Pensado & Speaker, 2020), which includes a sensitivity analysis of input parameters of the MACCS food chain model named COMIDA, and a description of each of those input parameters. The COMIDA sensitivity analysis revealed aspects of model implementation, addressing aspects of model validity and verification testing.

2 ATMOS MODULE

2.1 Test 2.1: Air Concentrations

The objective of the test was to verify the use of Gaussian plume equations for the computation of concentrations in air, centerline (z=h) and ground level (z=0). The Gaussian plume equations are defined in Section 2.5.1 of the MACCS Theory Manual (Nosek & Bixler, 2021)

$$\chi(x,y,z) = \frac{Q}{u}\frac{1}{\sqrt{2\,\pi}\,\sigma_y(x)}\exp\left(-\frac{1}{2}\frac{y^2}{\sigma_y(x)^2}\right)\psi(x,z) \tag{2-1}$$

with

$$\psi(x,z) = \frac{1}{\sqrt{2\,\pi}\,\sigma_z(x)}\sum_{n=-N}^{N}\left\{\exp\left[-\frac{1}{2}\frac{(z-h+2\,n\,H)^2}{\sigma_z(x)^2}\right]+\exp\left[-\frac{1}{2}\frac{(z+h+2\,n\,H)^2}{\sigma_z(x)^2}\right]\right\} \tag{2-2}$$

χ	—	time-integrated concentration (Bq-s/m^3)
Q	—	total activity in the plume segment (Bq)
u	—	windspeed (m/s)
h	—	centerline height (=plume release height in case of no plume rise) (m)
H	—	plume ceiling, maximum plume height (m)
n	—	integer
N	—	series limit
x	—	longitudinal distance (m)
y	—	lateral, across wind, distance (m)
z	—	vertical distance from the ground (m)
$\sigma_y(x)$	—	lateral Gaussian dispersion coefficient (m)
$\sigma_z(x)$	—	vertical Gaussian dispersion coefficient (m)

Equation (2-2) accounts for mirror boundary at z = 0 and z = H (particles reaching the ground and the plume ceiling are assumed to bounce back and remain in the region 0 ≤ z ≤ H). The accurate solution is an infinite series (N=∞); however, in practice the series converges after a few terms. In the tests, it was in general sufficient to consider N = 5 in the computation of $\psi(z)$, but more terms in the series were required when the Gaussian vertical dispersion coefficient, $\sigma_z(x)$, was large.

A second objective of the test was verifying the computation of a cloudshine dose for a simple case (one radionuclide, one organ). This test complements tests in Section 3 aimed at verifying computations by the EARLY module. From Section 3.3.1 of the MACCS Theory Manual, for organ k the cloudshine centerline dose is computed as

$$DC_k = \left[\sum_i DRCC_{\infty ik}\,\chi(x,y=0,z=h)\right] C\;F\;SFC \tag{2-3}$$

DC_k	—	cloudshine centerline dose to organ k (Sv)
$DRCC_{\infty ik}$	—	semi-infinite cloudshine dose coefficient to organ k by radionuclide i (Sv-m^3/Bq-s)
C	—	cloudshine factor, function of the plume height, h, and the dispersion coefficients σ_y and σ_z

F	—	fraction of the exposure time (=1, for non-evacuating and non-relocating individuals)
SFC	—	cloudshine protection factor specified by CSFACT in WinMACCS (CSFACT = 1 in the problem examined)

For the simple case of one radionuclide, non-evacuating and non-relocating individuals, and SFC=CSFACT=1, Eq. (2-3) becomes

$$DC_k = DRCC_{\infty ik}\ \chi(x, y = 0, z = h)\ C \tag{2-4}$$

Equation (2-4) was used to examine the computation of the cloudshine factor C.

2.1.1 Test Input

Default inputs from the LNT sample input file distributed with the MACCS code were selected, with modifications to simulate a simple case with the following features:

- One radionuclide, Cs-137
- One long-lasting plume segment, without plume rise
- Simple weather pattern: constant windspeed (10 m/s) blowing north
- One cohort, non-evacuating and non-relocating
- Cloudshine dose pathway only

The following were the explicit changes implemented to the MACCS inputs through the WinMACCS interface:

General Properties

- SCOPE
  - Atmospheric Transport and Dispersion: Gaussian
  - Early Consequences (no Late Consequences)
- TRANSPORT
  - Power Law Functions (NUM_DIST=0)
  - Plume Meander: None (MNDMOD=OFF)
- WEATHER
  - METCOD=4: constant weather
- PLUME
  - Plume Source: Area Source
  - Plume Rise: Power Model (plume rise controlled by power law and heat output, PLHEAT)
  - Plume Trapping/Downwash: Briggs (buoyancy flux)
- SITE DATA
  - Uniform: uniform population density
- DOSE
  - Linear No Threshold
  - Activate KI Model: FALSE (no KI ingestion model)
- EVAC/ROTATION
  - None (LASMOV=0): no evacuation

    - Wind Shift and Rotation: no wind shift with rotation (IPLUME = 1)
        - No wind shift: plume segments move with constant direction and speed
        - Rotation: means that wind direction is rotated according to user-defined probabilities
    - Number of cohorts = 1
- WIND ROSE
    - User Supplied (OVRRID = True)
- ANIMATION/HEALTH EFFECTS
    - AniMACCS files disabled under IPLUME=1
    - Early Effects: Early Fatality Effects, Early Injury Effects, Latent Cancer Effects from Early Exposure

ATMOS

- Spatial Grid
    - NUMCOR=16: compass subdivisions
    - SPAEND (km) defines the radial grid. Adjacent radial segments must be greater or equal than 0.1 km. The grid was log-spaced, from 0.1 to 100 km
- Deposition
    - Dry/Wet Depos Flags
        - DRYDEP = FALSE for Cs and Ba: no dry deposition
        - WETDEP = FALSE for Cs and Ba: no wet deposition
- Dispersion
    - Dispersion Function
        - CYSIGA, CYSIGB, CZSIGA, CZSIGB according to Table 2-5 of the MACCS Theory Manual (Nosek & Bixler, 2021)
    - Scaling Factors
        - YSCALE =1, factor for σ_y
        - ZSCALE = 1.0, 0.1, 0.01, factor for σ_z
- Plume Specifications
    - Plume Rise Scale Factor
        - SCLCRW = 0.001
        - SCLADP = 0.01
        - SCLEFP = 0.01
        - The smallest factors were selected to avoid plume rise. These factors should not matter when PLHEAT=0
- Radionuclides
    - Radionuclides
        - NUMISO = 16
        - CORINV (Bq): inventory for all isotopes, all 0 except for Cs-137 = 10^{15} Bq
    - Pseudostable radionuclides
        - NUMSTB = 17
        - Added Ba-137m, so that it would not contribute to dose computations with Cs-137 inventories
        - Removed Ba-137m from NUCNAM
- Release Description
    - Plume Parameters
        - One plume segment: variables NUMREL, PDELAY, PLHITE, REFTIM, PLUDUR
        - PDELAY = 18000 s
        - PLHITE (m) = 500 m: plume release height

        - REFTIM = 0.5 (midpoint representative location of plume segment)
        - PLUDUR = 18000 s
    - Daughter Ingrowth Flag
        - APLFRC = PROGENY: initial release controlled by chemical group
    - Release fractions: RELFRC
        - RELFRC = 1 for Cs, Plume 1, 0 for everything else
    - Release Fraction Scale Factors
        - NUMISO = 16
        - IGROUP: parameter defining the chemical group. Isotopes are part of the same chemical group
        - Reduced the radionuclide set until a minimum set was achieved that could run, including Cs-137
    - Heat
        - PLHEAT = 0, disables plume rise, sensible heat using ambient temperature as reference
    - Building Height Data
        - BUILDH (m) = 40 m
    - Initial Area Source
        - SIGYINIT (m) = SIGZINIT (m) = 0.1 m: initial values of the Gaussian dispersion coefficients
- Weather
    - Constant or Boundary Conditions
        - BNDMXH (m) = 1000: mixing layer height
        - IBDSTB = 4: stability class
        - BNDRAN (mm/hr) = 0: rain rate
        - BNDWND (m/s) = 10: windspeed
    - Fixed Start Time Data
        - ISTRDY = 1: day of the year when weather sequence starts
        - ISTRHR = 1: starting time of the weather trial (first hour)

EARLY

- Wind Rose Probabilities
    - WINROS: Segment 1 (north) = 1, 0 for all other segments. The wind was assumed to blow north.
- Uniform Site Data
    - IBEGIN = 1
    - POPDEN (1/km^2) = 10 people/km^2, population density
    - FRACLD = 1.0 land fraction
- Normal Relocation
    - DOSNRM (Sv) = 10^{10} Sv, set to high threshold to avoid normal relocation
- Hot Spot Relocation
    - DOSHOT (Sv) = 10^{10} Sv, set to high threshold to avoid relocation
- Emergency Phase Resuspension
    - RESCON (1/m) = 0
    - RESHAF (s) = 10^{10} s: long half-life to avoid resuspension
    - Parameters selected to avoid resuspension
- Emergency Cohort One
    - Cohort Fraction
        - WTFRAC = 1.0 (weight fraction)
    - Shielding and Exposure
        - CSFACT = 1 (cloudshine), and 0 for all other shielding factors

Output Controls

- Type 0 (NUM0) ATMOS Outputs
  - INDREL = 1 (plume segment)
  - INRAD = 1, 2, 3, …, 26 (all radial segments)
  - NUCOUT = Cs-137: radionuclide output by NUM0
- Type 6 (NUM6) Centerline Dose
  - ORGNAM = L-ICRP60ED
  - PATHNM = CLD: cloudshine
  - I1DIS6=1, I2DIS6=26: all radial segments
- Type A (NUMA) Peak Dose in a Grid Ring
  - NAME = L-ICRP60ED
  - I1DISA=1, I2DISA=26: all radial ring segments
- Type C (NUMC) Average Sector Dose
  - ORGNAM = L-ICRP60ED
  - ELEVDOSE (Sv) = 0: outputs all grid elements with dose > 0 Sv
  - PRINT_FLAG_C = True: outputs information for all grid elements

2.1.2 Test Procedure

Three different MACCS runs were executed with different values of ZSCALE (=0.01, 0.1, 1, 5, 10), to consider different cases of vertical plume spread, including very narrow plumes along the vertical direction. Results were extracted from MACCS output files Model1.out and tbl_outStat.txt. Python scripts were written to translate information in those files to Excel. Information in the Excel files were imported into Mathematica (Wolfram Reseach, 2021), to be queried, plotted, and compared to benchmark solutions.

Equations (2-1) and (2-2) were used to independently compute air concentrations along the centerline (y = 0, z=500 m) and along the ground (y = 0, z=0). The MACCS power law option was used to define the Gaussian dispersion coefficients, σ_y and σ_z as functions of the position x. The gaussian dispersion coefficients were computed using the coefficients for stability class D (class 4) of Table 2-5 of the MACCS Theory Manual, and the power law function (Eq. 2.21 of the MACCS Theory Manual) to compute $\sigma_y(x)$ and $\sigma_z(x)$. In addition, the virtual source position correction (Section 2.5.4 of the MACCS Theory Manual) was applied in the independent computations to match the assumed initial values of the dispersion coefficients at the source; i.e., $\sigma_y(x{=}0) = \text{SIGYINIT} = 0.1$ m, and $\sigma_z(x{=}0) = \text{SIGZINIT} = 0.1$ m.

Type 0 MACCS results (ATMOS module outputs) were compared to results directly computed based on Eqs. (2-1) and (2-2). Type 6 centerline doses and Type A peak doses were compared to Cs-137 cloudshine dose computed using Eq. (2-4).

Information output by the ATMOS module was also verified considering basic relationships, such as constant plume segment speed (= 10 m/s, controlled by the windspeed input) and decay rates of Cs-137.

2.1.3 Test Results

Results of the air concentration tests are presented in Figure 2-1. The MACCS outputs were extracted from the file tbl_outStat.txt marked by the labels “Centerline Air Concentration (Bq-s/m3)” and “Ground-Level Air Concentration (Bq-s/m3).” Excellent agreement was attained between the centerline and air concentrations computed with Eqs. (2-1) and (2-2) and the

MACCS outputs, demonstrating that MACCS computes air concentrations using the Gaussian plume equations, with Gaussian dispersion coefficients that have variable values as function of the downwind distance x.

The file tbl_outStat.txt includes additional outputs that allow for straightforward verification with simple independent computations. For example, values for the Gaussian dispersion coefficients σ_y and σ_z are tracked in tbl_outStat.txt under "Plume Crosswind Dispersion (m)" and "Plume Vertical Dispersion (m)," which were verified by direct comparison to dispersion coefficients independently computed using the power law function and the virtual source correction. Results of the verification are displayed in Figure 2-2. The independently computed dispersion coefficients match the MACCS outputs in tbl_outStat.txt. The file tbl_outStat.txt includes information on the plume travel time and the adjusted source strength under the labels "Plume Arrival Time (s)" and "Adjusted Source Strength (Bq)." The results were directly verified based on the windspeed (BNDWND=10 m/s), the plume delay (PDELAY = 18000 s), and the Cs-137 decay rate (half-life = 30.08 years). The verification results are included in Figure 2-3. The results agree with the expected values. A straight line fits the normalized source strength versus time, because the decay rate is small, and the exponential decay can be accurately approximated as a first order Taylor expansion.

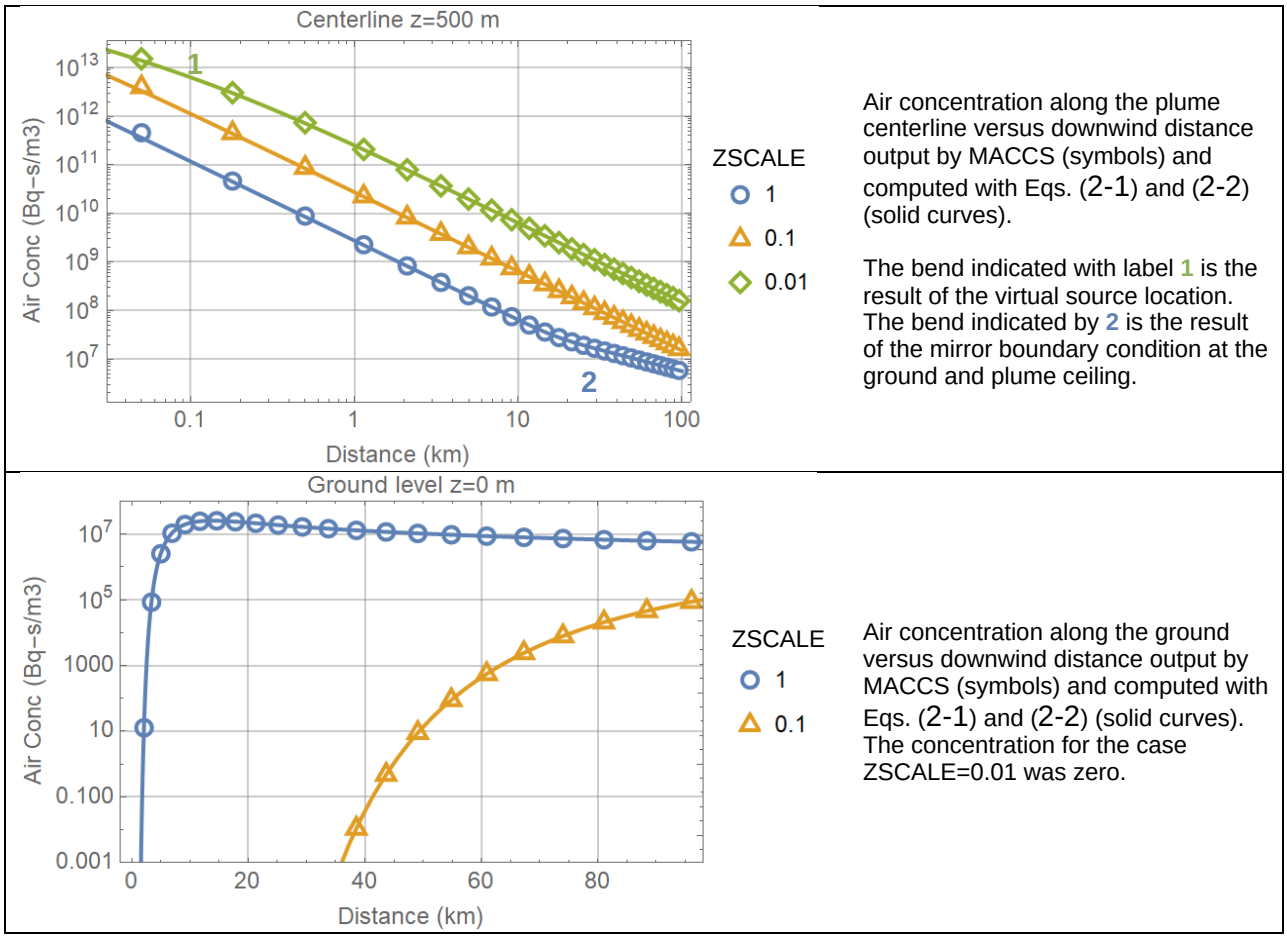

Figure 2-1. Air concentration along the centerline (y=500 m) and at the ground level (y=0 m) versus downwind distance. Symbols represent MACCS output; solid curves represent independent computations.

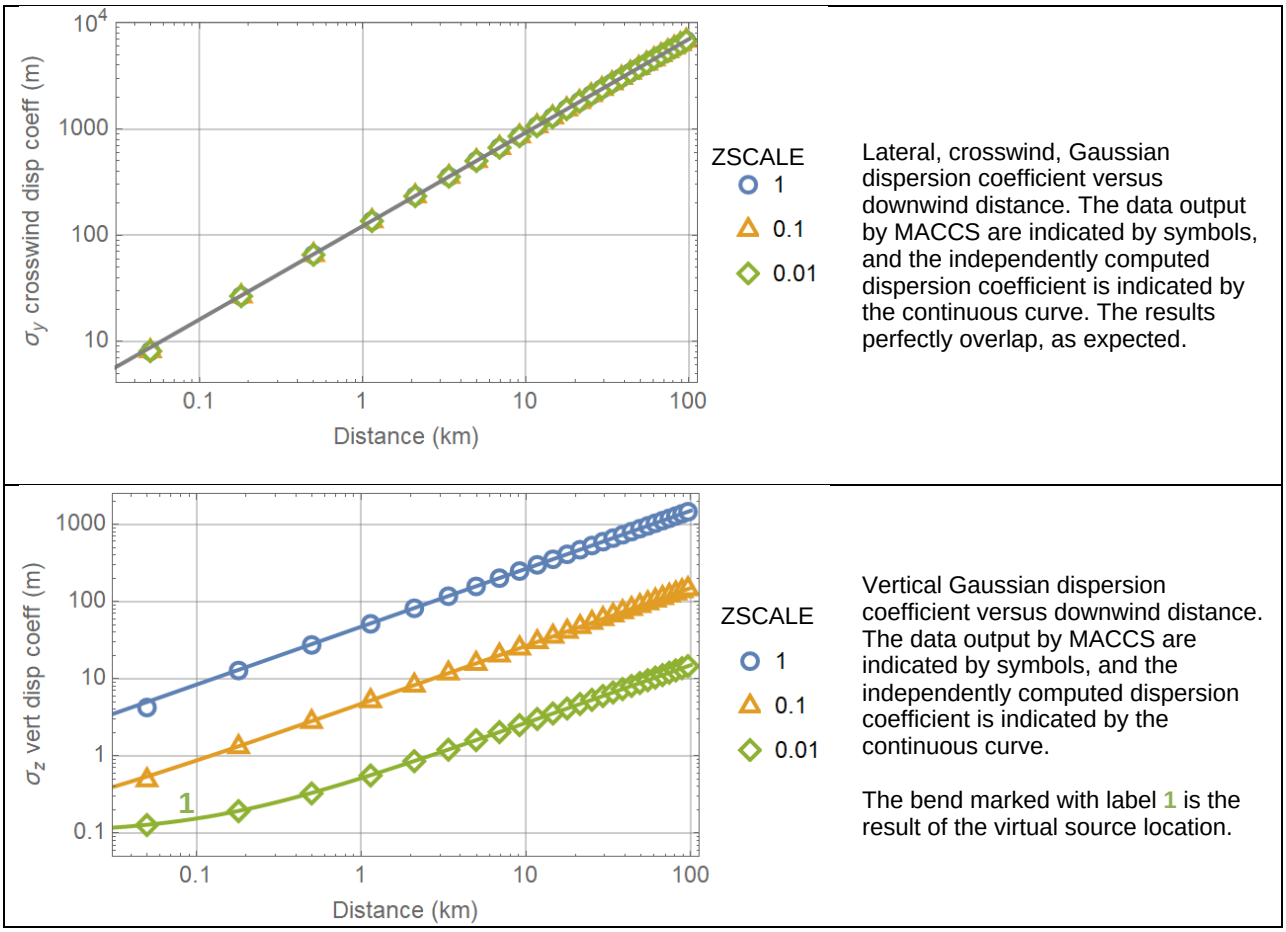

Figure 2-2. Lateral and vertical Gaussian dispersion coefficient versus downwind distance. Symbols represent MACCS output; solid curves represent independent computations.

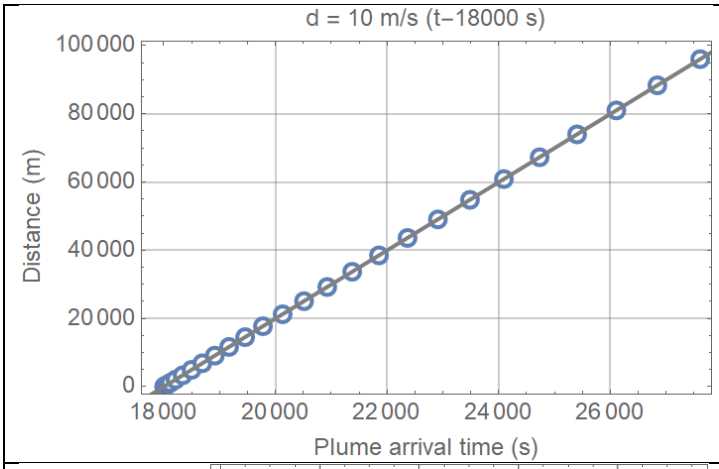

Plume distance versus time. MACCS output data are indicated by symbols, and the straight line was computed with the equations $d = 10\frac{m}{s}(t - 18000\ s)$, consistent with a windspeed BNDWND=10 m/s, and a delay PDELAY = 18000 s provided as input.

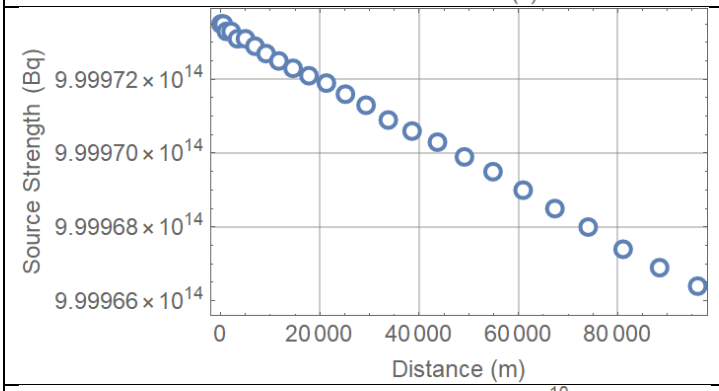

Source strength versus distance. The initial assumed inventory of Cs-137 was 10^{15} Bq (CORINV=10^{15} Bq).

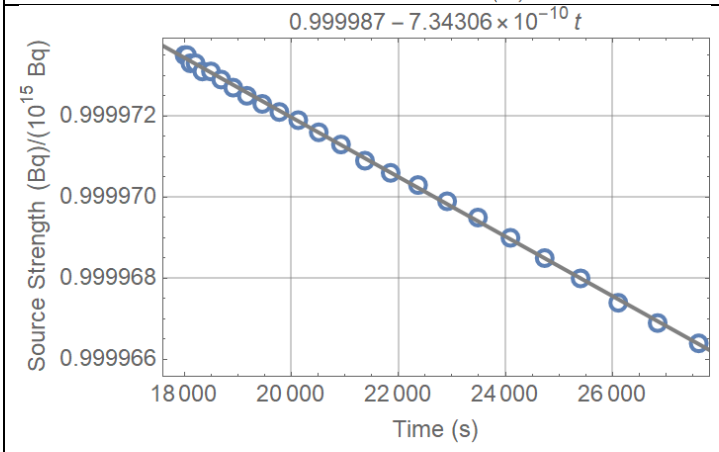

Normalized source strength versus time. The time was computed as a function of distance as

$$t = \frac{d}{10\ m/s} + 18000\ s$$

A straight line was fit, with a resulting slope of 7.34×10^{-10} 1/s. This slope corresponds to a half-life of 29.93 yr, which compares well to the Cs-137 half-life of 30.08 yr. A straight line fits the normalized source strength versus time because the decay rate is small, and a first order Taylor expansion is an accurate approximation:

$$\frac{Q}{Q_o} = e^{-\lambda t} \approx 1 - \lambda t$$

Q: source strength (Bq)
Q_o: initial source strength (CORINV=10^{15} Bq)

Figure 2-3. Plume travel time and source strength.

The following tests are focused on dose estimates associated with the cloudshine pathway. The dose computations are implemented by the EARLY module and corresponding tests are described in Section 3 of this report. However, a test of a cloudshine dose computation is included in the current Test 2.1 because it relates to air concentrations along the plume centerline, and data are readily available in the executed MACCS runs to complete a supplemental test (cloudshine dose) to tests documented in Section 3.

Type 6 (centerline doses) and Type A (peak dose) are output in the file Model1.out. It was verified that Type 6 and Type A doses are practically identical; however, the comparison is not shown herein, for brevity. The value of the Cs-137 cloudshine dose coefficient factor was extracted from the MACCS input database (file named Fgr13dcf.inp), $DRCC_{\infty ik}$ = 9.28×10^{-17}

Sv-m^3/Bq-s for the test. From Eq. (2-4), the cloudshine factor is computed from MACCS outputs as the ratio

$$C = \frac{DC_k}{DRCC_{\infty ik}\ \chi(x, y = 0, z = h)} \tag{2-5}$$

The numerator DC_k is the Type 6 centerline doe, the centerline concentration $\chi(x, y = 0, z = h = 500\ \mathrm{m})$ can be independently computed or extracted from the output Centerline Air Concentration (Bq-s/m^3) in the file tbl_outStat.txt.

The cloudshine factor C, computed from the MACCS outputs as described in Eq. (2-5), was compared to a cloudshine factor directly computed from a lookup table provided by the SNL software developers.[1] A plot of the cloudshine factor as a function of the effective plume size and the receptor distance from the centerline to the receptor location (located on the ground) is provided in Figure 2-4.

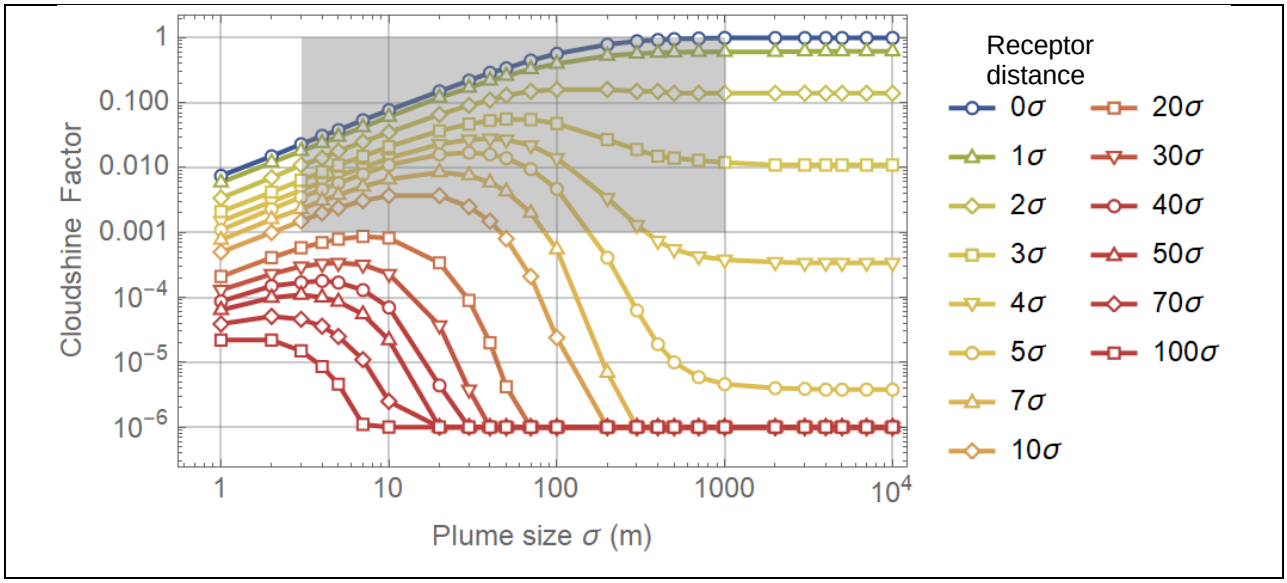

Figure 2-4. Cloudshine factor versus the effective plume size and the receptor distance to the plume centerline. This is lookup table data provided by MACCS software developers.[1] Markers represent points in the lookup table, which are joined by same-color lines to facilitate the visualization. The gray rectangle represents the domain considered in the prior MACCS Version 4.0.

The effective plume size, σ, is defined as the geometric mean of the lateral Gaussian dispersion coefficient, σ_y, and the vertical Gaussian dispersion coefficient, σ_z:

$$\sigma(x) = \sqrt{\sigma_y(x)\ \sigma_z(x)} \tag{2-6}$$

The relative receptor distance, rrd, is defined as

[1]Data obtained through personal communication. Update data in Figure 2-4 are not included in the MACCS Theory Manual (Nosek & Bixler, 2021).

$$rrd = \frac{receptor\ distance}{\sigma} = \frac{\sqrt{h^2 + y^2}}{\sigma} \quad (2\text{-}7)$$

where h is the plume centerline height (=500 m in the test problem), and the receptor is located at coordinates (x, y, z=0). The cloudshine factor lookup table updated for MACCS Version 4.1 defines the cloudshine factor as a function of σ ranging from 1 to 10000, and rrd ranging from 0 to 100.

The gray box in Figure 2-4 represents the approximated domain of the lookup table of MACCS Version 4.0 (σ ranged from 3 to 1000, and rrd from 0 to 5). Initial testing of MACCS Version 4.0 identified artefacts associated with effective plume sizes and relative receptor distances in the extrapolation domain of the cloudshine factor lookup table. Extending the (σ, rrd) domain of the cloudshine factor lookup table in MACCS Version 4.1 reduced the frequent need of extrapolation (implemented as edge interpolation in the MACCS algorithms) in the test problems in this report and associated artefacts.

Figure 2-5 displays the MACCS cloudshine factor. The symbols were computed based on Eq. (2-5) and MACCS outputs (centerline cloudshine dose and centerline concentration of Cs-137), and the continuous curves were computed from the lookup table (Figure 2-4), using a linear interpolation function available in Mathematica 12. The MACCS results are excellent in agreement with the independent computations.

Figure 2-6 displays the cloudshine factor versus the downwind distance for a wider range of ZSCALE factors (multiplicative factor to compute the vertical Gaussian dispersion coefficient σ_y), from 0.01 to 10. The independently computed cloudshine factor (solid curves) is in perfect agreement with the MACCS data for ZSCALE factors of 1 or less. The MACCS data exhibit a jump close to a value of 1 for the cases ZSCALE 5 and 10 possibly due to different and practical interpolation approaches to compute the cloudshine factor in the cases of broad plumes (large σ) and small relative receptor distance, rrd.

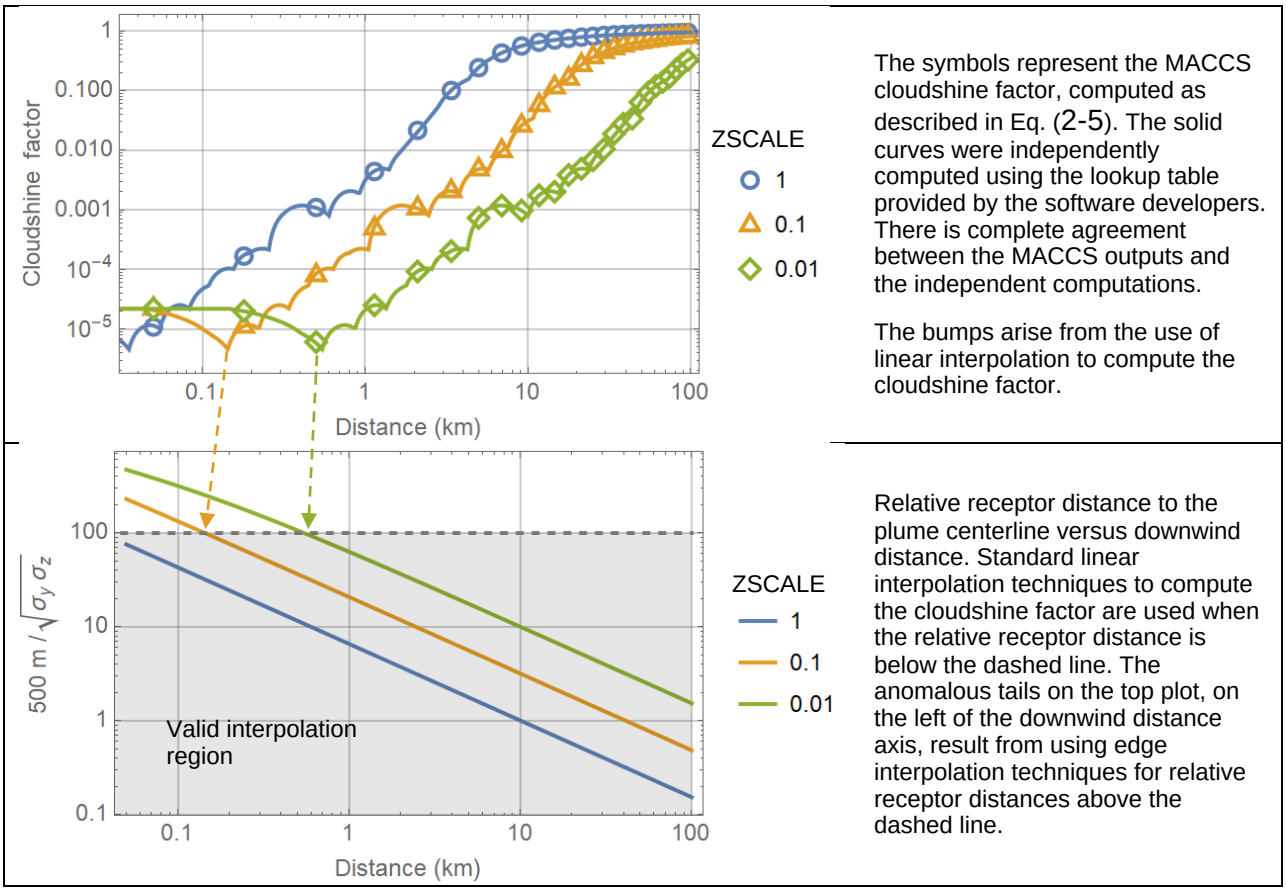

The symbols represent the MACCS cloudshine factor, computed as described in Eq. (2-5). The solid curves were independently computed using the lookup table provided by the software developers. There is complete agreement between the MACCS outputs and the independent computations.

The bumps arise from the use of linear interpolation to compute the cloudshine factor.

Relative receptor distance to the plume centerline versus downwind distance. Standard linear interpolation techniques to compute the cloudshine factor are used when the relative receptor distance is below the dashed line. The anomalous tails on the top plot, on the left of the downwind distance axis, result from using edge interpolation techniques for relative receptor distances above the dashed line.

Figure 2-5. Cloudshine factor versus downwind distance and relative receptor distance versus the downwind distance.

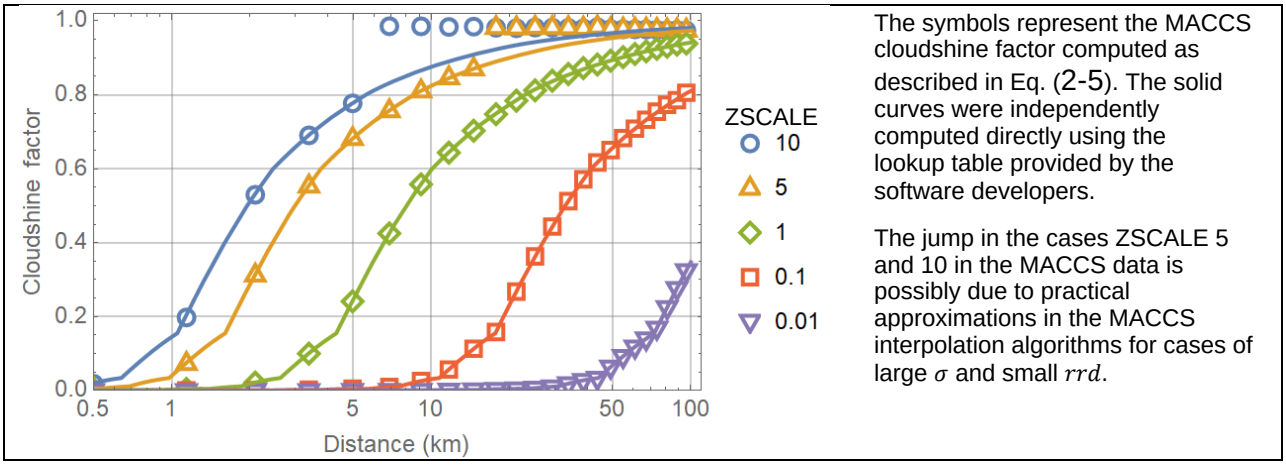

The symbols represent the MACCS cloudshine factor computed as described in Eq. (2-5). The solid curves were independently computed directly using the lookup table provided by the software developers.

The jump in the cases ZSCALE 5 and 10 in the MACCS data is possibly due to practical approximations in the MACCS interpolation algorithms for cases of large σ and small rrd.

Figure 2-6. Cloudshine factor versus downwind distance for additional ZSCALE cases.

The following test is associated with the computation of the mean concentration over a constant-radius arc in the MACCS polar grid. MACCS reports results in a polar coordinate grid. The Type C dose in the Model1.out file is the average dose along an arc of the MACCS grid. In the test problem, the 360° compass was divided into 16 sectors (NUMRAD=16), with each sector of angular length equal to π/8 radians. An arc of the MACCS grid is a constant radius curve of angular length π/8 radians.

MACCS does not implement a strict transformation of polar (r, θ) to Cartesian (x, y) coordinates. Instead, MACCS adopts the following approximated mapping, which is accurate only for laterally narrow plumes (narrow angle approximation):

$$x \to r$$
$$y \to \theta\, r \tag{2-8}$$

The average Type C dose for the north sectors is computed in MACCS as the average dose computed over a constant-radius segment spanning from – π/16 to π/16 (angle measured with respect to the north direction). The average dose was independently computed by applying the following steps:

1. Select a downwind distance x and a central sector (north sector)

2. The corresponding arc of the grid is identified: constant radius arc $r = x$, spanning from $-\pi$/16 to π/16, angle measured with respect to the north direction

3. The average cloudshine factor was computed as a line integral along the arc, considering the MACCS narrow angle approximation in Eq. (2-8). The average equals the line integral divided by the arc length.

4. A low-precision average also was computed as an alternative approach, sampling six equidistant points along the arc, and computing the average of those six points

The average cloudshine factor divided by the cloudshine factor at $y=0$ (or $\theta = 0$, centerline cloudshine factor) must be equivalent to the ratio of the Type C mean dose to the Type 6 centerline dose. The comparison of the independently computed average to the MACCS outputs is displayed in Figure 2-7. The independent computations (solid curves in Figure 2-7) agree with the MACCS data (symbols in Figure 2-7). The jump in the cases ZSCALE 5 and 10 have the same explanation as jumps in Figure 2-6 (due to different interpolation approaches to compute the cloudshine factor in the case of large σ and small rrd). The independent computations matching the MACCS data for the cases ZSCALE 1, 5, and 10 considered a high-precision average based on a line integral. On the other hand, the independent computations matching the MACCS data for the cases ZSCALE 0.01 and 0.001 (vertically narrow plumes) considered a simple average computed with 7 equidistant points on the arc of north sectors. It appears that MACCS employs different mean algorithms in the computation of the Type C cloudshine mean dose depending on the plume spread. For narrow plume cases, a simplified average considering few points along an arc is used; for broad plumes a high-precision algorithm to compute means is employed.

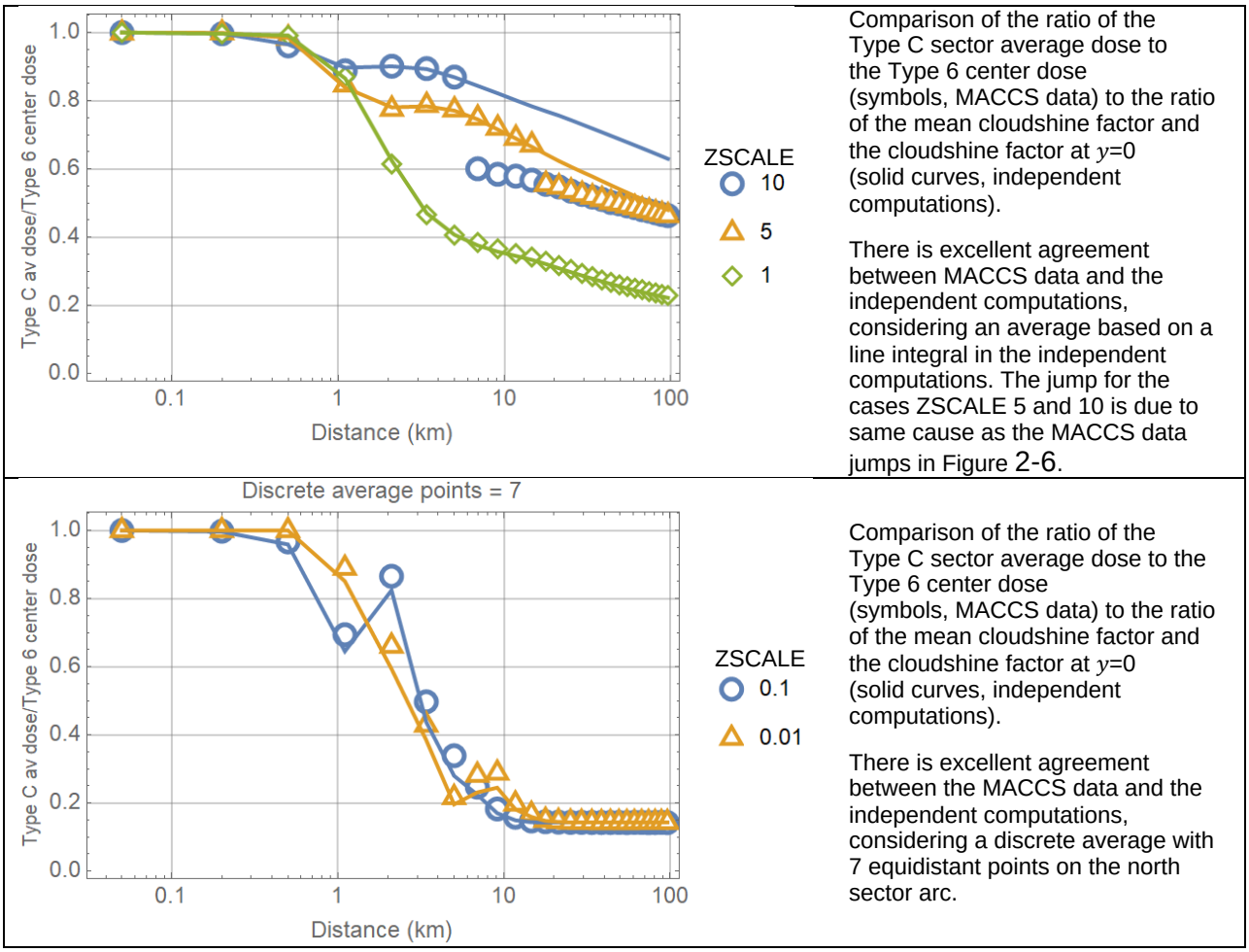

Comparison of the ratio of the Type C sector average dose to the Type 6 center dose (symbols, MACCS data) to the ratio of the mean cloudshine factor and the cloudshine factor at y=0 (solid curves, independent computations).

There is excellent agreement between MACCS data and the independent computations, considering an average based on a line integral in the independent computations. The jump for the cases ZSCALE 5 and 10 is due to same cause as the MACCS data jumps in Figure 2-6.

Comparison of the ratio of the Type C sector average dose to the Type 6 center dose (symbols, MACCS data) to the ratio of the mean cloudshine factor and the cloudshine factor at y=0 (solid curves, independent computations).

There is excellent agreement between the MACCS data and the independent computations, considering a discrete average with 7 equidistant points on the north sector arc.

Figure 2-7. Type C to Type 6 cloudshine dose ratio (symbols) versus the downwind distance compared to independent computations (solid curves).

2.1.4 Test Conclusions

Multiple aspects of the MACCS computations were tested; the MACCS ATMOS module passed the designed tests. The following aspects were verified to agree with descriptions in the MACCS Theory Manual:

- Computation of radionuclide concentrations in air, along the centerline and along the ground
- Computation of Gaussian dispersion coefficients according to power laws
- Computation of the Gaussian dispersion coefficients at x = 0, defined by the input parameters SIGYINIT and SIGZINIT
- Propagation of the plume, controlled by the windspeed
- Radioactive decay of the source
- Computation of the cloudshine pathway dose, accounting for the cloudshine factor
- Computation of an average cloudshine dose

A difference was noted in the computation of the cloudshine factor for broad plume cases (i.e., large σ) and small relative receptor distance, rrd (see Figure 2-6 and Figure 2-7) with respect to independent computations. This difference is likely a practical conservative approach in MACCS interpolation algorithms.

2.2 Test 2.2: Wet Deposition, Long Plume Under Constant Rain

The objective of the set of tests is to verify the implementation of the wet deposition model. Wet deposition is modeled as a first order decay (Eq. 2-44 of the MACCS Theory Manual)

$$\frac{dQ}{dt} = -C_1 \left(\frac{I}{I_0}\right)^{C_2} \cdot Q \tag{2-9}$$

Q — airborne activity (Bq)
I — rain rate (mm/hr), BNDRAN=1 mm/hr in the test
I_o — reference rain rate (=1 mm/hr)
C_1 — linear wet deposition coefficient (1/s), CWASH1
C_2 — exponential wet deposition coefficient (dimensionless), CWASH2=0 in the test

For a case with constant rain and no dry deposition, the solution to Eq. (2-9) is an exponentially decaying function. A plume under rain deposits mass on the ground according to an exponentially decaying function.

The reader is referred to the MACCS Theory Manual for detailed equations. A qualitative derivation is provided in the following description. If ΔQ_j is the deposited inventory on the ground, then the average concentration along the centerline y=0 on the ground is defined as

$$GC(y=0)_j = \frac{\Delta Q_j}{\sqrt{2\pi}\,\sigma_y(x_j)\,L_j} \tag{2-10}$$

$GC(y=0)_j$ — centerline ground concentration for grid element j (Bq/m^2)
ΔQ_j — inventory deposited on the ground for grid element j (Bq)
$\sigma_y(x_j)$ — dispersion coefficient at the x position of grid element j (m)
L_j — length of the grid element j (m)

The MACCS Theory Manual introduces a term denoted as $f_{av,j}$ to account for the plume segment dimensions projected along the ground and averaged in time. This factor is intended to constrain the amount of inventory carried by the plume which is available to wet deposition in a specific grid element j. For very long plume segments exceeding the dimensions of a plume element, the $f_{av,j}$ term is simply computed as

$$f_{av,j} = \frac{L_j}{2\,L_s} \tag{2-11}$$

L_j — length of the grid element j (m)
L_s — length of plume segment (m)

For a simple case of constant rain and constant wind direction and speed, the ground deposited inventory ΔQ_j is an exponentially decaying function of the elapsed time since the time of radionuclide release, i.e.,

$$\Delta Q_j = \Delta Q_o\, f_{av,j} \exp\left[-C_1 \left(\frac{I}{I_0}\right)^{C_2} (t - t_o)\right] = \Delta Q_o \frac{L_j}{2\,L_s} \exp\left[-C_1 \left(\frac{I}{I_0}\right)^{C_2} \frac{x_j}{u}\right] \tag{2-12}$$

ΔQ_o — reference ground inventory (Bq)
t_o — plume release time (s)

x_j — x-position of the grid element j (m)
u — wind speed (m/s)

Therefore, for a simple test problem of constant windspeed, long plume, and constant rain of long duration

$$GC(y=0)_j = \frac{\Delta Q_o}{2\ L_s} \frac{\exp\left[-C_1 \left(\frac{I}{I_0}\right)^{C_2} \frac{x_j}{u}\right]}{\sqrt{2\pi}\ \sigma_y(x_j)} \quad (2\text{-}13)$$

The ground concentration for grid element j is a Type 6 (centerline concentration) output in the file Model1.out. According to Eq. (2-13), the product $\sigma_y(x_j)\ GC(y=0)_j$ is proportional to $\exp\left[-C_1 \left(\frac{I}{I_0}\right)^{C_2} \frac{x_j}{u}\right]$. Thus, a plot of $\sqrt{2\pi}\ \sigma_y(x)\ GC(y=0)$ versus x should exhibit a linear decay (displayed as a straight line in a log-linear plot).

2.2.1 Test Input

The inputs were identical to inputs in the ATMOS Test 2.1 with the following changes

- Weather, Constant or Boundary Conditions
  - BNDMXH (m) = 1000: plume ceiling
  - IBDSTB = 4: stability class
  - **BNDRAN (mm/hr) = 1: rain rate**
  - BNDWND (m/s) = 10: windspeed
- Deposition
  - Wet / Dry Deposition Flags
    - DRYDEP = FALSE for Cs and Ba
    - WETDEP = TRUE for Cs
  - Wet Deposition
    - CWASH1 (1/s) = 10^{-5} (reference value)
    - CWASH2 = 0: makes wet deposition to be independent of the precipitation

Output Controls

- Same output controls of Test 2.1.

2.2.2 Test Procedure

Several runs of the MACCS code were executed with different values of CWASH1

- CWASH1 = 0 (0 × reference): case without wet deposition
- CWASH1 = 10^{-6} (0.1 × reference)
- CWASH1 = 10^{-5} (1 × reference)
- CWASH1 = 10^{-4} (10 × reference)
- CWASH1 = 10^{-3} (100 × reference)
- CWASH1 = 10^{-2} (1000 × reference)

Values of the Type 6 centerline concentration were extracted from Model1.out. Per Eq. (2-9) and for the simple system modeled (constant rain, constant windspeed), the air concentration

exponentially decays with elapsed time and x distance away from the source. The centerline concentration is computed as

$$\chi_j(x, y = 0, z = 500\ m) = \chi_j^o(x) \exp[-C_1(t - t_o)] = \chi_j^o(x) \exp\left[-C_1 \frac{x}{u}\right] \quad (2\text{-}14)$$

$\chi_j(x, y = 0, z = 500\ m)$ — air concentration along the centerline (Bq-s/m^3)
$\chi_j^o(x)$ — air concentration along the centerline (Bq-s/m^3) for a case with no wet deposition
u — windspeed (m/s), BNDWND=10 m/s in the test

Equation (2-14) does not include any dependence on the rain rate, because it was assumed CWASH2=0. The centerline air concentration $\chi_j^o(x)$ can be computed with a MACCS simulation with C_1=CWASH1=0, or with the methods of the test in Section 2.1.

The test in Section 2.1 demonstrated that the time since the plume release and plume element travel distance x are simply related

$$x = u(t - t_o) \quad (2\text{-}15)$$

t_o — initial time of the release (s), PDELAY=18000 s in the test

The quantity $\chi_j(x, y = 0, z = 500\ m)/\chi_j^o(x)$ was computed using MACCS outputs [Type 6 centerline dose, label Centerline Air Concentration (Bq-s/m3)]. A plot of $\chi_j(x, y = 0, z = 500\ m)/\chi_j^o(x)$ versus x should exhibit exponential decay with a decay rate equal to CWASH1/u.

The quantity $\sigma_y(x)\ GC(y = 0)_j$ was computed using MACCS outputs in the file tbl_outStat.txt for the lateral dispersion coefficient and the ground concentration marked by the labels “Plume Crosswind Dispersion (m)” and “Centerline Air Concentration (Bq-s/m3).” A plot of $\sigma_y(x)\ GC(y = 0)_j$ versus x should exhibit exponential decay with a decay rate equal to CWASH1/u.

2.2.3 Test Results

Figure 2-8 shows $\chi_j(x, y = 0, z = 500\ m)/\chi_j^o(x)$ versus x for different cases of CWASH1. The case legend was the factor applied to the reference CWASH1 = 10^{-5} 1/s. The log-linear plot demonstrates the expected linear decay.

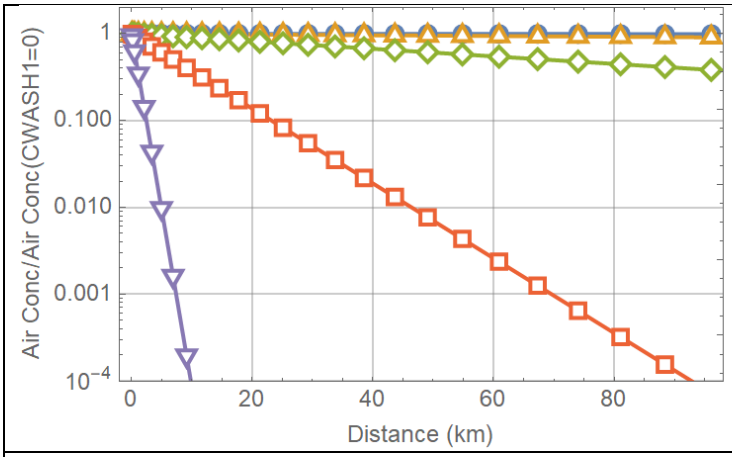

Plot of $\chi_j(x, y = 0, z = 500\ m)/\chi_j^o(x)$ versus downwind distance x for different cases of CWASH1. The case legend was the factor applied to the reference CWASH1 = 10^{-5} 1/s.

The log-linear plot demonstrates the expected exponential decay with distance. The decay rate equals CWASH1/wind speed, as expected.

	Fit	CWASH1 (1/s)	PDELAY (s)
CWASH1(1/s)=1E-6	$0.0179992 - 9.99967 \times 10^{-7}\ t$	9.99967×10^{-7}	17999.8
CWASH1(1/s)=1E-5	$0.179985 - 9.99919 \times 10^{-6}\ t$	9.99919×10^{-6}	18000.
CWASH1(1/s)=1E-4	$1.79856 - 0.0000999201\ t$	9.99201×10^{-5}	18000.
CWASH1(1/s)=1E-3	$17.8594 - 0.000992183\ t$	9.92183×10^{-4}	18000.1
CWASH1(1/s)=1E-2	$174.047 - 0.0096556\ t$	9.6556×10^{-3}	18025.5

The distance was transformed to a travel time using Eq. (2-15) with t_o=PDELAY=18000 s. Then the log of the vertical axis of the previous plot versus time was fit to a straight line, with results of the linear fit on the left table. The CWASH1 values computed from the fit well match the expected values of 10^{-6} 1/s, 10^{-5} 1/s, 10^{-4} 1/s, 10^{-3} 1/s, and 10^{-2} 1/s.

Figure 2-8. Ratio of Air concentration on the centerline to air concentration without wet deposition versus downwind distance, and results of a log-linear fit.

Figure 2-9 displays a plot of $\sqrt{2\,\pi}\ \sigma_y(x)\ GC(y = 0)$ versus x for different cases of CWASH1. The case legend was the factor applied to the reference CWASH1 = 10^{-5} 1/s. The results in Figure 2-9 and the embedded fit tables indicate that

$$\frac{\Delta Q_o}{2\ L_s} = C_1 \left(\frac{I}{I_0}\right)^{C_2} \frac{Q_o}{u} \qquad (2\text{-}16)$$

Q_o – plume segment inventory (Bq), CORINV=10^{15} Bq in the test
u – windspeed (m/s), BNDWND=10 m/s in the test

The intercept $\frac{\Delta Q_o}{2\ L_s}$ is the activity deposited on the ground per unit of length along the x-direction near the source (x = 0). Equation (2-16) can also be derived as a solution to Eq. (2-9), considering a total constant source Q_o at x=0. The right-hand side of Eq. (2-16) is independent of the plume length and the plume duration. As verification, another test was implemented by executing runs varying the plume length but keeping constant Q_o = 10^{15} Bq and keeping CWASH1 constant. It was verified that results (integrated air concentrations and ground concentrations) are independent of the plume duration (when the only quantity varied is the plume duration), as predicted by Eq. (2-16). Detailed results of that additional test are not included, for brevity.

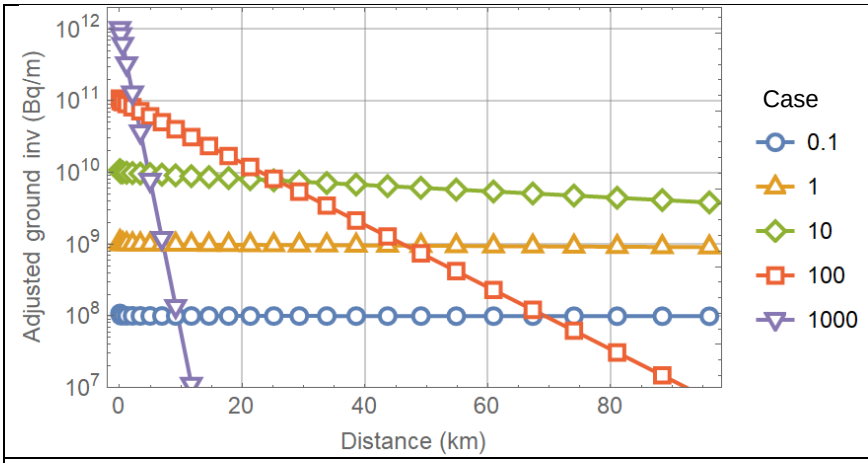

Plot of $\sqrt{2\,\pi}\,\sigma_y(x)\,GC(y=0)$ versus x for different cases of CWASH1. The case legend was the factor applied to the reference CWASH1 = 10^{-5} 1/s.

The log-linear plot demonstrates the expected exponential decay with distance.

The starting point of the different curves at x=0 is precisely spaced by factors of 10.

	Fit	CWASH1 (1/s)
CWASH1 (1/s) =1E−6	$18.4307 - 2.64633 \times 10^{-6}\,t$	2.64633×10^{-6}
CWASH1 (1/s) =1E−5	$20.7332 - 0.000011628\,t$	1.1628×10^{-5}
CWASH1 (1/s) =1E−4	$23.0358 - 0.000101598\,t$	1.01598×10^{-4}
CWASH1 (1/s) =1E−3	$25.3384 - 0.000998974\,t$	9.98974×10^{-4}
CWASH1 (1/s) =1E−2	$27.6904 - 0.00980354\,t$	9.80354×10^{-3}

The distance of the previous plot was divided by u=10 m/s to compute the elapsed time. Then a straight line was fit to the log of the vertical axis of the previous plot versus time, with results of the linear fit on the left table. The CWASH1 values computed from the fit match well with the expected values of 10^{-5} 1/s, 10^{-4} 1/s, 10^{-3} 1/s, and 10^{-2} 1/s. There is a sizable difference in the case CWASH1 = 10^{-6} 1/s because the corresponding slope is relatively flat, causing significant fitting uncertainty.

	Intercept $\frac{\Delta Q_o}{2\,L_s}$
CWASH1 (1/s) =1E−6	1.01012×10^{8}
CWASH1 (1/s) =1E−5	1.01002×10^{9}
CWASH1 (1/s) =1E−4	1.01×10^{10}
CWASH1 (1/s) =1E−3	1.00998×10^{11}
CWASH1 (1/s) =1E−2	1.06119×10^{12}

The intercepts of the plot at x=0 are spaced by factors of 10, as expected. The intercept equals Q_o CWASH1 u^{-1} (Q_o=plume segment inventory = 10^{15} Bq)

Figure 2-9. Adjusted ground concentration versus downwind distance, results of log-linear fits, and intercept values.

2.2.4 Test Conclusions

Basic MACCS equations modeling wet deposition were tested, considering a simple case (single plume segment, constant wind speed of constant direction, no dry deposition, constant rain rate). Air concentrations exhibit an exponential decay with downwind distance x, with a decay rate controlled by the rate of wet deposition, as expected. Ground concentrations balance the airborne mass lost and also exhibit an exponential decay with downwind distance x, of the same decay rate as the airborne concentration, as expected.

The MACCS ATMOS module passed the designed tests.

2.3 Test 2.3: Wet Deposition, Variable Plume Duration

Test 2.2 examined a limit case of long-plume duration and constant rain. In that case, at any location the plume undergoes wet deposition. In Test 2.2 it was concluded that the extent of wet deposition was independent of the plume duration if the rain duration was longer than the plume duration.

In this test, a case is examined where the rain is of short duration, and the plume duration is variable (shorter or longer than the rain duration). Per the Test 2.2, wet deposition must be independent of the plume duration when

Rain duration > plume duration

In the other case, Rain duration < plume duration, only a fraction of the plume inventory (the fraction exposed to rain) is subject to wet deposition, and the extent of wet deposition is inversely proportional to the plume duration.

For a case of short rain and plume duration, Eq. (2-16) is modified as

$$\frac{\Delta Q_o}{2\,L_s} = C_1 \left(\frac{I}{I_0}\right)^{C_2} \frac{Q_o}{u} \frac{\min\left(t_p, t_R\right)}{t_p} \tag{2-17}$$

I — rain rate (mm/hr), HRRAIN=1 mm/hr in the test
I_o — reference rain rate (=1 mm/hr)
C_1 — linear wet deposition coefficient (1/s), CWASH1=10^{-3} 1/s in the test
C_2 — exponential wet deposition coefficient (dimensionless), CWASH2=0 in the test
Q_o — plume segment inventory (Bq), CORINV=10^{15} Bq in the test
u — windspeed (m/s), HRWNDV = 10 m/s in the test
t_p — plume duration (s), PLUDUR
t_R — rain duration (s), 1 hr in the test

Equation (2-17) is related to the centerline ground concentration at x=0 as

$$GC(x=0, y=0) = C_1 \left(\frac{I}{I_0}\right)^{C_2} \frac{Q_o}{u} \frac{\min\left(t_p, t_R\right)}{t_p} \frac{1}{\sqrt{2\pi}\,\sigma_y(x=0)} \tag{2-18}$$

$\sigma_y(x=0)$ — initial lateral, across wind, Gaussian dispersion coefficient at the source

2.3.1 Test Input

The inputs were identical to inputs in Test 2.2 with the following changes.

General Properties

- WEATHER
  - METCOD=3: user supplied weather

Changes to Specific Input Parameters

- One plume segment: variables NUMREL, PDELAY, PLHITE, REFTIM, PLUDUR
  - PLHITE (m) = 500 m: plume release height (mid distance to ceiling)
  - PLUDUR (s): reference value 80000 s and decreased in factors of 10
  - PDELAY (s) = 0
- User-Supplied Weather
  - HRRAIN (mm/hr) = 1 for one hour, 0 after the first hour
  - HRWND (m/s) = 10 for 120 hours, windspeed
  - HRMXHT (m) = 1000 for 120 hours, plume ceiling
  - IHRSTB (-) = 4 for 120 hours, stability class 4
  - IHRDIR (-) = 1 for 120 hours, wind direction, 1=north direction
- Deposition
  - Wet Deposition
    - CWASH1 (1/s) = 10^{-3} (reference value)

Output Controls

- Same output controls of Test 2.1.

2.3.2 Test Procedure

Four runs of the MACCS code were executed, varying the plume duration, PLUDUR. The reference duration was 80000 s, with different runs decreasing PLUDUR in factors of 10.

- PLUDUR = 80000 (1 × reference)
- PLUDUR = 8000 (0.1 × reference)
- PLUDUR = 800 (0.01 × reference), case with plume duration less than the rain duration
- PLUDUR = 80 (0.001 × reference), case with plume duration less than the rain duration

Values of the centerline concentration were extracted from tbl_outStat.txt. The following ratio was computed

$$\frac{\chi_j(x, y = 0, z = 500\ m)}{\chi_j^o(x)} \tag{2-19}$$

$\chi_j(x, y = 0, z = 500\ m)$ — air concentration along the centerline (Bq-s/m^3), from tbl_outStat.txt

$\chi_j^o(x)$ — air concentration along the centerline (Bq-s/m^3), assuming no wet deposition, computed using Eqs. (2-1) and (2-2) of Test 2.1.

According to Test 2.2, the ratio in Eq. (2-19) is an exponentially decaying function of the downwind position x for cases with rain duration longer than the plume duration (cases 0.01 and 0.001 in this test). Per Test 2.2, the decay rate with distance equals CWASH1/HRWNDV. The test was aimed at verifying this expected trend and the magnitude of the decay rate. Wet deposition is restricted to 1 hour (rain duration). After 1 hour, the plume travels 36 kilometers at a speed of 10 m/s. Past 36 km, there must not be any wet deposition (the rain would be over after the plume traveled 36 km).

In a second test, the following quantity was computed

$$\sqrt{2\,\pi}\;\sigma_y(x)\;GC(x, y=0) \tag{2-20}$$

$GC(x, y=0)$ — ground concentration along the centerline (Bq/m^2), from tbl_outStat.txt
$\sigma_y(x)$ — lateral, across wind, Gaussian dispersion coefficient (m), computed using the method described in Test 2.1.

The test focused in verifying that the quantity in Eq. (2-20) is consistent with Eq. (2-18) at x=0. The quantity $\sqrt{2\,\pi}\;\sigma_y(x=0)\;GC(x=0, y=0)$ is inversely proportional to the plume duration, if the plume lasts longer than the rain.

2.3.3 Test Results

The results of the tests are presented in Figure 2-10. Expected trends and values were successfully verified. The agreement is reasonable, with differences due to different and detailed numerical integration algorithms implemented in MACCS. The verification computations are only simplified computations, not intended to reproduce the complexity and detail of the MACCS computations.

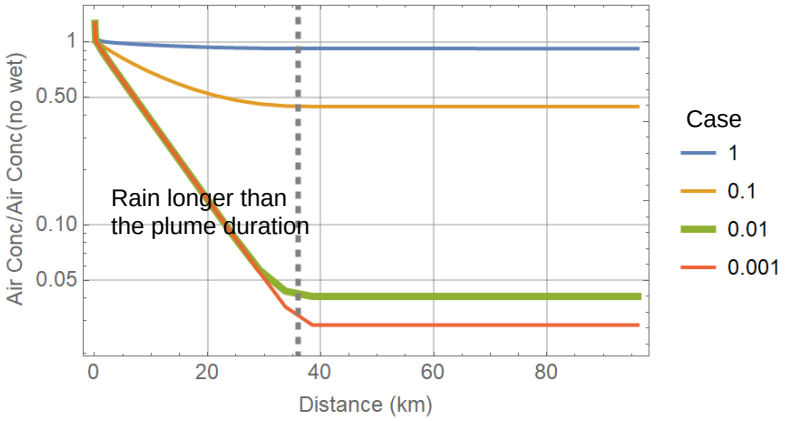

Plot of $\chi_j(x, y = 0, z = 500\ m)/\chi_j^0(x)$ versus x for different cases of the plume duration, PLUDUR. The case legend was the factor applied to the reference PLUDUR = 80,000 s.

The log-linear plot demonstrates the expected exponential decay, for the cases 0.01 and 0.001 (rain duration longer than the plume duration, green and red curves). The decay rate with x distance for those curves is CWASH1/HRWNDV=10^{-3} 1/s/10 m/s = 10^{-4} 1/m, as expected.

The curves become flat after 36 km, because rain only lasts 1 hour and 36 km is the distance traveled by the plume in 1 hour. The cases 1 and 0.1 do not exhibit exponential decay with distance because only a fraction of the plume intercepts the rain, with a fraction that is dependent on the downwind x location.

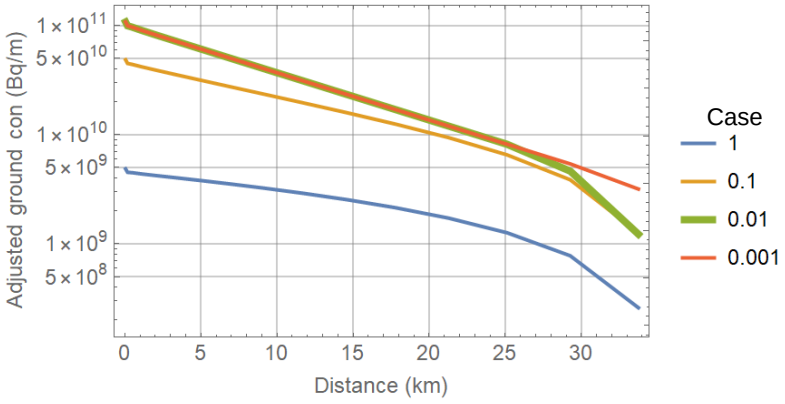

Adjusted ground concentration $\sqrt{2\,\pi}\,\sigma_y(x)\,GC(x, y = 0)$ versus x. For the cases 0.01 and 0.001 (rain duration longer than the plume duration, green and red curves), the curves exhibit exponential decay in most of the downwind distance domain as expected, with a decay rate equal to CWASH1/HRWNDV=10^{-4} 1/m.

The cases 1 and 0.1 do not exhibit exponential decay with distance because only a fraction of the plume intercepts the rain, with a fraction that is dependent on the sector x location.

Case	Intercept	Predicted
1	4.86232×10^9	4.5×10^9
0.1	4.85251×10^{10}	4.5×10^{10}
0.01	1.07687×10^{11}	$1. \times 10^{11}$
0.001	1.07687×10^{11}	$1. \times 10^{11}$

Intercept at x=0 of curves in the previous plot compared to predicted values based on Eq. (2-18). The agreement is reasonable, with differences due to different and detailed numerical integration algorithms implemented in MACCS. The simplified independent computations do not include the details of the MACCS computations.

The test verified that the intercept is inversely proportional to the plume duration for those cases where the plume lasts longer than the rain.

Figure 2-10. Ratio of Air concentration on the centerline to air concentration without wet deposition versus downwind distance; adjusted ground concentration versus downwind distance, and table with y-axis intercepts.

2.3.4 Test Conclusions

The test extended Test 2.2 to examine the effect of plume duration on the extent of ground deposition. Expected exponential decay rates were verified for derived quantities from the centerline air concentration and ground concentration, in the limit when the rain duration is longer than the plume duration. It was verified that the extent of wet deposition is inversely proportional to the plume duration.

The MACCS ATMOS module passed the designed tests.

2.4 Test 2.4: Wet Deposition, Variable Rain Duration

This test examined the effect of variable rain duration on wet deposition. Per Eq. (2-18), for cases with the plume duration longer than the rain, the wet deposition at x=0 is linearly proportional to the rain duration.

2.4.1 Test Input

The inputs were identical to inputs of Test 2.3, with the following changes

- One plume segment: variables NUMREL, PDELAY, PLHITE, REFTIM, PLUDUR
  - PLUDUR (s) = 86400 s (=24 hours)
  - PDELAY (s) = 0
- User-Supplied Weather
  - HRRAIN (mm/hr) = 1 for 1, 5, 10, 15, 25, and 30 hours

Output Controls

- Same output controls of Test 2.1.

2.4.2 Test Procedure

Six runs of the MACCS code were executed, varying the rain duration using HRRAIN inputs in the user-supplied weather. The user-supplied weather requires 120 hourly inputs. The hourly inputs were modified to attain a target rain duration, considering 6 cases:

- 1 hour
- 5 hours
- 10 hours
- 15 hours
- 25 hours (plume duration < rain duration)
- 30 hours (plume duration < rain duration)

The ratio defined in Eq. (2-19) was computed from data in tbl_outStat.txt, and the air concentration along the centerline, assuming no wet deposition, using Eqs. (2-1) and (2-2) of Test 2.1. According to Test 2.2, the ratio in Eq. (2-19) is an exponentially decaying function of the downwind distance x for cases with rain duration longer than the plume duration (cases 25 and 30 hours in this test). Per Test 2.2, the decay rate with distance equals CWASH1/HRWNDV = 10^{-4} 1/m for the cases 25 and 30 hours. For other cases (cases 1 to 15 hours), the ratio in Eq. (2-19) is not an exponentially decaying function of x; however, an exponential decay should be a reasonable approximation, with a decay rate that is proportional to 10^{-4} 1/m and to the ratio (rain duration)/(plume duration).

A second test was performed, computing the adjusted concentration in Eq. (2-20) as a function of x. For cases with rain duration longer than the plume duration (cases 25 and 30 hours in this test), the adjusted concentration must be an exponentially decaying function of x with decay rate equal to CWASH1/HRWNDV = 10^{-4} 1/m.

Per Eq. (2-18) at x=0, the quantity $\sqrt{2\,\pi}\,\sigma_y(x=0)\,GC(x=0,y=0)$ is directly proportional to the rain duration when the rain duration is less than the plume duration. The Test 2.4 verified this proportionality.

2.4.3 Test Results

Results of the tests are presented in Figure 2-11 and Figure 2-12.

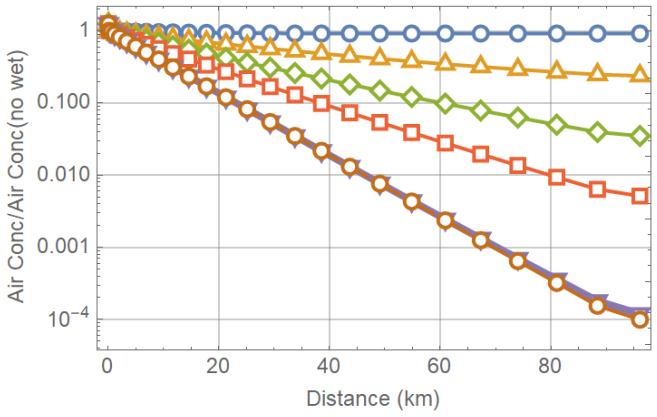

Plot of $\chi_j(x, y=0, z=500\,m)/\chi_j^o(x)$ versus x for different cases of the rain duration. The case legend was the rain duration in hours. The plume duration, PLUDUR, was 24 hours.

The log-linear plot demonstrates the expected exponential decay, for the cases 25 and 30 hours (rain duration longer than the plume duration). The decay rate with x distance for those bottom curves is CWASH1/HRWNDV=10^{-3} 1/s / 10 m/s = 10^{-4} 1/m, as expected.

The cases 1 to 15 hours can be well approximated with exponential decay. The computed decay rate is presented in the next entry.

Case	Decay rate (1/m)	Predicted
1	1.3×10^{-6}	4.2×10^{-6}
5	0.000016	0.000021
10	0.000037	0.000042
15	0.000057	0.000063
25	0.000097	0.0001
30	0.000099	0.0001

Decay rate computed as a log-linear fit, and decay rate predicted as

$$10^{-4}\,1/\mathrm{m}\,\frac{\min(t_p, t_R)}{t_p}$$

with t_p = plume duration and t_R = rain duration. The agreement is reasonable given simplifications adopted in the test (the independent computations do not reproduce all details of the MACCS computations).

The test demonstrates that the rain duration is accounted for in the MACCS numerical integrals defining the span of active wet deposition.

Figure 2-11. Ratio of air concentration on the centerline to the air concentration without wet deposition versus downwind distance, and effective decay rate computed with a log-linear fit.

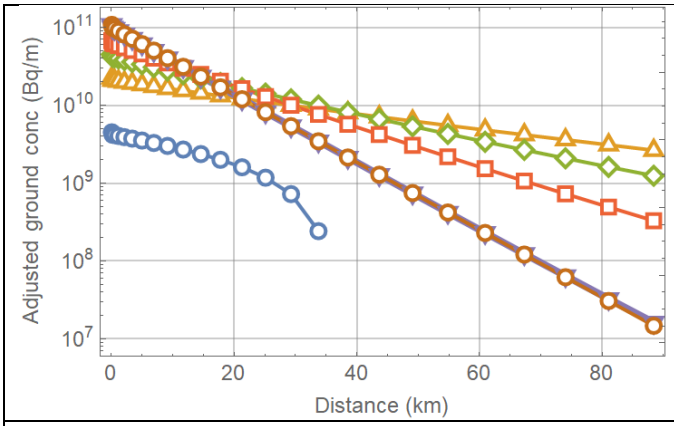

Adjusted ground concentration $\sqrt{2\,\pi}\,\sigma_y(x)\;GC(x, y=0)$ versus x. For the cases 25 and 30 hours (rain duration longer than the plume duration), the curves exhibit exponential decay with downwind distance, with an expected decay rate equal to CWASH1/HRWNDV=10^{-4} 1/m.

The other cases can be approximated as exponential decay functions, of decay rates identical to rates computed in the previous figure.

Case	Intercept (Bq/m)	Predicted
1	4.5×10^{9}	4.17×10^{9}
5	2.25×10^{10}	2.08×10^{10}
10	4.5×10^{10}	4.17×10^{10}
15	6.74×10^{10}	6.25×10^{10}
25	1.08×10^{11}	$1.\times10^{11}$
30	1.08×10^{11}	$1.\times10^{11}$

Intercept at x=0 of curves in the previous plot compared to predicted values based on Eq. (2-18). The agreement is reasonable, with differences due to different and detailed numerical integration algorithms implemented in MACCS. The verification computations are only simplified computations, not intended to reproduce the complexity and details of the MACCS computations.

The test verified that the intercept is proportional to the rain duration for those cases where the plume lasts longer than the rain.

Figure 2-12. Adjusted ground concentration versus downwind distance, results of log-linear fits, and table with y-intercept values.

2.4.4 Test Conclusions

The test extended Test 2.2 to examine the effect of rain duration on the extent of ground deposition. Expected exponential decay rates were verified for derived quantities from the centerline air concentration and ground concentration, in the limit when the rain duration is longer than the plume duration. It was verified that the extent of wet deposition is proportional to the rain duration when the plume lasts longer than the rain. The test demonstrated that the rain duration is accounted for in the MACCS numerical integrals defining the span of active wet deposition.

The MACCS ATMOS module passed the tests.

2.5 Test 2.5: Dry Deposition, Variable Speed

The objective of the test was to verify implementation of dry deposition equations, examining a simple case. For a single particle size, dry deposition is controlled by the equation 2-40 of the MACCS Theory Manual (Nosek & Bixler, 2021):

$$\frac{dQ}{dt} = -\frac{v_d}{\bar{z}(x)}\ Q \tag{2-21}$$

$$\frac{1}{\bar{z}(x)} = \frac{1}{\bar{z}(u\ t)} = \frac{\psi(x, z=0)}{\int_0^H \psi(x,z)\ dz} \tag{2-22}$$

Q — airborne activity (Bq)
v_d — vertical dry deposition velocity (m/s)
$\psi(x,z)$ — term defined by Eq. (2-2) (1/m)
$\bar{z}(x)$ — reference distance (m) [$1/\bar{z}(x)$ is a measurement of the plume spread along the vertical direction]
u — windspeed (m/s), HRWNDV = 10 m/s in the test
t — time measured since the plume release (s)
H — plume ceiling, maximum plume height (m), HRMXHT = 1000 m in the test

The general solution to Eq. (2-21) is

$$\frac{Q_1}{Q_o} = \exp\left[-v_d \int_0^t \frac{d\tau}{\bar{z}(u\ \tau)}\right] \tag{2-23}$$

Q_1 — airborne activity exiting a sector (Bq)
Q_o — airborne activity entering a sector (Bq)
t — relative time for a plume segment to cross a sector (s) (=sector length/u)

Equation (2-23) is a generalization of Eq. (2.40) of the MACCS Theory Manual. It is assumed in MACCS that dry deposition does not change the vertical distribution of the radioactive concentration. Therefore, Eq. (2-23) can be generalized for the computation of centerline concentrations (concentrations along the line y=0):

$$\frac{\chi_1(x = u\ t, y=0, z)}{\chi(x = u\ t, y=0, z)} = \exp\left[-v_d \int_0^t \frac{d\tau}{\bar{z}(u\ \tau)}\right] \tag{2-24}$$

$\chi_1(x,y,z)$ — integrated airborne concentration (Bq-s/m^3)
$\chi(x,y,z)$ — integrated airborne concentration (Bq-s/m^3) assuming no dry deposition, defined by Eqs. (2-1) and (2-2)
t — arbitrary time measured from the time of the plume release

The centerline ground concentration is computed as

$$GC(x = u\ t, y=0) = \chi_1(x = u\ t, y=0, z=0) v_d \tag{2-25}$$

$GC(x = u\ t, y=0)$ — centerline ground concentration (Bq/m^2)

The objective of the test was verifying that independently computed concentrations using Eqs. (2-24) and (2-25) agree with corresponding concentrations output in the file tbl_outStat.txt.

2.5.1 Test Input

Inputs were selected to simulate a single plume segment of constant speed (HRWNDV =10 m/s), constant wind direction (blowing north), only dry deposition (i.e., no wet deposition), one single long-lived radionuclide (Cs-137), and one particle size. The same input of Test 2.4 was used, with the following changes

- Deposition
  - Wet / Dry Deposition Flags
    - DRYDEP = TRUE for Cs
    - WETDEP = FALSE for Cs
  - Dry Deposition
    - VDEPOS (m/s) = 1 (reference value) for particle group 1, and 0 for other groups
- Release Description
  - Particle Size Distribution
    - PSDIST=1 for particle group 1, 0 for all other groups
- Weather / User-Supplied Weather
  - Constant weather for 120 hours
  - HRMXHT (m) = 1000
  - IHRSTB (-) = 4 (stability class 4 = D class, neutral class)
  - HRRAIN (mm/hr) = 0 (no rain)
  - HRWND (m/s) = 10
  - IHRDIR (-) = 1 (wind blowing in the north direction)

Output Controls

- Same output controls of Test 2.1.

2.5.2 Test Procedure

Individual runs of the MACCS code were executed varying only VDEPOS

- VDEPOS = 0 m/s
- VDEPOS = 0.01 m/s
- VDEPOS = 0.1 m/s
- VDEPOS = 0.3 m/s
- VDEPOS = 1 m/s
- VDEPOS = 10 m/s

The centerline air concentration, air concentration at the ground level, and ground concentration were extracted from the file tbl_outStat.txt, from outputs labeled

- Centerline Air Concentration (Bq-s/m3)
- Ground-Level Air Concentration (Bq-s/m3)
- Centerline Ground Concentration (Bq/m2)

The outputs were compared to results computed using Eqs. (2-24) and (2-25).

2.5.3 Test Results

Test results are presented in Figure 2-13.

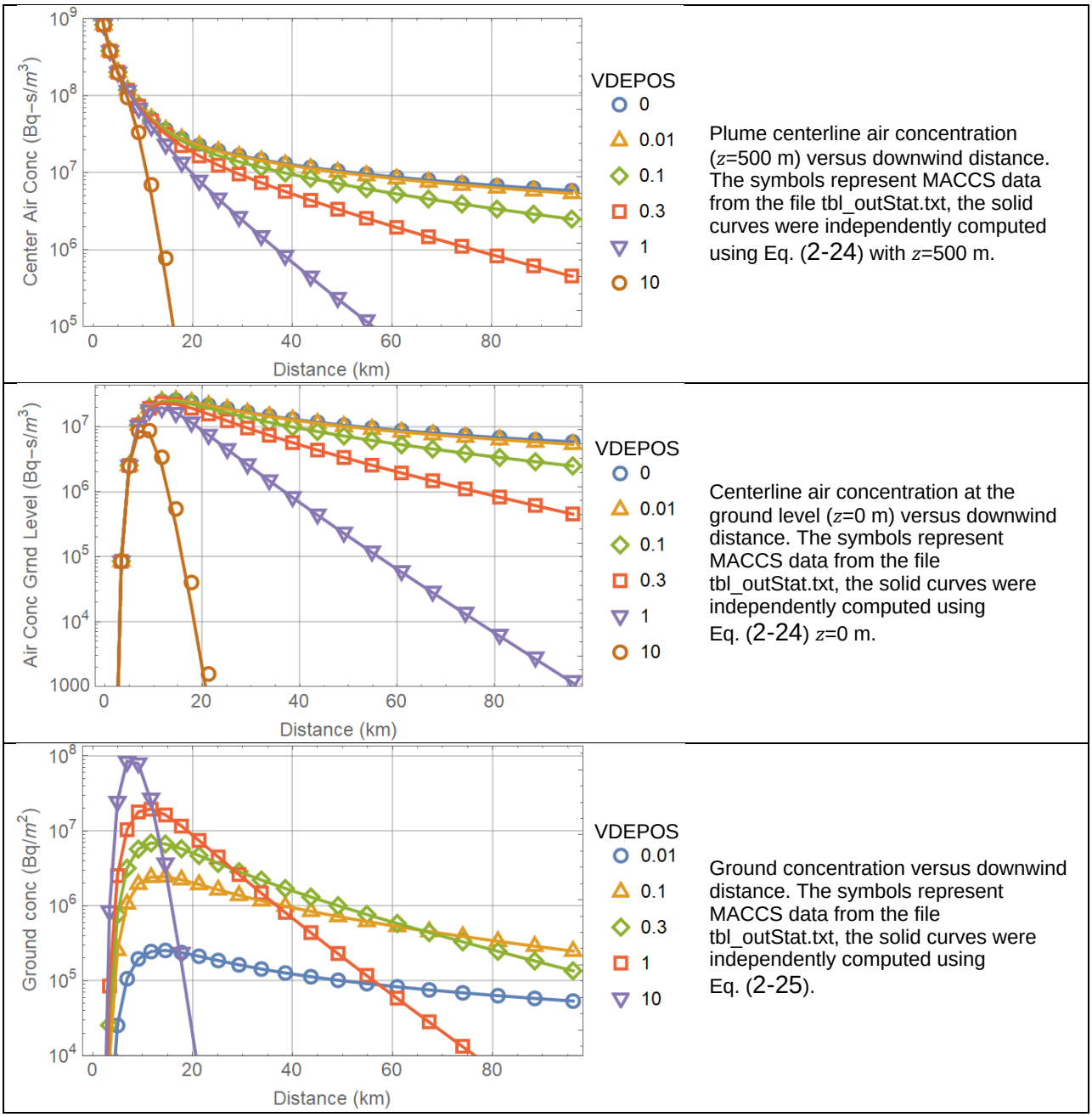

Figure 2-13. Centerline air concentration at y=500 m and at y=0 m, and centerline ground concentration versus downwind distance.

2.5.4 Test Conclusions

Concentrations independently computed successfully reproduced the MACCS concentrations under dry deposition.

2.6 Test 2.6: Comparison to CFD Simulations

This test was aimed at comparing air concentrations output from a computational fluid dynamics code to MACCS centerline air concentrations output by the ATMOS module. The test revealed that the level of lateral and vertical dispersion in the CFD simulations is in general less than predicted by the MACCS Gaussian plume dispersion equations. The differences prompted revisiting the fundamental theory behind the Gaussian plume equations, and particle tracking in CFD simulations, to examine whether reconciliation is possible or whether different solution approaches should be pursued under different scenarios. The investigation concluded that the approaches are fundamentally different, with CFD preferred when obstacles and the domain geometry, such as buildings or rugged domain, control the airflow, and Gaussian plume models preferred for open and flat spaces given knowledge of average atmospheric conditions (average windspeed, average wind direction and atmospheric stability class).

Summary of Gaussian Plume Equations

Given air moving with a windspeed $\vec{v}$, the mass flux of a substance of concentration c in air (e.g., a volatile radioactive substance mixed in air) is given by

$$\vec{J} = -\overline{\overline{D}}\,\nabla c + c\,\vec{v} \tag{2-26}$$

$\vec{J}$	—	mass flux or activity flux (mass/m^2-s or activity/m^2-s)
$\overline{\overline{D}}$	—	dispersion matrix with diagonal entries D_x, D_y, D_z (m^2/s)
c	—	substance or contaminant concentration in air (mass/m^3 or activity/m^3)
∇	—	3D gradient operator: $(\partial_x, \partial_y, \partial_z)$ (m^{-1})
$\vec{v}$	—	fluid (air) velocity vector (m/s)

The first term of Eq. (2-26), $-\overline{\overline{D}}\,\nabla c$, is a generalization of Fick's law of diffusion, representing mass fluxes in the opposing direction of concentration gradients of the substance (i.e., a substance migrates from regions of high concentration to regions of low concentration). The term $c\,\vec{v}$ is the advective component of the mass flux, corresponding to mass fluxes driven by air moving with a velocity $\vec{v}$. The terms D_x, D_y, D_z (m^2/s) are dispersion coefficients, and not classical diffusion coefficients arising from Brownian motion and particle collisions. The dispersion coefficients D_x, D_y, D_z are caused by fluctuations in the fluid speed and turbulence and other factors such as drag forces on particulates, and they must be established by experiments.

The mass conservation equation, controlling the evolution in time of the concentration of the substance in air is

$$\partial_t c = -\nabla \cdot \vec{J} = \nabla \cdot \left(\overline{\overline{D}}\,\nabla c\right) - \nabla \cdot (c\vec{v}) \tag{2-27}$$

Under steady state, $\partial_t c = 0$, and if the direction x is selected to align with the wind direction such that $\vec{v} = (u, 0, 0)$ (u is the windspeed magnitude), Eq. (2-27) is simplified as

$$\nabla \cdot \left(\overline{\overline{D}}\,\nabla c\right) - \partial_x\,(c\,u) = 0 \tag{2-28}$$

The direction x aligns with the downwind direction, y is a lateral horizontal direction, and z is a vertical direction. To derive the Gaussian plume solution, it is assumed that

1. The dispersion coefficients D_y, D_z are independent of the positions y and z but they could be function of the variable x; i.e., $D_y = D_y(x)$ and $D_z = D_z(x)$

2. The dispersion coefficient D_x is negligible, which is equivalent to assuming that the substance moves along the downwind direction x with a speed u (i.e., the substance moves with the fluid along the downwind direction x, undispersed in that direction)

3. The windspeed u is constant

Under those three assumptions, Eq. (2-28) simplifies to

$$\frac{D_y}{u}\,\partial_{yy}c + \frac{D_z}{u}\,\partial_{zz}c - \partial_x\,c = \alpha_y\,\partial_{yy}c + \alpha_z\,\partial_{zz}c - \partial_x\,c = 0 \tag{2-29}$$

The parameters $\alpha_y = D_y/u$ and $\alpha_z = D_z/u$ are commonly referred to as dispersivities, which have units of length. Dispersivities are generally defined as a fraction of the transport path length. For example, a common rule of thumb in problems of contaminant transport in groundwater is selecting a dispersivity as 10 percent of the transport path length; however, in air dispersion problems this rule of thumb does not apply.

A point source at located (x=0, y=0, z=h) is represented as

$$u\,c(x=0,y,z) = r\,\delta(y)\delta(z-h) \tag{2-30}$$

r — release rate of the substance (mass/s or activity/s)
$\delta()$ — Dirac delta function (1/m)
h — source height (m)
u — windspeed (m/s)

The solution to the steady-state Eq. (2-29) with a point source at (x=0, y=0, z=h) is a Gaussian function

$$c(x,y,z) = \frac{e^{-\frac{y^2}{4\,x\,\alpha_y}}}{2\sqrt{\pi\,\alpha_y\,x}}\;\frac{e^{-\frac{(z-h)^2}{4\,x\,\alpha_z}}}{2\sqrt{\pi\,\alpha_z\,x}}\;\frac{r}{u} \tag{2-31}$$

Equation (2-31) can be written as a multi-normal distribution by defining “standard deviation” parameters σ_y and σ_z as

$$\sigma_y(x) = \sqrt{2\,\alpha_y\,x} \text{ and } \sigma_z(x) = \sqrt{2\,\alpha_z\,x} \tag{2-32}$$

which yields

$$c(x,y,z) = \frac{e^{-\frac{y^2}{2\,\sigma_y(x)^2}}}{\sqrt{2\,\pi}\,\sigma_y(x)}\;\frac{e^{-\frac{(z-h)^2}{2\,\sigma_z(x)^2}}}{\sqrt{2\,\pi}\,\sigma_z(x)}\;\frac{r}{u} \tag{2-33}$$

For any downwind location x, the solution in Eq. (2-33) extends over infinite planes in the lateral y direction and vertical z direction. An additional zero flux condition can be imposed at the ground level, so that the contaminant substance is only contained in a vertical region between 0 and infinity

$$\partial_z c(x, y, z = 0) = 0 \tag{2-34}$$

The solution to the point source at the height z=h with a zero-flux boundary condition at the ground can be derived from Eq. (2-33) by the method of images, adding a virtual source at the location (x=0, y=0, z=−h) to compensate for the mass crossing the ground plane, which yields

$$c(x, y, z) = \frac{r}{u} \frac{e^{-\frac{y^2}{2\,\sigma_y(x)^2}}}{\sqrt{2\,\pi}\sigma_y(x)} \left[\frac{e^{-\frac{(z-h)^2}{2\,\sigma_z(x)^2}}}{\sqrt{2\,\pi}\,\sigma_z(x)} + \frac{e^{-\frac{(z+h)^2}{2\,\sigma_z(x)^2}}}{\sqrt{2\,\pi}\,\sigma_z(x)} \right] \tag{2-35}$$

In MACCS, contaminants are assumed constrained between the ground and an upper plane at a distance z=H (referred in MACCS as mixing layer height). The solution to the advective-dispersive mass balance equation with a point source at (x=0, y=0, z=h) and zero-flux boundary conditions at the planes z=0 and z=H

$$\partial_z c(x, y, z = 0) = 0 \text{ and } \partial_z c(x, y, z = H) = 0 \tag{2-36}$$

can also be derived with the method of images. In this case, virtual sources must be considered mirrored on the planes z=0 and z=H, which results in an infinite series of virtual sources (such as the infinite images reflected by two parallel mirrors) yielding the following solution

$$c(x, y, z) = \frac{r}{u} \frac{1}{\sqrt{2\,\pi}\,\sigma_y(x)} e^{-\frac{1}{2}\frac{y^2}{\sigma_y(x)^2}} \psi(x, z) \tag{2-37}$$

with

$$\psi(x, z) = \frac{1}{\sqrt{2\,\pi}\,\sigma_z(x)} \sum_{n=-N}^{N} [e^{-\frac{1}{2}\frac{(z-h+2\,n\,H)^2}{\sigma_z(x)^2}} + e^{-\frac{1}{2}\frac{(z+h+2\,n\,H)^2}{\sigma_z(x)^2}}] \tag{2-38}$$

The series limit N in Eq. (2-38) must approach infinity for an accurate solution, but in practice relatively few elements of the series are sufficient to achieve solutions of reasonable accuracy.

Equations (2-37) and (2-38) are identical to the equations defining the integrated plume concentration $\chi(x, y, z)$, Eqs. (2-1) and (2-2), with a different interpretation of the release rate term r.

The Gaussian plume Eq. (2-37) is a solution to a steady-state system, defining concentrations everywhere in the domain. For any downwind location x, the integral over a semi-infinite plane perpendicular to the downwind x direction (i.e., plane extending from −∞ to ∞ along the lateral y direction and from 0 to H along the vertical z direction) of $u\,c(x, y, z)$ equals the total release rate, r, at the source. In other words, at steady state the total release rate over any plane perpendicular to the downwind direction x is the constant r. In practice, it may take a long time for such steady-state solution to be experimentally achieved, and extensive amounts of the contaminant substance to be inserted to the system.

MACCS uses the concept of “plume segment.” A plume segment encloses a finite amount of mass or activity, and it is released over a limited time. The plume segment moves along the downstream direction according to the windspeed, dispersing only in the lateral and vertical directions. At any point (x, y, z) of the semi-infinite domain, the concentration is assumed to be at the steady state as soon as the plume arrives to such location. This steady-state

concentration is an overestimate of a concentration that would be computed with a transient solution because concentrations build up from 0 to the steady-state value, and it is an appropriate approximation for the decision-making purposes of MACCS (i.e., the steady-state concentration is a conservative concentration).

The MACCS plume segment concentration can be easily integrated over time by direct multiplication by the plume duration. In that case, the release rate r in Eq. (2-37) with units of activity/s is simply replaced by the total release Q with units of activity, and an equation identical to Eq. (2-1) is recovered:

$$\chi(x,y,z) = \frac{Q}{u}\frac{1}{\sqrt{2\,\pi}\,\sigma_y(x)}\; e^{-\frac{1}{2}\frac{y^2}{\sigma_y(x)^2}}\,\psi(x,z) \tag{2-39}$$

with χ being an integrated concentration with units of activity-s/m^3.

The coefficients $\sigma_y(x)$ and $\sigma_z(x)$ are consistently referred to in this report as Gaussian dispersion coefficients, which should not be confused with the dispersion coefficients D_y, D_z, or the dispersivities α_y, α_z. Dispersion coefficients (D) and dispersivities (α) correspond to general concepts for mass balance equations, while the Gaussian dispersion coefficients (σ) are intended to be used exclusively with the normal distribution functions of Eq. (2-39) or Eq. (2-35) and related variants.

Although Eq. (2-32) defines the Gaussian dispersion coefficients as proportional to $x^{1/2}$ for the case of constant dispersivity, seminal works by Pasquill (Pasquill, 1961), Gifford (Gifford, 1961), and Turner (Turner, 1970) define those coefficients as empirical functions of the downstream distance x. Alternative functions have been proposed to define the empirical Gaussian dispersion coefficients σ as functions of x, such as power law functions with parameters as in Table 2-5 of the MACCS Theory Manual (Nosek & Bixler, 2021) or lookup tables used in the MACCS Nearfield Report (Clayton, 2021), both alternatives aimed at computing concentrations consistent with empirical data.

If the Gaussian dispersion coefficients are defined as arbitrary functions of the downwind distance, $\sigma_y(x)$ and $\sigma_z(x)$, what is the corresponding mass-balance equation satisfied by the Gaussian functions in Eqs. (2-35) or (2-37)? By direct computation of partial derivatives, the following is the general mass balance equation satisfied by the Gaussian functions with arbitrary definitions of $\sigma_y(x)$ and $\sigma_z(x)$:

$$\frac{1}{2}\frac{d}{dx}\left[\sigma_y(x)^2\right]\partial_{yy}c + \frac{1}{2}\frac{d}{dx}\left[\sigma_z(x)^2\right]\partial_{zz}c - \partial_x\, c = 0 \tag{2-40}$$

By comparing Eq. (2-41) to Eq. (2-29), arbitrary dispersivities $\alpha_y(x)$ and $\alpha_z(x)$ associated with arbirtrary functions $\sigma_y(x)$ and $\sigma_z(x)$ are defined as

$$\alpha_y(x) = \tfrac{1}{2}\tfrac{d}{dx}\left[\sigma_y(x)^2\right] \text{ and } \alpha_z(x) = \tfrac{1}{2}\tfrac{d}{dx}\left[\sigma_z(x)^2\right] \tag{2-41}$$

If $\alpha_y(x)$ and $\alpha_z(x)$ are constant, the definition in Eq. (2-32) is recovered aside from integration constants. Therefore, Gaussian functions modified with empirical corrections $\sigma_y(x)$ and $\sigma_z(x)$ are also solutions of the steady-state advection-dispersion mass balance equation, with dispersivities defined as in Eq. (2-41) under the assumption of constant windspeed. A visualization of Gaussian dispersion coefficients based on lookup tables of the MACCS

Nearfield Report (Clayton, 2021) and the derived dispersivities are presented in Figure 2-14. The lateral dispersivity is a power law of the downwind distance in Figure 2-14, but the vertical dispersivity can be a non-monotonic function, depending on the atmospheric stability class. Dispersion coefficients, D_y and D_z, or dispersivities α_y and α_z appear in mass balance equations and are possibly more directly connected to parameters of CFD models than the empirical Gaussian dispersion coefficients σ. However, the non-trivial trends in Figure 2-14, especially in the vertical dispersivity, suggest difficulties in direct connection to CFD model concepts. In the next section and the Test Results section, basic concepts of CFD models are presented and the possibility of reproducing outputs of Gaussian plume dispersion models with CFD models is examined.

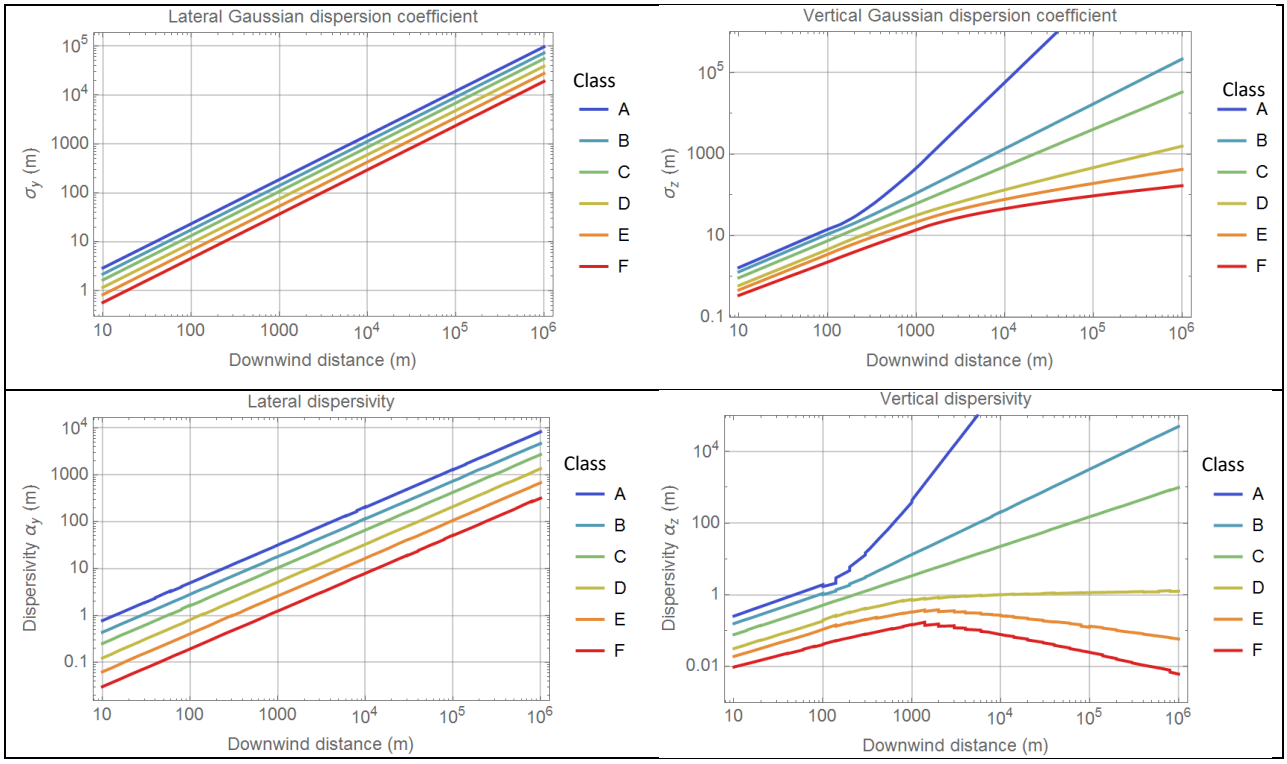

Figure 2-14. Gaussian dispersion coefficients (top plots) and derived dispersivities (bottom plots) based on Eq. (2-41). Wiggles in the bottom plots are artefacts of numerical derivatives.

Computational Fluid Dynamics Model Concepts

The main goal of computational fluid dynamics (CFD) modeling is describing the motion of fluids. The motion of fluids is solved based on solution of the Navier-Stokes equations for the conservation of mass and momentum. It is also common to consider equations of state and to solve the conservation of energy equation to fully characterize the flow. The equations account for fluid pressures, viscous forces, friction, and gravity. The equations are commonly simplified as an average form, with alternative models to account for turbulence in the fluid. Turbulence can be introduced into the model as a boundary condition or be generated from the interaction of the fluid with walls of a domain. CFD models output pressure distributions, temperature distributions, and lines of flow, among other outputs.

With respect to particle dispersion, when the particles have low inertia, CFD models commonly implement a one-way coupling approach, in which the lines of flow are first established by the

approximated solution of the Navier Stokes equations, and then individual particles are launched and allowed to travel in the fluid. Particle concentrations are established from statistics of thousands and thousands of particles individually tracked. Particles move in the lines of flow and are subject to forces with respect to a Lagrangian frame of reference moving with the fluid. The particles have mass and shape and are subject to forces such as drag, gravity, and buoyancy. The physical processes involved in particle tracking in a CFD model are much more complex than in the advection-dispersion mass balance equation, Eq. (2-27). Particles can disperse vertically for example due to the action of gravity, buoyancy, and turbulence, and laterally due to turbulence. In the absence of turbulence (e.g., away from walls), and ignoring gravity and buoyancy, particles would move coherently with the lines of flow. This differs from the advection-dispersion equation, which predicts dispersion in uniform flow fields. The dispersion coefficients of the advection-dispersion mass-balance equation implicitly account for fluctuations in the flow fields. As previously stated, the dispersion coefficient must be empirically determined.

In the following sections, results are presented comparing the Gaussian plume and CFD outputs.

2.6.1 Test Input

For the MACCS simulations, a similar input to Test 2.1 was adopted, with the following changes

General Properties

- TRANSPORT
  - Lookup Tables

ATMOS

- Spatial Grid
  - NUMCOR = 16: number of circumferential sectors
  - NUMRAD = 34: discretization number along the radial direction
  - SPAEND (km): end radius of each ring grid
    - 0.1, 0.2, 0.3, 0.4, 0.5, 0.6, 0.7, 0.8, 0.9, 1.0, 1.1, 1.539, 2.657, 4.096, 5.854, 7.932, 10.33, 13.05, 16.08, 19.44, 23.12, 27.11, 31.43, 36.06, 41.02, 46.29, 51.89, 57.8, 64.04, 70.59, 77.46, 84.66, 92.17, 100.0
- Radionuclides
  - CORINV = 1 Bq for Cs-137, 0 for other radionuclides
- Dispersion
  - Dispersion Table
    - Lookup table for σ_y and σ_z following the parameterization of (Eimutis & Konicek, 1972), and extracted from the Appendix D input files in (Clayton, 2021)
  - Scaling Factors
    - YSCALE = 1
    - ZSCALE = 1
- Release Description
  - Plume Parameters
    - One plume segment
    - PDELAY (s) = 18000 s (=24 hours)

        - PLHITE (m) = 0: release height, ground release
        - REFTIM (-) = 0.5: midpoint grid
        - PLUDUR (s) = 18000 s (=24 hours)
    - Building Height Data
        - BUILDH (m) = 40
    - Initial Area Source
        - SIGYINIT (m) = SIGZINIT (m) = 0.1
- Deposition
    - Wet / Dry Deposition Flags
        - DRYDEP = FALSE for Cs
- Weather
    - Constant or Boundary Conditions
        - BNDMXH (m) = 1000 (mixing layer height)
        - IBDSTB (-) = 1 to 6: stability class A to F
        - BNDRAN (mm/hr) = 0: rain rate
        - BNDWND (m/s) = 2: windspeed

Output Controls

Same outputs as Test 2.1 were used, with the following additional outputs:

- Type 0 (NUM0) ATMOS Outputs
    - INDREL = 1 (plume segment)
    - INRAD = 1, 2, 3, …, 34 (all radial segments)
    - NUCOUT = Cs-137: radionuclide output by NUM0
- Type D (NUMD) Average Sector Concentrations
    - I1DISD = 34 (outer radial interval)
    - NUCLIDE = Cs-137
    - ELEVCONC (Bq/m^2) = 0 (threshold value, all sectors are reported when 0)
    - PRINT_FLAG_D = True
    - Report Options = REPORT
- Type 6 (NUM6) Centerline Dose
    - ORGNAM = L-ICRP60ED; PATHNM = INH LIF: inhalation lifetime; I1DIS6=1, I2DIS6=34: all radial segments; Report Options = NONE
    - ORGNAM = L-ICRP60ED; PATHNM = CLD: cloudshine dose; I1DIS6=1, I2DIS6=34: all radial segments; Report Options = NONE
- Type A (NUMA) Peak Dose in a Grid Ring
    - NAME = L-ICRP60E; I1DISA=1, I2DISA=34: all radial ring segments; Report Options = NONE
- Type C (NUMC) Land Area Exceeding Dose
    - ORGNAM = L-ICRP60ED; ELEVDOSE (Sv) = 0: outputs all grid elements with dose > 0 Sv; PRINT_FLAG_C = True; Report Options = NONE

Ansys CFX

The code Ansys CFX was selected for the CFD simulations. Ansys CFX is a tool used predominantly for turbomachinery applications. It includes modules for turbulence modeling, including the Generalized κ-ω model, with adjustable parameters to simulate different flow regimes, and modules for multi-phase and multi-fluid modeling. The following inputs were selected in the CFD modeling with Ansys CFX:

- Domain dimensions: 1005 m length × 300 m height × 800 m width (Figure 2-15)

- Windspeed: 2 m/s uniform air velocity at the inlet face of the domain box, atmospheric pressure at the outlet face of the domain box (Figure 2-15)
- Turbulence model: laminar and shear stress transport (SST) with high-intensity turbulence (20%)
- Source: located 100 m away the from the box domain inlet face, on the ground
- Particle emission rate: 1 kg/s, the contaminant substance is injected from a circular hole on the ground in the form of a vertical jet of slow vertical velocity
- The contaminant substance was modeled equivalent to air (i.e., same density as ambient air) to minimize or avoid settlement and deposition.

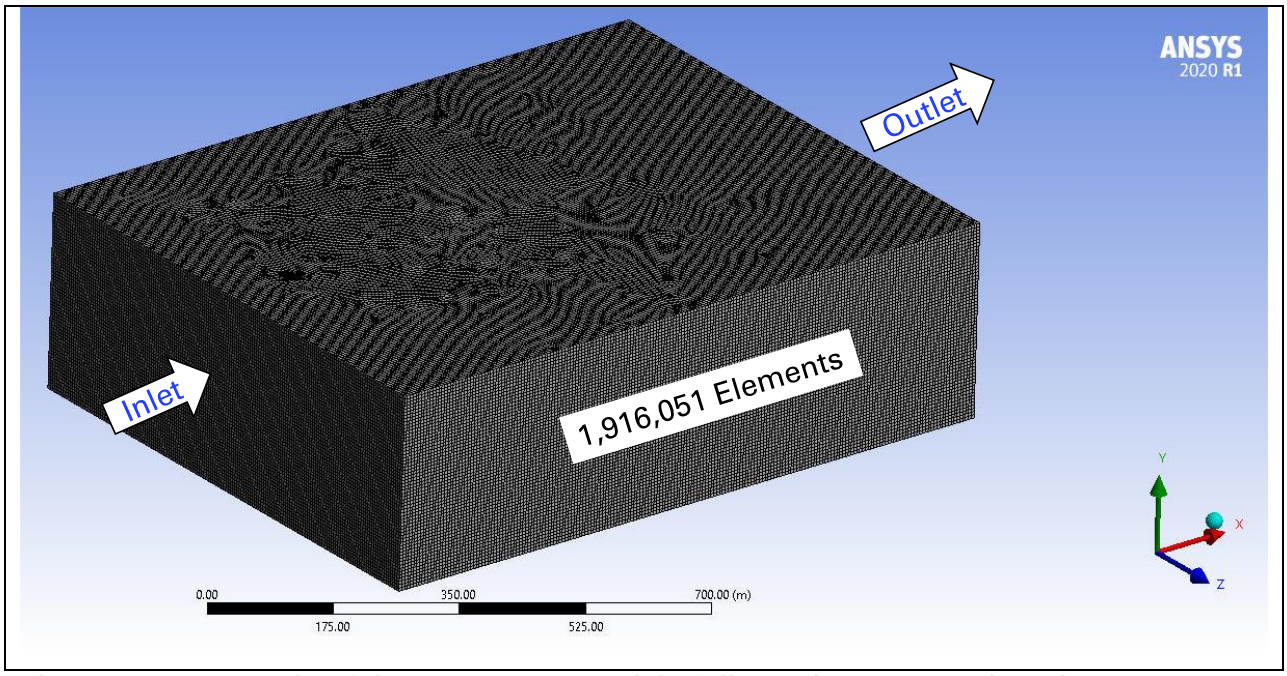

Figure 2-15. Domain of the Ansys CFX model of dimensions 1005 m length × 300 m height × 800 m width. A constant windspeed, 2 m/s, was imposed at the inlet face and atmospheric pressure was imposed at the outlet face.

2.6.2 Test Procedure

Several options were investigated to simulate dispersion of particles using Ansys CFX. Simulations tracking individual particles of given densities and dimensions caused deposition of particles on the ground due to the consideration of gravity, a deposition process that is not explicitly accounted for in the basic Gaussian plume model associated with Eq. (2-39). For that reason, it was decided to simulate a source as a jet of a gas (of the same density as air) initially moving vertically and mixing with air moving at the defined horizontal windspeed, to avoid settlement of particles. The system was modeled as a mixing of two similar fluids, one fluid representing the background air moving with a speed of 2 m/s, and a second fluid representing the contaminant substance injected at a rate of 1 kg/s and dispersing in air. In the steady-state simulations it was verified that the rate at which the contaminant crossed the outlet face of the domain was approximately equal to 1 kg/s (i.e., equal to the source injection rate), so that the substance deposition rate was minimal.

Ansys CFX was executed to solve for a steady-state system, assuming a constant contaminant injection rate r = 1 kg/s. The steady-state concentration $c(x, y, z)$ was normalized by the input

injection rate r, to compute the ratio $c(x, y, z)/r$ which is has the same units and is equivalent to the $\chi(x, y, z)/Q$ ratio (s/m^3 units) output by MACCS.

$\chi(x, y, z)/Q$ concentrations were computed with MACCS using the Type 0 outputs along the centerline. The Eqs. (2-38) and (2-39) were independently programmed using Mathematica 12, to allow computation of integrated concentrations or $\chi(x, y, z)/Q$ ratios at locations other than the centerline. The Mathematica functions included the MACCS correction for virtual source location (i.e., correction to σ_y and σ_z to attain specific values, e.g., 0.1 m, at an initial x=0 location) and an approximation to the term $\psi(x, y)$ to equal 1/H when $\sigma_z(x) > H/0.03$, which is the same efficient approximation implemented in MACCS to avoid many terms of the Eq. (2-38) series. The mixing layer height was H=1000 m in the simulations. Figure 2-16 compares the MACCS Type 0 centerline outputs to the computations using Mathematica, showing that the independent Mathematica functions accurately reproduced the MACCS centerline outputs. Therefore, the Mathematica functions can be reliably used to compute concentrations at arbitrary (x, y, z) locations.

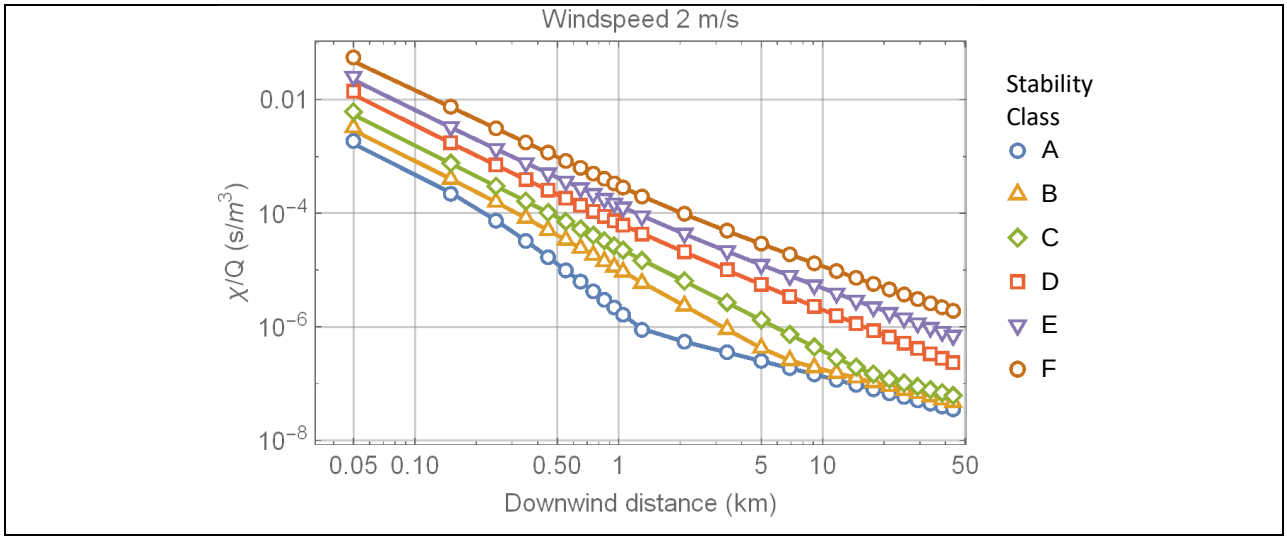

Figure 2-16. Comparison of MACCS Type 0 centerline concentrations (symbols) to independent computations using Mathematica functions and Eqs. (2-38) and (2-39) (solid curves).

2.6.3 Test Results

Figure 2-17 shows a comparison of MACCS χ/Q centerline air concentrations to c/r centerline air concentrations computed with Ansys CFX. The dots are the MACCS Type 0 centerline concentrations of a case with windspeed 2 m/s and wind under atmospheric stability class F (highest stability class, lowest extent of dispersion). Two alternative CFD simulations were considered. In the first simulation (blue curve) it was assumed that the incoming jet of contaminants had density equivalent to air (so that the particulates would remain airborne) and airflow lines were laminar (no turbulence case). In the second simulation (yellow curve), it was assumed that the air at the inlet face of the domain box was of high turbulence (turbulence intensity 20%). Both CFD simulations predict sudden decrease in the concentration and flatter concentration gradients than the MACCS Gaussian plume outputs. The air concentration of the high turbulence case is lower than the air concentration of the laminar case (because contaminants mix faster in the vertical direction in the high turbulence case) and attains a plateau at approximately 500 m. At that point, the plume does not laterally disperse at greater downwind distances (i.e., the plume travels coherently with the laminar lines of airflow).

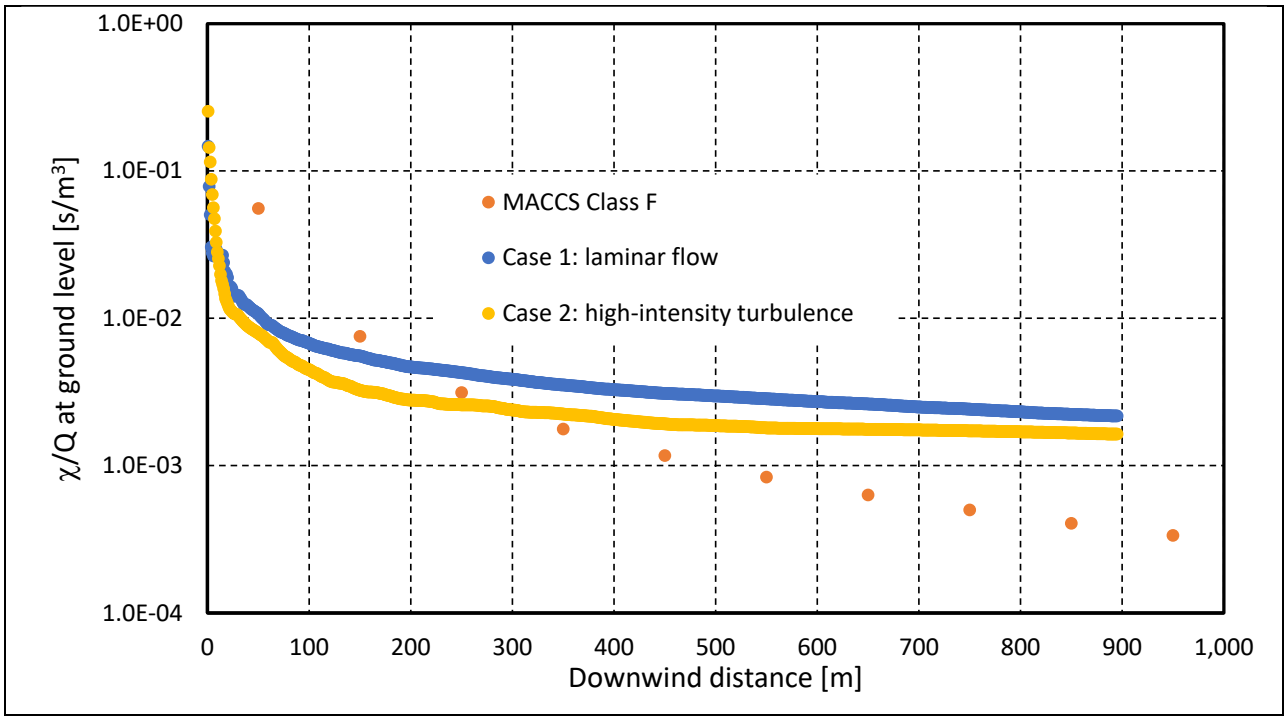

Figure 2-17. Comparison of MACCS Type 0 centerline concentrations for stability class F simulation (dots) to Ansys CFX outputs considering two alternative cases (solid curves). The Case 1 (blue curve) is for a laminar airflow case, and the Case 2 (yellow curve) corresponds to a high-intensity turbulence case.

Figure 2-18 displays contour plots of the ratio c/r for the two CFD cases examined. In the Case 2 (high-intensity turbulence case) the contours of the highest concentrations become parallel lines at around 500 m from the source, at the same point at which the c/r versus x distance reaches a plateau in Figure 2-17. At further downwind distances, the contours remain parallel indicating that the plume does not laterally disperse. The contaminant plume is trapped in the uniform wind, and it travels coherently with the wind without further lateral dispersion. The Case 1 (laminar airflow case) exhibits increasing lateral dispersion with downwind x distance in the top contour plot of Figure 2-18. The corresponding centerline concentration versus distance (blue curve) in Figure 2-17 exhibits a flattening gradient tending towards a plateau. Therefore, the slowly expanding contours in the top plot of Figure 2-18 are expected to also become parallel lines at increasing downwind distances, similar to the parallel contours in the bottom plot of Figure 2-18. The parallel concentration contours and constant width plume at far downwind distances in a uniform airflow field is a feature of CFD models in open domains. Absent irregularities in the spatial model domain (such as roughness on the ground and obstacles), there is no source for turbulence, which is the only mechanism that can cause lateral dispersion of a plume. In other words, under a uniform airflow field, in a smooth and regular domain (such as the box in Figure 2-15), at downwind distances after turbulence eddies have subsided, a plume becomes constant width (i.e., exhibits no further lateral dispersion).

Case 1 laminar airflow

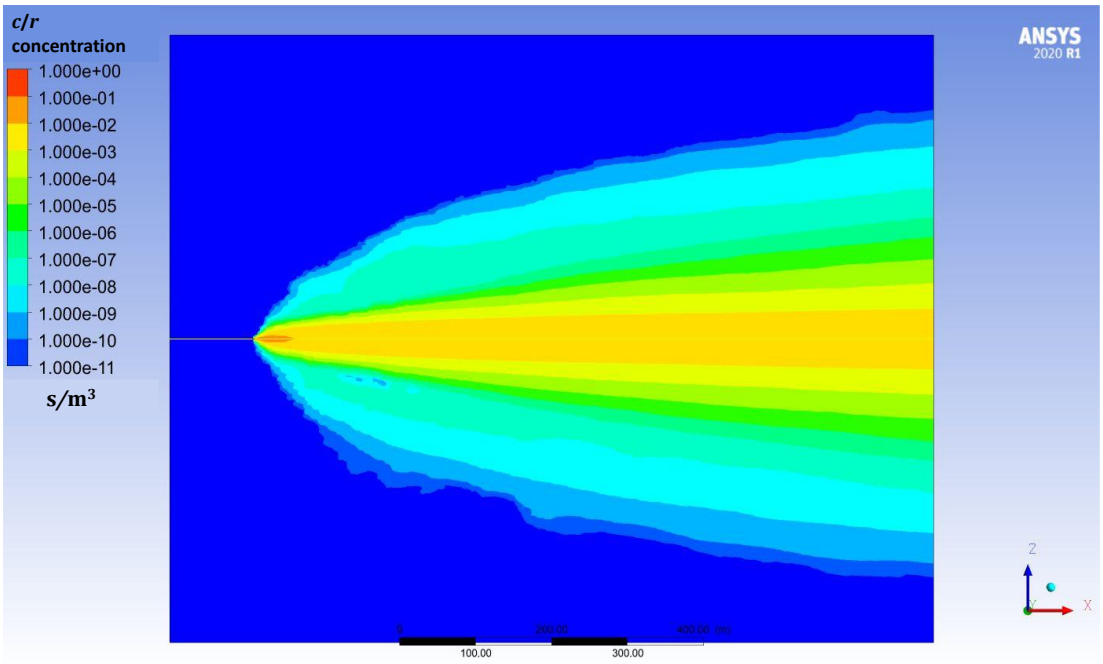

Case 2 high-intensity turbulence

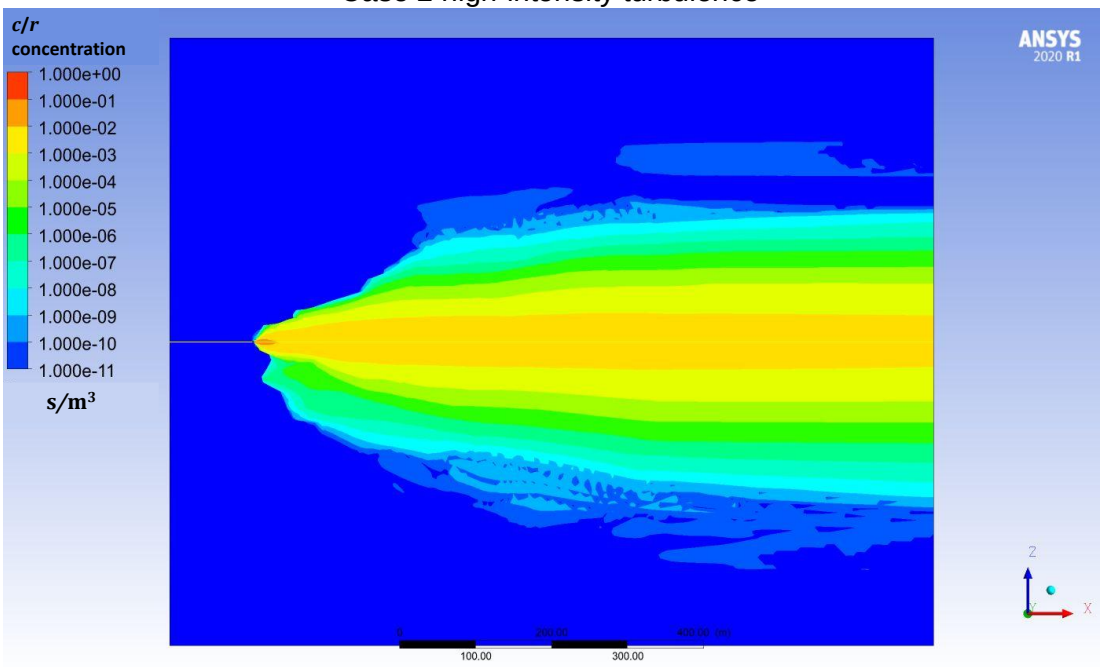

Figure 2-18. Contour plots of the *c/r* ratios for Case 1, laminar airflow, and Case 2, high-intensity turbulence.

Multiple alternative simulations were examined using CFD and in all cases, the centerline concentrations exhibited flatter gradients than the MACCS outputs; the concentrations were lower than MACCS outputs close to the source and higher than the MACCS outputs at distant locations from the source. CFD concentrations tended to plateau.

The observation that CFD simulations tend to produce less dispersion than Gaussian plume models is consistent with other studies. For example, Demael and Carissimo highlighted difficulties of simulating the extent of lateral dispersion of Gaussian plume dispersion models (which empirical Gaussian dispersion coefficients) with a Eulerian CFD code, especially in open and flat terrains (Demael & Carissimo, 2008). The CFD models require turbulence to drive lateral dispersion, and turbulence tends to subside and dissipate in flat model domains. A relatively recent study was aimed at reconciling Gaussian plume modeling with CFD models of particle dispersion (Joseph, Hargreaves, & Lowndes, 2020). Joseph, Hargreaves, and Lowndes noted that CFD particle tracking models underestimate lateral dispersion compared to Gaussian plume models. They attempted to reconcile the models by implicitly incorporating variability in the direction of the wind. These authors combined independent CFD runs with blowing wind at different angles, θ with respect to the x direction, by computing average results from the multiple runs assuming that the angle θ follows a normal distribution with zero mean, and a standard deviation computed as a function of the windspeed. The standard deviation of the angle θ could be significant for cases of low windspeed, which would implicitly simulate plume meander. Joseph, Hargreaves, and Lowndes had to also modify a time scale parameter of the k-ε turbulence model to increase the agreement of the CFD and Gaussian plume model (the focus of the analysis was on particle accretion rates). Although the work by Joseph, Hargreaves, and Lowndes (2020) appears to reconcile CFD and Gaussian plume models, such is only accomplished by the introduction of additional empirical and model fitting corrections (such as the standard deviation of the wind direction angle θ), and therefore it is unclear how those corrected/adjusted/fitted CFD models fundamentally improve the empirical Gaussian plume dispersion model. In summary, CFD models of flat domains yield less lateral dispersion than Gaussian plume models. Lateral dispersion arises from turbulence patterns, and turbulence becomes weak and dissipates in flat domains. To recover the lateral dispersion, some authors have introduced lateral variation of the wind direction as a post-processing step to combine results of multiple independent (single wind direction) CFD simulations. The post-processing strategy includes a level of fitting which could be regarded equivalent to Gaussian dispersion coefficients empirically determined. CFD is better fitted to model dispersion when the geometry of the domain (e.g., sets of buildings) drives the airflow patterns, but not to model dispersion in open and flat terrains.

Figure 2-19 displays contour plots of the χ/Q integrated air concentration at the ground level, computed using the MACCS Gaussian plume functions programmed in Mathematica, which contours qualitatively differ from contours in Figure 2-18 computed using CFD simulations. The three plots correspond to three atmospheric stability class states. Class A is the lowest stability, showing greatest dispersion in the form of fat ovals. Class F is the highest stability, showing the least dispersion in the form of very narrow ovals. This is the case with the most constrained lateral dispersion of the cases displayed in Figure 2-19. Even in the stability class F, the plume continuously laterally widens with downwind distance (note that σ_y and σ_z increase with downwind distance in the top plots of Figure 2-14), which is the trend consistent with empirical data, but different from the CFD simulations. Such plume widening in the Gaussian model most likely arises from variation in the magnitude and direction of the wind, combined and aggregated effect of irregularities on the ground, and thermal effects.

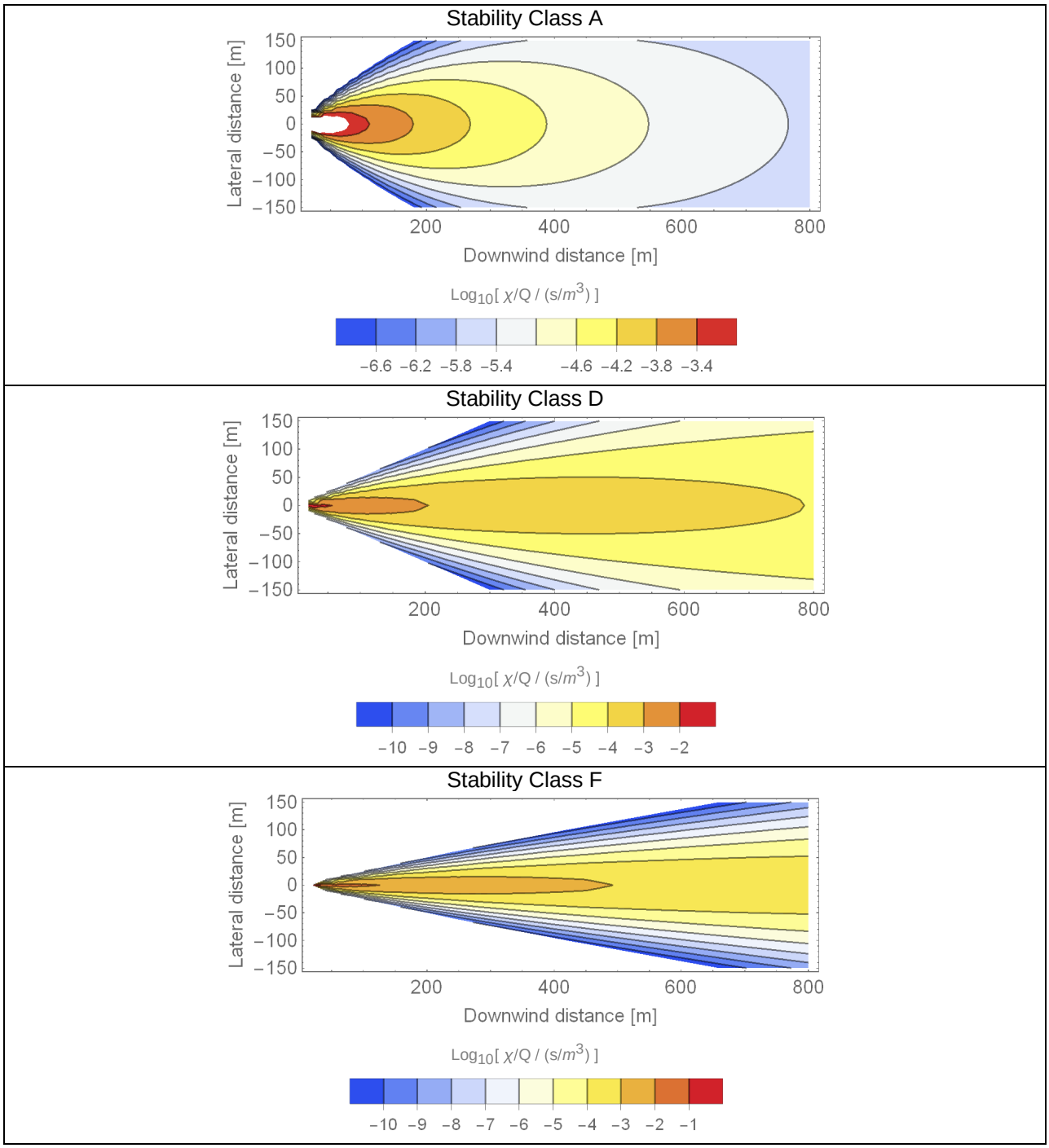

Figure 2-19. Contour plots of χ/Q concentrations computed with Mathematica reproducing the MACCS Gaussian plume equations, for three atmospheric stability classes.

2.6.4 Test Conclusions

This was a special test, aimed at examining difficulties of reconciling Gaussian plume models with CFD models. Ansys CFX was used to execute CFD simulations considering a simple domain and a source injecting airborne contaminants in air at a constant rate at the ground level. Steady-state simulations were considered based on the fact that the Gaussian plume concentration functions are steady-state solutions to the advection/dispersion mass balance differential equation. In all the CFD simulations examined (of which only two are reported in this test), concentration versus downwind distance always exhibited flatter trends that the outputs of the Gaussian plume function of MACCS and its ATMOS module. This finding is consistent with studies in the literature (Demael & Carissimo, 2008; Joseph, Hargreaves, & Lowndes, 2020). Specific studies have managed to reconcile to some extent CFD models with Gaussian plume models but only after the adoption of empirical corrections (Joseph, Hargreaves, & Lowndes, 2020). Care should be exercised in using CFD to simulate contaminant plume dispersion in open and flat domains. In those simple domains, CFD models predict propagation of a plume of constant width moving coherently with the wind, after turbulence has subsided and dissipated, which is inconsistent with the empirical observation of plumes widening with downwind distance. CFD may be better suited to model contaminant dispersion if the airflow is controlled by the geometry of the domain, such as contaminant dispersion in a city with buildings. CFD may be used to examine relative effects, such as redistribution of contaminants due to the presence of a building or a set of buildings, compared to cases where those buildings are not present. For open and flat domains, the empirical Gaussian plume models are adequate, given their empirical basis and consistency with experiments.

2.7 Test 2.7: Plume Rise

The test was aimed at examining the implementation of the improved plume rise equations described in Section 2.4.2 of the MACCS Theory Manual (Nosek & Bixler, 2021). The MACCS plume rise model accounts for buoyancy of hot gases less dense than the surrounding air, causing the plume centerline to rise above the initial release height up to a plateau at a downwind distance. Accounting for plume rise causes lower air concentrations at the ground level compared to scenarios without plume rise.

2.7.1 Test Input

The input was similar to inputs of Test 2.6, with the following changes

General Properties

- TRANSPORT
  - Lookup Tables
- PLUME
  - Plume Source: Area Source
  - Plume Rise: Power Model (buoyancy flux equal to 8.79×10^{-6} PLHEAT)
  - Plume Trapping/Downwash: Briggs (buoyancy flux)

ATMOS

- Radionuclides
  - CORINV = 1 Bq for Cs-137, 0 for other radionuclides
- Dispersion
  - Dispersion Table
    - Lookup table for σ_y and σ_z following the parameterization of (Eimutis & Konicek, 1972), and extracted from the Appendix D input files in (Clayton, 2021)
- Plume Specifications
  - Plume Rise Scale Factor
    - SCLCRW = 1E6: large scale factor on the critical windspeed selected to force plume rise (plume rise occurs when the windspeed is less than a critical speed, which is a function of the buoyancy flux)
    - SCLADP = 1 scaling factor on plume rise for classes A through D
    - SCLEFP = 1 scaling factor on plume rise for classes E and F
- Release Description
  - Plume Parameters
    - One plume segment
    - PDELAY (s) = 0 s: plume segment release delay
    - PLHITE (m) = 50: release source height
    - REFTIM (-) = 0.5: midpoint grid
    - PLUDUR (s) = 18000 s (=24 hours)
  - Building Height Data
    - BUILDH (m) = 50
  - Initial Area Source
    - SIGYINIT (m) = SIGZINIT (m) = 0.1

    - Heat
        - PLHEAT (W) = 1E6, 1E7, 1E8: sensible heat release rate
- Deposition
    - Wet / Dry Deposition Flags
        - DRYDEP = FALSE for Cs
- Weather
    - Constant or Boundary Conditions
        - BNDMXH (m) = 1000 (mixing layer height)
        - IBDSTB (-) = 1 to 6: stability class A to F
        - BNDRAN (mm/hr) = 0: rain rate
        - BNDWND (m/s) = 0.5: windspeed

Output Controls

The same outputs of Test 2.6 were selected for this test.

2.7.2 Test Procedure

The improved plume rise equations described in Section 2.4.2 of the MACCS Theory Manual (Nosek & Bixler, 2021) were programmed in Mathematica, including functions for final relative plume rise (Δh_f), windspeed as a function of height (u), average windspeed between the initial and final heights ($\bar{u}$), buoyancy heat flux (F), and relative plume rise (Δh) as a function of the downwind distance, the buoyancy heat flux, and the average windspeed. The plume centerline height as a function of the downwind distance was compared to Type 0 MACCS outputs indicated by the label "Plume Height (m)" in the file Model1.out. In addition, the Cs-137 χ/Q air concentration on the plume centerline and at the ground level were computed using Eqs. (2-1) and (2-2), using an approximated term $\psi(x,z)$ (= 1/H when $\sigma_z(x) > H/0.03$) as described in Test 2.6 Section 2.6.2, and in Eq. (3-23). The independently computed air concentrations were compared to Type 0 outputs in Model1.out labeled as "Cs-137 Center Air Conc. (Bq-s/m3)" and "Cs-137 Ground Air Conc. (Bq-s/m3)." Multiple MACCS runs were executed varying PLHEAT (=10^6, 10^7 and 10^8 watts) and the atmospheric stability class (from A to F), and MACCS outputs of the ATMOS module were compared to computations of the plume height and integrated air concentrations.

2.7.3 Test Results

Figure 2-20 compares independently computed plume height versus downwind distance (solid curves) to MACCS outputs (symbols) for 3 cases of the sensible heat release rate (PLHEAT = 10^6, 10^7 and 10^8 watts). The trends are consistent; however, there are differences between the MACCS outputs and the independent computations, potentially due to roundup error or differences in programmed equations with respect to descriptions in the MACCS documentation. The equations in Mathematica were carefully checked against descriptions in Section 2.4.2 of the MACCS Theory Manual (Nosek & Bixler, 2021). Figure 2-21 displays the integrated χ/Q centerline air concentration versus distance. The independent computations closely matched the MACCS centerline air concentrations, despite differences in the plume height in Figure 2-20. Figure 2-22 compares the integrated χ/Q air concentration at the ground level, showing minor differences between MACCS outputs and independent computations, entirely due to the differences in the plume height (Figure 2-20).

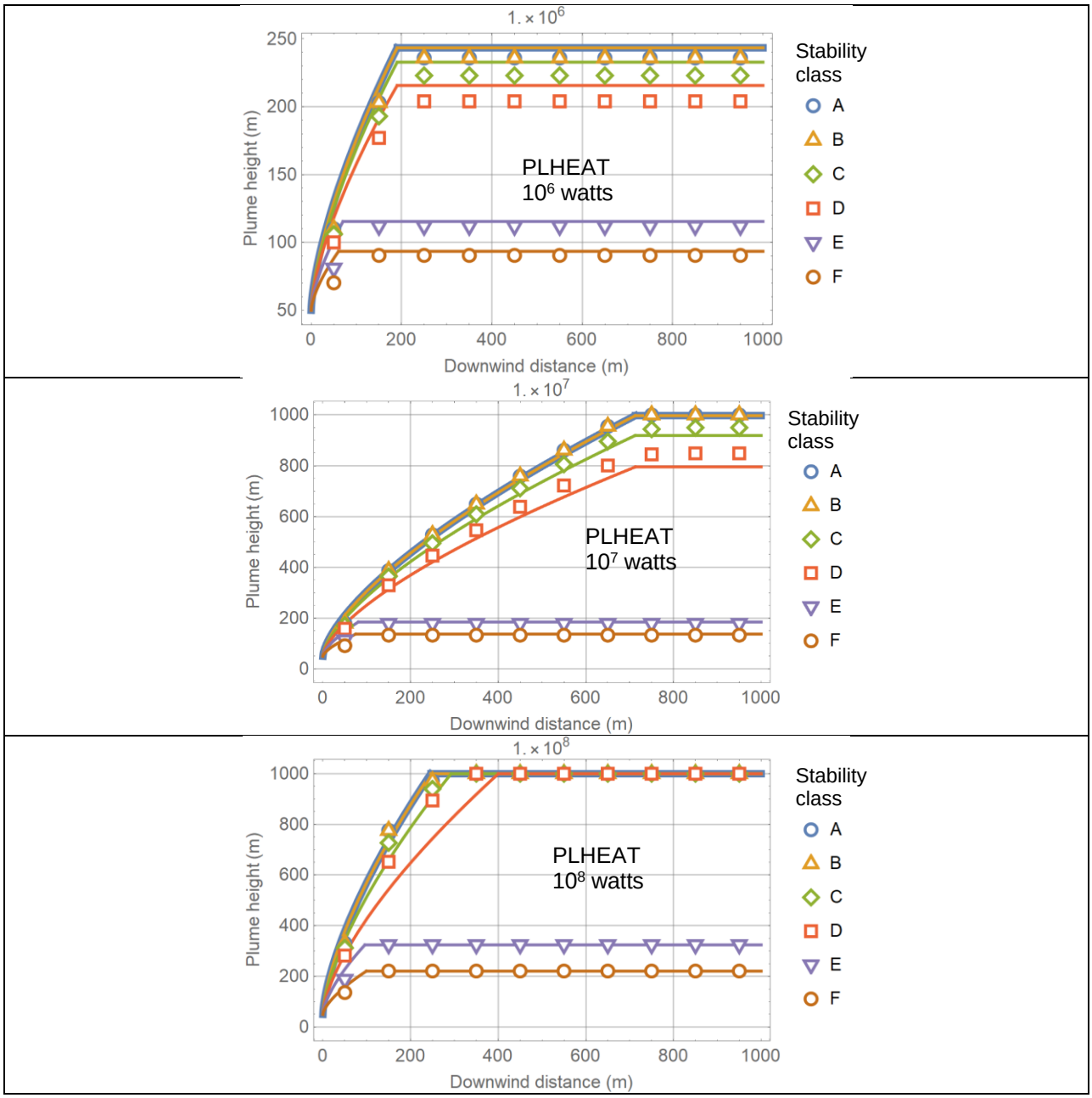

Figure 2-20. Plume height versus downwind distance for 3 cases of sensible heat release rate (PLHEAT). MACCS outputs are presented in symbols and the solid curves represent the independent computations.

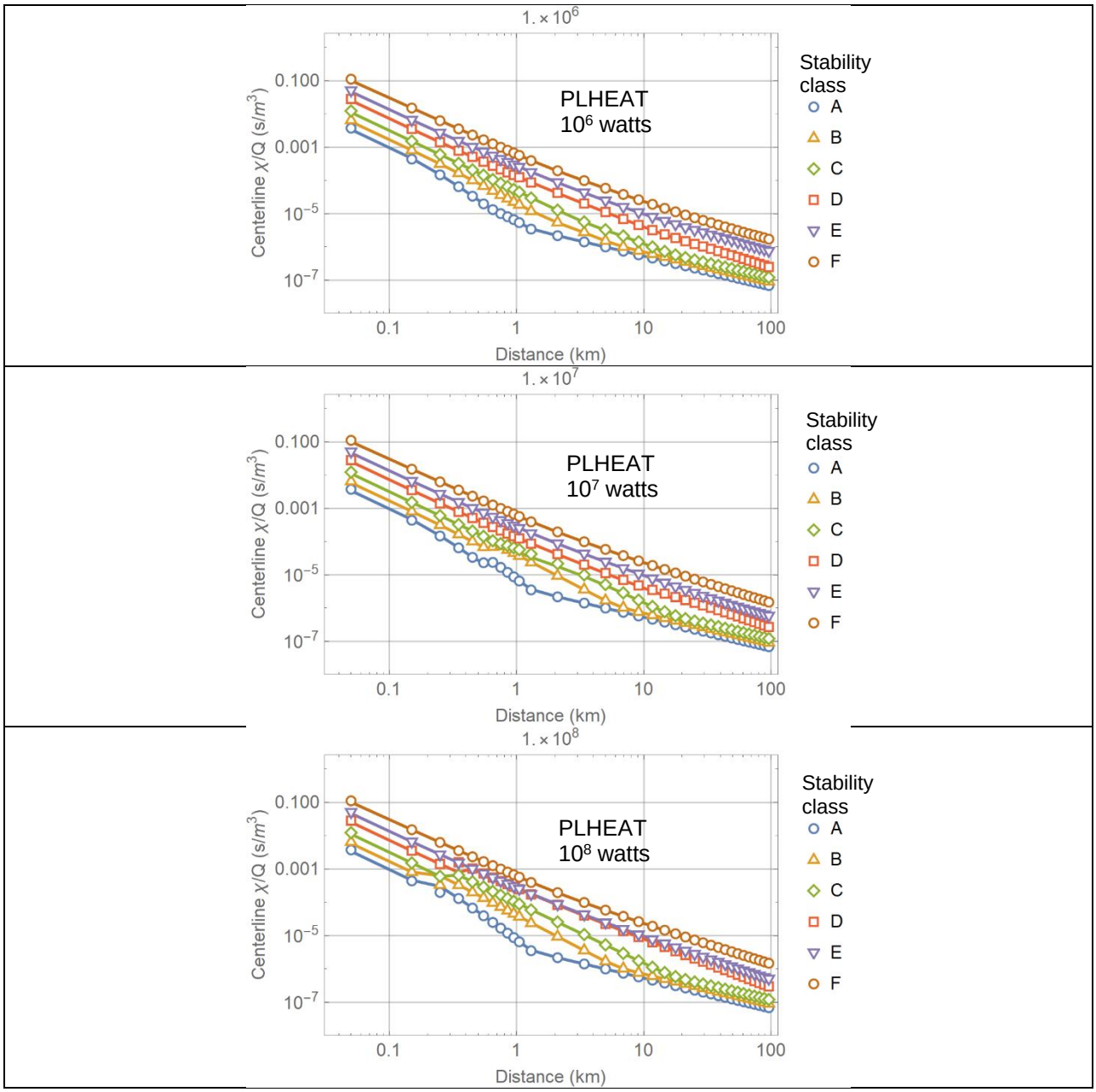

Figure 2-21. Integrated χ/Q centerline air concentration versus distance for 3 cases of sensible heat release rate (PLHEAT). MACCS outputs are presented in symbols and the solid curves represent the independent computations.

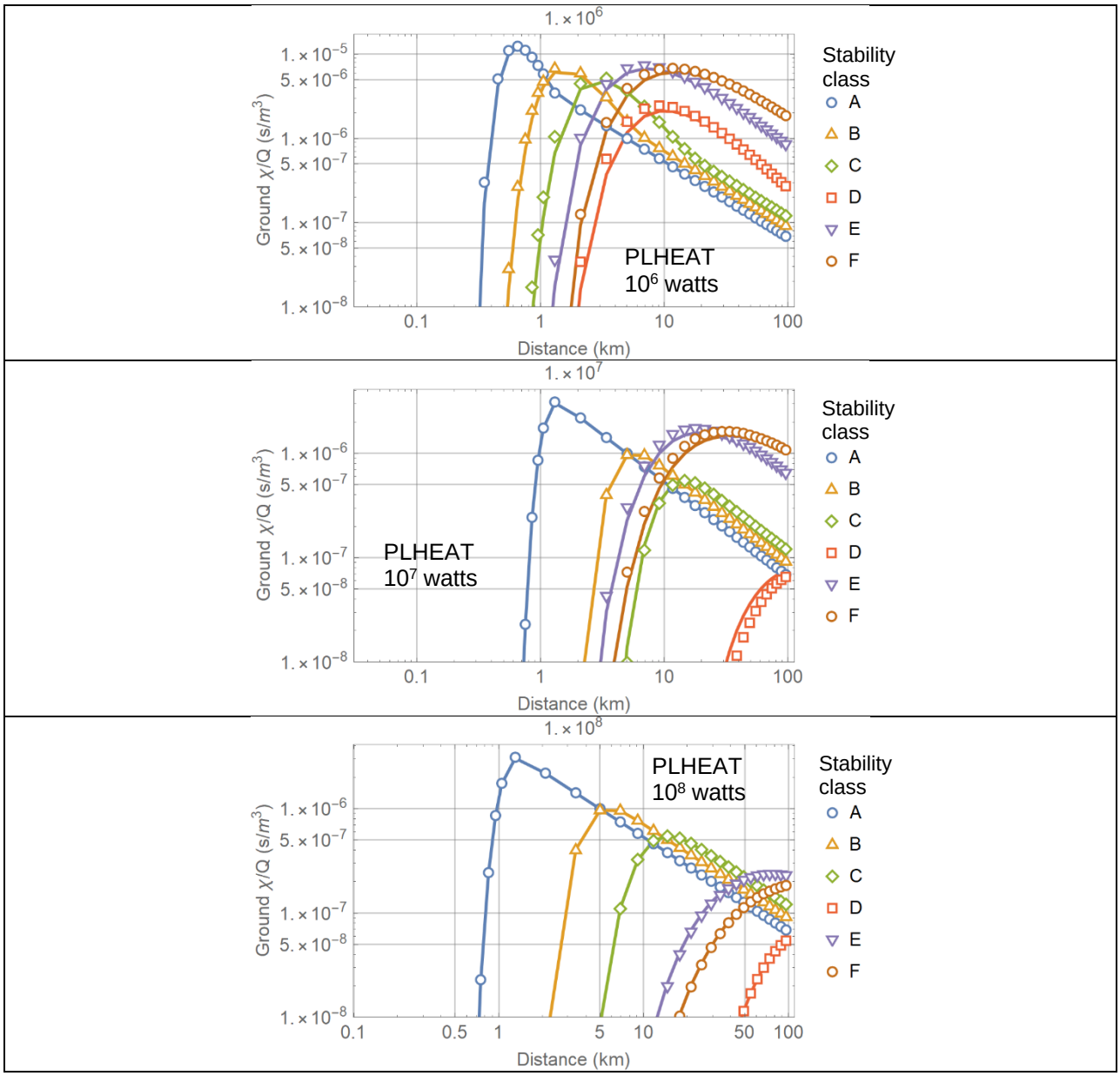

Figure 2-22. Integrated χ/Q air concentration at the ground level versus distance for 3 cases of sensible heat release rate (PLHEAT). MACCS outputs are presented in symbols and the solid curves represent the independent computations.

2.7.4 Test Conclusions

Independent computations approximately verified the MACCS implementation of the improved plume rise equations, as described in Section 2.4.2 of the MACCS Theory Manual (Nosek & Bixler, 2021). However, differences were noted between the MACCS plume height outputs and independent computations, potentially due to roundup error in the MACCS computations or slight variation in programmed equations with respect to descriptions in the MACCS documentation. In the analyzed examples, errors in the plume height do not propagate as significant errors in the integrated air concentrations. Nonetheless, it is recommended that MACCS software developers examine whether programmed equations to compute the plume height are perfectly consistent with the MACCS documentation.

3 EARLY MODULE

3.1 Test 3.1: Groundshine, Inhalation, Cloudshine, and Skin Dose

The objective of the test was to verify equations to compute individual doses from concentrations and given dose rate coefficients for simple cases. The simple case considered is summarized in the following bullets:

- One radionuclide, Cs-137
- One long-lasting plume segment, without plume rise
- Simple weather pattern: constant windspeed (10 m/s), north direction
- One cohort, non-evacuating and non-relocating

The groundshine, inhalation, cloudshine, and skin dose equations that were examined in the test are presented in the following paragraphs.

Groundshine dose (equation 3-10 of the MACCS Theory Manual):

$$GDR_k = \left(\sum_i DRCG_{ik}\ GC_i\ T_i \right) J\ SFG \tag{3-1}$$

GDR_k	—	sector average groundshine dose rate to organ k (Sv)
$DRCG_{ik}$	—	groundshine dose rate coefficient to organ k by radionuclide i (Sv-m^2/Bq-s)
GC_i	—	ground concentration along the plume centerline (Bq/m^2)
T_i	—	effective exposure time (s)
J	—	off-centerline factor to compute the sector average from the centerline dose
SFG	—	Groundshine shielding factor, specified by GSHFAC (=0 or 1 in the test runs)

The effective exposure time T_i accounts for linear buildup in time while the plume is passing, and radioactive decay while and after the plume passage. For the simple problem examined of a fast-moving plume, non-evacuating and non-relocating cohort, and a long-lived radionuclide, the effective exposure time is approximately equal to the duration of the early phase, specified by ENDEMP (=7 days in the test runs).

Inhalation dose (equation 3-12 of the MACCS Theory Manual):

$$DI_k = \left(\sum_i DCI_{ik}\ \chi_i(x, y = 0, z = 0) \right) BR\ J\ F\ SFI \tag{3-2}$$

DI_k	—	sector average inhalation dose to organ k from passage of a plume (Sv)
DCI_{ik}	—	inhalation dose coefficient to organ k from radionuclide i (Sv/Bq)
$\chi_i(x, y = 0, z = 0)$	—	integrated air concentration of radionuclide i at the ground level, along the plume centerline (Bq-s/m^3), Eq. (2-1) and (2-2)
BR	—	air breathing rate, specified by BRRATE (m^3/s) (BRRATE = 10^{-4} m^3/s in the test runs)

J	—	off-centerline factor to compute the sector average from the centerline dose
F	—	fraction of exposed time (=1 for non-evacuating and non-relocating cohort)
SFI	—	inhalation shielding factor, specified by PROTIN (=0 or 1 in the test runs

Cloudshine dose (equation 3-9 of the MACCS Theory Manual):

$$DC_k = \left[\sum_i DRCC_{\infty ik}\ \chi_i(x, y=0, z=h)\right] C(x,y)\ F\ SFC \tag{3-3}$$

DC_k	—	cloudshine centerline dose to organ k (Sv)
$DRCC_{\infty ik}$	—	semi-infinite cloudshine dose coefficient to organ k by radionuclide i (Sv-m^3/Bq-s)
$\chi_i(x, y=0, z=h)$	—	integrated air concentration of radionuclide i at the center level (y=h), along the plume centerline (Bq-s/m^3), Eq. (2-1) and (2-2)
$C(x,y)$	—	cloudshine factor at the location (x, y), which is a function of the plume height, h, and the dispersion coefficients $\sigma_y(x)$ and $\sigma_z(x)$
F	—	plume exposure time fraction (=1, for non-evacuating and non-relocating individuals)
SFC	—	cloudshine protection factor specified by CSFACT (=0 or 1 in the test runs)

Skin acute dose (derived from equations 3-15 and 3-16 of the MACCS Theory Manual, assuming a slow decay rate):

$$DS = T\ DRCS\ \ V_d\ J\ F\ SFS \sum_i \chi_i(x, y=0, z=0) \tag{3-4}$$

DS	—	sector average acute dose from skin deposition during passage of a plume (Sv)
T	—	exposure time, fixed to 8 hours = 28800 s in MACCS
$DRCS$	—	acute skin dose coefficient from deposition of radioactive contaminants on the skin, fixed to 5.4×10^{-14} Sv-m^2/Bq-s in MACCS, independently of the radionuclide
V_d	—	deposition velocity, fixed to 0.01 m/s in MACCS
J	—	off-centerline factor to compute the sector average from the centerline dose
F	—	fraction of the exposure duration during the plume passage, set to 1 in the test runs (due to no relocation and no evacuation assumptions)
SFS	—	skin shielding factor, specified by SKPFAC (=0 or 1 in the test runs)
$\chi_i(x, y=0, z=0)$	—	integrated air concentration of radionuclide i at the ground level, along the plume centerline (Bq-s/m^3), Eq. (2-1) and (2-2)

The MACCS computation of the air concentrations $\chi_i(x, y=0, z=h)$, $\chi_i(x, y=0, z=0)$, and centerline ground concentration GC_i were verified in the ATMOS module tests in Section 2. The same methods of Section 2 were applied to provide additional verification of concentration computations.

In the tests, doses were independently computed from Type 0 and Type D concentrations and compared to the Type 6 and Type C doses. The Type 0 and Type D concentrations were already verified for central sectors (sectors in the north direction in the tests) in Section 2 tests based on analytical steady-state Gaussian plume concentration equations, and equations to model dry and wet deposition.

3.1.1 Test Input

The input was similar to the Test 2.1 input with the following changes:

- Deposition
  - Wet / Dry Deposition Flags
    - DRYDEP = TRUE for Cs
    - WETDEP = FALSE for Cs
  - Dry Deposition
    - VDEPOS (m/s) = 0.3 m/s for particle group 1, and 0 for other groups
- Release Description
  - Plume Parameters
    - PDELAY (s) = 0 (plume delay)
    - PLUDUR (s) = 86400 s (=24 hours, plume duration)
  - Particle Size Distribution
    - PSDIST=1 for particle group 1, 0 for all other groups

Output Controls

Same outputs Test 2.1 were used, with the following additional outputs:

- Type D (NUMD) Average Sector Concentrations
  - I1DISD = 26 (outer radial interval)
  - NUCLIDE = Cs-137
  - ELEVCONC (Bq/m^2) = 0 (threshold value, all sectors are reported when 0)
  - PRINT_FLAG_D = True
  - Report Options = REPORT

For the skin acute dose tests, additional outputs were generated with the following settings:

- Type 6 (NUM6) Centerline Dose
  - ORGNAM = A-SKIN (acute skin dose)
  - PATHNM = TOT ACU
  - I1D1S6 = 1
  - I2DIS6 = 26
  - Report Options = NONE
- Type A (NUMA) Peak Dose
  - NAME = A-SKIN
  - I1DISA = 1
  - I2DISA = 26
  - Report Options = NONE
- Type C (NUMC) Land Area Exceeding Dose
  - ORGNAM = A-SKIN
  - ELEVDOSE (Sv) = 0
  - PRINT_FLAG_C = True
  - Report Options = NONE

For the groundshine, inhalation, and cloudshine dose tests, the extracted doses from the MACCS output files corresponded to ORGNAM = L-ICRP60ED. For the skin acute dose test, the dose extracted from the MACCS output files corresponded to ORGNAM = A-SKIN.

3.1.2 Test Procedure

Multiple runs of the MACCS code were executed with the following selections of the Gaussian dispersion coefficient factors:

- YSCALE = ZSCALE = 0.1
- YSCALE = ZSCALE = 0.5
- YSCALE = ZSCALE = 1
- YSCALE = ZSCALE = 2

The shielding and exposure factors were set to output groundshine dose only (GSHFAC=1, other shielding factors = 0), inhalation dose only (PROTIN=1, other shielding factors = 0), cloudshine dose only (CSFACT=1, other shielding factors = 0), or skin dose only (SKPFAC=1, other shielding factors = 0).

A total of 16 runs (= 4 dispersion coefficient factors × 4 shielding factor selections) were executed. Different runs with a specific value of the dispersion coefficient factor correspond to cases with identical air and ground concentrations (the only difference of runs with the same dispersion coefficient is the type of dose tracked in the output files). A total of 4 runs for each dispersion coefficient factor were executed to itemize the different pathway doses (groundshine, inhalation, cloudshine, or skin) in the MACCS outputs.

Air and ground concentrations were extracted from the file tbl_outStat.txt and compared to independently computed concentrations using closed-form analytical equations from Section 2. In addition, those concentrations were compared to

- Type 0 concentrations, air and ground concentrations along the centerline
- Type D concentrations, sector average air concentration at the ground level and sector average ground concentration

The off-centerline factor *J* was verified by computing the ratio Type D concentration/Type 0 concentration (= *J* factor), and comparing the ratio to independently computed values of *J* computed based on line integrals along constant radius arcs.

Multiplying appropriate dose coefficient and exposure factors by the Type 0 and Type D concentrations, alternative dose estimates were computed, which were compared to the Type 6 dose (centerline dose) and Type C dose (sector average dose).

In addition, the Type A dose (peak dose) was compared to the Type 6 dose (centerline dose). The following inequality must be true

$$\text{Type A dose} < \text{Type 6 dose}$$

Violation of that inequality reveals artefacts in the MACCS computations. In initial testing with MACCS Version 4.0, it was found that the inequality was violated for broad plume cases. In discussing with MACCS software developers, it was concluded that the anomalous result was due to failing to constrain the lateral plume domain to $\pm 2.15\ \sigma_y$ around the plume centerline. In

MACCS Version 4.1, the appropriate lateral constraints were implemented and, in addition, runs with extremely large values of σ_y are not permitted. These changes fixed anomalies identified in testing of MACCS Version 4.0.

3.1.3 Test Results

Figure 3-1 shows MACCS concentrations from the tbl_outStat.txt output files (symbols), compared to concentrations computed using Eqs. (2-1), (2-2), and (2-24) with $N=20$ in the series in Eq. (2-2) (solid curves). The agreement between the MACCS outputs and the independently computed concentrations was excellent. The legends represent the value input for YSCALE = ZSCALE (scale factor for the Gaussian dispersion coefficients). This test provides additional verification of air and ground concentration computations, based on steady-state Gaussian plume concentration equations and equations to model dry deposition, complementing Test 2.5.

Figure 3-2 compares concentrations in the output file tbl_outStat.txt (symbols) to Type 0 concentrations in Model1.out output file. The concentrations in both output files are identical, as expected.

Figure 3-3 compares Type 0 centerline air and ground concentrations (solid curves), to Type D sector average air and ground concentrations (dashed curves). As expected, Type D (sector average) < Type 0 (centerline). The ratio Type D/Type 0 is equivalent to the off-centerline factor *J* of the central grid sector. The off-centerline factor was independently computed as the average of the normal distribution function of 0 mean and $\sigma_y(r)$ standard deviation, over an arc of constant radius r spanning an angle θ from $-\pi/16$ to $\pi/16$ (the angle θ is measured with respect to the north direction), divided by the center value of the normal distribution (i.e., normal distribution evaluated at y=0 or angle θ=0). The small-angle approximation in Eq. (2-8) was adopted to transform Cartesian coordinates to polar coordinates. In Figure 3-3, the independently computed value of the off-centerline factor as a function of the downwind distance is in excellent agreement with the Type D/Type 0 concentration ratio.

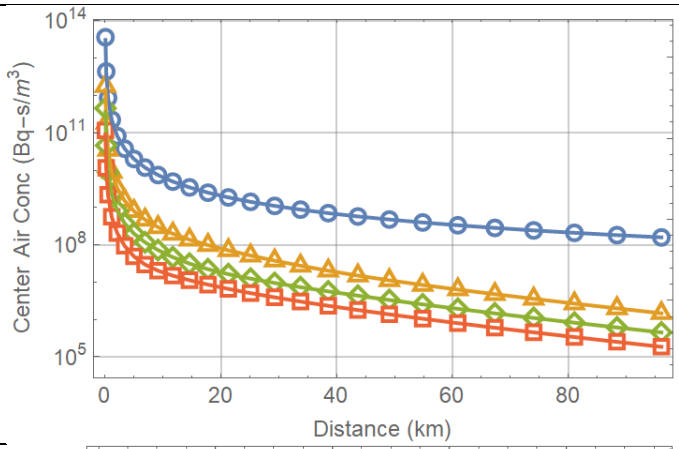

Centerline air concentration (z=h=500 m) versus downwind distance. The symbols represent MACCS data from the file tbl_outStat.txt, and the solid lines were independently computed using Eq. (2-24). A total of N = 20 terms were used in the series of Eq. (2-2).

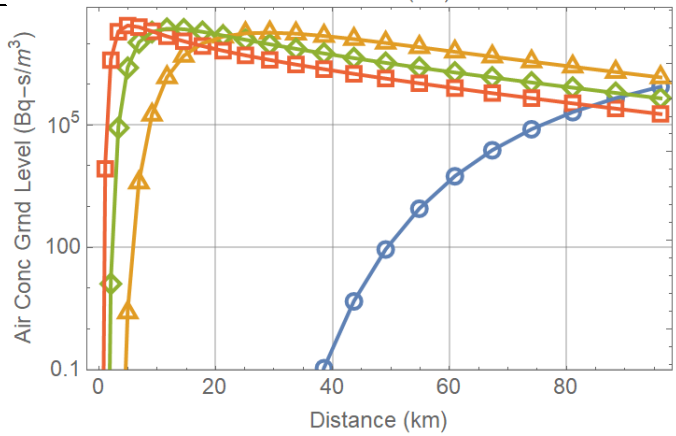

Centerline air concentration at the ground level (z=0 m) versus downwind distance. The symbols represent MACCS data from the file tbl_outStat.txt, and the solid curves were independently computed using Eq. (2-24). A total of N = 20 terms were used in the series of Eq. (2-2).

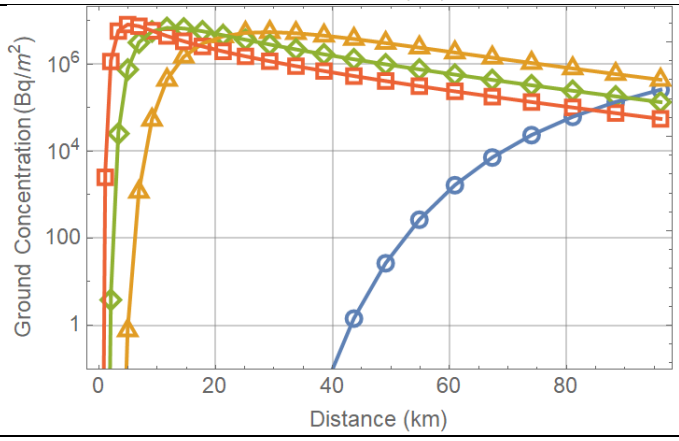

Ground concentration versus downwind distance. The symbols represent MACCS data from the file tbl_outStat.txt, and the solid curves were independently computed using Eq. (2-25). A total of N = 20 terms were used in the series of Eq. (2-2).

Figure 3-1. Centerline air concentration at a height, z=500 m and at z=0 m (ground level), and centerline ground concentration versus downwind distance; comparison of MACCS outputs to independent computations. Four cases were considered: YSCALE = ZSCALE = 0.1, 0.5, 1, and 2.

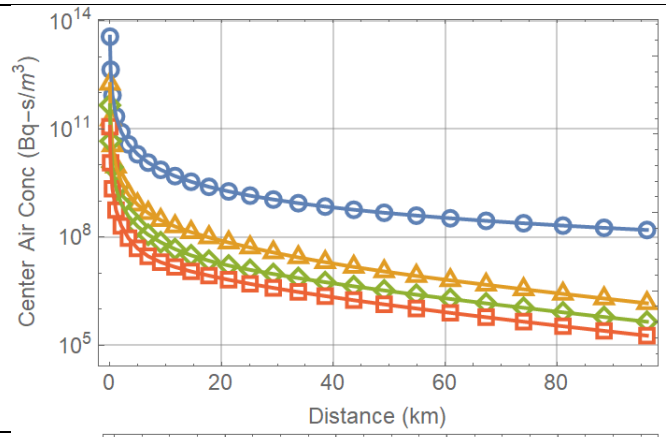

Comparison of centerline air concentrations in tb_outStat.txt (symbols) and Type 0 air concentrations (solid curves) at z=500 m.

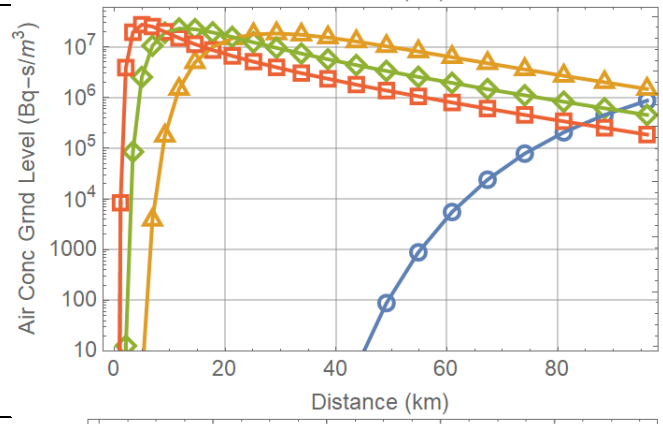

Comparison of centerline air concentrations in tb_outStat.txt (symbols) and Type 0 air concentrations (solid curves) at z=0 m.

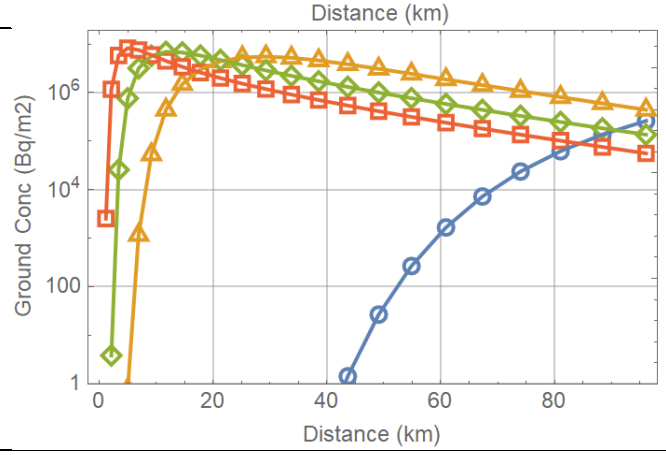

Comparison of centerline ground concentrations in tb_outStat.txt (symbols) and Type 0 ground concentrations (solid curves).

Figure 3-2. Centerline air concentration at a height, z=500 m and at z=0 m (ground level), and centerline ground concentration versus downwind distance; comparison of MACCS outputs in tbl_outStat.txt to Type 0 outputs in Model1.out. Four cases were considered: YSCALE = ZSCALE = 0.1, 0.5, 1, and 2.

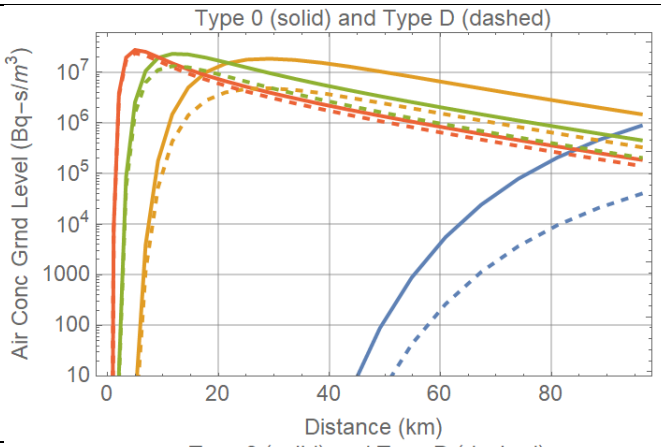

Comparison of Type 0 air concentration at the ground level (solid curves) and Type D grid sector average air concentration (dashed curves). As expected, Type D < Type 0.

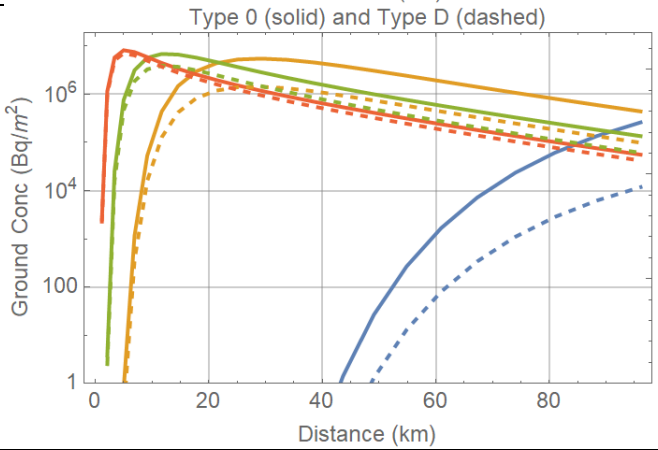

Comparison of Type 0 ground concentration (solid curves) and Type D grid sector average ground concentration (dashed curves). As expected, Type D < Type 0.

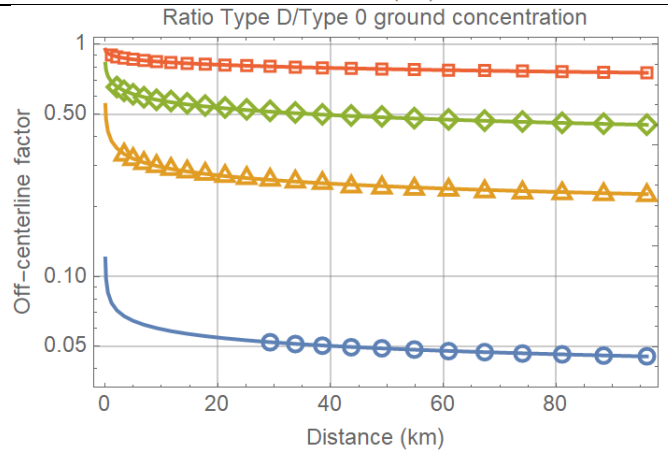

Comparison of the ratio Type D/Type 0 (air or ground) concentration (MACCS data in symbols) to the independently computed off-centerline factor of the grid sector (solid curves). The independently computed off-centerline factor is in excellent agreement with the Type D/Type 0 ratio.

Figure 3-3. Comparison of Type 0 (solid curves) to Type D sector average concentrations (dashed curves), including centerline air concentration at the ground level (z=0) and centerline ground concentration. The bottom plot is the off-centerline factor J (MACCS data in symbols, independent computations in solid curves) versus the downwind distance.

The following tests verify dose outputs. A specific dose pathway output (groundshine, inhalation, cloudshine, or skin) was produced by a MACCS run by setting the appropriate shielding factor to 1 (GSHFAC, PROTIN, CSFACT, SKPFAC) and the complementary factors set to zero.

Groundshine Dose

The test verified that the groundshine dose is computed by MACCS according to Eq. (3-1). In Figure 3-4, groundshine doses (Type 6 centerline and Type C average) were compared to doses independently computed from ground concentrations (Type 0 and Type D), the Cs-137 dose coefficient for groundshine ($DRCG_{ik} = 2.99 \times 10^{-18}$ Sv-m^3/Bq-s), and $T_i \approx 6.048 \times 10^5$ seconds ignoring radioactive decay (=7 days —assumed duration of the EARLY emergency response period). The MACCS groundshine dose outputs were in excellent agreement with the independently computed groundshine doses.

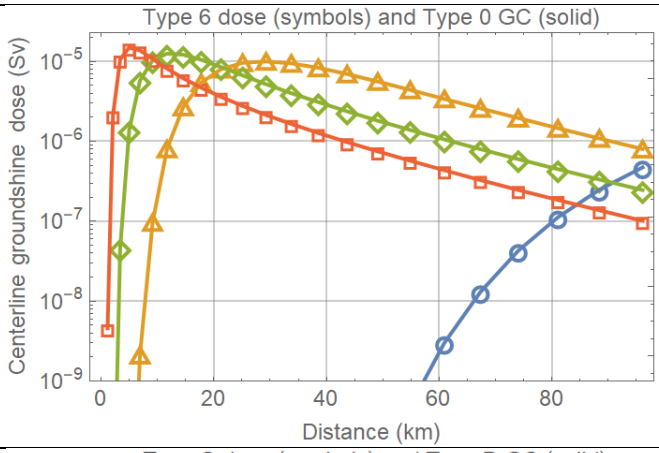

Comparison of Type 6 centerline groundshine dose (symbols) to independently computed doses using the Type 0 centerline ground concentration (solid curves).

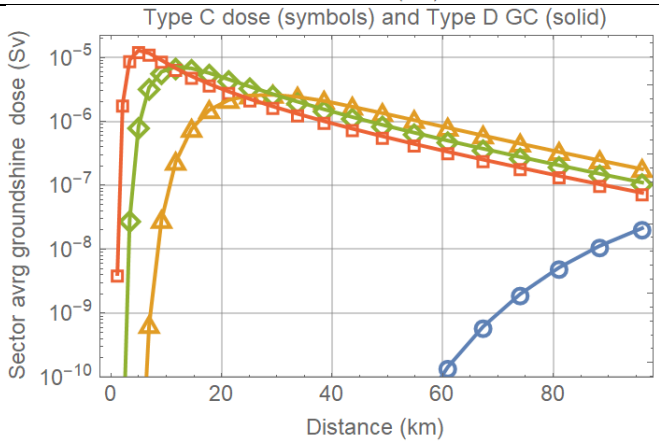

Comparison of Type C grid sector average (north sectors) groundshine dose (symbols) to independently computed doses using the Type D sector average ground concentration of north sectors (solid curves).

Figure 3-4. Centerline groundshine dose, and sector-average groundshine dose (north sector) versus downwind distance.

The Type 6 centerline groundshine dose was compared to the Type A grid sector maximum groundshine dose. It was expected that

Type A groundshine dose ≤ Type 6 centerline dose

The Type A groundshine dose and the Type 6 centerline dose should differ by the off-centerline factor, which is approximately equal to 1 for well spread plume cases (e.g., cases 1 and 2). The comparison is displayed in Figure 3-5. As expected, the Type A doses are below Type 6 doses. For the Case 2, the solid and dashed curves almost overlap in Figure 3-5.

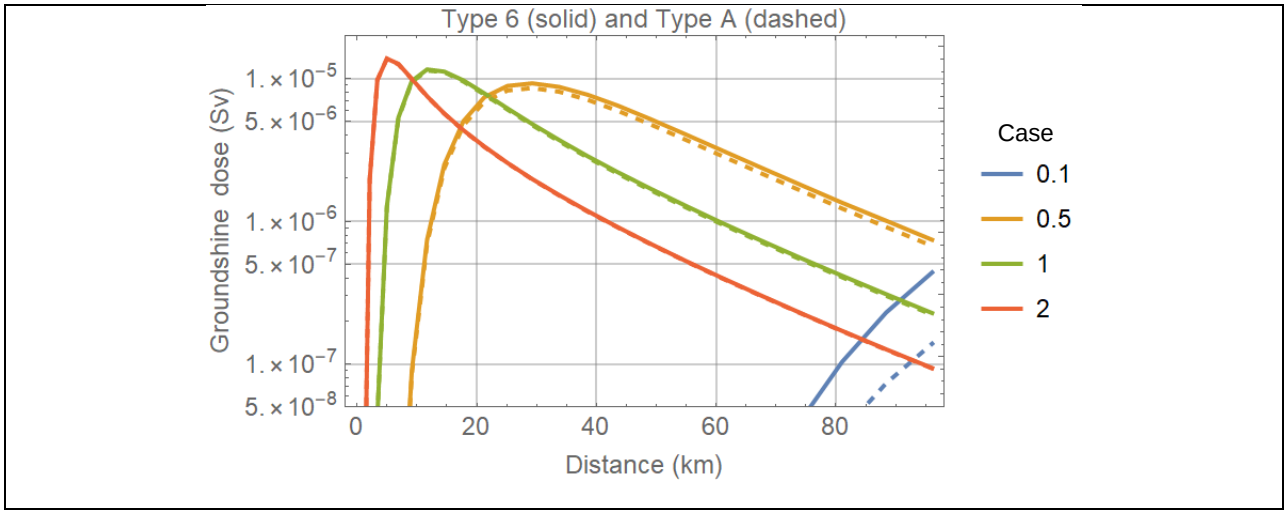

Figure 3-5. Comparison of the Type 6 centerline groundshine dose (solid curves) to the Type A maximum dose (dashed curves).

Inhalation Dose

The test verified that the inhalation dose is computed by MACCS according to Eq. (3-2). Inhalation doses (Type 6 and Type C) were compared to doses independently computed from air concentrations at the ground level (Type 0 and Type D), the Cs-137 dose coefficient for inhalation ($DCI_{ik} = 4.88 \times 10^{-9}$ Sv/Bq), and the input breathing rate BRRATE $= BR = 10^{-4}$ m^3/s. Figure 3-6 shows that MACCS inhalation dose outputs were in excellent agreement with the independently computed inhalation doses.

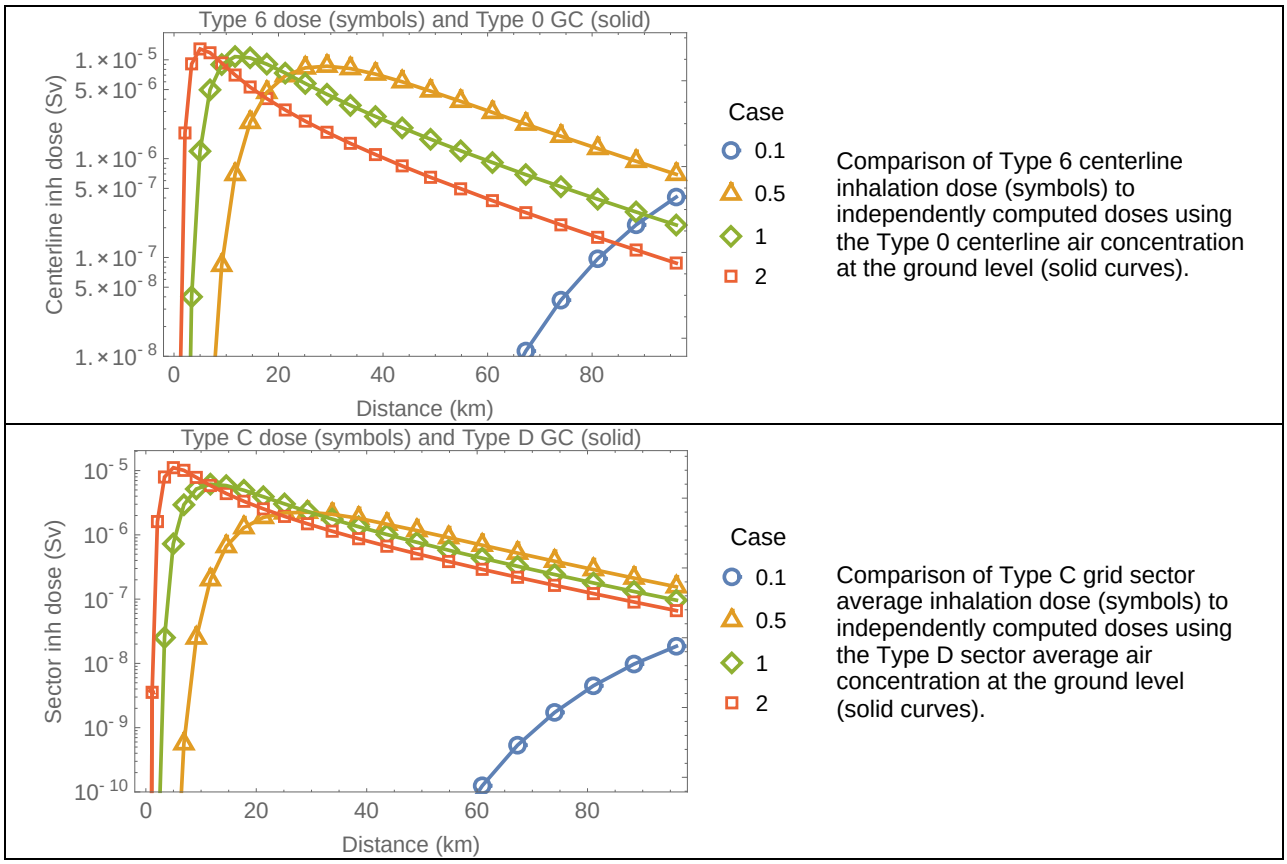

Figure 3-6. Centerline inhalation dose, and sector-average inhalation dose (north sector) versus downwind distance.

The Type 6 centerline inhalation dose was compared to the Type A grid sector maximum inhalation dose in Figure 3-7. The test verified that

Type A inhalation dose ≤ Type 6 centerline dose

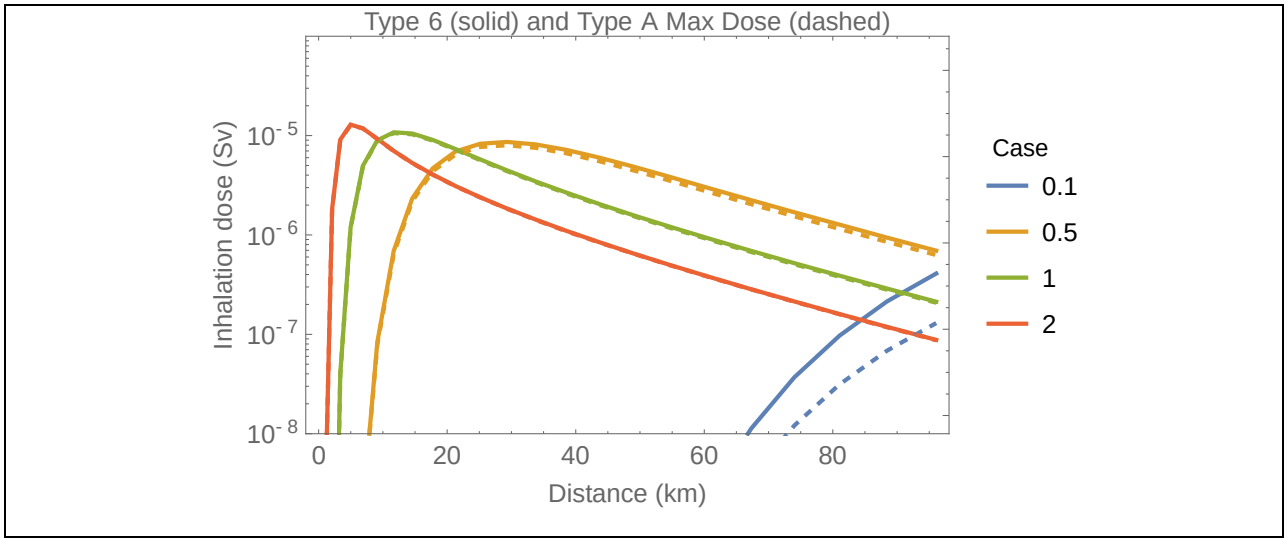

Figure 3-7. Comparison of Type 6 centerline inhalation dose (solid curves) to the Type A sector maximum inhalation dose (dashed curves).

Cloudshine Dose

The approach to verifying the cloudshine dose computation is summarized as follows. From Eq. (3-3), the cloudshine factor C can be computed from the Type 6 cloudshine dose (DC_k) and the Type 0 centerline air concentration [$\chi_i(x, y = 0, z = h)$] as the ratio

$$C = \frac{DC_k}{DRCC_{\infty ik}\ \chi_i(x, y = 0, z = h)} \tag{3-5}$$

The Cs-137 dose coefficient for cloudshine in the test is $DRCC_{\infty ik} = 9.28 \times 10^{-17}$ Sv-m^3/Bq-s. The value of C computed with the MACCS outputs was compared to the cloudshine factor directly computed by linear interpolation from a lookup table supplied by the MACCS software developers. The results of the test are presented in Figure 3-8. The MACCS data are in excellent agreement with the independent computations. A jump is noted in the MACCS data for the Case 2 (YSCALE = ZSCALE = 2), which has the same explanation than similar jumps in Figure 2-6. The jump is due to a practical approach to computing the cloudshine factor in cases with large effective plume size and small relative receptor distance. Figure 3-8 also compares the MACCS Type 6 centerline cloudshine dose (symbols) to independent computations based on Eq. (3-3) and Type 0 MACCS centerline concentrations (solid curves). The agreement between the independent computations and the MACCS data is excellent.

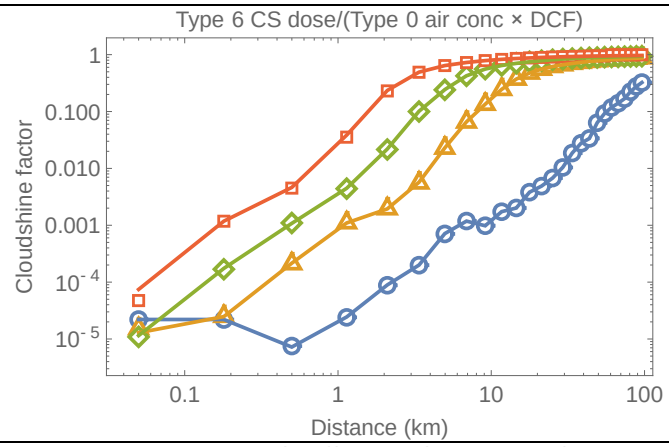

Comparison (in logarithmic scale) of the cloudshine factor computed based on Eq. (3-5) and Type 6 centerline dose and Type 0 centerline air concentration (symbols), to the cloudshine factor directly computed by linear interpolation from a lookup table supplied by MACCS software developers (solid curves).

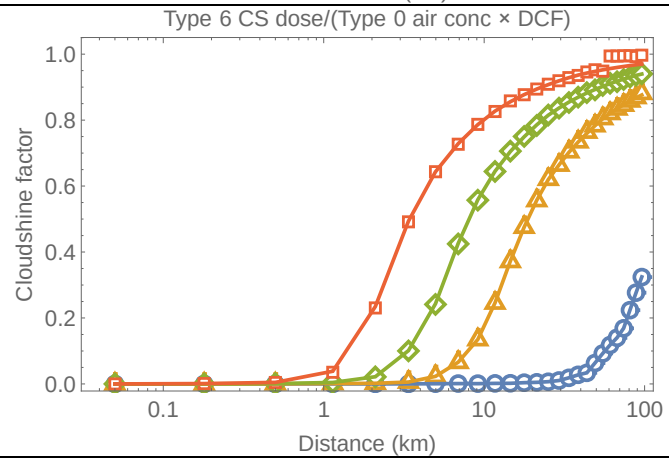

Same as the previous plot, but with the vertical axis in linear scale. The small jump in the Case 2 has the same explanation than similar jumps in Figure 2-6.

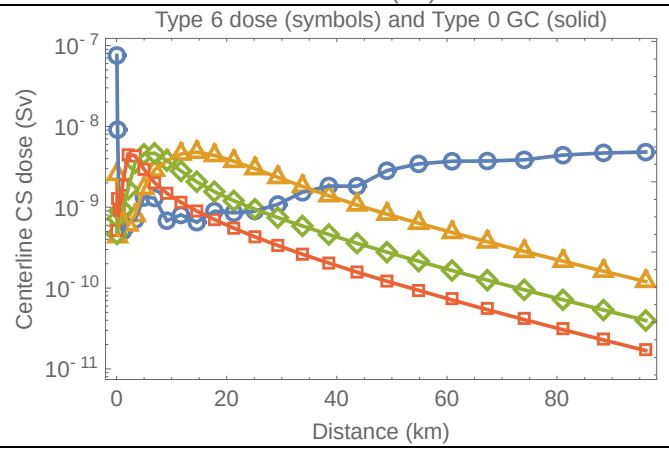

Type 6 centerline cloudshine dose MACCS outputs (symbols) compared to independent computations based on Eq. (3-3) and Type 0 air concentration MACCS outputs at the plume center (solid curves).

Figure 3-8. Cloudshine factor in logarithmic and linear scale displays, and centerline cloudshine dose versus downwind distance.

The relationship of the Type 6 centerline dose to the Type C sector average dose was examined. The Type 6 and Type C MACCS outputs are compared in Figure 3-9. As expected, the Type 6 centerline cloudshine dose (solid curve) is greater than the Type C sector average dose (dashed curve). The ratio Type C/Type 6 is equivalent to the average cloudshine factor computed along a constant radius arc (arc of angular length $\pi/8$ radians) divided by the cloushine factor at the arc center. See the Figure 2-7 of Test 2.1 for a detailed description of the computation of the arc average of the cloudshine factor, accounting for Eq. (2-8) to transform Cartesian to polar coordinates. The cloudshine factor arc average was computed considering a line integral and using a simple average from seven equidistant points along the arc. A

comparison of the ratio Type C/Type 6 (symbols) to the independent computations (solid curves) is also displayed in Figure 3-9. The Type C/Type 6 MACCS output ratio compares well to the independent computations. The computations considering a line integral average matched the MACCS Type C/Type 6 ratio for the Cases 1 and 2 (broad plumes, ZSCALE=YSCALE=1 and ZSCALE=YSCALE=2). On the other hand, the computations considering a simple seven-point average matched the Type C/Type 6 ratio for the Cases 0.1 and 0.5 (narrow plumes). This result is consistent with the result in Figure 2-7 of Test 2.1, indicating that MACCS implements different algorithms to compute the Type C cloudshine dose average depending on the relative plume size. The MACCS data in the middle plot of Figure 3-9 exhibit a jump for the Case 2. The jump has the same explanation than similar jumps in Figure 2-7 and Figure 3-8. The jump is due to practical approximations in MACCS interpolation algorithms to compute the cloudshine factor for cases of large effective plume size and small relative receptor distance.

Type 6 centerline cloudshine dose was compared to the Type A grid sector maximum cloudshine dose in Figure 3-10. It was expected that

Type A maximum cloudshine dose = Type 6 centerline dose

The off-centerline *J* factor concept is not used in the cloudshine dose, for that reason, the Type A and Type 6 doses should be identical. The test verified that the Type A and Type 6 doses are strictly identical.

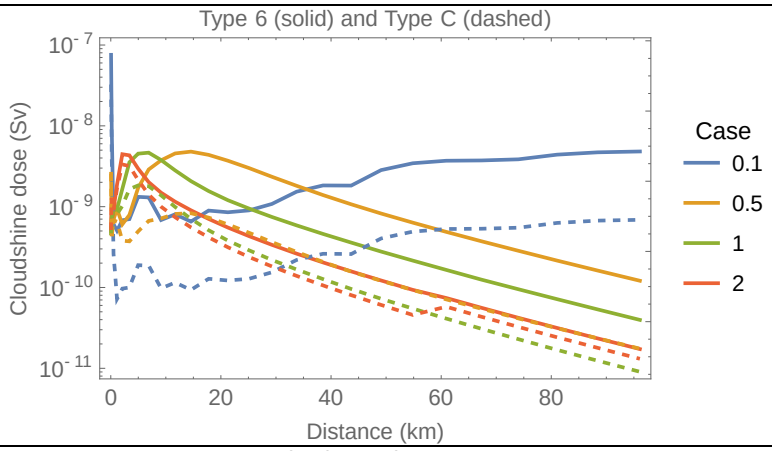

Comparison of the Type 6 centerline dose to the Type C sector average dose. As expected, Type 6 > Type C.

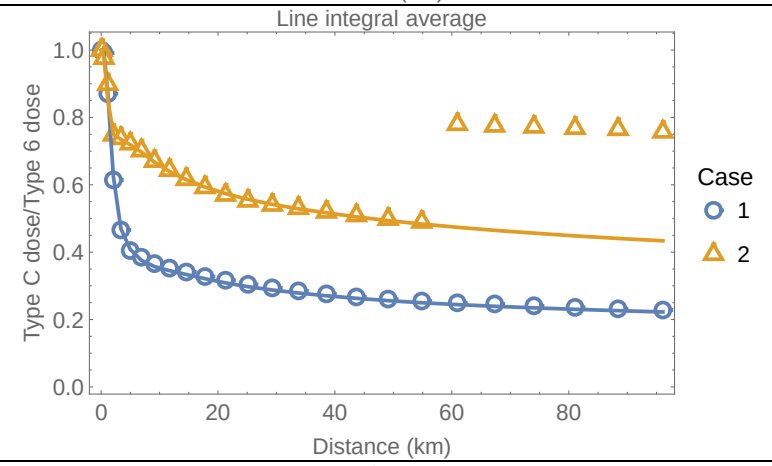

Type C/Type 6 MACCS output ratio (symbols) compared to the average cloudshine factor divided by the cloudshine factor at the arc center (solid curves). The arc average was computed based on line integration.

The jump for the Case 2 is due to practical approximations in MACCS interpolation algorithms to compute the cloudshine factor. See the explanation of similar jumps in Figure 2-7.

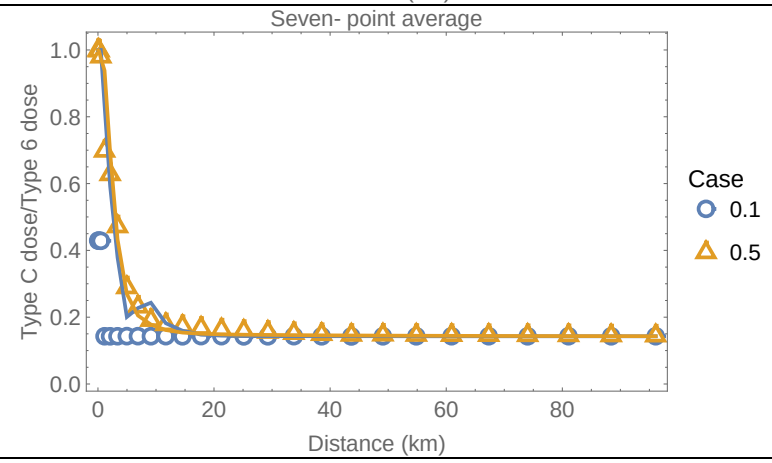

Type C/Type 6 MACCS output ratio (symbols) compared to the average cloudshine factor divided by the cloudshine factor at the arc center (solid curves). The arc average was computed based on a simple seven-point average.

Figure 3-9. Comparison of Type 6 centerline dose to the Type C sector (north sectors) average dose, and Type C/Type 6 ratio versus downwind distance.

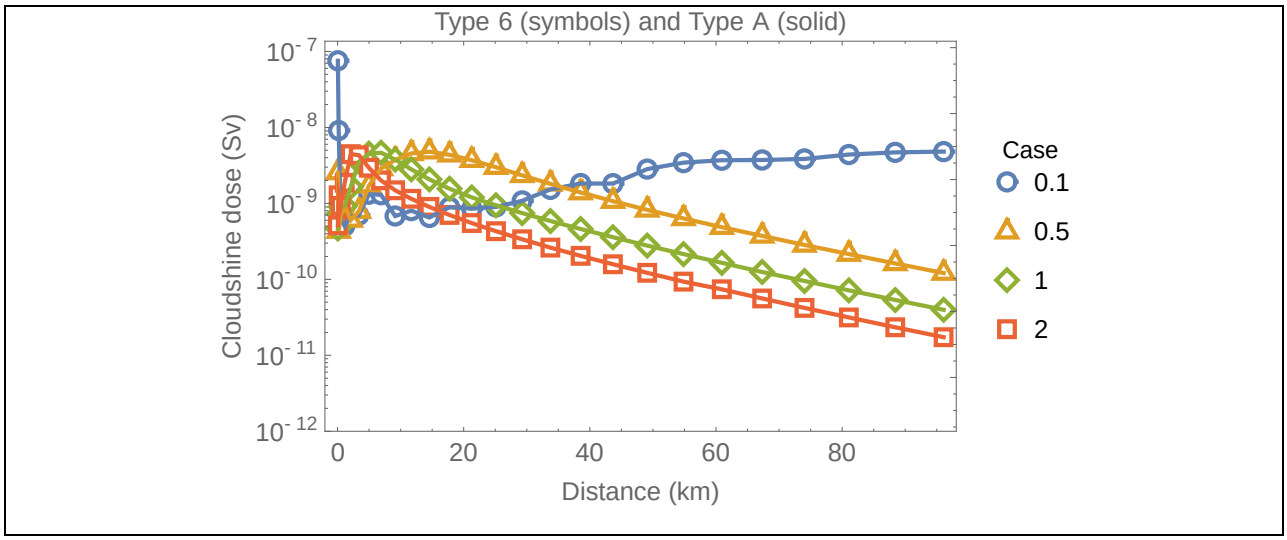

Figure 3-10. Comparison of Type 6 centerline groundshine dose (symbols) to the Type A maximum dose (solid curves).

Skin Acute Dose

It was verified that the skin acute dose is computed by MACCS according to Eq. (3-4). Figure 3-11 displays the skin acute doses (Type 6 and Type C) compared to doses independently computed based on air concentrations at the ground level (Type 0 and Type D) and Eq. (3-4). The MACCS skin dose outputs were in excellent agreement with the independently computed skin acute doses.

Figure 3-12 compares the Type 6 centerline dose to the Type A maximum dose. The test verified that the Type 6 is greater than the Type A dose.

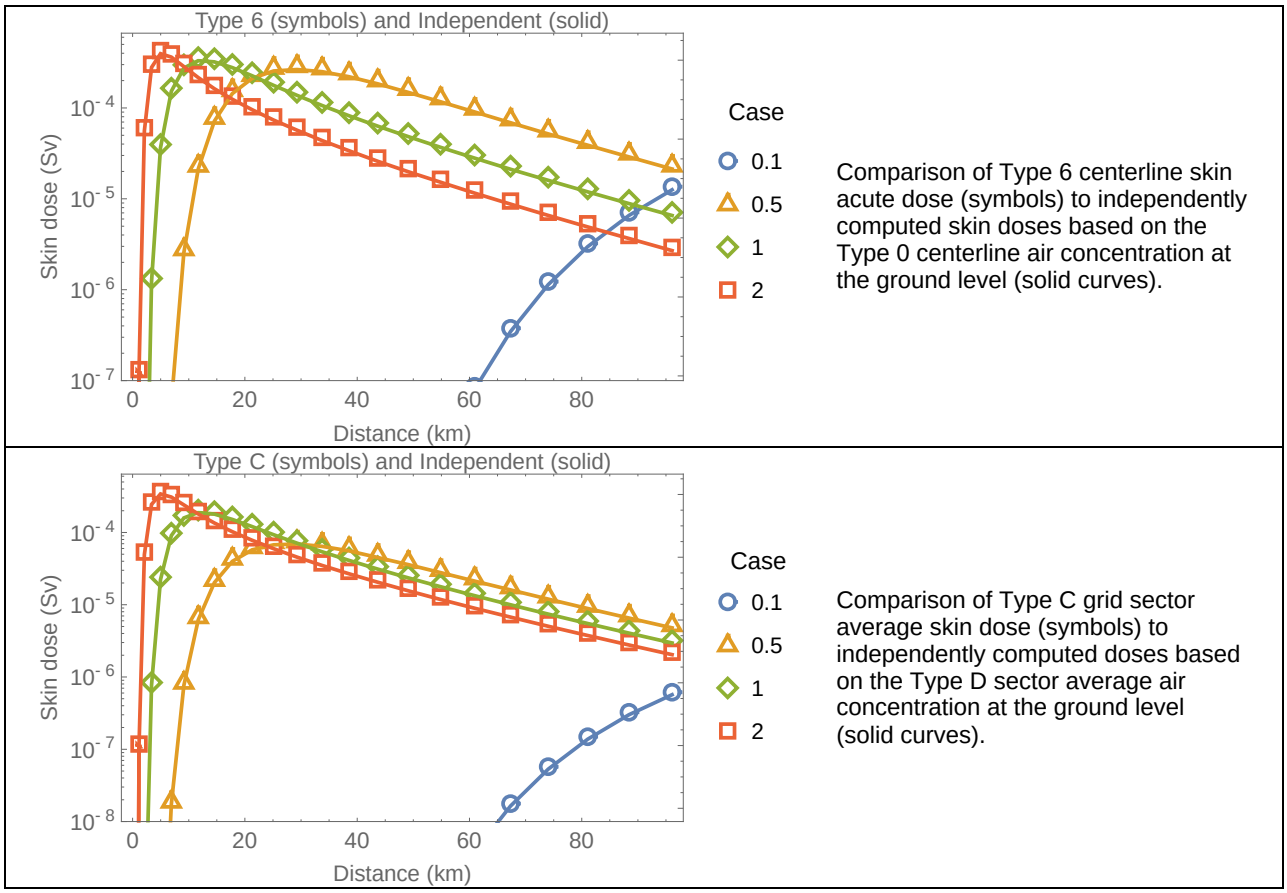

Figure 3-11. Centerline skin acute dose, and sector-average skin acute dose (north sector) versus downwind distance.

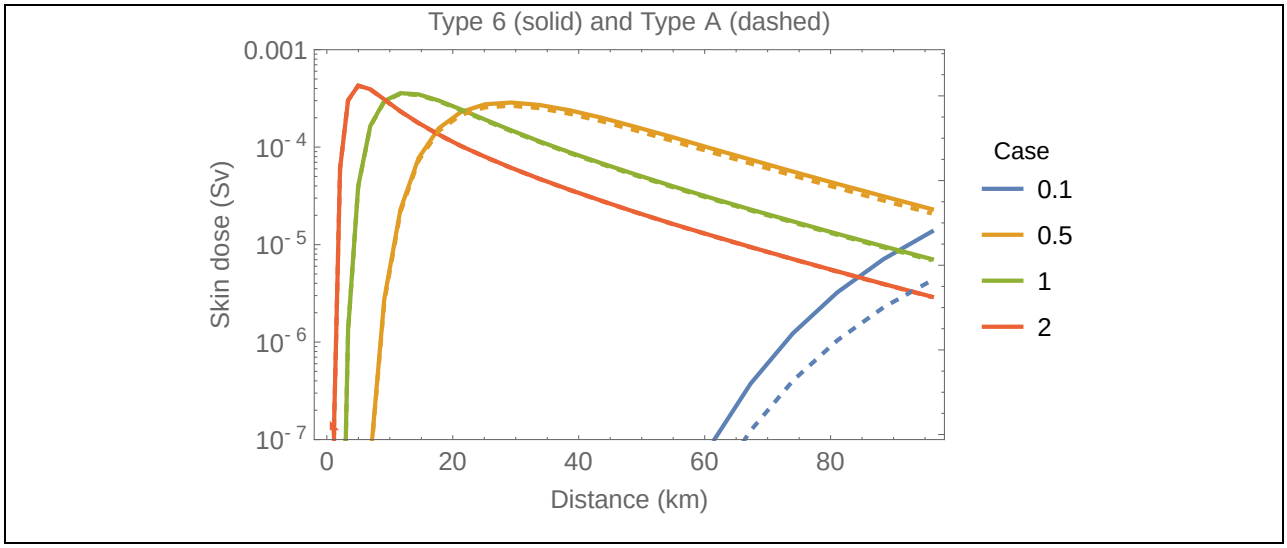

Figure 3-12. Comparison of Type 6 centerline skin dose (solid curves) to the Type A maximum dose (dashed curves).

3.1.4 Test Conclusions

The computations of groundshine, inhalation, cloudshine, and skin doses were verified for a simple case based on independent computations of air concentrations along the plume center, air concentrations at the ground level, and ground concentrations. The approaches to compute sector average concentrations and doses were also verified. MACCS successfully passed the designed tests.

3.2 Test 3.2: Population Dose

In this test the approach to computing the population dose was examined. For simple cases of non-evacuating and non-relocating cohorts, the population dose for a MACCS sector equals the average individual dose for the sector times the number of people residing in the sector. The population dose is a Type 5 output of the EARLY module. The average dose per sector is a Type C output of the EARLY module.

3.2.1 Test Input

The MACCS input was identical to the Test 3.1.

Output Controls

Same outputs Test 2.1 with the following addition:

- Type 5 (NUM5) Population Dose per 360° Grid Ring
  - NAME = L-ICRP60ED
  - I1DIS5 = 1 to 26
  - I2DIS5 = 1 to 26
  - Report Options = NONE

The specified Type 5 inputs cause the EARLY module to itemize population doses for each of the 26 rings of the test problem.

3.2.2 Test Procedure

Multiple runs of the MACCS code were executed with the following selections of the Gaussian dispersion coefficient factors:

- YSCALE = ZSCALE = 0.1
- YSCALE = ZSCALE = 1
- YSCALE = ZSCALE = 2
- YSCALE = ZSCALE = 2.6[1]

The shielding and exposure factors were set to output the inhalation dose only (PROTIN=1, other shielding factors = 0), groundshine dose only (GSHFAC=1, other shielding factors = 0), or cloudshine dose only (CSFACT=1, other shielding factors = 0).

A total of 12 runs (= 4 dispersion coefficient factors × 3 shielding factor selections) were executed. Different runs with a specific value of the dispersion coefficient factor correspond to a single case with identical air and ground concentrations. The runs only differ in the outputs, itemizing different pathway doses. A total of 3 runs for each dispersion coefficient factor were executed to manually itemize the different pathway doses (groundshine, inhalation, or cloudshine) in the Type C dose MACCS outputs.

[1]Testing of MACCS Version 4.0 identified issues related to the inadvertent lack of constraints on the lateral spread of plumes. The issue was fixed in Version 4.1. For example, a value YSCALE = 2.7 triggers an error message requesting the user to adjust the lateral spread of the plume, and MACCS is aborted. The largest YSCALE value with one decimal point not triggering the error message in this test was 2.6.

The population dose for each MACCS sector was independently computed as

Number of people in a sector × Type C average sector dose

The number of people in a sector was computed as the sector area times the population density (POPDEN = 10 people/km^2). The independently computed population dose (inhalation, groundshine, cloudshine), aggregated over 360° rings, was compared to the Type 5 population dose.

3.2.3 Test Results

Inhalation Dose (PROTIN=1, other shielding factors = 0)

The Type C average sector inhalation dose (left plots) and the independently computed population doses per sector (right plots) are presented in Figure 3-13. The color scheme is based on a logarithmic scale. The plots display only the sectors with non-zero doses. With increasing values of the dispersion coefficient factor, more sectors exhibit non-zero doses. For every case of specific dispersion coefficient values (e.g., case YSCALE = ZSCALE=2.6), there is consistency in the sectors with non-zero individual and population doses.

The independently computed population dose was aggregated over 360° concentric rings for direct comparison to the Type 5 population dose. The comparison is presented in Figure 3-14. There is excellent agreement between the MACCS Type 5 population dose and the independent computations.

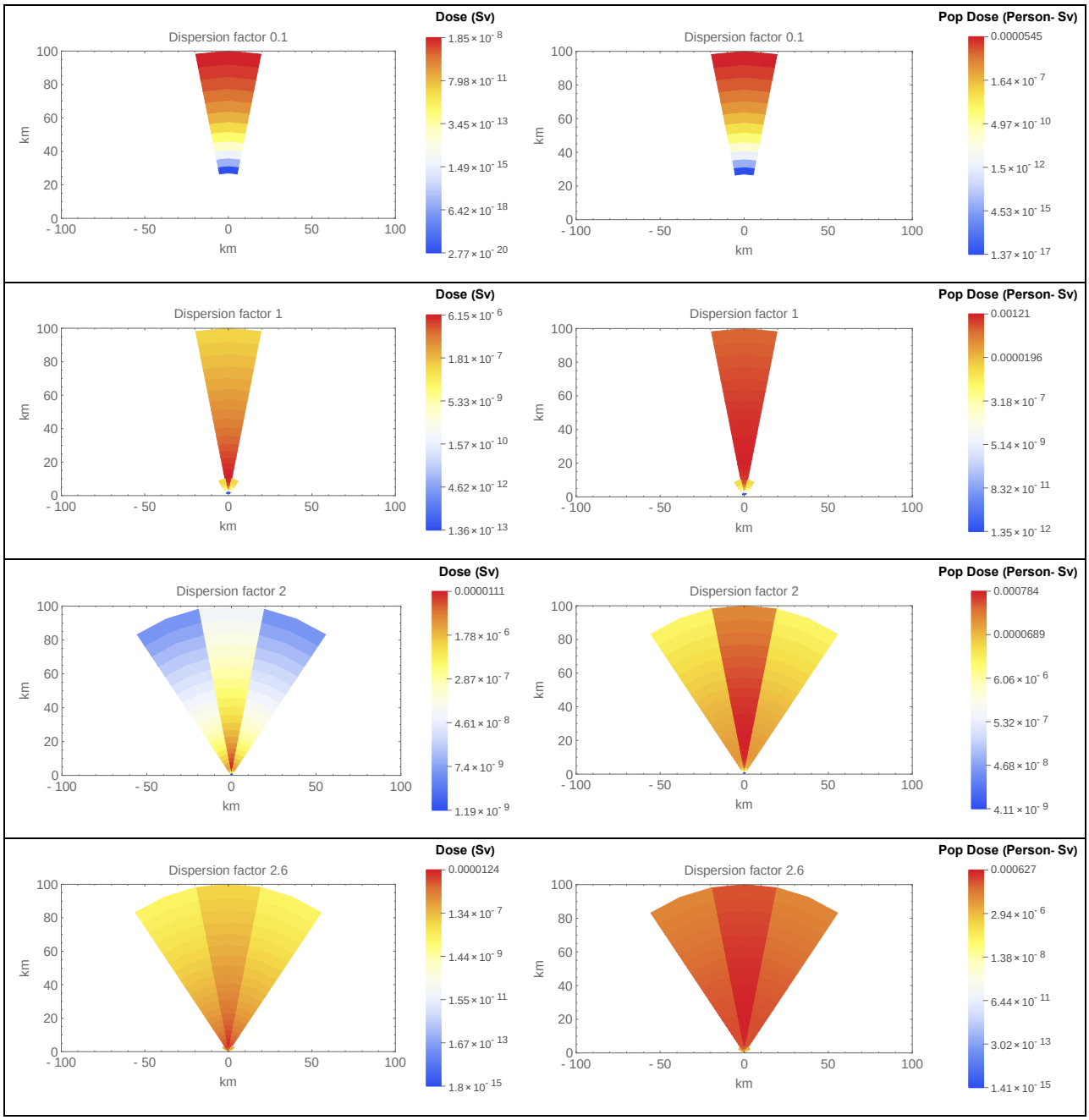

Figure 3-13. Sector plots of Type C inhalation dose and Type 5 population dose, with a color scheme representing a log-scale in the dose and population dose.

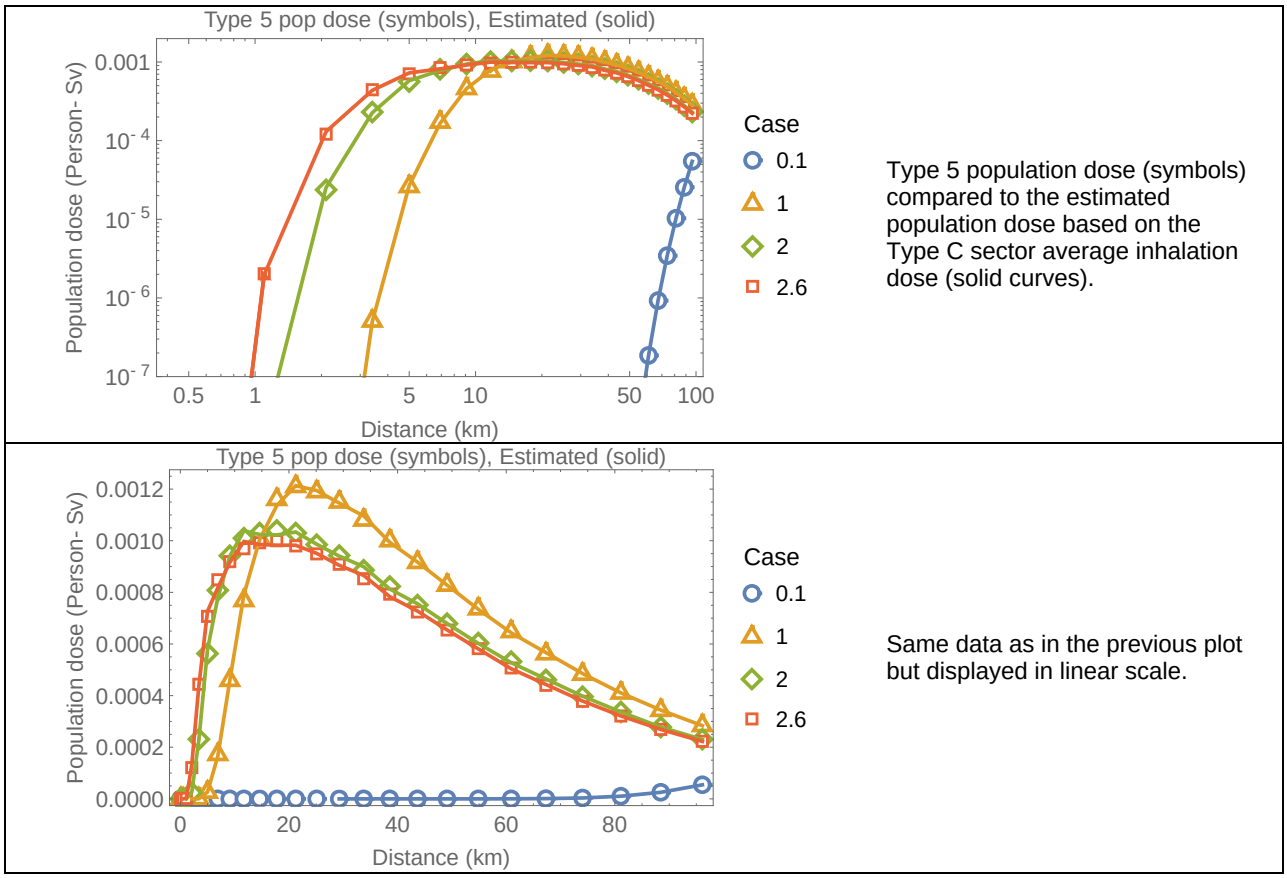

Figure 3-14. Population dose (inhalation) versus distance.

Groundshine Dose (GSHFAC=1, other shielding factors = 0)

The population dose was computed based on the Type C sector average groundshine dose, following the same approach described previously (inhalation dose example). Sector plots of groundshine dose and population dose are similar to the corresponding plots based on the inhalation dose, and not presented in this report for brevity. The independently computed population dose was aggregated over concentric rings for direct comparison to the Type 5 population dose. The comparison is presented in Figure 3-15.

The results are very similar to the inhalation dose results (because the example examined only considered dry deposition, and the ground concentration is proportional to the air concentration at the ground level).

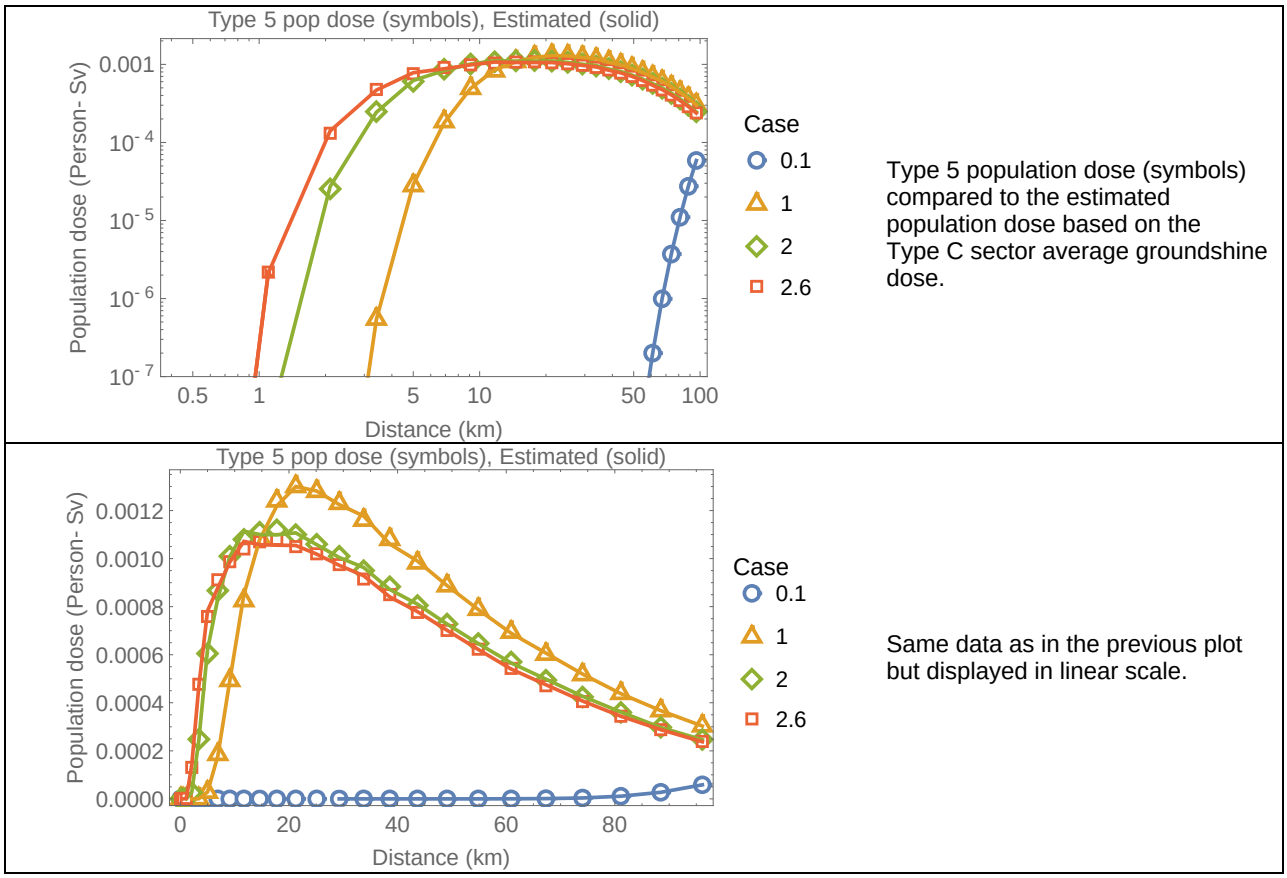

Figure 3-15. Population dose (groundshine) versus distance.

Cloudshine Dose (CSFACT=1, other shielding factors = 0)

The Type C average sector cloudshine dose (left plots) and the independently computed population doses per sector (right plots) are presented in Figure 3-16. The color scheme is based on a logarithmic scale. The plots display only the sectors with non-zero doses. With increasing values of the dispersion coefficient factor, more sectors exhibit non-zero doses.

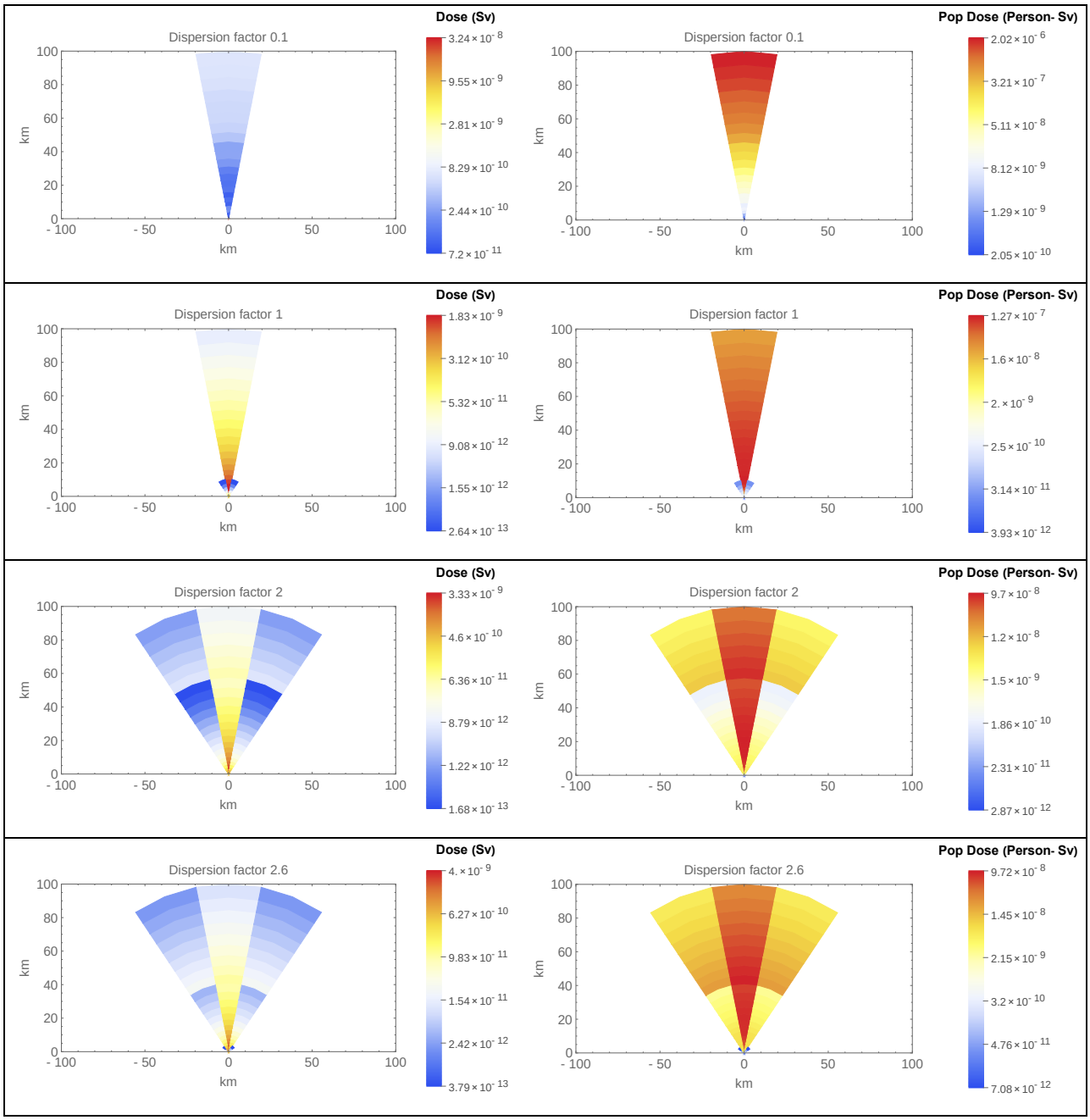

Figure 3-16. Sector plots of Type C cloudshine dose and Type 5 population dose, with a color scheme representing a log-scale in the dose and population dose.

The independently computed population dose was aggregated over 360° concentric rings for direct comparison to the Type 5 population dose. The comparison is presented in Figure 3-17.

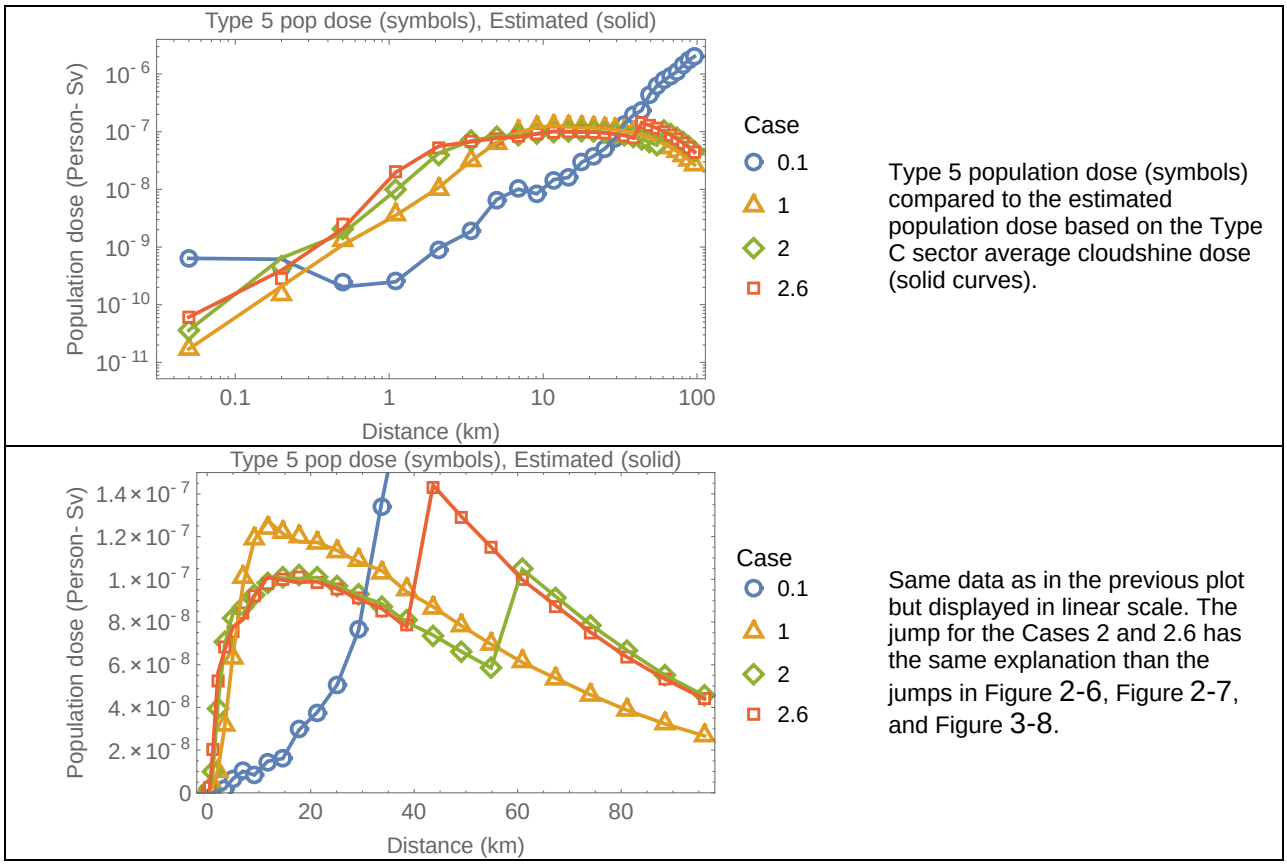

Figure 3-17. Population dose (cloudshine) versus distance.

There is excellent agreement between the MACCS Type 5 population dose and the independent computations. The jump for the Cases 2 and 2.6 in Figure 3-14 is of the same nature than similar jumps in other tests, for example the jump on Figure 2-7 of Test 2.1. The jump is due to simplifications in MACCS interpolation algorithms for the computation of the cloudshine dose in case of large effective plume size and small relative receptor distance.

3.2.4 Test Conclusions

Population doses were independently computed based on Type C sector average individual doses. The independently computed population doses agree with the Type 5 population doses. MACCS successfully passed the designed tests.

3.3 Test 3.3: Early Health Effects and Stochastic Health Effects

This test was aimed at computations of the expected number of people to experience non-lethal injuries during the early period due to acute doses, and stochastic health effects (cancer fatalities and non-fatal cancer — referred to as cancer *injuries*) due to latent doses incurred due to the plume passage.

The equation to compute the number of early injuries due to acute doses is the following (equation 6-1 of the MACCS Theory Manual)

$$N_k = f_k \, POP \left[1 - e^{-H_k(D_k)}\right] \tag{3-6}$$

N_k — number of injured people (early health effect k) in a sector due to an acute dose
POP — number of people residing in a sector
f_k — fraction of people susceptible to early health effect k, specified by EISUSC (=1 in this test)
$H_k(D_k)$ — Hazard function for early health effect k as a function of the acute dose D_k

The hazard function is defined as follows (equation 6-4 of the MACCS Theory Manual)

$$H_k(D_k) = \begin{cases} 0 & D_k < D_{T,k} \\ \left(\dfrac{D_k}{D_{50,k}}\right)^{\beta_k} \ln(2) & D_k \geq D_{T,k} \end{cases} \tag{3-7}$$

D_k — acute dose to a target organ inducing health effect k (Gy)
$D_{T,k}$ — threshold acute dose for the onset of health effect k, specified by EITHRE
$D_{50,k}$ — dose causing half of the population to experience early health effect k (Gy), specified by EIFACA
β_k — shape parameter, specified by EIFACB

For a small dose D_k and assuming $D_{T,k} = 0$, Eq. (3-6) simplifies to (after applying a first order Taylor expansion to the exponential function)

$$N_k = f_k \, POP \left(\frac{D_k}{D_{50,k}}\right)^{\beta_k} \ln(2) \tag{3-8}$$

If the shape factor β_k is one, then the number of early injuries is linearly related to the acute dose D_k.

The individual risk of cancer fatality or cancer injury in the long term due to a lifetime dose arising from the plume passage is computed as (based on equations 6-5 and 6-6 of the MACCS Theory Manual)

$$r_k^E = \begin{cases} f_k \, RC_k \, D_k^E & D_k^E \geq D_\alpha \\ f_k \, RC_k \dfrac{D_k^E}{\alpha_k} & D_k^E < D_\alpha \end{cases} \tag{3-9}$$

r_k^E — risk of an individual to experience health effect k, due to a lifetime early dose D_k^E

f_k — fraction of people susceptible to health effect k, specified by ACSUSC (=1 in the test runs)

RC_k — lifetime risk factor early health effect k (Gy), specified by CFRISK for cancer fatalities or CIRISK for cancer injuries (1/Sv)

D_k^E — lifetime dose associated with the early period causing the health effect k in a sector (Sv)

α_k — dose and dose rate effectivity factor, specified by DDREFA

D_α — threshold dose (Sv), specified by DDTHRE

To compute the number of people in a sector that would experience the health effect k, r_k^E is multiplied by the number of people residing in a sector of the spatial grid.

The test was aimed at computing the number of people with early injuries, and late fatalities and cancer injuries (Type 1 output) based on sector average acute and lifetime doses (Type C output).

3.3.1 Test Input

The input was identical to the Test 3.1, with the following changes

- Shielding and Exposure
  - PROTIN = 1, inhalation dose pathway
  - BRRATE = 1 m^3/s, exaggerated breathing rate to cause sizable risk
  - CSFACT (cloudshine) = SKPFAC (skin dose) = GSHFAC (ground dose) = 0
- Early Injury Parameters
  - EINAME = HYPOTHYROIDISM
  - ORGAN = A-THYROID
  - EITHRE (Gy) = 0 Gy, zero threshold dose
  - EIFACA (Gy) = 1 Gy
  - EIFACB = 1, selection to make the risk linearly dependent on the acute dose, per Eq. (3-8)
- Latent Cancer Parameters
  - ACNAME = LUNG
  - ORGNAM = L-LUNGS
  - ACSUSC = 1 (fraction of people affected)
  - CFRISK (1/Sv) = 0.026 1/Sv
  - CIRISK (1/Sv) = 0 1/Sv (no long-term injury)
  - DDREFA = 1 (no risk reduction)

  - ACNAME = THYROID
  - ORGNAM = L-THYROID
  - ACSUSC = 1
  - CFRISK (1/Sv) = 6.34×10^{-4} 1/Sv
  - DDREFA = 1 (no risk reduction)

Output Controls

The same outputs used for Test 3.2 were selected with the following addition:

- Type 1 (NUM1) Health-Effect Cases
  - NAME = ERL INJ/HYPOTHIROIDISM (early hypothyroidism due to acute dose A-THYROID)

    - I1DIS1 = 1 to 26
    - I2DIS1 = 1 to 26
    - Report Options = NONE

    - NAME = CAN FAT/LUNG (lung cancer fatality due to lifetime dose L-LUNGS during the early period)
    - I1DIS1 = 1 to 26
    - I2DIS1 = 1 to 26
    - Report Options = NONE

    - NAME = CAN INJ/THYROID (lung cancer injury due to lifetime dose L-THYROID during the early period)
    - I1DIS1 = 1 to 26
    - I2DIS1 = 1 to 26
    - Report Options = NONE
- Type 4 (NUM4) Average Individual Risk
    - NAME = ERL INJ/HYPOTHIROIDISM
    - IDIS4 = 1 to 26
    - Report Options = NONE

    - NAME = CAN FAT/LUNG
    - I1DIS4 = 1 to 26
    - Report Options = NONE

    - Note: an error was produced when trying to add more outputs, such as CAN INJ/THYROID
- Type 8 (NUM8) Population-Weighted Individual Risk
    - NAME = ERL INJ/HYPOTHIROIDISM
    - I1DIS1 = 1 to 26
    - I2DIS1 = 1 to 26
    - Report Options = NONE

    - NAME = CAN FAT/LUNG
    - I1DIS1 = 1 to 26
    - I2DIS1 = 1 to 26
    - Report Options = NONE
- Type C (NUMC) Average Sector Dose
    - ORGNAM = L-ICRP60ED
    - ELEVDOSE (Sv) = 0: outputs all grid elements with dose > 0 Sv
    - PRINT_FLAG_C = True: outputs information for all grid elements

    - ORGNAM = A-LUNGS
    - ELEVDOSE (Sv) = 0: outputs all grid elements with dose > 0 Sv
    - PRINT_FLAG_C = True: outputs information for all grid elements

    - ORGNAM = L-LUNGS
    - ELEVDOSE (Sv) = 0: outputs all grid elements with dose > 0 Sv
    - PRINT_FLAG_C = True: outputs information for all grid elements

    - ORGNAM = A-THYROID
    - ELEVDOSE (Sv) = 0: outputs all grid elements with dose > 0 Sv
    - PRINT_FLAG_C = True: outputs information for all grid elements

- ORGNAM = L-THYROID
- ELEVDOSE (Sv) = 0: outputs all grid elements with dose > 0 Sv
- PRINT_FLAG_C = True: outputs information for all grid elements

3.3.2 Test Procedure

Six runs of the MACCS code were executed with the following selections of the Gaussian dispersion coefficient factors:

- YSCALE = ZSCALE = 0.1
- YSCALE = ZSCALE = 0.5
- YSCALE = ZSCALE = 1
- YSCALE = ZSCALE = 2
- YSCALE = ZSCALE = 2.6

The shielding and exposure factors were set to output the inhalation dose only (PROTIN=1, other shielding factors = 0).

The expected number of people with early injuries (hypothyroidism) due to an acute dose (A-THYROID) was independently computed using Eq. (3-6) and the Type C average sector dose (A-THYROID). The number of people in a sector (POP) was computed as the sector area times the population density (POPDEN = 10 people/km^2).

The risk of cancer fatalities and injuries due to lifetime doses to the lungs (L-LUNGS) or to the thyroid (L-THYROID) was independently computed using the corresponding Type C sector average dose (L-LUNGS or L-THYROID) and Eq. (3-9). The expected number of affected people per sector was computed by multiplying the computed risk number and the number of people in a sector (in this test problem it was assumed a constant population density, POPDEN = 10 people/km^2).

The independently computed number of health effects (e.g., early injury, cancer fatalities and injuries), aggregated over 360° rings, were compared to the Type 1 health-effect cases.

The average individual risk (early injury risk, cancer fatality risk, cancer injury risk) in a MACCS grid ring was computed as the average of 16 risk values (one independently computed risk value for each of the 16 sectors in a 360° ring). The average individual risk per grid ring was compared to Type 4 outputs of the EARLY module.

The test did not evaluate early fatality risk. In the test runs, the early fatalities were zero. Although the early fatality results were not explicitly tested, the early injury computations are identical to the early fatality computations.

3.3.3 Test Results

The independently computed individual risk of early injury (hypothyroidism) from acute doses to the thyroidal gland was compared to the corresponding Type 4 MACCS output in Figure 3-18. The MACCS outputs are in excellent agreement with the independent computations. Particularly noteworthy is that the Type 4 risk considers sectors located upwind from the source (i.e., sectors south of the source in the test problem), with zero dose, in the computation of the average risk. Figure 3-18 also compares the Type 1 MACCS population risk output to the independently computed number of people affected by hypothyroidism, showing complete

agreement. Finally, Figure 3-18 includes a comparison of Type 8 population-weighted individual risk to Type 4 average individual risk (in the form of a ratio of Type 8/Type 4 versus distance). As expected, Type 8 and Type 4 are identical due to the consideration of uniform population density in the test problem.

The independently computed individual lung cancer fatality risk (based on the Type C sector average lifetime lung dose, L-LUNGS) was compared to the corresponding Type 4 MACCS output in Figure 3-19. Figure 3-19 also includes the independently computed number of people with fatal lung cancer compared to the corresponding Type 1 output, as well as a comparison of Type 8 population-weighted individual risk to Type 4 average individual risk (in the form of a ratio of Type 8/Type 4 versus distance). As expected, Type 8 MACCS outputs are identical to Type 4 MACCS outputs, due to the assumption of uniformly distributed population.

The independently computed number of people affected by thyroidal cancer (based on the Type C sector average lifetime thyroidal dose, L-THYROID) was compared to the corresponding Type 1 output in Figure 3-20. The MACCS outputs are in excellent agreement with the independent computations.

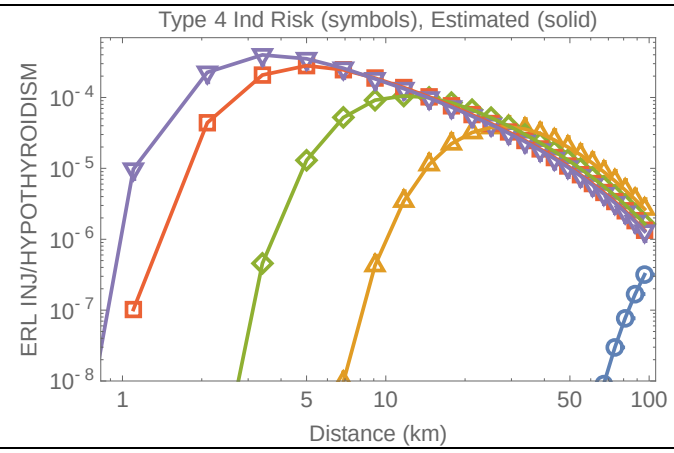

Type 4 average individual risk (symbols, early injury, hypothyroidism) compared to the independently computed average risk based on the Type C sector average inhalation A-THYROID dose (solid curves).

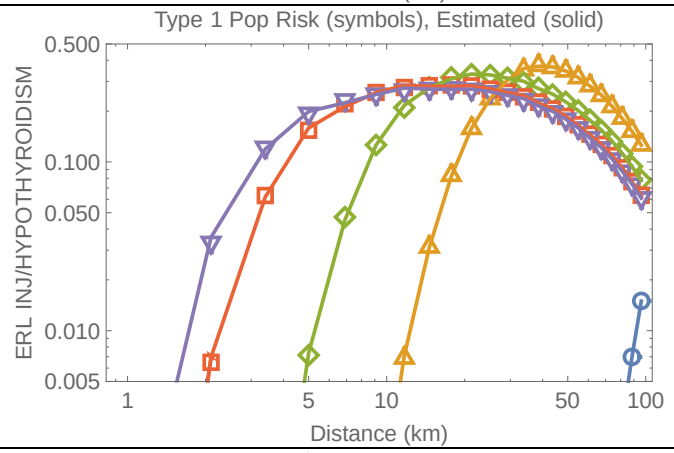

Type 1 population risk (symbols, early injury, hypothyroidism) compared to the independently computed average risk based on the Type C sector average inhalation A-THYROID dose (solid curves).

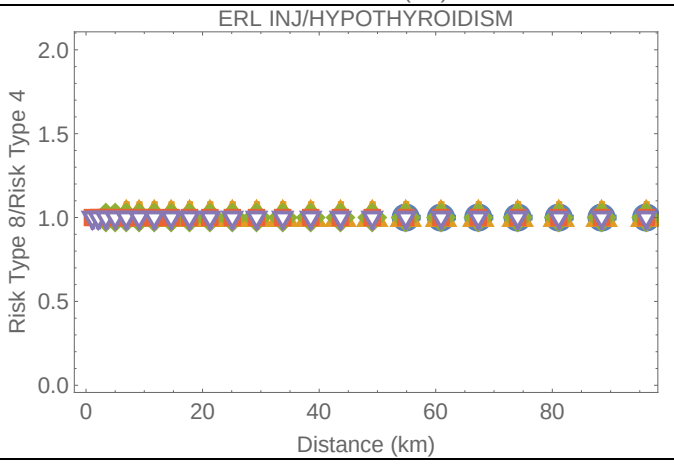

Comparison of Type 8 population-weighted individual risk and Type 4 average individual risk of early injury (hypothyroidism), presented as a ratio Type 8/Type 4.

As expected, Type 4 and Type 8 results are strictly identical due to the use of a uniform population density in the test.

Figure 3-18. Individual average risk (Type 4 output) and population risk (Type 1 output) from acute doses to the thyroidal gland versus radial distance from the source. The third plot is a ratio comparison of Type 4 and Type 8 MACCS outputs (the results are strictly identical).

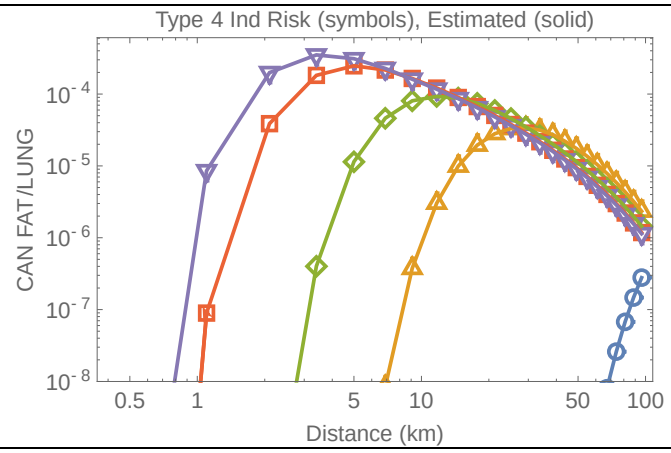

Type 4 MACCS average individual risk (symbols, lung cancer fatality) compared to the independently computed average risk, based on the Type C sector average inhalation L-LUNG dose (solid curves).

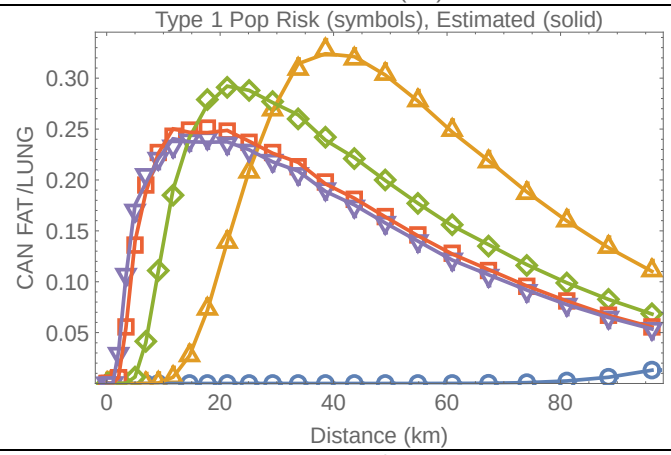

Type 1 MACCS population risk (symbols, lung cancer fatality) compared to the independently computed number of affected people based on the Type C sector average inhalation L-LUNGS dose (solid curves).

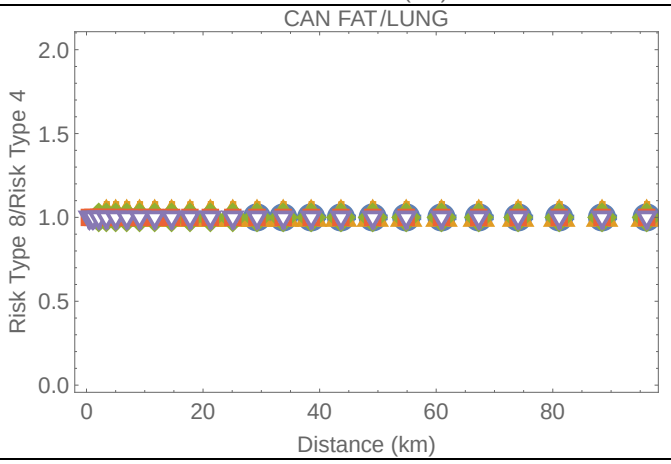

Comparison of Type 8 population-weighted individual risk and Type 4 average individual risk of early injury (lung cancer fatality), presented as a ratio Type 8/Type 4.

As expected, Type 4 and Type 8 results are identical due to the use of a uniform population density in the test.

Figure 3-19. Average individual risk (Type 4 output) and population risk (Type 1 output) from long-term lung doses from inhalation of radioactivity carried by the plume, versus radial distance from the source. The third plot is a ratio comparison of Type 4 and Type 8 MACCS outputs (the results are strictly identical).

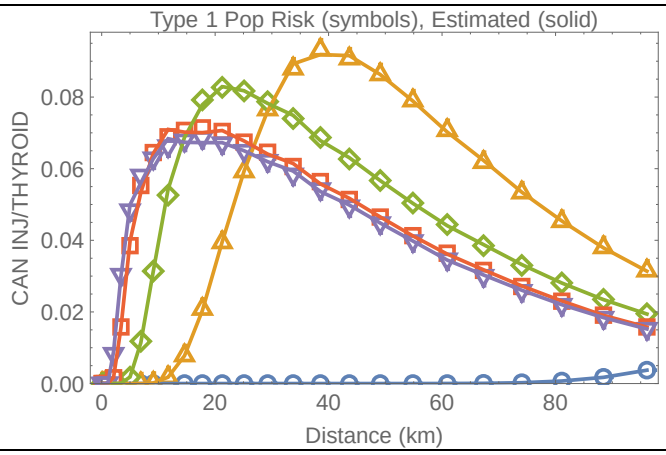

Type 1 population risk (symbols, thyroidal cancer injury) compared to the independently computed number of affected people by thyroidal cancer based on the Type C sector average inhalation L-THYROID dose (solid curves).

Figure 3-20. Population risk (from long-term doses to the thyroid from inhalation of radioactivity carried by the plume) versus radial distance from the source.

3.3.4 Test Conclusions

The test verified the MACCS algorithms to compute individual risk and the number of people exhibiting specific health effects due to acute doses of lifetime doses incurred during the early phase. Independent computations verified the computation of risk indices and the number of affected people. MACCS successfully passed the designed tests.

3.4 Test 3.4: Dependence of Results on Lateral Dispersion σ_y

Tests 3.1, 3.2, and 3.3 with MACCS Version 4.0 identified anomalies related to lack of numerical constraints on the spread of plumes. Test 3.4 was originally designed as a complementary test, to identify whether anomalies in Version 4.0 were related to scenarios with large values of vertical or lateral Gaussian dispersion coefficients. The causes of the identified anomalies in the referred tests were already addressed in MACCS Version 4.1, but the Test 3.4 with Version 4.1 is documented herein for the sake of completeness.

In Tests 3.1, 3.2, and 3.3, the vertical and lateral dispersion coefficients were adjusted through the factors YSCALE and ZSCALE. In all those previous tests, YSCALE = ZSCALE. In the current Test 3.4, the effect of lateral dispersion was independently examined by setting ZSCALE=1 and varying YSCALE. Similarly, vertical dispersion effects were examined by setting YSCALE=1 and varying ZSCALE. Anomalies in MACCS Version 4.0 were related to lateral dispersion (acrosswind direction) and numerical artefacts in the computation of concentrations, doses, and health effects on non-central grid sectors. As previously stated, those anomalies do not exist in MACCS Version 4.1, given the constraints on the allowed extent of lateral spread of plumes.

3.4.1 Test Input

Identical inputs and outputs than Test 3.3 were used.

3.4.2 Test Procedure

Five runs of the MACCS code were executed with ZSCALE=1 and the following selections of the lateral Gaussian dispersion coefficient factors:

- YSCALE = 0.1
- YSCALE = 1
- YSCALE = 2
- YSCALE = 2.6

In addition, four runs of the MACCS code were executed with YSCALE=1 and the following selections of the vertical Gaussian dispersion coefficient factors:

- ZSCALE = 0.1
- ZSCALE = 1
- ZSCALE = 10
- ZSCALE = 100

Tests exhibiting anomalous results using MACCS Version 4.0 were repeated, following procedures in Tests 3.1, 3.2, and 3.3.

3.4.3 Test Results

ZSCALE = 1 and variable YSCALE

The Type A maximum dose and Type 6 centerline inhalation dose were compared in Figure 3-21. Figure 3-22 includes multiple plots of MACCS outputs (symbols) to independent

computations (solid curves), with excellent agreement and no anomalies. Note that population doses and health effects in Figure 3-22 were aggregated over 360° rings. The aggregated results are almost independent of the lateral plume spread.

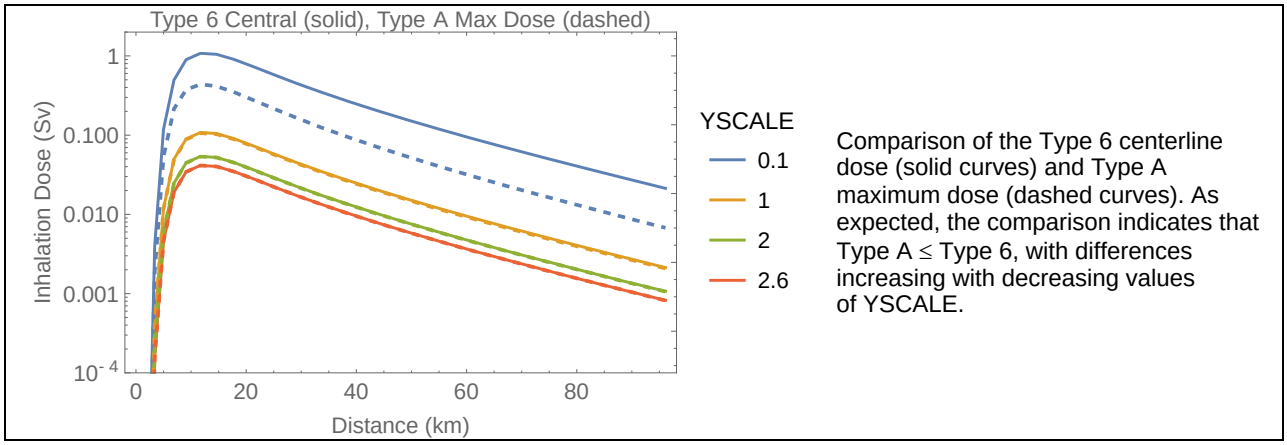

Figure 3-21. Comparison of Type 6 centerline inhalation dose (solid curves) to the Type A maximum dose (dashed curves).

Figure 3-23 shows sector plots of the air concentration on the left column (air concentration of Cs-137 at the ground level extracted from Type D outputs) and individual inhalation dose on the right column (L-ICRP60ED inhalation dose extracted from Type C outputs). The concentration plots are visually identical to the dose plots because the inhalation dose is proportional to the air concentration at ground level.

Figure 3-24 is an alternative visual display of the same data shown in Figure 3-23: the air concentration and inhalation dose were plotted versus the sector angle, for the different radial distances of the sector centers. Each curve in each plot in Figure 3-24 represents information of sectors on a single ring of the MACCS spatial grid (i.e., sectors located at the same radial distance from the source). The color scale represents the ring radius (blue is for a small radius close to the source, red is for a radius far from the source). The angle was measured with respect to the east direction: i.e., east = 0°, north = 90°, west = 180°. The air concentration plots (left hand side plots) and the inhalation dose plots (right hand side plots) are visually identical because the inhalation dose is proportional to the air concentration at the ground level. The expected shape of a concentration or dose versus angle curve is a bell shape: a value that is maximal in the central sectors (90°) and with smaller values for angles farther away from the central angle. There are no visual anomalies in the MACCS outputs.

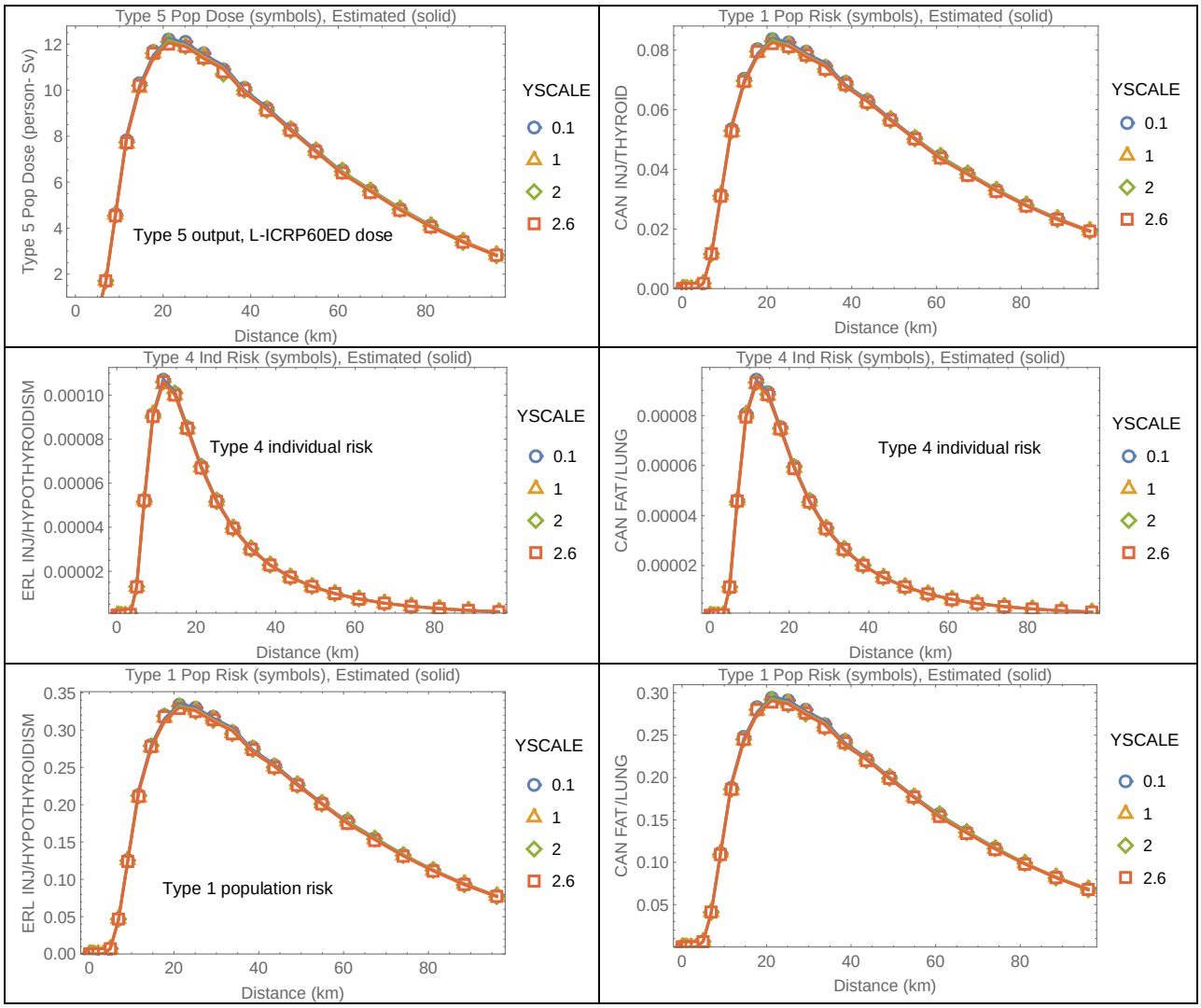

Figure 3-22. Comparison of several MACCS outputs (symbols) to independent computations (solid curves). Health effects arise from acute and long-term lung and thyroid doses from inhalation of radioactive material carried in the plume. Results are combined over 360° rings.

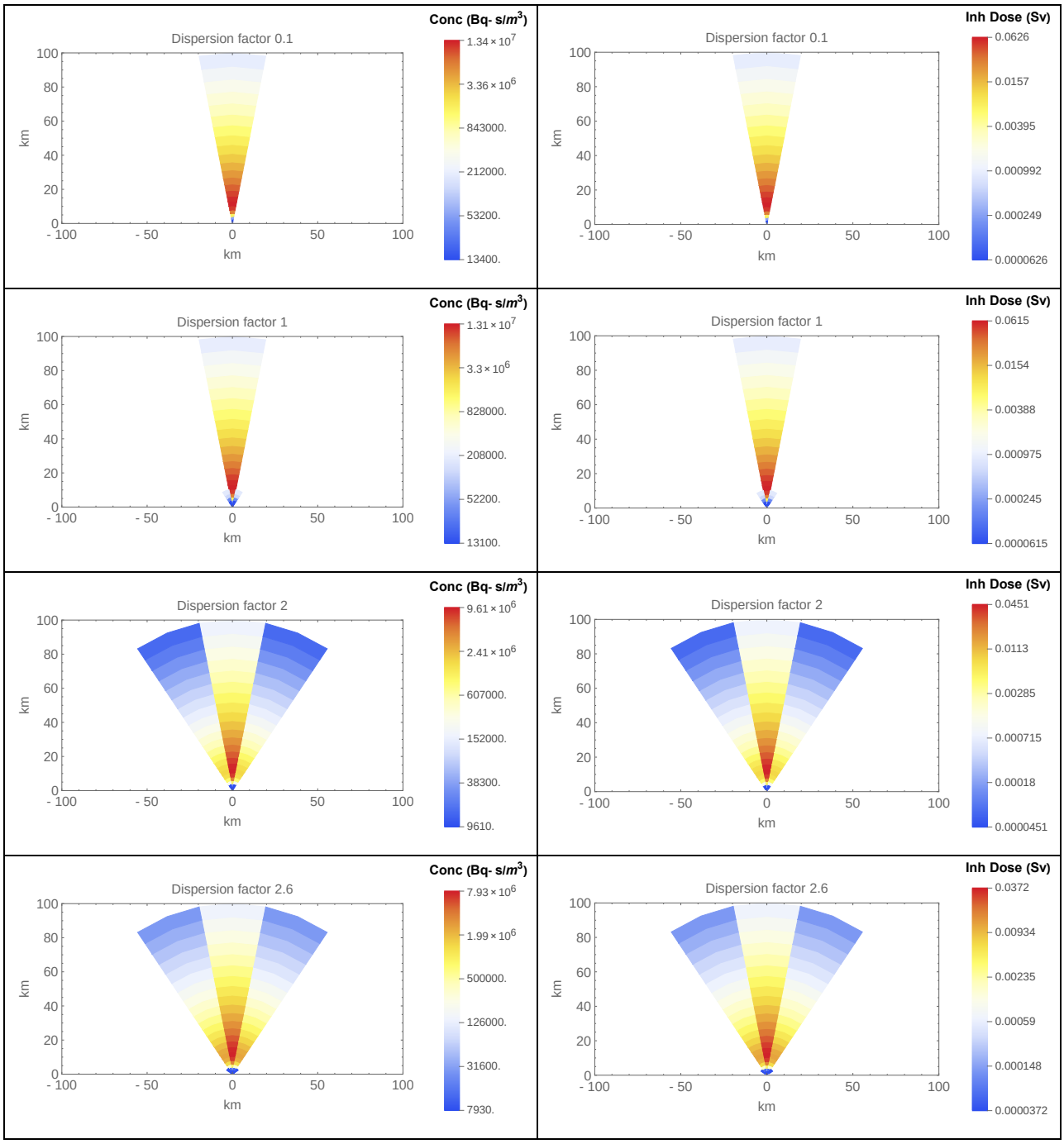

Figure 3-23. Sector plots of Type D average air concentration at the ground level and Type C average inhalation dose, with a color scheme representing a log-scale in the dose and population dose and truncated to span 3 orders of magnitude.

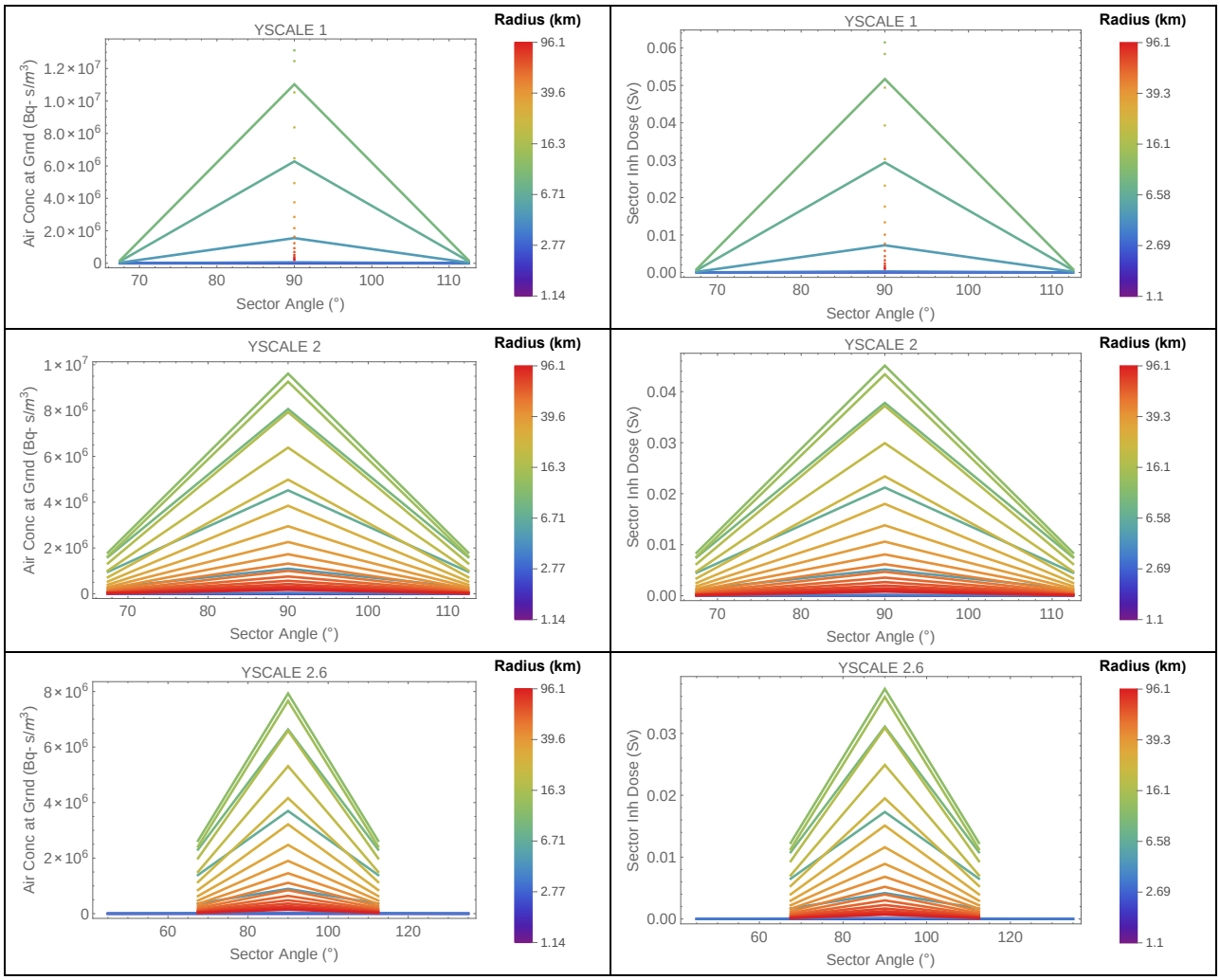

Figure 3-24. Sector average air concentration at the ground level (Type D output) and sector average inhalation dose (Type C output) versus sector angle and radial distance to the source. The color scheme represents radial distances in a log-scale (blue for near distances and red for far distances).

YSCALE = 1 and variable ZSCALE

A final test was implemented to independently examine variation of vertical dispersion. The following figure compares the Type A maximum dose to the Type 6 centerline dose.

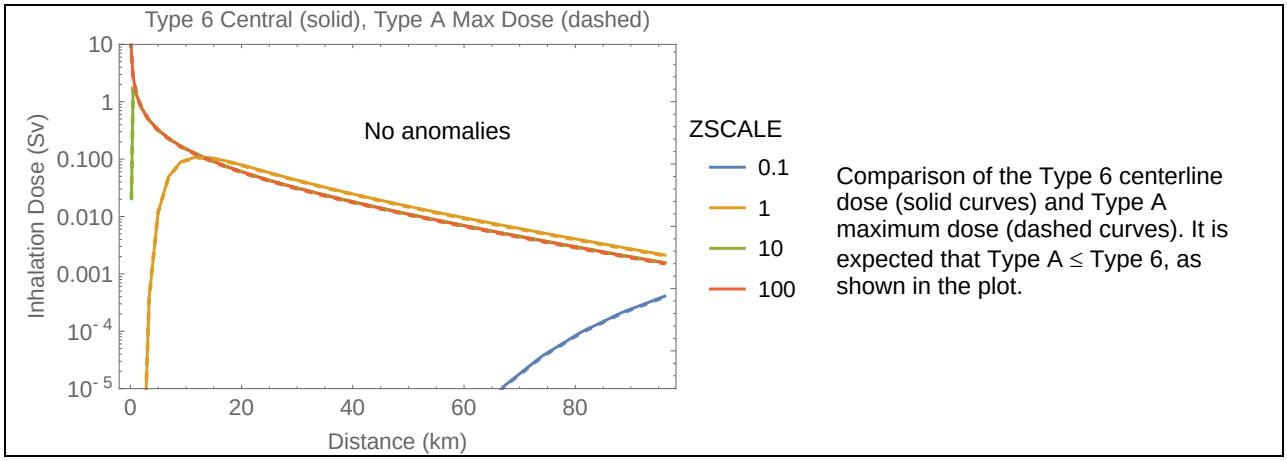

Figure 3-25. Comparison of Type centerline inhalation dose (solid curves) to the Type A maximum dose (dashed curves).

Figure 3-26 shows no anomalies in the population dose and health effects. The plots compare the MACCS outputs (symbols) to independent computations (solid curves). The MACCS outputs agree with the expected results. For the case ZSCALE = 0.1, the plume is narrow and the inhalation dose is small (source height = 500 m). Other cases correspond to wider plumes, causing greater Cs-137 air concentration at the ground level. The cases ZSCALE = 10 and ZSCALE = 100 correspond to well spread plumes along the vertical direction, and the results are nearly identical. There were no anomalies in the results.

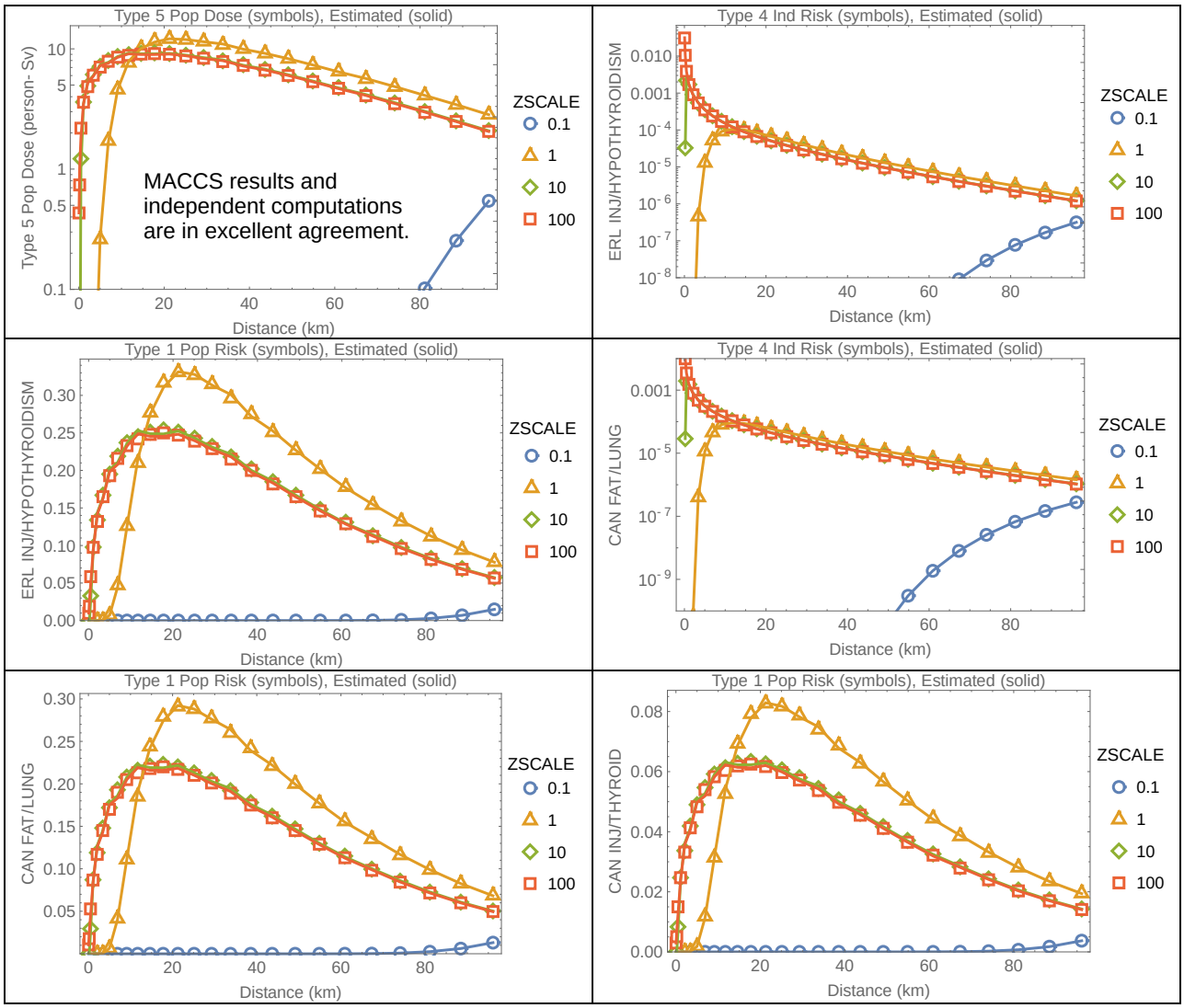

Figure 3-26. Comparison of Type 5 population dose, Type 4 average individual risk, and Type 1 population health effects (from inhalation of radioactivity in a plume) to independent computations. The MACCS outputs are in excellent agreement with the independent computations.

3.4.4 Test Conclusions

MACCS Version 4.1 successfully passed the designed tests. There were no anomalies in the MACCS outputs.

3.5 Test 3.5: Off-Center Sector Air Concentrations and Cloudshine Doses

The EARLY module considers fine grid concentrations/doses to compute a coarse sector representative concentration/dose, as an average of the fine grid concentrations/doses. The computation of coarse sector averages was examined in Tests 2.1 and 3.1, but focusing only on central sectors (i.e., north sectors in the test runs). In this test, the examination is extended to concentrations in non-central sectors (i.e., other sectors than the north sectors).

If dry and wet deposition is ignored and radioactive decay is negligible, air concentrations at an arbitrary 3D location (x, y, z) can be computed using Eqs. (2-1) and (2-2). However, MACCS tracks results in a cylindrical grid; thus, MACCS requires transformation of cylindrical to Cartesian coordinates to use Gaussian steady-state concentration functions expressed in Cartesian coordinates. If (r, θ, z) are the equivalent cylindrical coordinates of a point (x, y, z), with the radial distance r measured with respect to source location, and the angle θ measured with respect to the east direction, the integrated air concentration at a point (r, θ, z) should be computed as

$$\chi(r \sin\theta\,, r\cos\theta\,, z) \tag{3-10}$$

$\chi(x,y,z)$	—	integrated air concentration defined by Eq. (2-1), Bq-s/m^3
r	—	radial distance to the source, m
θ	—	angle measured with respect to the east direction
z	—	vertical distance, m

However, MACCS does not implement a strict cylindrical to Cartesian coordinates conversion. Instead, MACCS adopts a narrow plume approximation, which does not require trigonometric functions:

$$\begin{aligned} x &\approx r \\ y &\approx \left(\theta - \frac{\pi}{2}\right) r \end{aligned} \tag{3-11}$$

This approximation is valid for θ angles close to $\pi/2$ and becomes inaccurate for angles far from $\pi/2$. See Figure 3-27 for a graphical representation of the approximation, and how the narrow plume approximation diverges for sectors towards the east or west directions. MACCS computes the integrated air concentration at an arbitrary location (r, θ, z) as

$$\chi\left(r, r\,\theta - r\frac{\pi}{2}, z\right) \tag{3-12}$$

which, again, is a good approximation to Eq. (3-10) for θ angles close to $\pi/2$.

The objective of the test was to examine the use of Eq. (3-12) to compute representative or average air concentrations of sectors. Average concentrations were independently computed and compared to Type D outputs. The test was extended to include the cloudshine dose. Per Eq. (3-3), the cloudshine dose at any receptor location (located on the ground) of Cartesian coordinates (x, y) is computed based on the plume centerline air concentration $\chi(x, y = 0, z = h)$ (h is the source height, 500 m in the test runs), and the cloudshine factor computed at the location (x, y). The cloudshine factor, $C(\sigma, rrd)$, is computed by linear interpolation from a lookup table as a function of two independent variables, the effective plume size σ and the relative receptor distance, rrd, defined as

$$\sigma(x) = \sqrt{\sigma_y(x)\,\sigma_z(x)}$$

$$rrd(x,y) = \frac{\sqrt{h^2+y^2}}{\sigma(x)} = \sqrt{\frac{h^2+y^2}{\sigma_y(x)\,\sigma_z(x)}} \quad (3\text{-}13)$$

$\sigma_y(x)$ — lateral, acrosswind, Gaussian dispersion coefficient, m
$\sigma_z(x)$ — vertical Gaussian dispersion coefficient, m
h — source height, m
(x,y) — receptor coordinates on the ground, m

The cloudshine dose at an arbitrary location (x, y) is proportional to the factor

$$\chi(x,0,h)\; C[\sigma(x), rrd(x,y)] \quad (3\text{-}14)$$

MACCS implements the narrow plume approximation of Eq. (3-11) in the computation of the cloudshine dose to transform polar to Cartesian coordinates. Specifically, the cloudshine dose at a position on the ground of polar coordinates (r,θ) is computed in MACCS as

$$DC_k(r,\theta) = DRCC_{\infty k}\;\chi(r,0,h)\;C\left[\sigma(r), rrd(r, r\,\theta - r\frac{\pi}{2})\right]\;F\;SFC \quad (3\text{-}15)$$

$DC_k(r,\theta)$ — cloudshine dose to organ k at the location (r,θ) (Sv)
$DRCC_{\infty k}$ — semi-infinite cloudshine dose coefficient to organ k for a specific radionuclide (Sv-m^3/Bq-s) (=9.28×10^{-17} S-m^3/Bq-s for Cs-137 in the test problem)
$\chi(r,0,h)$— integrated air concentration at the plume centerline (Bq-s/m^3), Eqs. (2-1) and (2-2)
$C[\cdots]$ — cloudshine factor computed at the position $x = r, y = r\,\theta - r\frac{\pi}{2}$
F — fraction of the exposure time (=1, for non-evacuating and non-relocating individuals)
SFC — cloudshine protection factor specified by CSFACT (CSFACT = 1 in the test runs)

The test examined the MACCS implementation of Eq. (3-15) to compute the cloudshine dose in non-central sectors (i.e., sectors at other orientations than π/2 or 90°).

3.5.1 Test Input

The input was identical to the Test 3.3, with the following changes:

ATMOS
- Deposition / Wet/Dry Depos Flags
  - DRYDEP=WETDEP=False for Cs-137 (no wet deposition, no dry deposition)
- Dispersion / Scaling Factors
  - YSCALE = 1, 2, 2.6
  - ZSCALE = 1

EARLY
- Shielding and Exposure (**Set 1**)
  - PROTIN = 1, inhalation dose pathway only
  - BRRATE = 1 m^3/s, exaggerated breathing rate to cause sizable risk

    - CSFACT (cloudshine) = SKPFAC (skin dose) = GSHFAC (ground dose) = 0
- Shielding and Exposure **(Set 2**)
    - CSFACT = 1, cloudshine pathway only
    - PROTIN (inhalation) = SKPFAC (skin dose) = GSHFAC (ground dose) = 0

Identical outputs than Test 3.3 were used.

3.5.2 Test Procedure

The MACCS code was executed to simulate a case of

- Wind blowing in the north direction at constant speed (10 m/s)
- No dry/wet deposition
- Release and transport of Cs-137 only (long-lived radionuclide)
- One plume segment

Several runs of the MACCS code with variable lateral dispersion coefficient were executed with the following inputs, ZSCALE = 1 (vertical Gaussian dispersion coefficient factor) and

- YSCALE = 1
- YSCALE = 2
- YSCALE = 2.6

Two sets of runs were executed, in the Set 1, the shielding and exposure flags were set to output only inhalation doses, and in the Set 2, the shielding and exposure flags were set to output only cloudshine doses.

An alternative method was designed to compute representative average concentrations and cloudshine doses of coarse spatial sectors. Points were sampled within a coarse sector (e.g., north-north-east, NNE, sector), exemplified by the red points in Figure 3-27. The red dots in Figure 3-27 are located along an arc of constant radius passing through the center of each of the three sectors and at equidistant angles. The sector average concentration/cloudshine dose was defined as the average of the air concentrations/cloudshine doses computed at the red points falling within a sector. To increase accuracy of the mean, the average was computed based on a numerical line integral determined by trapezoidal integration. The average so computed must be equivalent to Type D sector average concentrations output by the EARLY module in the case of air concentrations, and to Type C sector average doses in the case of cloudshine doses. The objective of the test was verifying that Type D sector average concentrations and Type C sector average cloudshine doses are equivalent to concentrations/doses computed with the independent average method, accounting for the MACCS narrow plume approximation, Eq. (3-12). An additional test was designed to consider accurate polar to Cartesian coordinate transformation, to evaluate the effect of the MACCS narrow plume approximation. Figure 3-27 displays points located on a horizontal line (constant x). Those points are the true locations where concentrations and doses are computed, using the MACCS narrow plume approximation in the north-north-east (NNE) and north-east (NE) sectors.

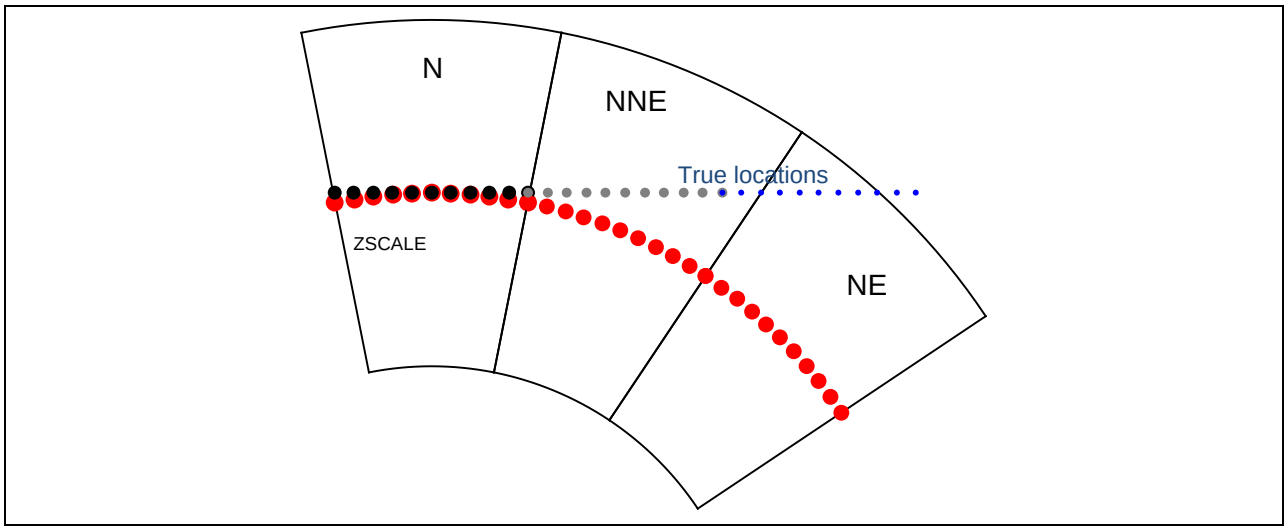

Figure 3-27. Example of red points sampled within three sectors (N, NNE, NE) to compute average concentrations or cloudshine doses. The red points fall along a constant radius arc passing through the center of each sector and are located at equidistant angles.

3.5.3 Test Results

Air Concentrations at the Ground Level, Set 1 Runs

Figure 3-28 displays sector plots prepared with Type D MACCS outputs, air concentration at the ground level. The color scheme represents concentrations in log-scale (red for high concentration, blue for low concentration). Each plot corresponds to a different value of the dispersion coefficient factor YSCALE. The dashed lines in each plot enclose a region ± 2.15 $\sigma_y(x)$ around the center, with a distance 2.15 $\sigma_y(x)$ measured along constant-radius arcs (r=x). The boundaries define the point at which the concentration becomes a factor of 10 lower than the central concentration. The ± 2.15 $\sigma_y(x)$ boundaries are practical boundaries in MACCS to define sectors with non-zero concentrations and to avoid numerical underflow. Figure 3-28 verifies that the sectors farthest away from the center with non-zero concentrations are the sectors intercepting the ± 2.15 $\sigma_y(x)$ boundaries, as expected.

Plots in Figure 3-29 compare the MACCS outputs to average concentrations independently computed. The plots display the sector average air concentration at the ground level versus the radial distance (distance measured with respect to the source), for the different runs (different cases of YSCALE dispersion factor). MACCS outputs are represented by symbols and the independent computations by the solid curves. The different plots correspond to different sector sets oriented at specific angles (90°, 67.5°, and 45°).

Figure 3-29 shows reasonable agreement between the MACCS Type D concentrations and the independent computations. There are differences in the concentrations in the north-east (45°) sectors, most likely due to round-off error and the different treatment of concentrations beyond the ± 2.15 $\sigma_y(x)$ boundaries in the independent computations.

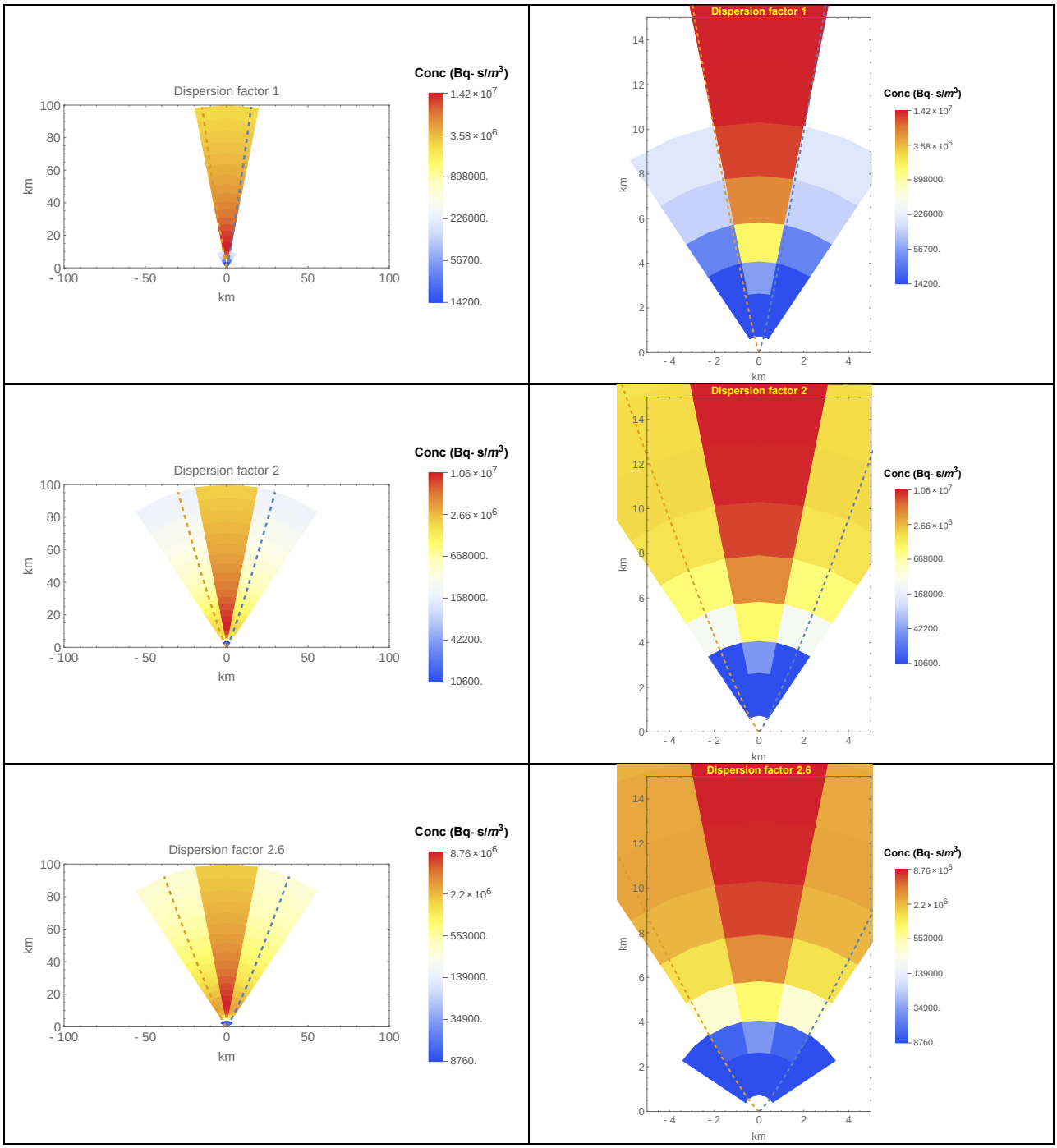

Figure 3-28. MACCS Type D sector average air concentrations at the ground level for different cases of YSCALE. Plots on the right are amplified scale plots. The dashed curves represent the ± 2.15 $\sigma_y(x)$ boundaries.

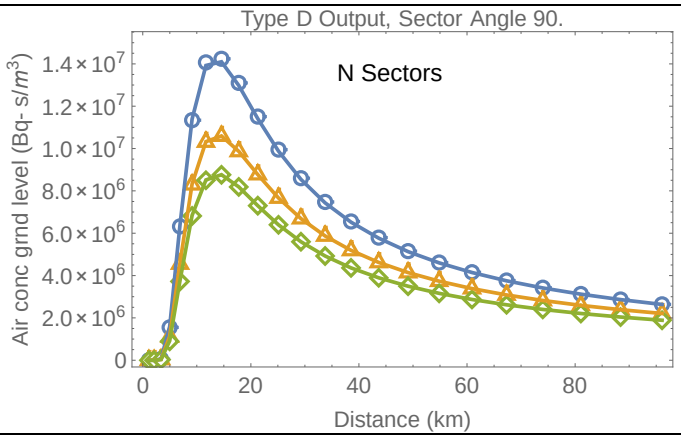

Sector average air concentration at the ground level versus radial distance. MACCS results, Type D concentrations, are indicated by symbols and the independent computations by solid curves. The results are in excellent agreement for the 90° sectors (north sectors).

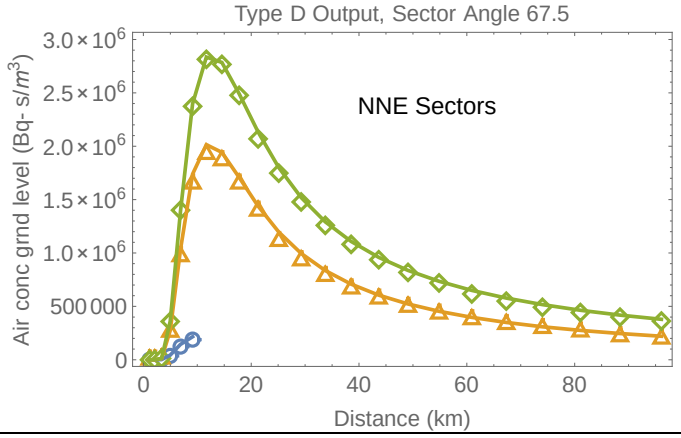

Same type of data as in the previous plot, but for north-north-east sectors. The results are in excellent agreement for the 67.5° sectors.

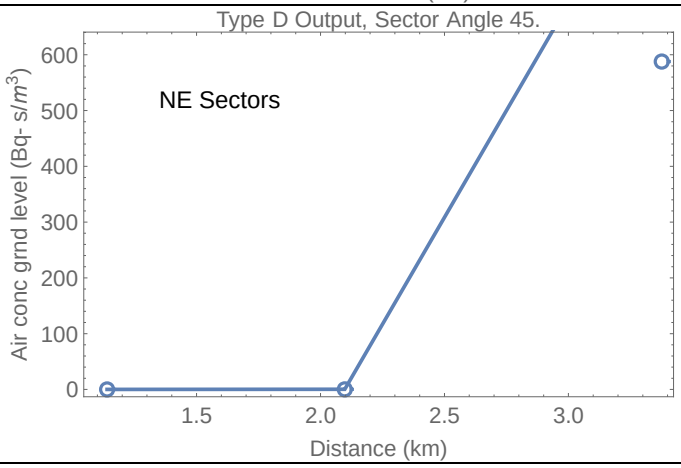

Same type of data as in the previous plot, but for north-east sectors. The results are comparable for the 45° sectors. It is likely that differences are due to round-off errors and different treatment of concentrations beyond the ±2.15 σ_y boundaries in the independent computations.

Figure 3-29. Type D sector average air concentration (symbols) versus radial distance for sectors of different orientation compared to independently computed average air concentrations (solid curves).

Figure 3-30 presents similar information than Figure 3-29, in the form of concentration versus the sector angle. Each plot corresponds to different values of the dispersion factor YSCALE. The color code is based on the radial distance (blue for short distance, red for far distance) in logarithmic scale. The plots indicate there is excellent agreement between the MACCS results (symbols) and the independent computations (solid lines). The last plot, with points at 45°, makes evident that differences in Figure 3-29 correspond to very small air concentrations.

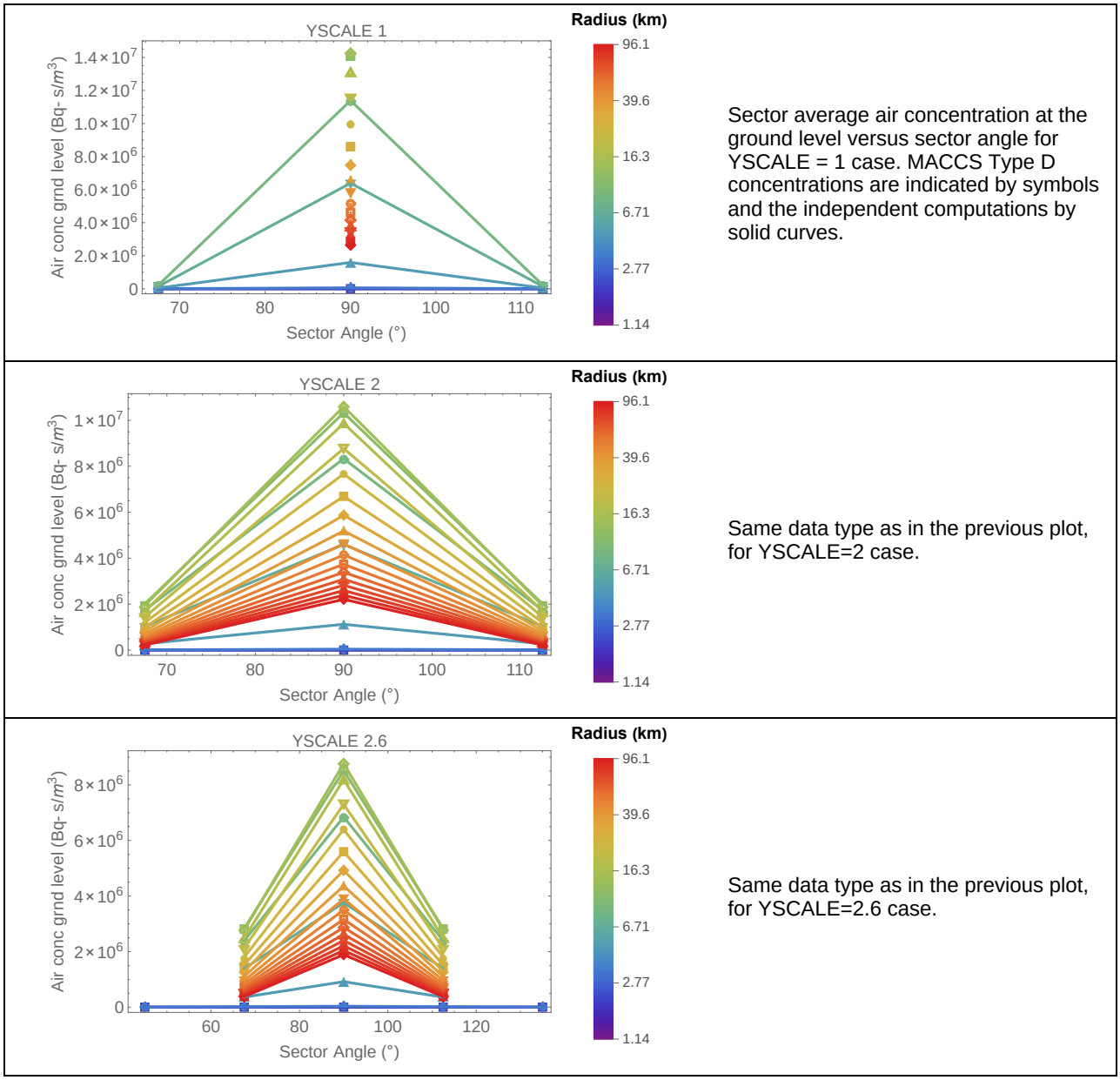

Figure 3-30. Comparison of Type D sector average air concentrations (symbols) versus sector angle to independent computations (solid lines) for different cases of YSCALE.

It is highlighted that the independent computations also adopted the MACCS narrow plume approximation to transform polar coordinates to Cartesian coordinates, Eq. (3-11). The approximation becomes inaccurate for sectors away from north. For example, the points along a horizontal (constant x) line in Figure 3-27, represent the true locations where concentrations

and doses are effectively computed by MACCS to define averages on the polar grid. Only in the north sector are the true locations close to the red point locations in Figure 3-27. The MACCS polar locations (red dots in Figure 3-27) increasingly deviate from the true locations in north-north-east and north-east sectors. The MACCS narrow plume approximation should be kept in mind when using MACCS for consequence assessments, because it could lead to non-intuitive results especially when examining consequences of radionuclide releases under atmospheric conditions of low stability (leading to the formation of broad plumes). To explore the effect of the MACCS narrow plume approximation, an additional test was performed adopting a strict polar to Cartesian coordinate conversion, i.e.,

$$x = r \sin\theta$$
$$y = r \cos\theta \tag{3-16}$$

Concentrations and average concentrations computed along constant radius arcs were computed and compared to the MACCS outputs, following the described approaches, and using the Eq. (3-16) transformation. The results are displayed in Figure 3-31. In the north sectors, the MACCS Type D outputs are in excellent agreement with the independent computations accounting for precise polar to Cartesian conversions, as expected. For non-central sectors, the MACCS Type D outputs tend to be greater than the independently computed average concentrations. However, the independent results are still relatively close to the MACCS outputs for the NNE sectors. In testing performed with MACCS Version 4.0, which allowed laterally broader plumes, there were differences that increased in sectors away the north sector (i.e., increasing differences in the sector sequence NNE, NE, ENE, E), and always with MACCS Type D outputs greater than the independently computed values considering precise polar to Cartesian coordinate conversions. Those differences are constrained in MACCS Version 4.1 by limiting the allowed values of lateral Gaussian dispersion coefficients. In the tests, no examples were found with outputs beyond the 45° or NE sectors.

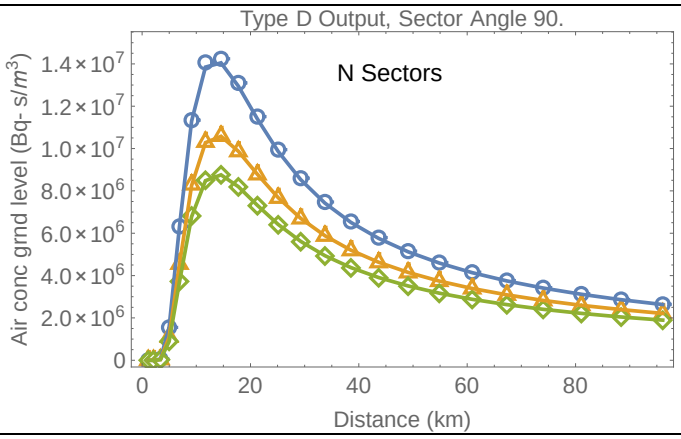

YSCALE
1
2
2.6

Sector average air concentration at the ground level versus radial distance. MACCS results, Type D concentrations, are indicated by symbols and the independent computations by solid curves. The results are in excellent agreement for the 90° sectors (north sectors).

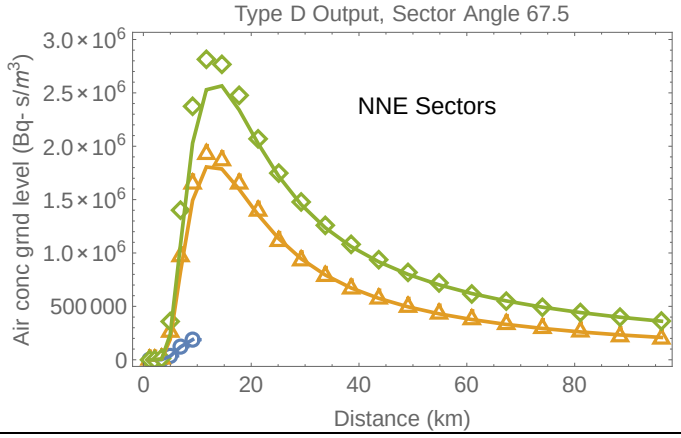

YSCALE
1
2
2.6

Same type of data as in the previous plot, but for north-north-east sectors. The independent computations (solid curves) with accurate polar to Cartesian coordinate conversion tend to be below the MACCS outputs.

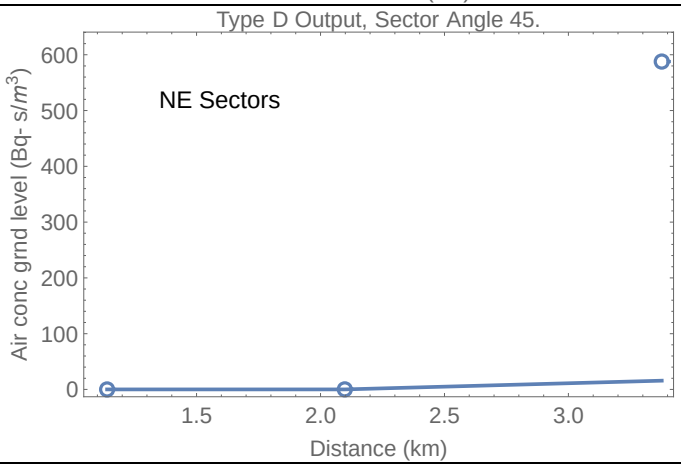

YSCALE
2.6

Same type of data as in the previous plot, but for north-east sectors. The independent computations (solid curves) with accurate polar to Cartesian coordinate conversion are below the MACCS outputs.

Figure 3-31. Type D sector average air concentration (symbols) versus radial distance for sectors of different orientation compared to independently computed average air concentrations (solid curves) using accurate polar to Cartesian coordinate conversion.

Cloudshine Dose, Set 2 Runs

Figure 3-32 compares the Type 6 MACCS centerline cloudshine doses (symbols) to independently computed cloudshine doses (solid curves) based on Eq. (3-15) with angle θ=90°=π/2 radians. The Type 6 centerline doses are in excellent agreement with the independent computations. Figure 3-33 compares the Type C sector average doses (L-ICRP60 cloudshine dose, symbols) to independently computed average doses (solid curves) based on the method described in Section 3.5.2.

There is reasonable agreement between the MACCS Type C outputs and the independently computed doses in Figure 3-33, with differences possibly due to different interpolation algorithms to compute the cloudshine factor. The differences in the middle plot of Figure 3-33 are likely related to jumps noted in other tests of the Type C cloudshine dose (e.g., Figure 2-6, Figure 2-7, Figure 3-8, Figure 3-9, and Figure 3-17), and explained due to differences in interpolation algorithms to compute the cloudshine factor for cases of large effective plume size, σ, and small relative receptor distance, rrd. To complete the test, additional independent computations were executed considering the accurate polar to Cartesian coordinate conversion, Eq. (3-16), in the computation of the cloudshine dose and the Type C average cloudshine dose. The independent computations (solid curves) and the corresponding Type C MACCS outputs (symbols) are displayed in Figure 3-34.

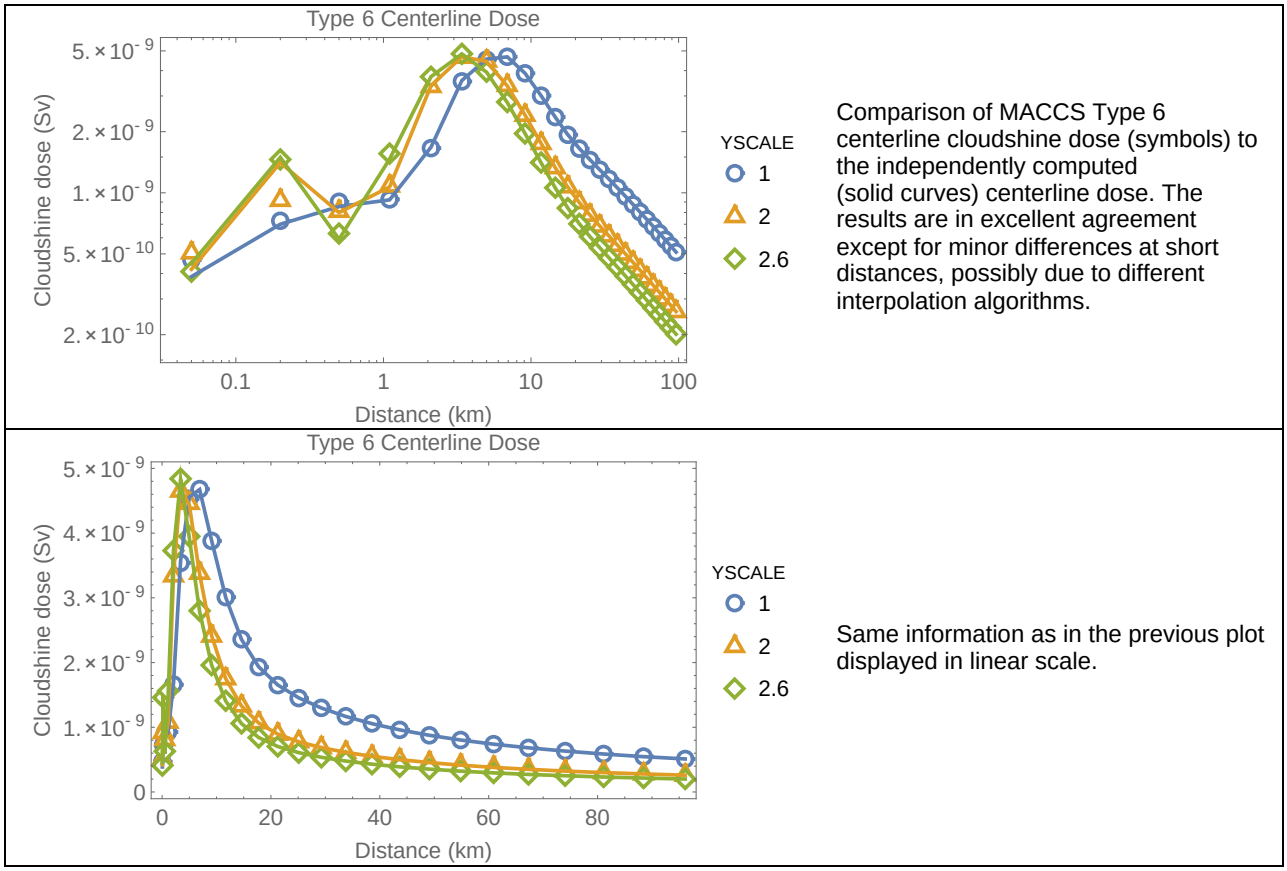

Figure 3-32. Comparison of Type 6 centerline dose outputs (symbols) to independent computations (solid curves) in logarithmic and linear scales.

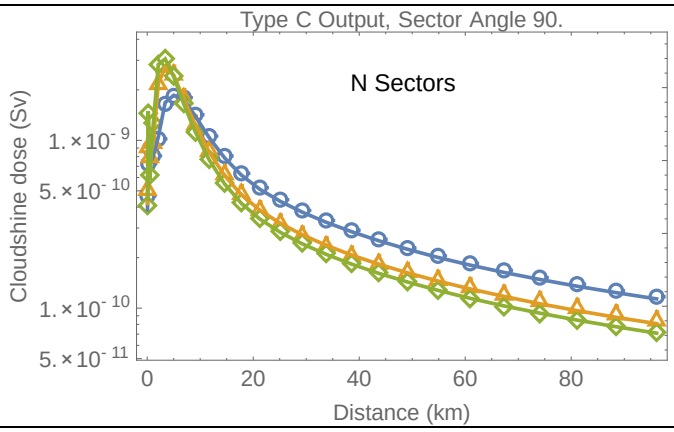

YSCALE
1
2
2.6

Comparison of MACCS Type C cloudshine dose (symbols, L-ICRP60ED) to the independent computations (solid curves) for north sectors. The results are in excellent agreement.

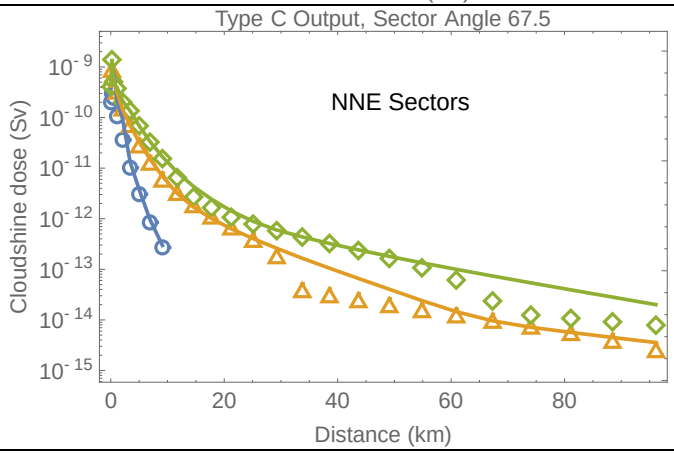

YSCALE
1
2
2.6

Same data type as in the previous plot, for north-north-east sectors. The results are in excellent agreement, except at far distances for the cases YSCALE = 2 and 2.6. Those differences are very likely due to differences in interpolation algorithms to compute the cloudshine factor for cases of large effective plume size and small relative receptor distance. Those differences may be related to jumps noted in other tests of the Type C cloudshine dose (e.g., Figure 2-6, Figure 2-7, Figure 3-8, Figure 3-9, and Figure 3-17)

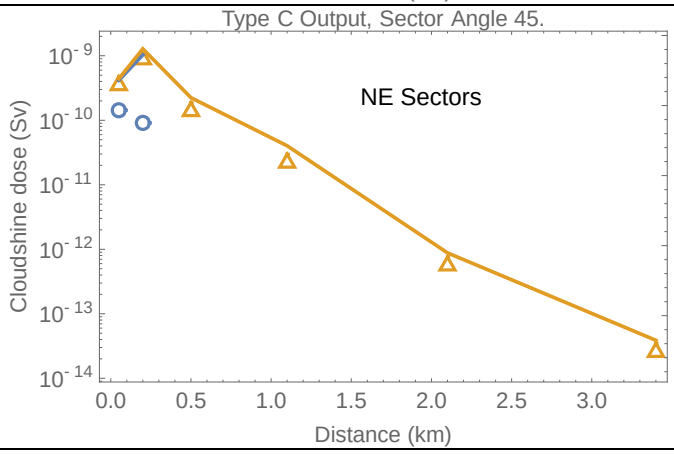

YSCALE
2
2.6

Same data type as in the previous plot, for north-east sectors. The results are in reasonable agreement, with differences possibly due to different interpolation algorithms to compute the cloudshine factor.

Figure 3-33. Type C sector average cloudshine dose versus radial distance for different sectors (symbols), compared to independent computations (solid curves) using the MACCS narrow plume approximation, Eq. (3-11).

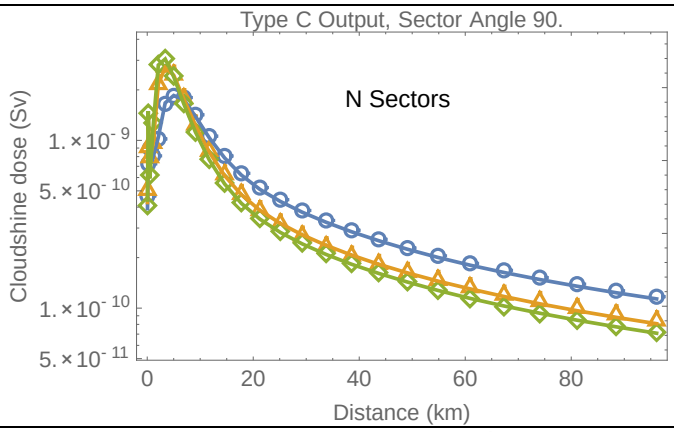

YSCALE
1
2
2.6

Comparison of MACCS Type C cloudshine dose (symbols, L-ICRP60ED) to the independent computations (solid curves) for north sectors. The results are in excellent agreement.

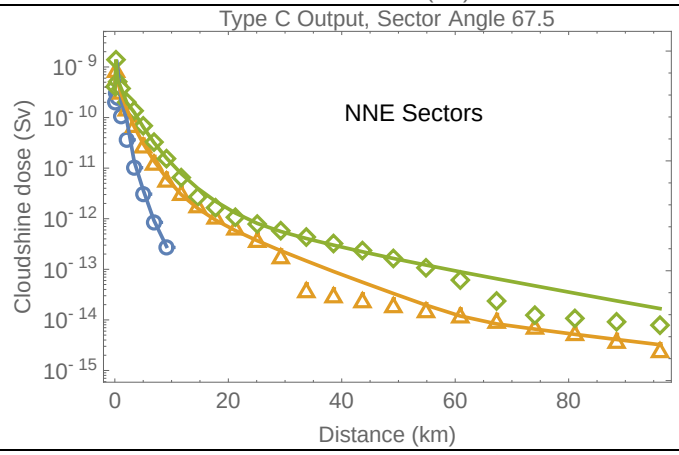

YSCALE
1
2
2.6

Same data type as in the previous plot, for north-north-east sectors. The results are in excellent agreement, except at far distances for the cases YSCALE = 2 and 2.6. Those differences are very likely due to differences in interpolation algorithms to compute the cloudshine factor for cases of large effective plume size and small relative receptor distance. Those differences may be related to jumps noted in other tests of the Type C cloudshine dose (e.g., Figure 2-6, Figure 2-7, Figure 3-8, Figure 3-9, and Figure 3-17)

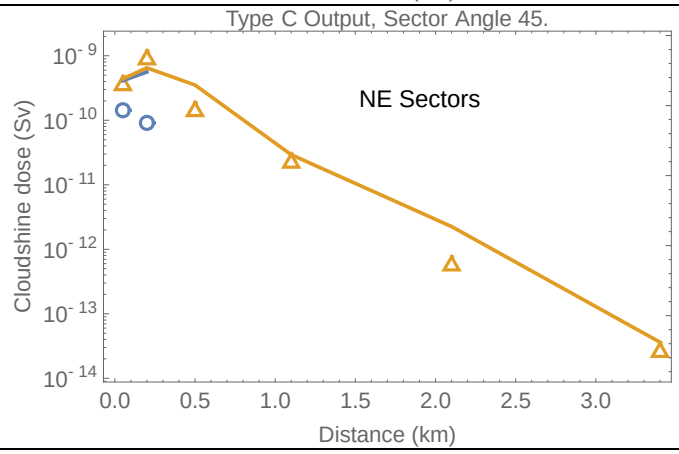

YSCALE
2
2.6

Same data type as in the previous plot, for north-east sectors. The results are in reasonable agreement, with differences possibly due to different interpolation algorithms to compute the cloudshine factor

Figure 3-34. Type C sector average cloudshine dose versus radial distance for different sectors (symbols), compared to independent computations (solid curves) using the accurate polar to Cartesian coordinate conversion, Eq.(3-16).

The results of the independent computations in Figure 3-34, using the accurate polar to Cartesian coordinate conversion, Eq.(3-16), are very similar to results in Figure 3-33, using the MACCS narrow plume approximation to transform polar to Cartesian coordinates, Eq. (3-11), with the greatest differences exhibited in the north-east sector (45° sector). It may be concluded that that extending the narrow plume approximation to sectors other than the central sectors does not seem to significantly degrade the results, although caution is recommended to generalize this conclusion for any situation. In the tests, no examples were found with outputs beyond the 45° or north-north-east sectors. For example, increasing YSCALE from 2.6 to 2.7 triggers an error message in MACCS Version 4.1 and the run is aborted. The user is requested by MACCS to reduce the extent of lateral dispersion for the run to proceed.

3.5.4 Test Conclusions

The MACCS Type D air concentrations and Type C cloudshine doses in off-center sectors agreed with independently computed values. The following aspects of the MACCS computations were verified:

- MACCS adopts a narrow plume approximation to transform polar coordinates to Cartesian coordinates in the computation of time-integrated air concentrations and cloudshine doses, in the central sector and any other sector.

- MACCS applies a criterion based on a ± 2.15 $\sigma_y(x)$ arc distance around a centerline to identify sectors that are output in result files with non-zero concentrations.

- Averages based on numerical line integrals along constant-radius arcs well reproduced the MACCS Type D average time-integrated air concentrations and the Type C average cloudshine doses.

There were some differences, associated with very small concentrations, in the Type D MACCS results with respect to the designed benchmarks possibly due to the different treatment of concentrations beyond the 2.15 $\sigma_y(x)$ limits in the independent computations. Also, there were some differences in the Type C cloudshine doses possibly due to different interpolation algorithms to compute the cloudshine factor. Those differences are not considered to be errors of the MACCS code. They reflect the fact that the independent computations were not intended to precisely incorporate all the details of the MACCS computations. Minor differences with respect to the designed benchmarks were expected.

MACCS Version 4.1 introduced limits to avoid simulations with very broad plumes. For example, in the test problems, simulations with YSCALE=2.6 were allowed, but simulations with YSCALE=2.7 were aborted by MACCS Version 4.1. The farthest sectors with non-zero concentrations were the 45° or north-north-east sectors in the tests. Although the MACCS narrow plume approximation tends to overestimate the Type D average concentrations, the results are still comparable to detailed simulations using accurate polar to Cartesian coordinate conversions. Similarly, independent computations using accurate polar to Cartesian coordinate conversions to compute Type C cloudshine doses produced results very similar to computations based on the MACCS narrow plume approximation. The comparison of results using the narrow plume approximation to results relying on accurate polar to Cartesian coordinate conversions suggests that errors caused by the narrow plume approximation in non-central sectors are not significant provided broad plumes are avoided. Only a few examples were examined, however, so caution is recommended in generalizing this conclusion to any scenario.

3.6 Test 3.6: Potassium Iodide Ingestion Model

The objective of this test was examining the implementation of the potassium-iodide (KI) ingestion model. The ingestion of KI pills to mitigate the effect of inhalation of radioactive isotopes of iodine is simulated in MACCS as an adjustment factor to the dose (equation 4-4 of the MACCS Theory Manual):

$$DP_{I,thyroid} = (1 - \varepsilon_{KI})\, DB_{I,thyroid} \tag{3-17}$$

$DP_{I,thyroid}$ — thyroid dose from inhalation of radioiodine considering ingestion of KI pills (Sv)

$DB_{I,thyroid}$ — thyroid dose from inhalation of radioiodine without any mitigation effects by the ingestion of KI pills (Sv)

ε_{KI} — Efficacy factor to reduce the radioiodine (1 = 100% effectivity, 0 = no effectivity), specified by EFFACY

In addition, the MACCS code includes another factor, POPFRAC, to define the fraction of people taking KI pills. To simplify computations, MACCS computes individual inhalation doses as a weighted average of the dose by individuals taking KI pills and those not taking any KI pills:

$$\overline{DP}_{I,thyroid} = POPFRAC\ (1 - \varepsilon_{KI})\, DB_{I,thyroid} + (1 - POPFRAC)\, DB_{I,thyroid} \tag{3-18}$$

$\overline{DP}_{I,thyroid}$ — average thyroid dose from inhalation of radioiodine considering ingestion of KI pills, and the fraction of the population taking and not taking KI pills (Sv)

Note that when ε_{KI} = EFFACY = 1, Eq. (3-18) reduces to

$$\overline{DP}_{I,thyroid} = (1 - POPFRAC)\, DB_{I,thyroid} \tag{3-19}$$

And when POPFRAC=1, Eq. Eq. (3-18) becomes

$$\overline{DP}_{I,thyroid} = (1 - \varepsilon_{KI})\, DB_{I,thyroid} \tag{3-20}$$

Both Eqs. (3-19) and (3-20) are identical. Therefore, a run with EFFACY = 1 and POPFRAC = 0.25 must yield identical inhalations doses to a run with POPFRAC = 1 and EFFACY = 0.25. This test was implemented herein, as well as a test of the linearity of Eqs. (3-19) and (3-20).

3.6.1 Test Input

The input was identical to the Test 3.3, with the following changes:

General Properties

- DOSE
  - Linear No Threshold
  - Activate KI Model: TRUE

Changes to specific input parameters

ATMOS

- Radionuclides/Pseudostable Radionuclides
  - Remove I-129 from list
- Radionuclides/Radionuclides
  - Add I-129 to list
- Release Description/Release Fractions
  - RELFRC
    - I = 1
    - Other elements = 0
- Deposition, Wet/Dry Depos Flags
  - DRYDEP = WETDEP = False for I-129
- Dispersion/Scaling Factors
  - YSCALE = ZSCALE = 1
- Output Control
  - NUCOUT = I-129

EARLY

- Emergency Cohort One/KI Ingestion Linear No Threshold
  - POPFRAC = 1, EFFACY = 0, 0.25, 0.5, 0.75, 1.0
  - POPFRAC = 0, 0.25, 0.5, 0.75, 1.0, EFFACY = 1
- Shielding and Exposure
  - PROTIN = 1, inhalation dose pathway
  - BRRATE = 1 m^3/s, exaggerated breathing rate to cause sizable risk
  - CSFACT (cloudshine) = SKPFAC (skin dose) = GSHFAC (ground dose) = 0

Output Controls

- The same outputs of Test 3.3 were used.

3.6.2 Test Procedure

Two sets of MACCS runs were executed with the following inputs:

Set 1

- POPFRAC = 1
- EFFACY = 0, 0.25, 0.5, 0.75, 1.0

Set 2

- POPFRAC = 0, 0.25, 0.5, 0.75, 1.0
- EFFACY = 1

The results from Set 1 must be identical to the results from Set 2. Results from Set 1 must exhibit linear variation with the variable EFFACY. Results from Set 2 must exhibit linear variation with the variable POPFRAC. The following results were compared between Sets 1 and 2:

- Type C sector average dose
- Type 6 centerline dose
- Type 5 population dose
- Type 1 health effects
- Type 4 average individual risk

- Type 8 population-weighted individual risk

In addition, it was demonstrated that Type C results vary linearly with EFFACY for the Set 1 runs and vary linearly with POPFRAC for the Set 2 runs.

3.6.3 Test Results

Figure 3-35 displays Type C sector average inhalation doses. Type 6 centerline inhalation doses are presented in Figure 3-36. The plots in Figure 3-35 and Figure 3-36 demonstrate that the Set 1 runs (POPFRAC = 1, EFFACY = 0, 0.25, 0.5, 0.75, 1.0) and the Set 2 runs (POPFRAC = 0, 0.25, 0.5, 0.75, 1.0, EFFACY = 1) output identical results. The Set 1 results are indicated with symbols, and the Set 2 results with solid curves. The plot legend represents values of EFFACY for Set 1, or values of POPFRAC for Set 2.

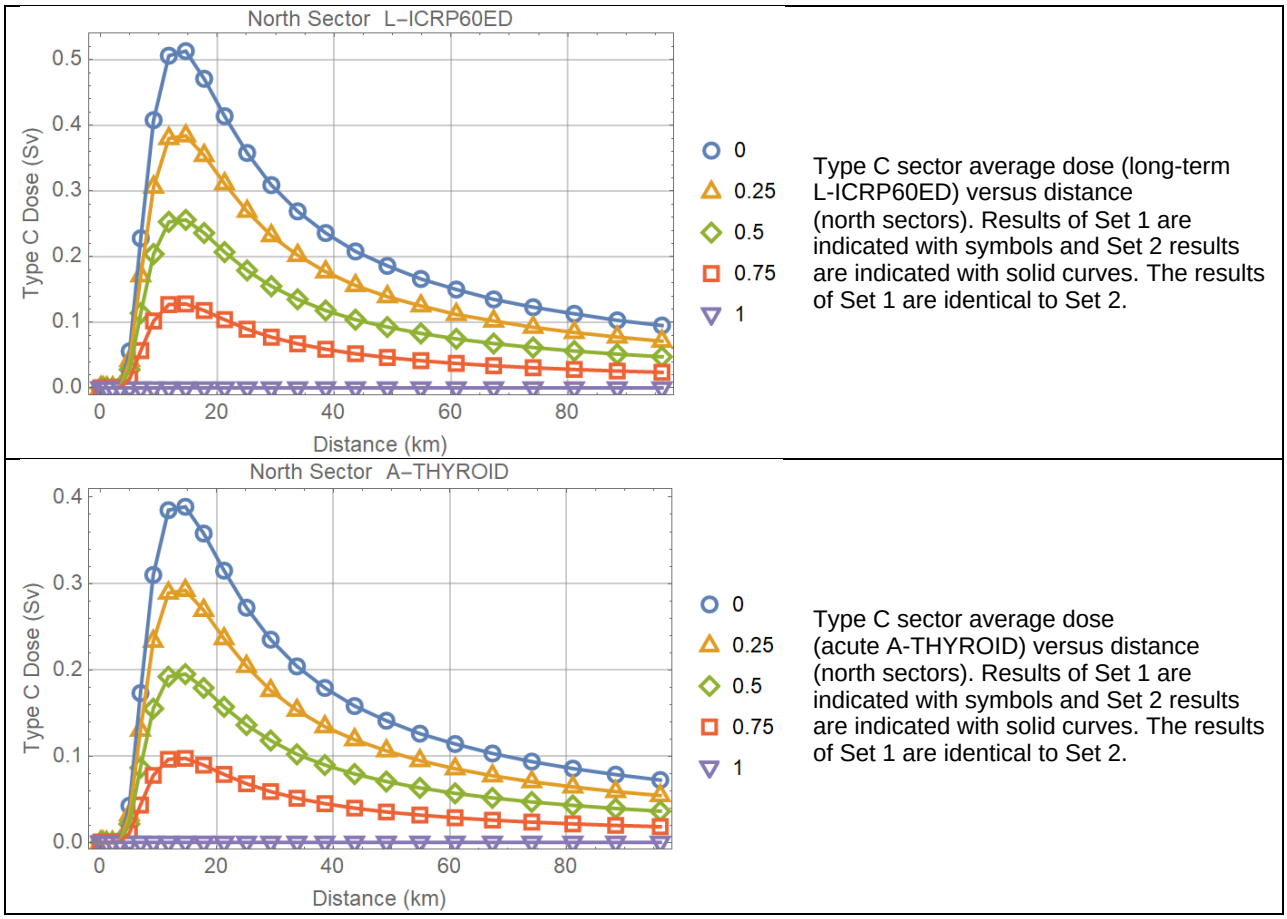

Figure 3-35. Type C inhalation dose versus distance. Each plot displays a different kind of Type C dose. The plots compare Set 1 and Set 2 results.

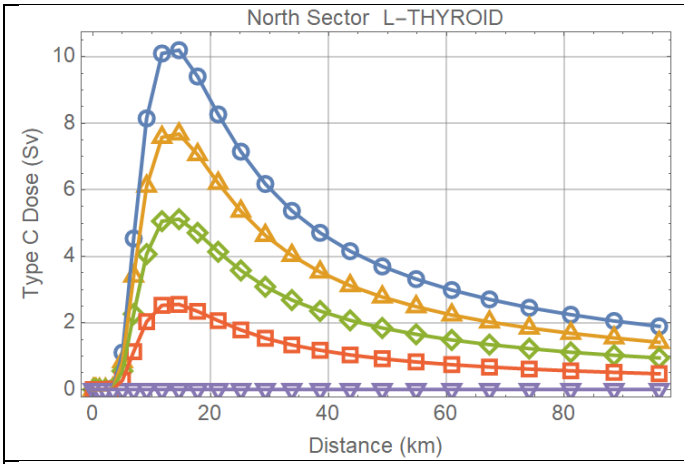

Type C sector average dose (long-term L-THYROID) versus distance (north sectors). Results of Set 1 are indicated with symbols and Set 2 results are indicated with solid curves. The results of Set 1 are identical to Set 2.

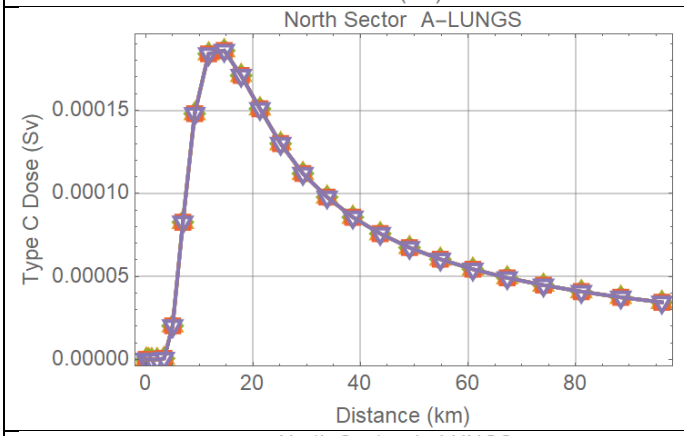

Type C sector average dose (acute A-LUNGS) versus distance (north sectors). In this case, results are independent of the value of POPFRAC and EFFACY because the acute doses to the lung are not reduced by the ingestion of KI pills (only doses to the thyroidal gland are reduced by the ingestion of KI pills).

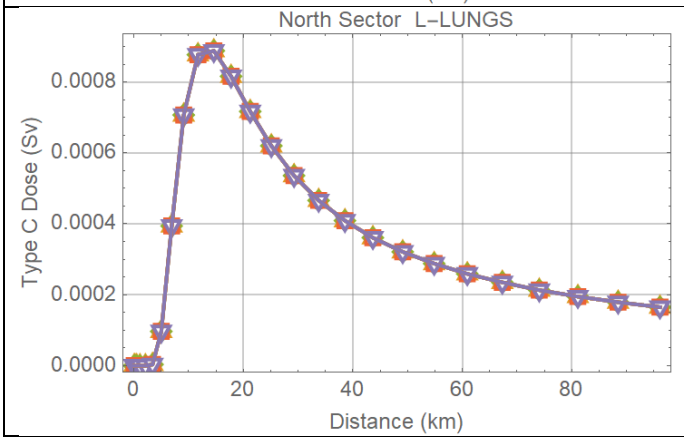

Type C sector average dose (long-term L-LUNGS) versus distance (north sectors). In this case, results are independent of the value of POPFRAC and EFFACY because the lifetime doses to the lung are not reduced by the ingestion of KI pills (only doses to the thyroidal gland are reduced by the ingestion of KI pills).

Figure 3-35 (continued). Type C inhalation dose versus distance. Each plot displays a different kind of Type c dose. The plots compare Set 1 and Set 2 results.

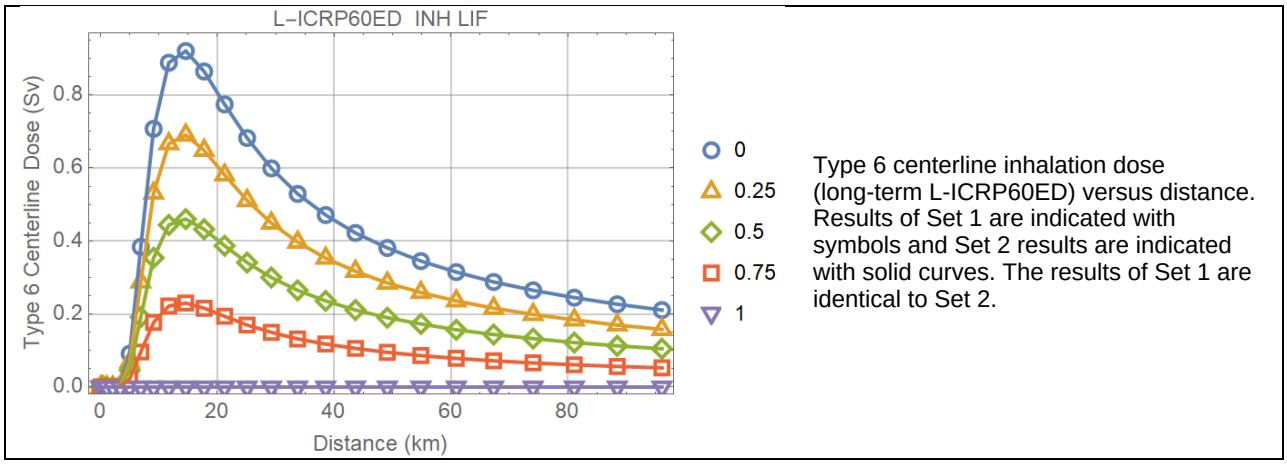

Figure 3-36. Type C inhalation dose versus distance. Each plot displays a different kind of Type c dose. The plots compare Set 1 and Set 2 results.

Figure 3-37 shows the population dose (Type 5 output), population health effects (Type 1 output), and average individual risk (Type 4 output), and population-weighted individual risk (Type 8 output).

Figure 3-38, Figure 3-39, and Figure 3-40 demonstrate the linearity of Type C sector average results on the EFFACY factor, when POPFRAC = 1 (Set 1). Since the results of Set 1 are identical to Set 2, the figure also demonstrates the linear dependence of the Type C results on POPFRAC when EFFACY = 1.

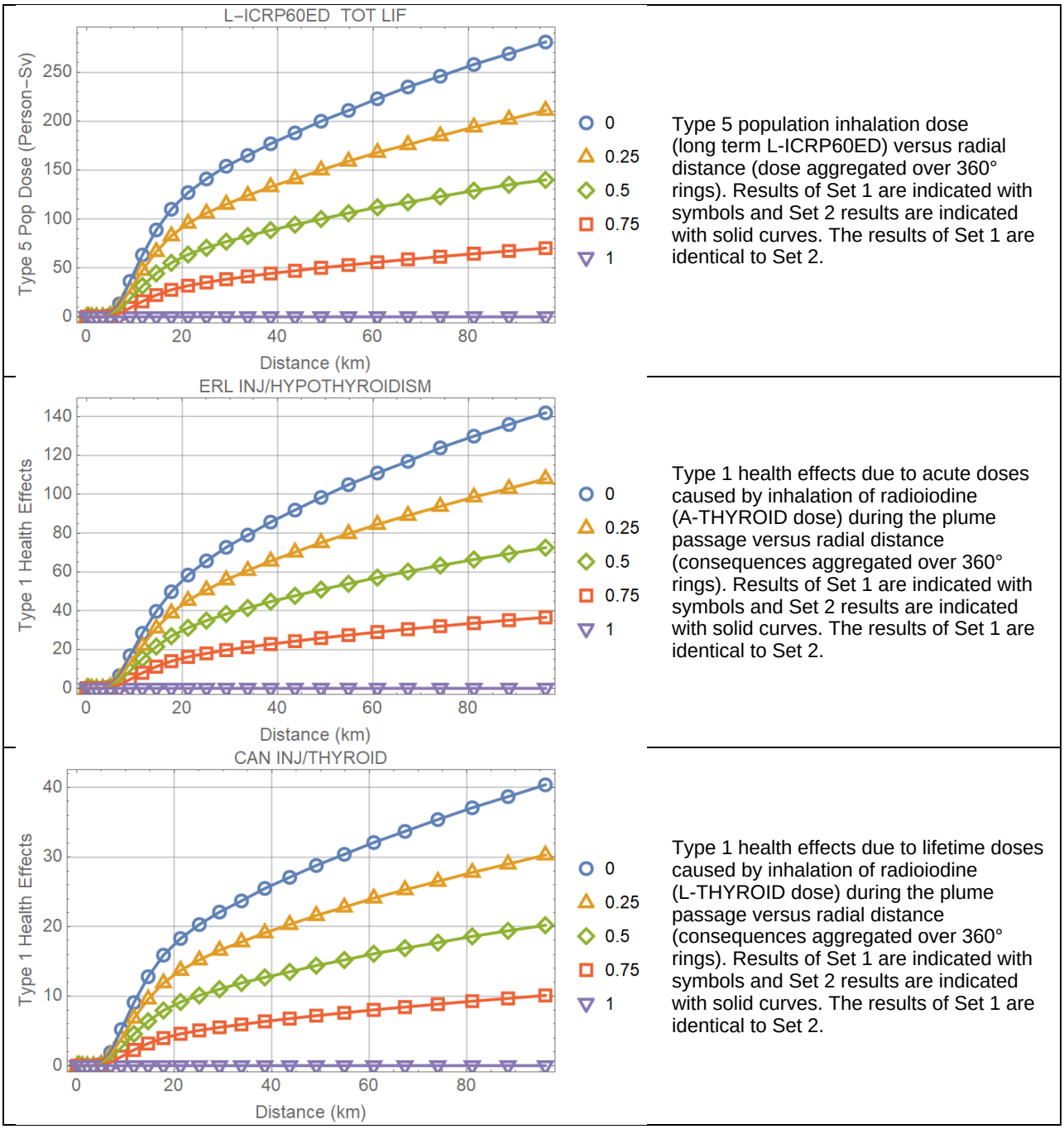

Figure 3-37. Type 5 population dose, Type 1 population health effects, Type 4 average individual risk, and Type 8 population-weighted individual risk versus radial distance. Each plot displays a different kind of output. The plots compare Set 1 and Set 2 results (they are identical).

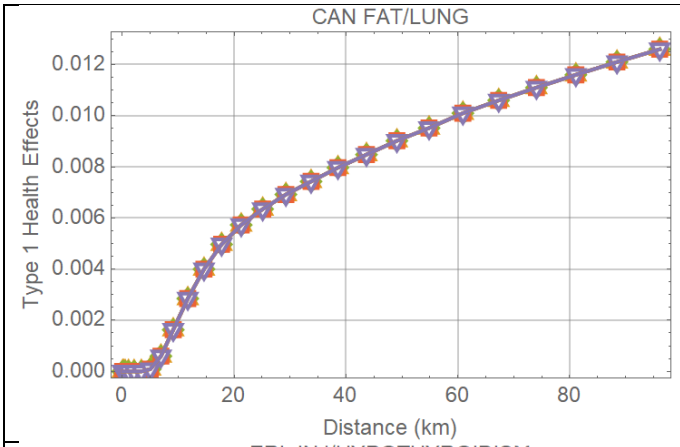

Type 1 health effects (cancer fatalities) due to lifetime doses caused by inhalation of radioiodine (L-THYROID dose) during the plume passage versus radial distance (consequences aggregated over 360° rings). In this case, results are independent of the value of POPFRAC and EFFACY because lifetime doses to the lung are not reduced by the ingestion of KI pills (only doses to the thyroidal gland are reduced by the ingestion of KI pills).

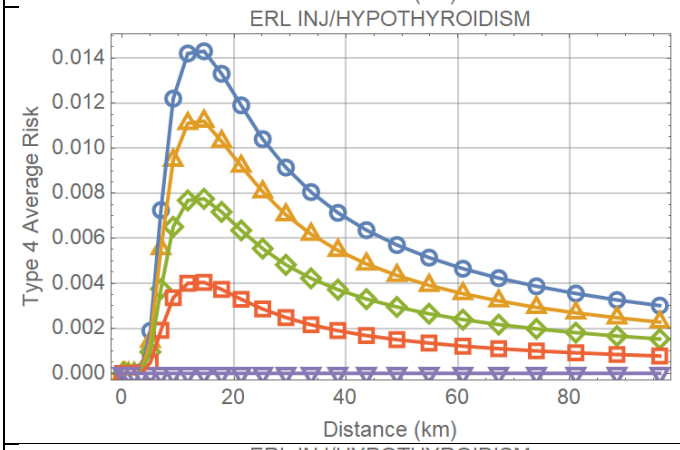

Type 4 average individual risk due to acute doses caused by inhalation of radioiodine (A-THYROID dose) during the plume passage versus radial distance (consequences averaged over 360° rings). Results of Set 1 are indicated with symbols and Set 2 results are indicated with solid curves. The results of Set 1 are identical to Set 2.

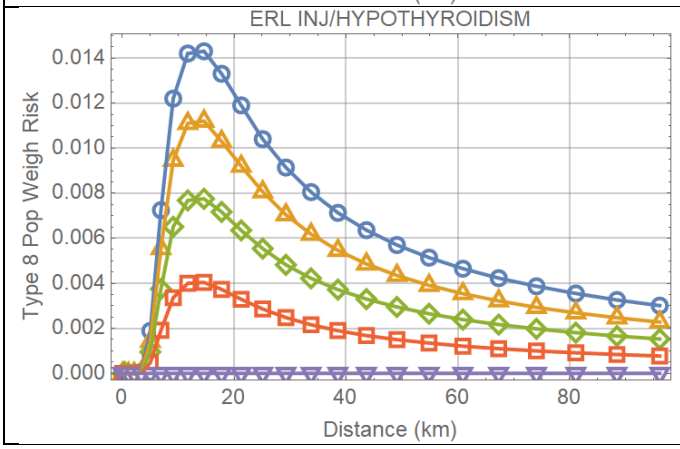

Type 8 population-weighted individual risk due to acute doses caused by inhalation of radioiodine (A-THYROID dose) during the plume passage versus radial distance (consequences aggregated over 360° rings). Results of Set 1 are indicated with symbols and Set 2 results are indicated with solid curves. The results of Set 1 are identical to Set 2.

As expected, Type 4 and Type 8 results are identical due to the use of a uniform population density in the test.

Figure 3-37 (continued). Type 5 population dose, Type 1 population health effects, Type 4 average individual risk, and Type 8 population-weighted individual risk versus radial distance. Each plot displays a different kind of output. The plots compare Set 1 and Set 2 results (they are identical).

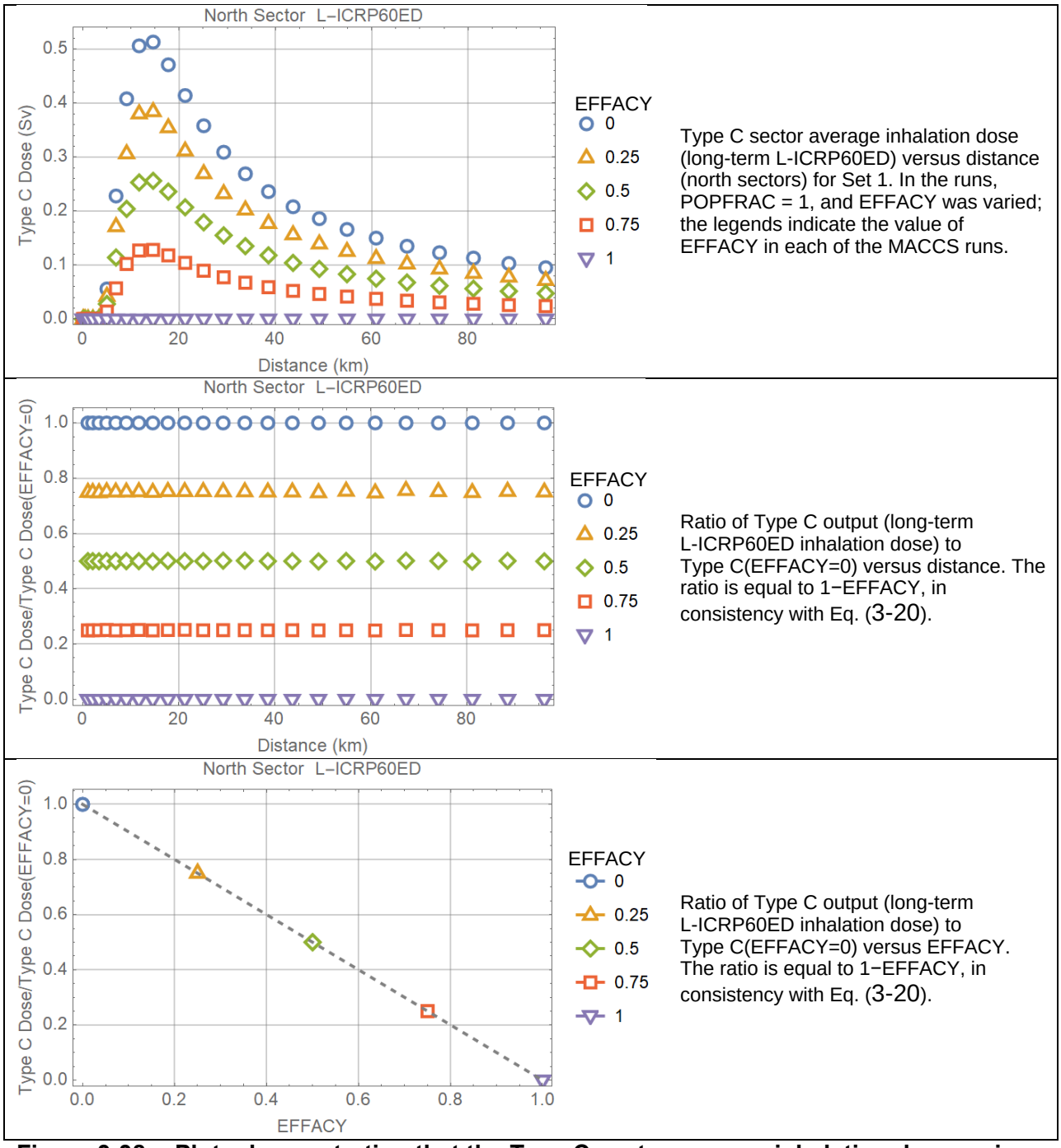

Figure 3-38. Plots demonstrating that the Type C sector average inhalation dose varies linearly with the parameter EFFACY.

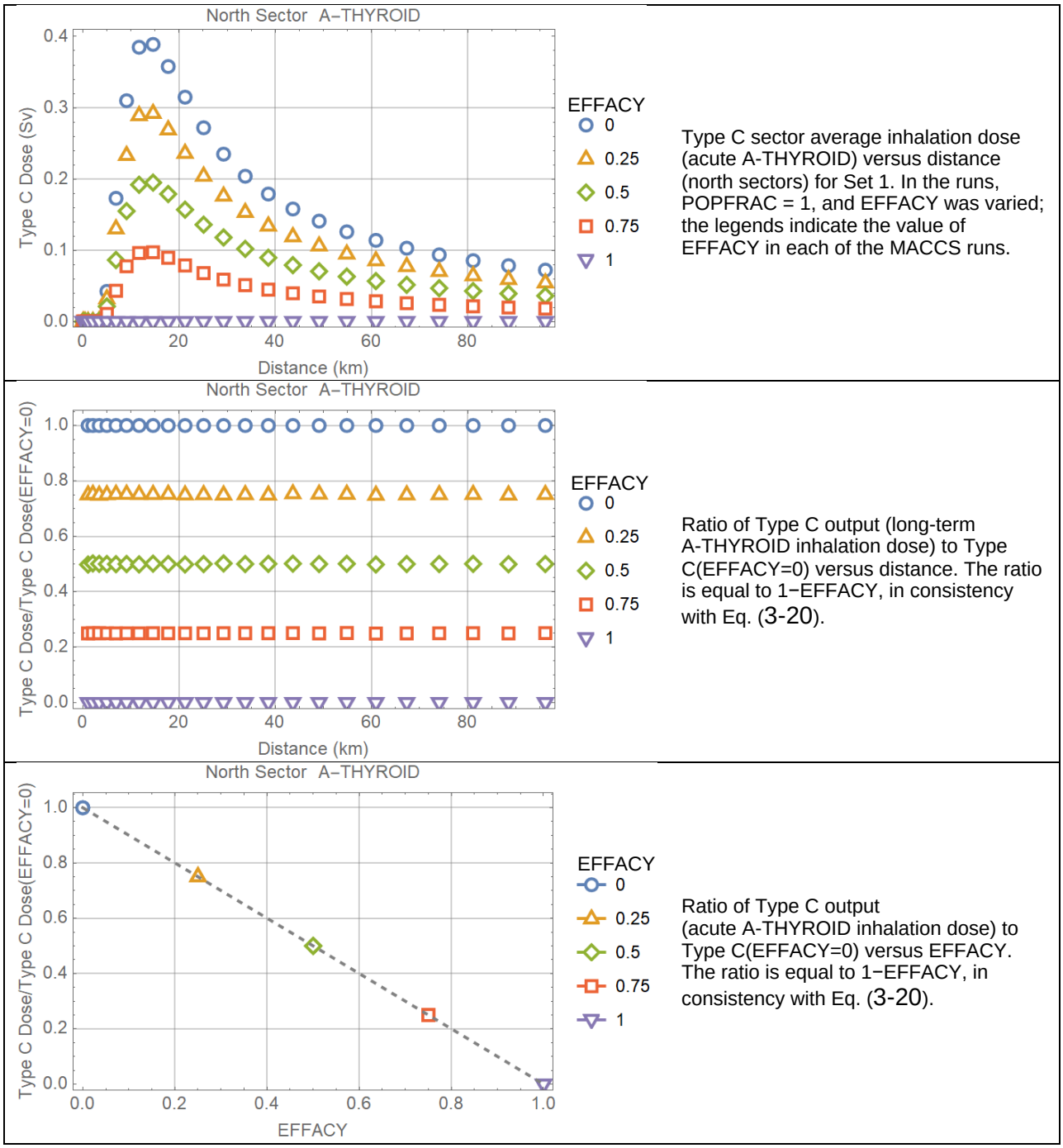

Figure 3-39. Plots demonstrating that the Type C sector average inhalation dose (acute dose to the thyroid) varies linearly with the parameter EFFACY.

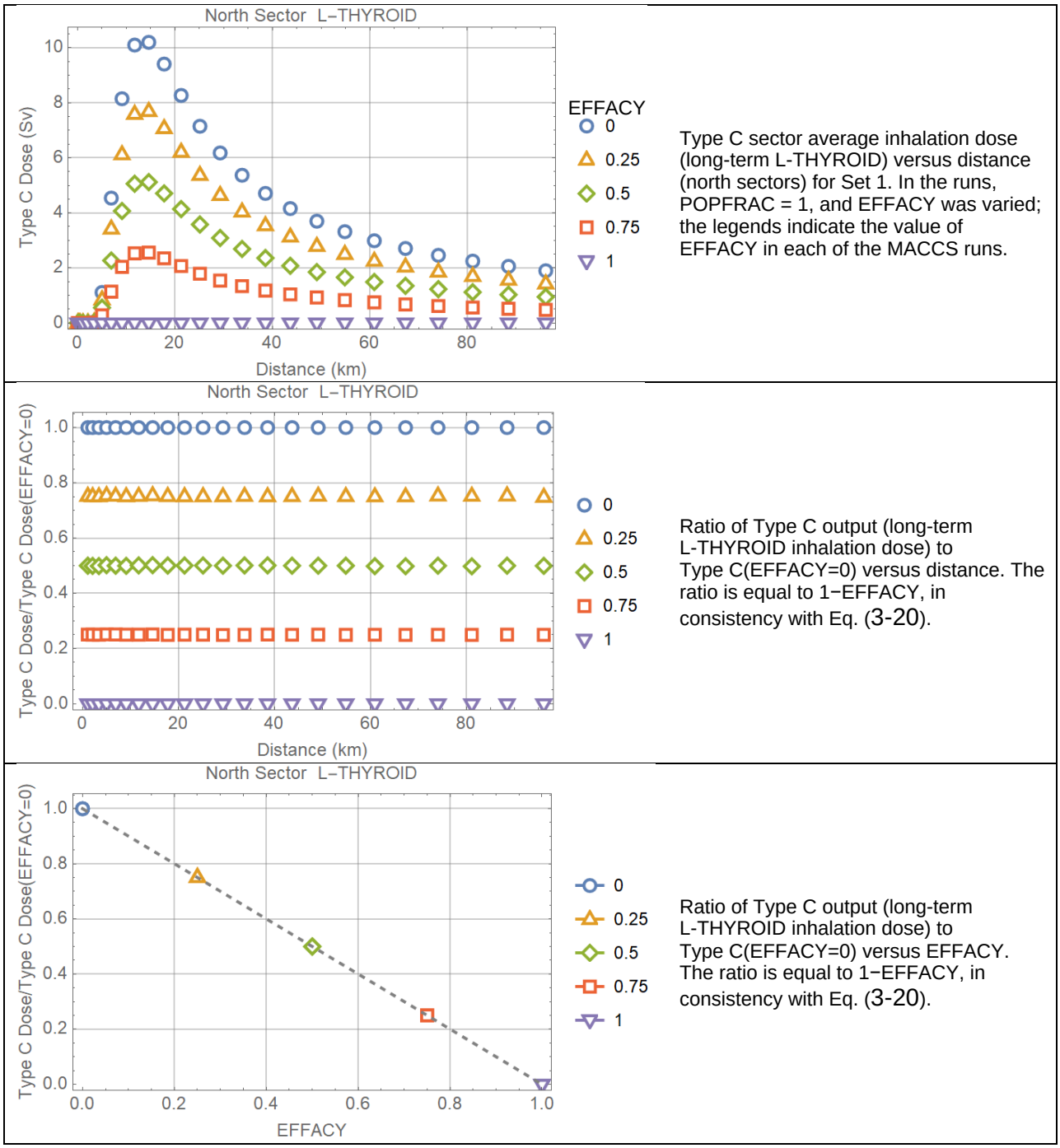

Figure 3-40. Plots demonstrating that the Type C sector average inhalation dose (long-term dose to the thyroid from inhalation of radioactivity during the passage of the plume) varies linearly with the parameter EFFACY.

3.6.4 Test Conclusions

The tests were aimed at examining the implementation of the KI pill ingestion model to mitigate doses to the thyroidal gland in case of inhalation of radioiodine during the plume passage. The tests were successful and verified that the MACCS model is consistent with Eqs. (3-17) to (3-20). The tests indirectly demonstrated that when one cohort is considered with a POPFRAC<1, then averages doses are computed for the different MACCS sectors considering the fraction of the population ingesting and not ingesting KI pills. Average health effects per sector are then computed based on the average doses. If non-linear health effects are modeled (e.g., considering beta shape parameters of risk functions, EFFACB and EIFACB, different than one), the number of health effect cases, Type 1 outputs, are approximations. To derive more accurate results, it is recommended instead to consider two cohorts: one cohort ingesting KI pills and a second cohort not ingesting the KI pills. Again, the two-cohort approach may only be considered when the parameters EFFACB and EIFACB differ from 1. In general, the approximated results are reasonable.

3.7 Test 3.7: Broad Plume Run Interrupt

MACCS Version 4.1 includes a check on the lateral spread of the plume. A run is stopped when the following condition occurs

$$2.15\ \frac{\sigma_y(x)}{x} > \frac{\pi}{2} \tag{3-21}$$

where x is the downwind distance from the source along the plume centerline, and the lateral Gaussian dispersion coefficient $\sigma_y(x)$ includes all adjustment factors (e.g., YSCALE factor and/or plume meander factors) and is based on input values for atmospheric stability class A (lowest stability class, highest plume spread). The condition in Eq. (3-21) is only checked for distances x > 1,000 m (details of the run stop are not yet described in MACCS documentation). The rationale for the run stop is to avoid plumes (under atmospheric stability class A conditions) with a spread angle broader than 180° for x distances greater than 1,000 m. For shorter distances, the condition in Eq. (3-21) does not trigger a run stop. In case of a run stop, MACCS issues a message requesting the user to modify inputs to attain narrower plumes.

Figure 3-41 summarizes the approach described in the MACCS documentation to define the spread of a plume. [Recall that MACCS employs a narrow plume approximation to map polar to Cartesian coordinates, Eq. (3-11); concentrations on the horizontal orange line are mapped to locations on the blue circular arc.] The point A is defined such that the length of the blue arc AB is $2.15\ \sigma_y(x)$. The circular arc ABC encloses 97% of the concentration that would be spread along a horizontal line of constant x from $-\infty$ to ∞ (orange line in Figure 3-41). This concentration is called herein the total Cartesian concentration for the constant x line. The MACCS documentation states that the remaining 1.5% of the total Cartesian concentration is assigned to the last red grid sector enclosing point A, and a complementary 1.5% is assigned to the last red grid sector enclosing the point C. The current test considered an alternative computational approach, accounting for non-zero concentrations only for locations on the north arc enclosed by points E and D and ignoring other tail concentrations (corresponding to concentrations at farther distances on the horizontal Cartesian line).

A Gaussian plume extends laterally from $-\infty$ to ∞; however, as a practical approach, MACCS constrains the outputs so that grid sectors with non-zero concentrations are the sectors that enclose the arc ABC (i.e., grid sectors enclosed by the "bookend" red-outline sectors in Figure 3-41, including those red sectors). The last grid sectors with non-zero concentration in the output files are the red-outline sectors containing the points A and C in Figure 3-41. Sectors south of the red outline sectors, such as the green outline sector, are assigned by MACCS a zero concentration.

MACCS applies the narrow angle approximation to transform polar to Cartesian coordinates, Eq. (3-11), also to broad angles (which validity is examined to some extent in this test). MACCS considers a plume spread valid if the angle φ subtended by the blue arc AB in Figure 3-41 is less than 90° or π/2 radians. The subtended angle φ is computed as

$$\varphi = 2.15\ \frac{\sigma_y(x)}{x} \tag{3-22}$$

The run stop condition in Eq. (3-21) indicates that the subtended angle φ exceeded 90° for that run, and therefore the plume would extend in the upwind direction, which is not allowed for farfield distances (defined in MACCS as distances x > 1,000 meters).

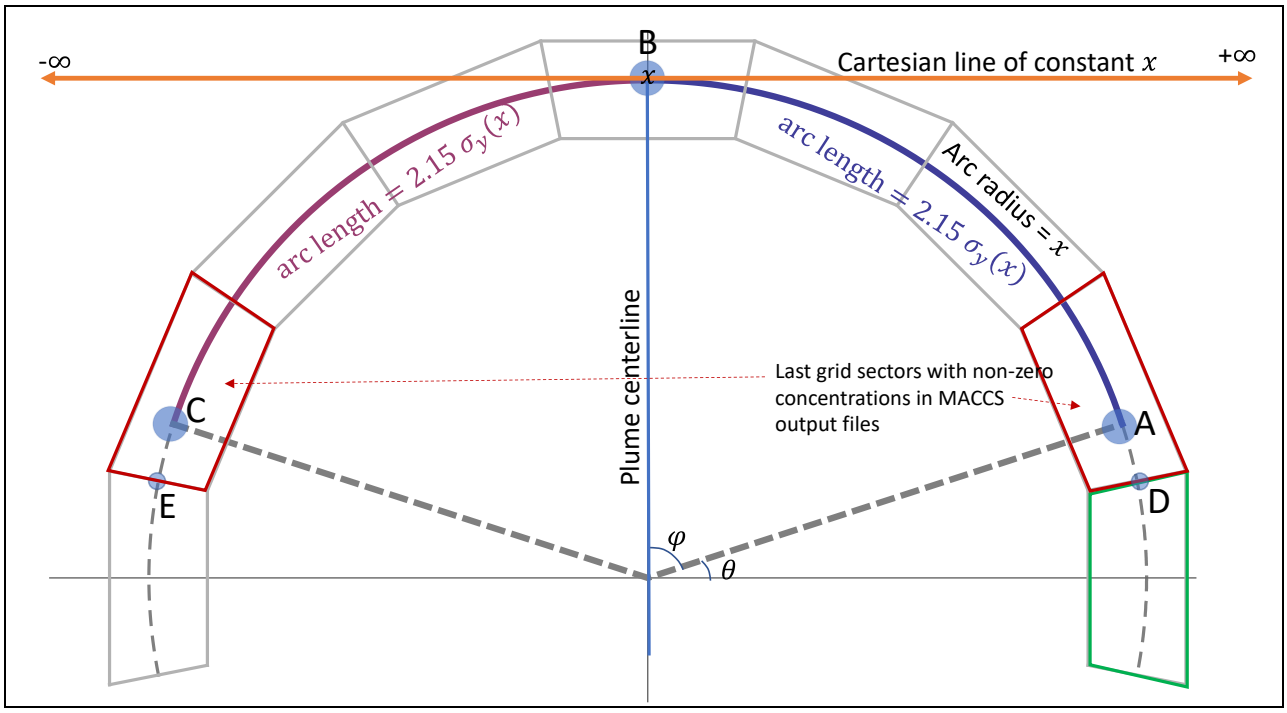

Figure 3-41. Example of MACCS computation of the plume spread

The purpose of this test is twofold:

- Examine the implementation of the run interrupt criterion, Eq. (3-21)
- Examine the accuracy of the narrow angle approximation (i.e., for which sectors does the narrow angle approximation become a poor approximation?)

3.7.1 Test Input

The same inputs of Test 2.1 were used, with the following changes:

General Properties

- Transport
  - Dispersion: Lookup Tables
  - Plume Meander: None (MNDMOD = OFF)
- Plume
  - Plume Source: Area Source
  - Plume Rise: Power Model
  - Plume Trapping/Downwash: Briggs (buoyancy flux)

ATMOS

- Spatial Grid
  - NUMCOR = 16: number of circumferential sectors
  - NUMRAD = 34: discretization number along the radial direction
  - SPAEND (km): end radius of each ring grid
    - 0.1, 0.2, 0.3, 0.4, 0.5, 0.6, 0.7, 0.8, 0.9, 1.0, 1.1, 1.539, 2.657, 4.096, 5.854, 7.932, 10.33, 13.05, 16.08, 19.44, 23.12, 27.11, 31.43, 36.06, 41.02, 46.29, 51.89, 57.8, 64.04, 70.59, 77.46, 84.66, 92.17, 100.0
- Radionuclides
  - CORINV = 1 Bq for Cs-137, 0 for other radionuclides
- Dispersion
  - Dispersion Table
    - Lookup table for σ_y and σ_z following the parameterization of (Eimutis & Konicek, 1972), and extracted from the Appendix D input files in (Clayton, 2021)
  - Scaling Factors
    - YSCALE = 1, 2, 3, 3.9 in independent runs
    - ZSCALE = 1
- Release Description
  - Plume Parameters
    - One plume segment
    - PDELAY (s) = 0
    - PLHITE (m) = 0: release height, ground release
    - REFTIM (-) = 0.5: midpoint grid
    - PLUDUR (s) = 86400 s (=24 hours)
  - Building Height Data
    - BUILDH (m) = 40
  - Initial Area Source
    - SIGYINIT (m) = SIGZINIT (m) = 0.1
- Deposition
  - Wet / Dry Deposition Flags
    - DRYDEP = FALSE for Cs
- Weather
  - Constant or Boundary Conditions
    - BNDMXH (m) = 1000
    - IBDSTB (-) = 1: stability class A
    - BNDRAN (mm/hr) = 0: rain rate
    - BNDWND (m/s) = 2: windspeed

Output Controls

Same outputs Test 2.1 were used, with the following additional outputs:

- Type 0 (NUM0) ATMOS Outputs
  - INDREL = 1 (plume segment)
  - INRAD = 1, 2, 3, …, 34 (all radial segments)
  - NUCOUT = Cs-137: radionuclide output by NUM0
- Type D (NUMD) Average Sector Concentrations
  - I1DISD = 34 (outer radial interval)

    - NUCLIDE = Cs-137
    - ELEVCONC (Bq/m^2) = 0 (threshold value, all sectors are reported when 0)
    - PRINT_FLAG_D = True
    - Report Options = REPORT
- Type 6 (NUM6) Centerline Dose
    - ORGNAM = L-ICRP60ED; PATHNM = INH LIF: inhalation lifetime; I1DIS6=1, I2DIS6=34: all radial segments; Report Options = NONE
    - ORGNAM = L-ICRP60ED; PATHNM = CLD: cloudshine dose; I1DIS6=1, I2DIS6=34: all radial segments; Report Options = NONE
- Type A (NUMA) Peak Dose in a Grid Ring
    - NAME = L-ICRP60E; I1DISA=1, I2DISA=34: all radial ring segments; Report Options = NONE
- Type C (NUMC) Land Area Exceeding Dose
    - ORGNAM = L-ICRP60ED; ELEVDOSE (Sv) = 0: outputs all grid elements with dose > 0 Sv; PRINT_FLAG_C = True; Report Options = NONE

3.7.2 Test Procedure

MACCS was executed with different inputs of the parameter YSCALE= 1, 2, 3, 3.9. A value of YSCALE=4.0 triggered the broad plume run interrupt, and for that reason the maximum value of YSCALE=3.9 was used in the test.

Type D concentrations were extracted from the output file Model1.out. Air concentrations at the ground level are identified by the label "Air Concentration by Grid Element (Bq-s/m3)" in the output files. Because the Cs-137 inventory in the run was 1 Bq, these air concentrations are numerically equivalent to the quantity χ/Q in s/m^3 units. Concentrations were independently computed using Eqs. (2-1) and (2-2). The number of elements in the sum in Eq. (2-2) was N=50. The sum in Eq. (2-1) to compute $\psi(x,z)$ was used when $\sigma_z(x) \leq H/0.03$, where H is the maximum plume height (m) (H=1000 m in the test). Otherwise, if $\sigma_z(x) > H/0.03$, the term $\psi(x,z)$ was approximated as

$$\psi(x,z) = \frac{1}{H} \text{ if } \sigma_z(x) > H/0.03 \tag{3-23}$$

which is the same approximation adopted in the MACCS algorithms.

The Type D air concentrations are sector average concentrations. The sector average concentration was computed by integrating the Gaussian function along the y direction, using closed-form integrals available in Mathematica based on the complementary error function. For the last sectors (i.e., the red-outline sectors including the points A and C in Figure 3-41), alternative approaches were examined where the concentrations of Gaussian distributions tails were added (i.e., case 1) or not added (i.e., case 2). Either case produces similar results. When adding tails, the last sectors had slightly higher concentrations.. Results of the independent computations were compared to the MACCS outputs.

An alternative approach to computing the χ concentration was examined using the general Eq. (3-10), which does not use the MACCS narrow plume approximation [Eq. (3-12)]. In that general case, the sector average concentration was independently computed using numerical integration with a 1/3 Simpson rule and 21 points. This alternative approach was implemented to examine the accuracy of the MACCS narrow plume approximation for broad plumes.

3.7.3 Test Results

Air concentrations at the ground level, expressed as χ/Q, from MACCS Type D outputs are displayed in Figure 3-42 for the cases YSCALE=1, 2, 3, and 3.9. The dashed curves are the $\pm 2.15\ \sigma_y(x)$ boundaries. The graphic verifies that the last sectors of the plume with non-zero concentrations are the sectors enclosing the $\pm 2.15\ \sigma_y(x)$ curves (see Figure 3-41 for a visual on how the distance $2.15\ \sigma_y(x)$ is measured along a circular arc). The plot at the bottom of Figure 3-42 is an expanded view of the $\pm 2.15\ \sigma_y(x)$ boundaries for the case YSCALE=3.9, showing that the plume spreads upwind for radial distances less than 1000 m. For the case YSCALE=3.9, the plume spreads at an angle exceeding 180°; the $2.15\ \sigma_y(x)$ limit is south to the source in the upwind region. MACCS Version 4.1 only checks the condition in Eq. (3-21) for distances x>1000 m to trigger a run stop. In other words, at distances less than 1000 m, the plume spread could exceed 180°, as shown in the lower plot of Figure 3-42.

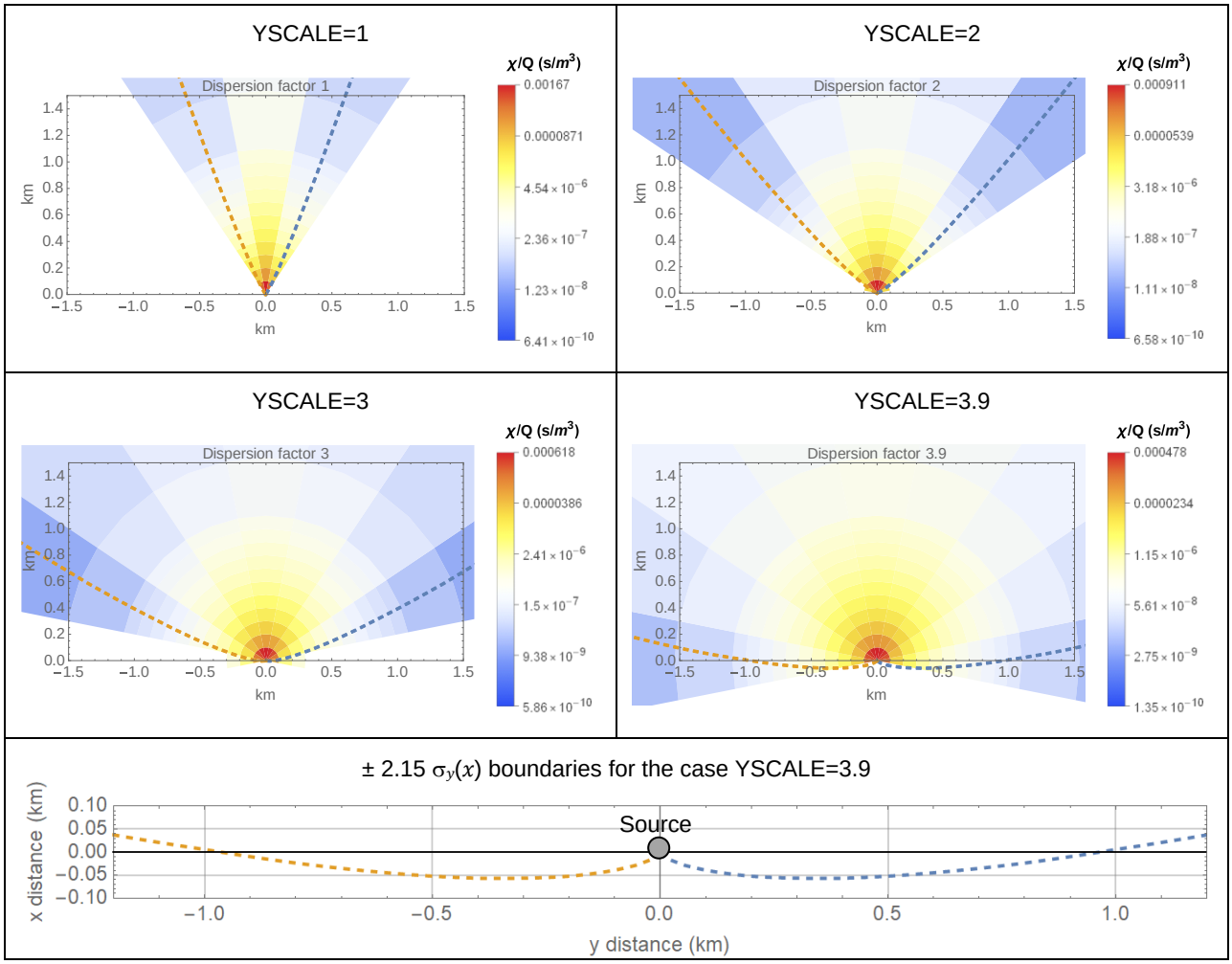

Figure 3-42. MACCS Type D sector average air concentrations at the ground level for different cases of YSCALE. The dashed curves represent the ± 2.15 $\sigma_y(x)$ boundaries. The plot at the bottom is an expanded-scale display of the ± 2.15 $\sigma_y(x)$ boundaries for the case YSCALE=3.9.

Figure 3-43 and Figure 3-44 compare MACCS outputs (symbols), χ/Q at z=0 versus radial distance, to independent computations (solid curves). Each plot corresponds to same-orientation sectors, indicated by the angle on the top title in each plot. The legends on the right of the plots indicate the value of YSCALE used in the runs. The solid curves on the plots on the left used the MACCS narrow plume approximation, Eq. (3-12). Differences between the MACCS outputs (symbols) and the independent computations are minor in the left plots, possibly due to roundup error and different precision in the approaches to compute sector average concentrations. Nonetheless, the results are in close agreement. The solid curves successfully verified that the MACCS computations are implemented as described in the MACCS Theory Manual (Nosek & Bixler, 2021). Differences considering whether the remaining 1.5% Cartesian concentration (tail concentration) is added to the last sector or not are minor, and insufficient to discern whether those minor differences contribute to differences between the MACCS outputs and the independently computed sector-average air concentrations.

The right-hand side plots in Figure 3-43 and Figure 3-44 are provided to evaluate the accuracy of the MACCS narrow plume approximation. The solid curves were computed considering accurate polar to Cartesian coordinate conversion, Eq. (3-10). The top plot for east sectors (0° sectors), indicates the MACCS narrow plume approximation is a poor approximation, with MACCS concentrations being at least four orders of magnitude greater than concentrations computed with the accurate polar to Cartesian coordinate conversions for the test case considered. For the east-north-east sectors (22.5° sectors), the MACCS narrow plume approximation is still a poor approximation, but with smaller differences than the 0°-sector results. For the north-east sectors (45° sectors), the MACCS narrow plume approximation surprisingly yields reasonable results, comparable to the more accurate results using accurate polar to Cartesian coordinate conversions. The right-hand-side plots in Figure 3-44 indicate that the MACCS results for the north-east-north (67.5° sectors) and north (90°) sectors are relatively accurate. The comparison in the right-hand-side plots in Figure 3-43 and Figure 3-44 suggest care should be exercised in interpreting results associated with broad plumes (such as those arising from plume meander). In the example examined in this test, MACCS results relying on the narrow plume approximation overestimated air concentrations at times by several orders of magnitude for the 0° and 22.5° sectors. However, for the 45° sectors, the MACCS results can be lower than concentrations computed using accurate polar to Cartesian coordinate conversions. Therefore, the reader is cautioned to extrapolate the conclusion that *MACCS integrated air concentrations with the narrow plume approximation are always conservative*. This conclusion is not true. For plumes not spreading beyond the north-east-north sectors (67.5° sectors), the test example indicates MACCS results accurately reflect Gaussian plume model concentrations, but examination of additional examples is recommended to establish the generality of this conclusion of numerical accuracy.

Additional Cases Examined

The test included additional examples, but for the sake of brevity the results are only summarized herein. Corresponding output files are archived with the quality assurance records of this report.

Additional runs were executed considering atmospheric stability class D or E, and varying the parameter YSCALE. It was verified that the broad plume run interrupt is triggered for the same value of YSCALE, independently of the assumed atmospheric stability class in the run. The run stop is based on the value of the lateral dispersion $\sigma_y(x)$ computed considering the atmospheric stability class A (causing the broadest plume), independently of the atmospheric stability class controlling the spread of the plume. As expected, the plume in output files is narrower when carried in winds of higher stability.

Additional runs were executed assuming power law functions to define the Gaussian dispersion coefficients as function of the downwind distance x (NUM_DIST=0 to enable the power law functions). The parameters of the power law functions (CYSIGA, CYSIGB, CZSIGA, CZSIGB) were input the numerical values recommended in Table 2-5 of the MACCS Theory Manual (Nosek & Bixler, 2021). In this case, runs were successfully completed with YSCALE up to 2.45. A value YSCALE=2.46 triggered a run stop. The condition in Eq. (3-21) triggers a run stop for distances x>1000 m. For distances x<1000 m, the condition in Eq. (3-21) does not trigger a run stop, and as a consequence, the plume can span more than 180° for radial distances less than 1000 m.

Solid curves computed using the MACCS narrow plume approximation, Eq. (3-12), to map polar to Cartesian coordinates	Solid curves computed using the general polar to Cartesian coordinate conversion, Eq. (3-10)

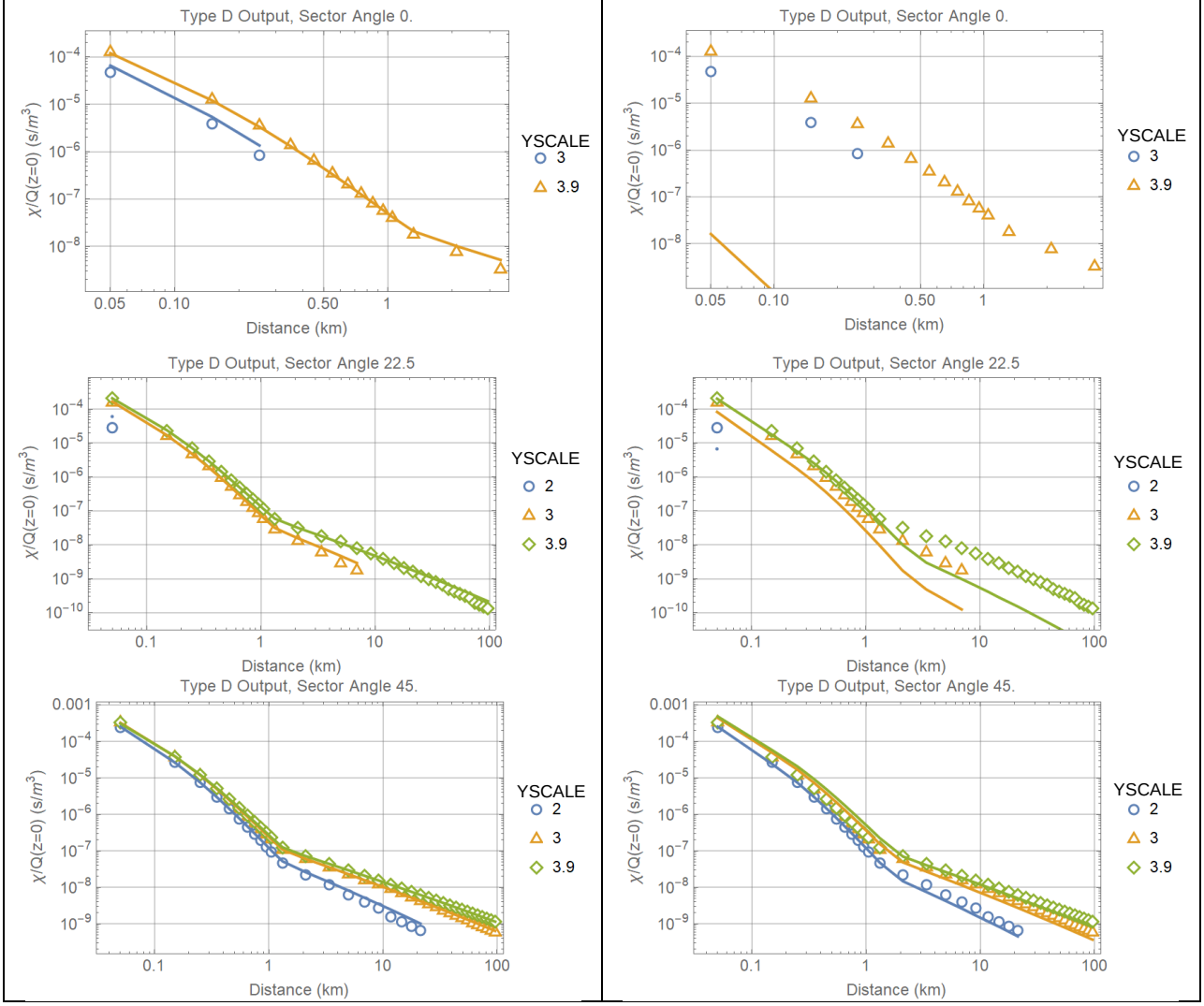

Figure 3-43. MACCS Type D sector average air concentrations at the ground level versus radial distance. Each plot corresponds to grid sectors at the same orientation, identified by the label at the top of the plot. The different cases of YSCALE are indicated by the plot legend. The symbols are MACCS outputs and the solid curves are independent computations. The solid curves on the left plots incorporate the MACCS narrow plume approximation, and solid curves on the right plots accounted for accurate polar to Cartesian coordinate conversions.

Solid curves computed using the MACCS narrow plume approximation, Eq. (3-12), to map polar to Cartesian coordinates	Solid curves computed using the general polar to Cartesian coordinate conversion, Eq. (3-10)
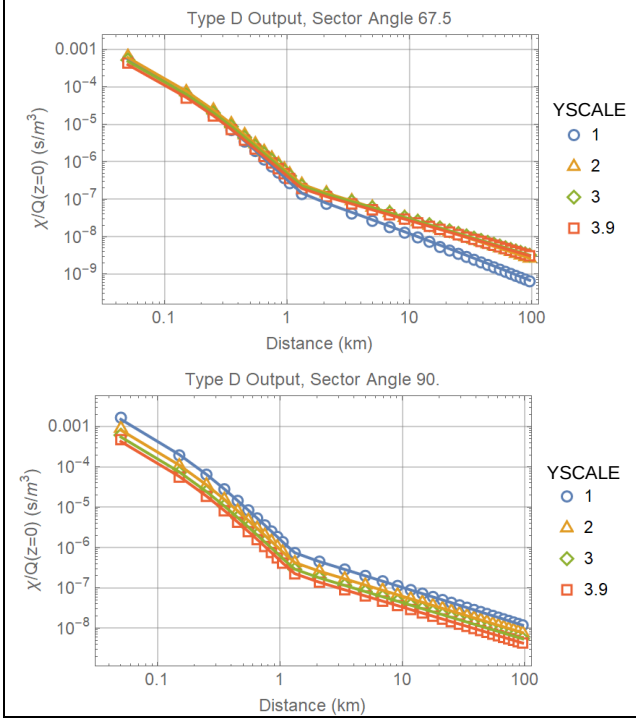	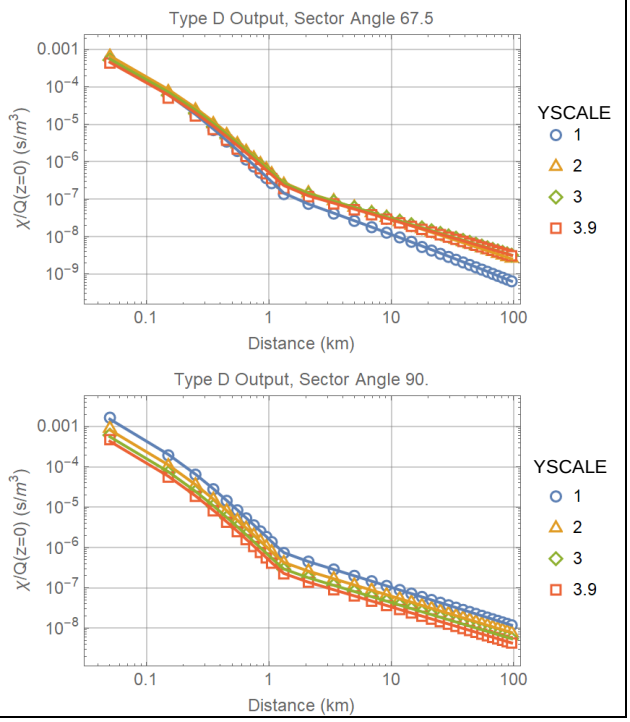

Figure 3-44. MACCS Type D sector average air concentrations at the ground level versus radial distance. Each plot corresponds to grid sectors at the same orientation, identified by the label at the top of the plot. The different cases of YSCALE are indicated by the plot legend. The symbols are MACCS outputs and the solid curves are independent computations. The solid curves on the left plots incorporate the MACCS narrow plume approximation, and solid curves on the right plots account for accurate polar to Cartesian coordinate conversions.

3.7.4 Test Conclusions

The test identified the condition used in MACCS to trigger a run interrupt in case the user inputs cause a plume that is too broad. MACCS Version 4.1 does not allow plumes carried under atmospheric stability class A to exceed an angular span of 180°, for radial distances greater than 1000 m. The spreads can exceed 180° for radial distances less than 1000 m (i.e., upwind plume spread is allowed).

For plumes with a centerline aligned with the north direction, the MACCS narrow plume approximation is poor for computing concentrations in east and east-north-east sectors, but reasonable for computing concentrations in the north-east sectors, and excellent for concentrations in the north and north-east-north sectors. Care should be exercised when interpreting results of broad plumes, especially those arising from plume meander at nearfield distances (x<1000 m).

3.8 Test 3.8: Plume Meander Models

The nearfield plume meander models were updated with MACCS 4.1, as described in the Nearfield Report (Clayton, 2021). The focus of Test 3.8 was on the Ramsdell and Fosmire model (enabled by MNDMOD=RAF). Substantial testing was documented by Sandia National Laboratories (SNL) (Clayton, 2021), and testing herein was limited to verifying the magnitude of the lateral Gaussian dispersion coefficient, $\sigma_y(x)$, and its relationship to the broad plume run stop discussed in detail in Test 3.7.

3.8.1 Test Input

Similar inputs than Test 3.7 were adopted with the following changes:

General Properties

- Transport
  - Lookup tables
  - Plume Meander: Ramsdell and Fosmire (MNDMOD=RAF)
- Plume
  - Plume Source: Point Source
  - Plume Rise: Power Model
  - Plume Trapping/Downwash: Briggs (buoyancy flux)

ATMOS

- Dispersion
  - Dispersion Table
    - Lookup table for σ_y and σ_z following the parameterization of Eimutis and Konicek (1972), and extracted from the Appendix D input files of the SNL nearfield report (Clayton, 2021)
  - Scaling Factors
    - YSCALE = ZSCALE = 1
- Plume Specifications
  - Ramsdell and Fosmire Meander
    - Input parameters based on Table 2-1 of the SNL nearfield report (Clayton, 2021)
- Release Description
  - Building Height Data
    - BUILDH (m) = 20
  - Additional Building Data
    - BUILDW (m) =20, BUILDL (m) = 20, BUILDA (degrees) = 0
  - Initial Area Source
    - Parameters disabled
    - SIGYINIT and SIGZINIT are defaulted to 0.1 m for a point source
- Weather
  - Constant or Boundary Conditions
    - BNDMXH (m) = 1000
    - IBDSTB (-) = 1: stability class A
    - BNDRAN (mm/hr) = 0: rain rate
    - BNDWND (m/s) = 0.55, 0.8, 1: windspeed in independent runs

Output Controls

- Same output controls of Test 3.7

3.8.2 Test Procedure

Equations (2-12) to (2-23) of the SNL nearfield report (Clayton, 2021), defining the Ramsdell and Fosmire meander model, were used to compute the plume meander adjustment factors to the lateral Gaussian dispersion coefficient as a function of the windspeed, building dimensions, with empirical input parameters defined in Table 2-1 of the same SNL report. The computed total effective lateral dispersion coefficient, $\sigma_y(x)$, including the Ramsdell and Fosmire meander factor, was compared to ATMOS outputs in the file tbl_outStat.txt labeled as "Plume Crosswind Dispersion (m)," considering different values of the windspeed (e.g., 0.55, 0.8, and 1 m/s) and atmospheric stability Class A. The windspeed was systematically decreased until a broad-plume run interrupt was triggered. A successful run was completed with 0.55 m/s windspeed, but a windspeed equal to 0.54 m/s triggered the run stop.

Type D outputs, integrated χ air concentrations at the ground level, identified by the label “Air Concentration by Grid Element (Bq-s/m3)” were extracted from the file Model1.out. Sector plots were prepared to examine the spread of the plume for nearfield distances (x<1,000 m). A commentary is provided related to the MACCS narrow plume approximation, and how this approximation affects the nearfield plume meander model.

3.8.3 Test Results

Figure 3-45 shows a comparison of the independently computed lateral Gaussian dispersion coefficient $\sigma_y(x)$ (solid curves) to the MACCS outputs (symbols) versus the downwind distance x for three different windspeeds. The lower plot in Figure 3-45 has an expanded horizontal scale. The algorithm described in the SNL nearfield report (Clayton, 2021) states that the meander factor is only used at distances x < 1,200 m, and a virtual source approach is implemented at x = 1,200 m to ensure continuity of the Gaussian dispersion coefficient. The change at x = 1,200 m was considered in the independent computations, which accurately reproduced the MACCS outputs.

Figure 3-46 displays sector plots of the integrated χ/Q concentration, colored according to a logarithmic scale. The sector plots include the $\pm 2.15\ \sigma_y(x)$ plume boundary. See Figure 3-41 for a description of the MACCS plume boundary for a radial distance x. For the windspeed cases of 0.55 m/s and 0.8 m/s the boundaries fall below the horizontal axis, indicating that internally MACCS keeps track of plume spreading angles greater than 180°. MACCS considers those concentrations in the internal computations of sector averages and assigns those concentrations to the last[a] east (0° orientation) and west (180° orientation) sectors. The wider the plume angle beyond 180°, the larger is the average sector average output for the last[a] east and west sectors. In principle, MACCS allows for internal plume spreads even beyond 360°; the concentration in the spread exceeding 180° is symmetrically assigned to the last east (0° orientation) and west sectors (180° orientation).

[a]See Figure 3-41 for a visual definition of “last” sectors

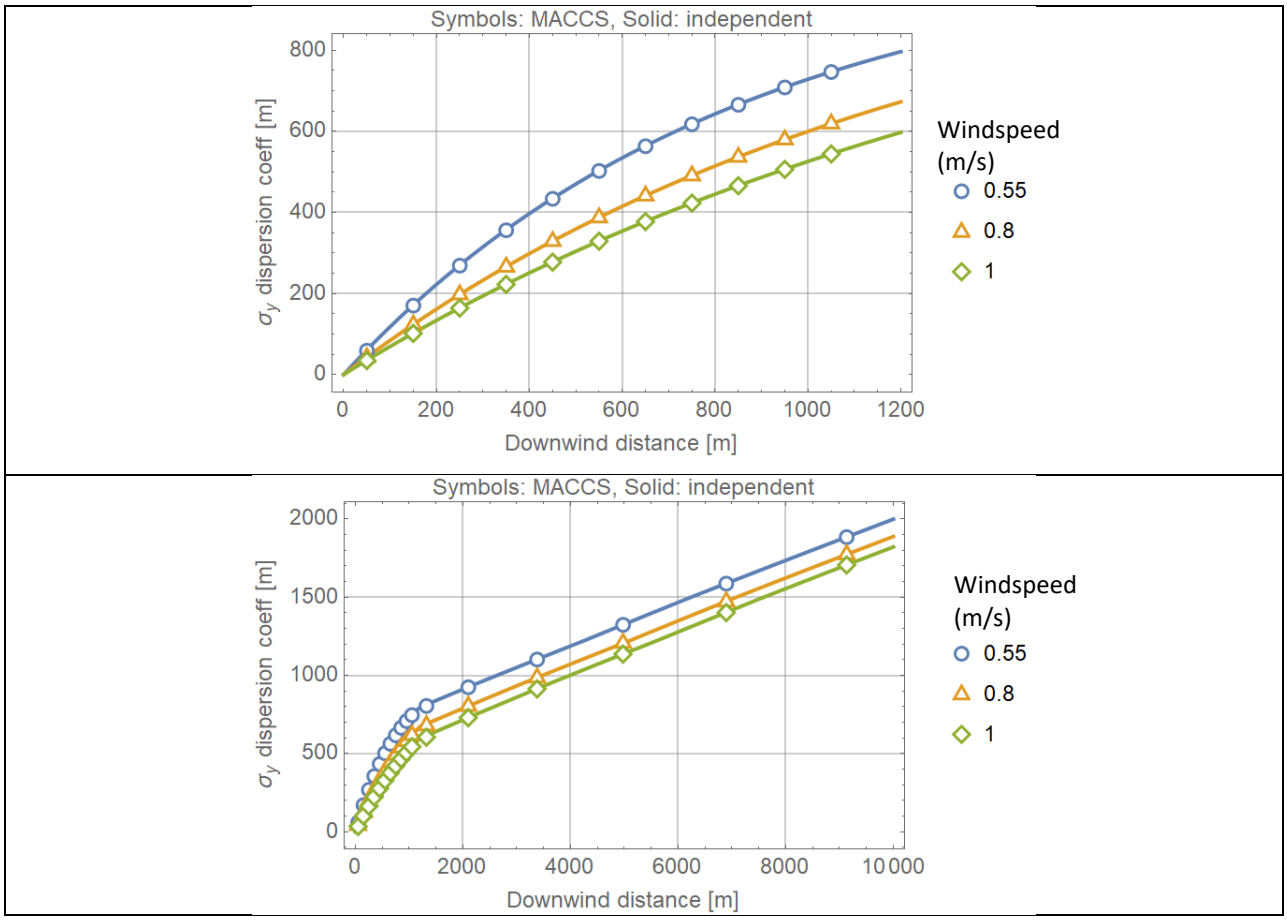

Figure 3-45. Adjusted lateral Gaussian dispersion coefficient, $\sigma_y(x)$, including the meander factor, as a function of the downwind distance x, for three windspeeds (atmospheric stability class A). Symbols correspond to the MACCS outputs, and the independent computations are the continuous curves.

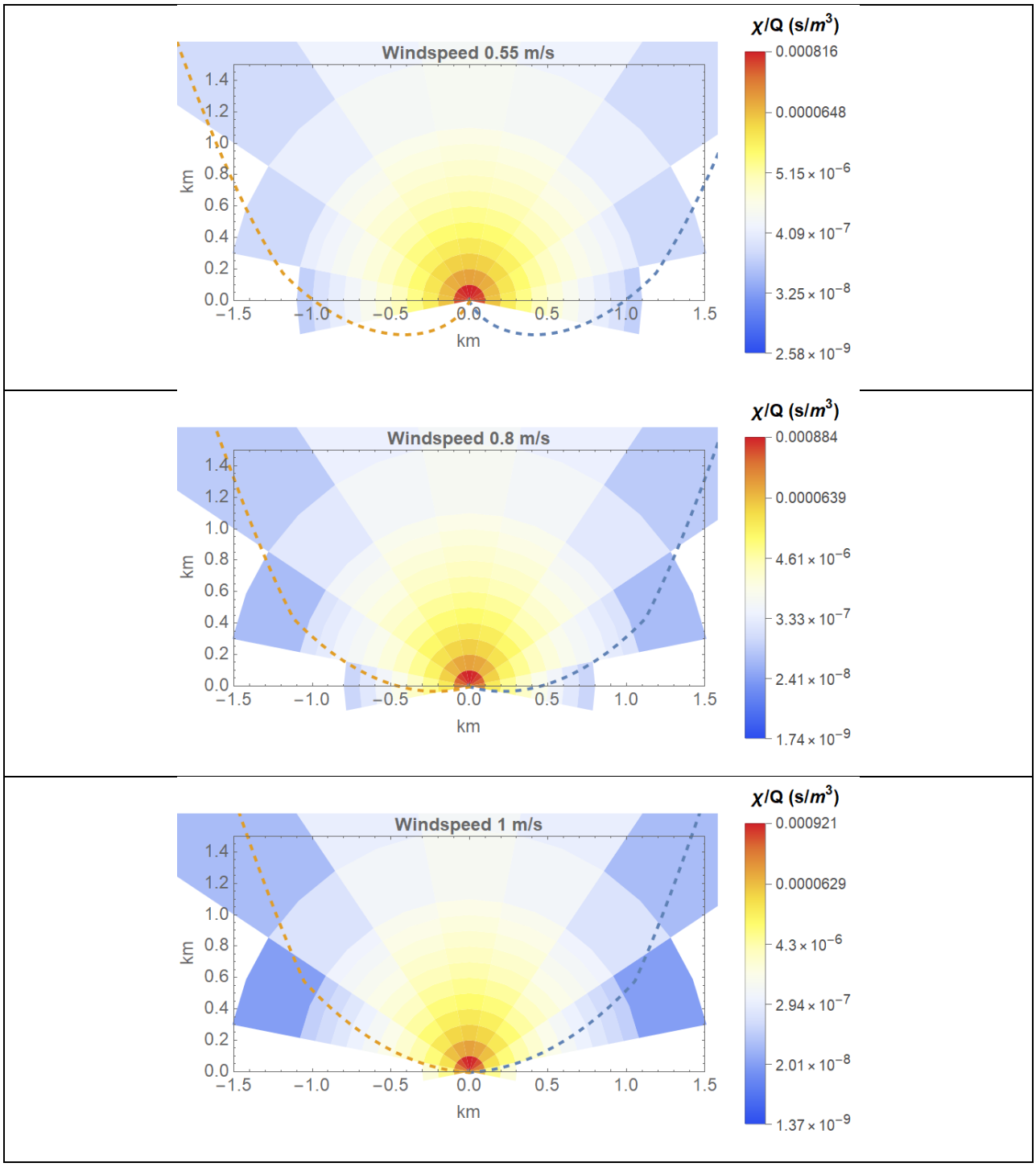

Figure 3-46. Sector plots of the integrated χ/Q concentration, colored according to a logarithmic scale, for three different speeds. The dashed curves define the location of the ±2.15 $\sigma_y(x)$ boundaries.

Figure 3-47 displays the angular spread of the plume internally tracked in MACCS versus the downwind distance x, which is equivalent to a radial distance under the MACCS narrow plume approximation. For distances close to the source and windspeed 0.55 m/s, the plume spread exceeds 300°. At x=1000 m, the plume spread is slightly less than 180° (180° is indicated by a dashed horizontal line). For smaller windspeeds, the plume spread at 1000 m exceeds 180°, MACCS stops the run and issues a warning requesting users to adjust inputs controlling the plume spread.

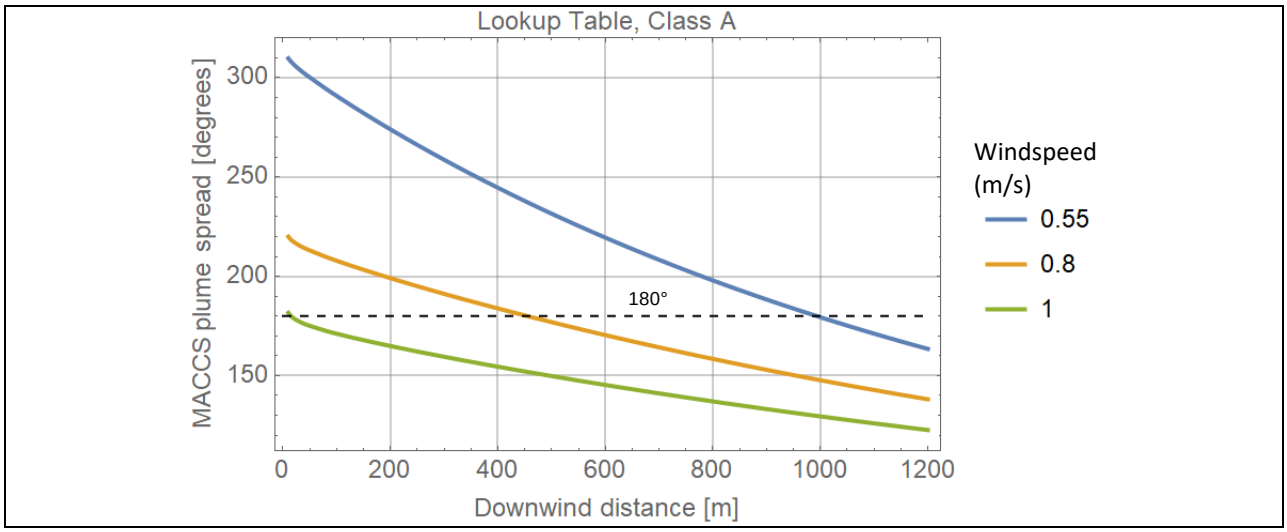

Figure 3-47. MACCS plume spread in degrees, based on ±2.15 $\sigma_y(x)$ boundaries, versus the downwind (or radial) distance x.

MACCS internally tracks plumes exceeding 180°, and concentrations in arcs beyond 180° are assigned to the last east and west sectors. Figure 3-48 shows the integrated χ/Q sector-average concentration versus the sector angle for three different windspeeds. All data in Figure 3-48 are MACCS outputs. Each curve displays information for sectors located at the same radius to the source (the color legend to the right of the plot indicates the radial distance of the sector center to the point source). The last sectors at 0° and 180° include the internal concentrations beyond 180°. In the top plot of Figure 3-48, the curve for radius 50 m (top purple curve in the plot), the total integrated concentration at 0° and 180° is such that the concentration almost exceeds the concentration in the prior sectors oriented 22.5° and 157.5°. Concentrations in the last 0° and 180° sectors are already inaccurate, due to the use of the MACCS narrow plume approximation in non-narrow plumes. The addition of the excess concentration of plumes exceeding 180° further overestimates the concentrations of the sectors oriented 0° (east sector) and 180° (west sector).

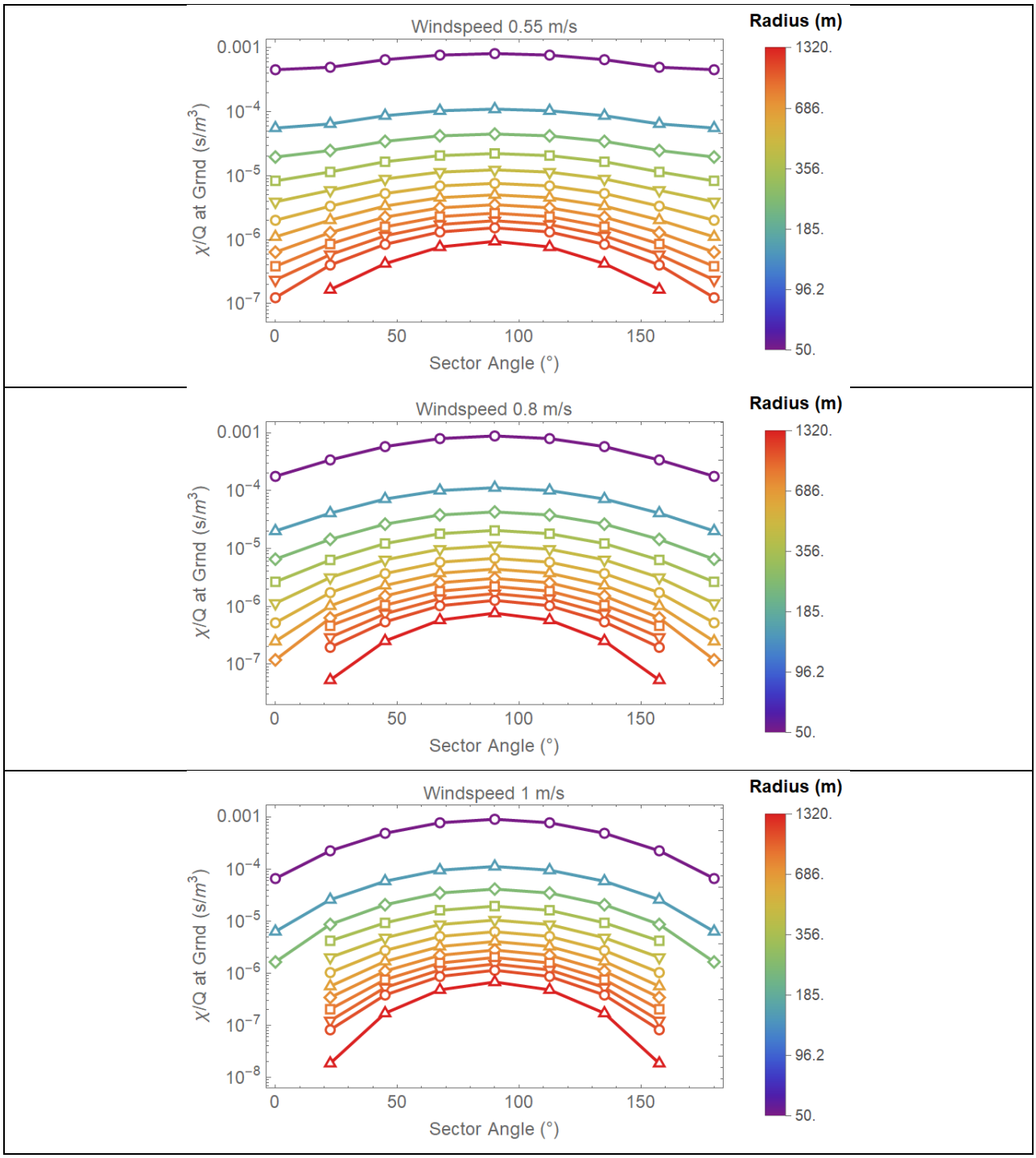

Figure 3-48. Integrated χ/Q sector-average concentration versus sector angle for three different speeds output by MACCS. Each curve displays information of sectors at a constant radius, with a radial distance of the sector center to the source indicated by the color legend on the right of the plot.

The test was repeated considering plumes under atmospheric stability Class D and F. The results for low windspeed conditions (e.g., 0.55 m/s) are very similar, because after applying the Ramsdell and Fosmire meander factor to the Gaussian dispersion coefficient, the total effective Gaussian dispersion coefficient is almost independent of the stability class. For example, Figure 3-49 displays the total Gaussian dispersion coefficient (including the Ramsdell and Fosmire meander factor) versus the downwind distance x, for three windspeeds, 0.55 m/s, 1 m/s, and 5 m/s. For each windspeed, there are three curves of the same color corresponding to stability class A, D, and F. For the windspeed 0.55 m/s, the three curves are of similar magnitude. Therefore, the plume spreads exceed 180° also for stability classes up to F when low windspeeds are considered.

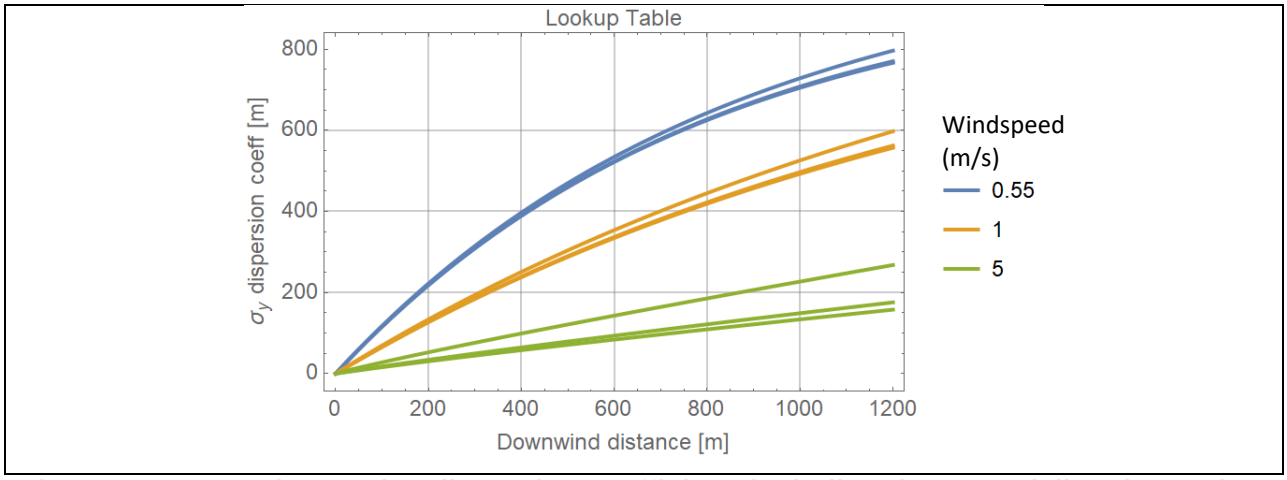

Figure 3-49. Total Gaussian dispersion coefficient, including the Ramsdell and Fosmire plume meander factor, versus the downwind distance x. Each family of curves (curves of the same color) includes three curves corresponding to stability class A, D, and F.

Additional runs were executed considering Gaussian dispersion coefficients based on power law functions with empirical parameters following Table 2-5 of the MACCS Theory Manual (Nosek & Bixler, 2021). In this case, the broad-plume run stop was not triggered. The YSCALE factor was systematically varied until the run-stop was triggered. Runs with YSCALE=2.1 were successfully executed, but YSCALE=2.2 triggered a run stop. Figure 3-50 shows the plume spread internally tracked in MACCS versus the radial distance x, for runs with windspeed 0.5 m/s (the lowest windspeed allowed in MACCS) and YSCALE = 1 and 2.1. Note that the blue curve (YSCALE=1) in Figure 3-50 well exceeds 180° at 1000 m, and the yellow curve (YSCALE=2.1) well exceeds 360°; however, the MACCS broad-plume run stop was not triggered. It appears that the broad-plume run stop is inconsistently applied when Gaussian dispersion coefficients are computed based on power law functions.

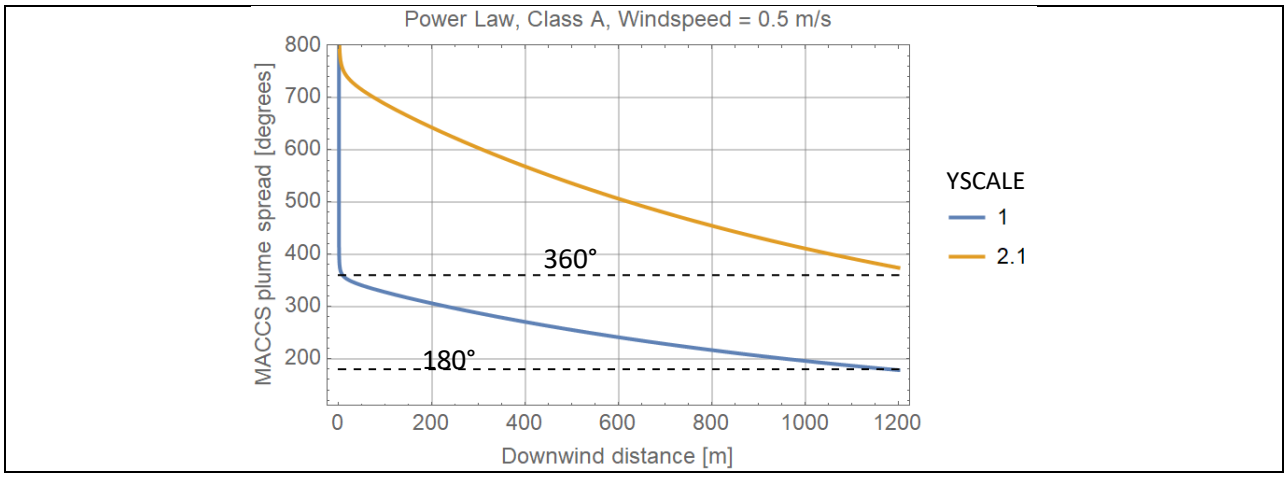

Figure 3-50. MACCS internal plume spread in degrees, based on ±2.15 $\sigma_y(x)$ boundaries, versus the radial distance x. The dispersion coefficients were computed based on power law functions.

Figure 3-51 shows sector plots of sector-average χ/Q concentration outputs by MACCS, considering stability Class A and Gaussian dispersion coefficients defined based on power law functions and a windspeed equal to 0.5 m/s. Note the ±2.15 $\sigma_y(x)$ plume boundaries are located well south of the source for the YSCALE=1 case (top plot). The lower plot is the sector plot for the case YSCALE=2.1, with an internal plume spreading beyond a full circle.

Figure 3-52 displays the information from Figure 3-51 as sector-average χ/Q concentration versus the sector angle. Note that the concentration in the last 0° and 180° sectors exceeds the concentration in the prior sectors oriented 22.5° and 157.5°. This anomaly arises because of the MACCS approach of keeping track of plumes exceeding 180° and adding concentrations of plumes beyond 180° to the last sectors oriented 0° and 180°. As indicated in Figure 3-50, the internal plume spread well exceeds a full circle, and those exceedance arcs are added to the last 0° and 180° sectors. Under the MACCS algorithm, cases of extremely large Gaussian dispersion coefficient result in low concentrations in central sectors, but high concentrations on the sectors oriented 0° (east) and 180° (west). As implied by Figure 3-49 (showing that the plume spread is very similar for any stability class at low windspeeds —close to 0.5 m/s), this extremely broad spread issue is manifested with any stability class at low windspeeds, and care is recommended in using the MACCS meander models to examine low windspeed conditions.

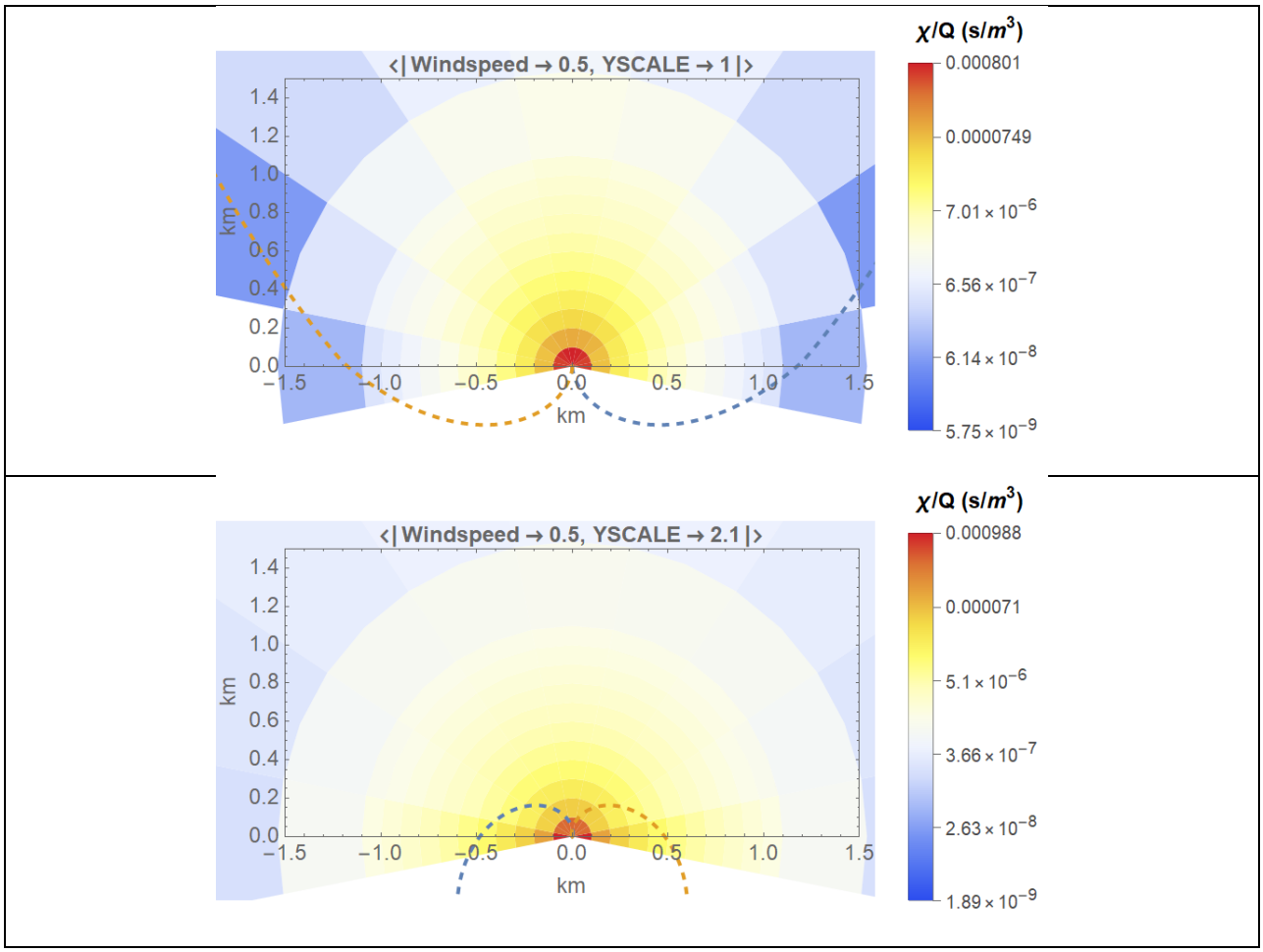

Figure 3-51. Sector plots of the integrated χ/Q sector-average concentration output by MACCS, colored according to logarithmic scales. The dashed curves indicate the ± 2.15 $\sigma_y(x)$ plume boundaries. The stability class in the run was Class A, the windspeed was 0.5 m/s, and the Gaussian dispersion coefficients were computed based on power law functions.

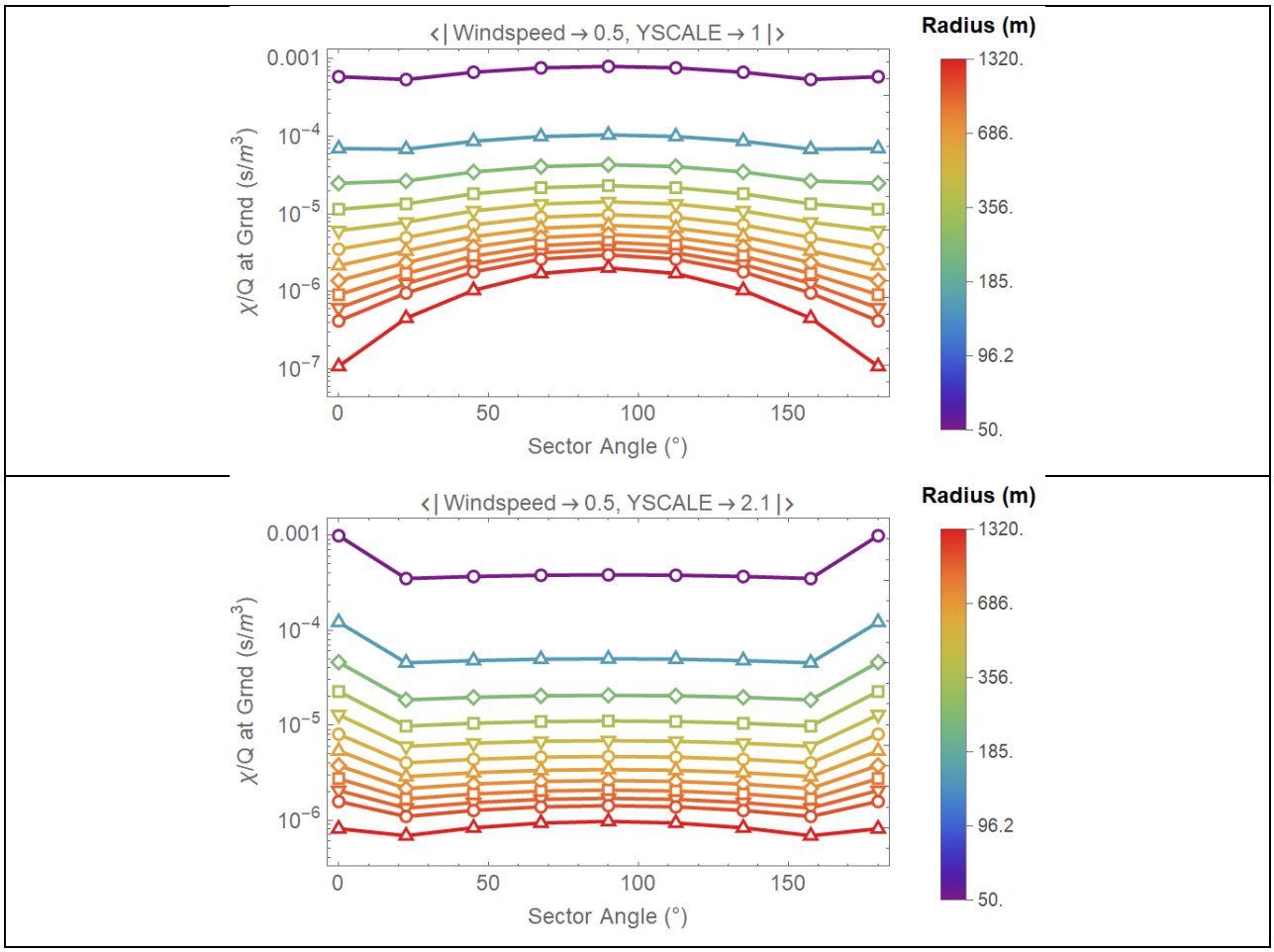

Figure 3-52. Integrated χ/Q sector-average concentration output by MACCS versus the sector angle, for two cases of YSCALE (1 and 2.1). Each curve displays information of sectors at a constant radius, with a radial distance of the sector center to the source indicated by the color legend on the right of the plot. The stability class in the run was Class A, the windspeed was 0.5 m/s, and the Gaussian dispersion coefficients were computed based on power law functions.

Additional Cases Examined

The test included additional cases, but for the sake of brevity the results are only summarized herein. Corresponding output files are archived with the quality assurance records of this report. Runs were executed to examine the Regulatory Guide 1.145 meander model (MNDMOD=NEW) with a point source. Runs considering Gaussian dispersion coefficients based on lookup tables [lookup table values extracted from the Appendix D input files of the SNL nearfield report (Clayton, 2021)] completed successfully. Values output by MACCS of the total lateral Gaussian dispersion coefficient were verified to include meander factors defined by equations (2-1) to (2-11) of the SNL nearfield report (Clayton, 2021). However, changing from lookup tables to power law functions, with coefficients according to Table 2-5 of the MACCS Theory Manual (Nosek & Bixler, 2021) triggered a broad-plume run interrupt, independently of the stability class and windspeed. This is highly anomalous because the plume spread is significantly less than 180° at x=1000 m. Figure 3-53 shows the internal plume spreads computed based on a lookup

table (top plot) and on power law functions (bottom plot), demonstrating that the plume spread is less than 180° at x=1000 m for both cases.

Additional runs were executed considering the original plume meander model in MACCS 4.0 (MNDMOD=OLD), with a plume meander factor computed as a function of the windspeed and stability class according to equations (2-1) to (2-5) of the SNL nearfield model (Clayton, 2021). Also in this test, MACCS runs successfully completed when Gaussian dispersion coefficients were computed from a lookup table but runs that used the power law functions triggered a broad-plume run stop, independently of the stability class and the windspeed magnitude. In the original MACCS 4.0 plume meander model, the meander factor for stability class A is 1 independent of the windspeed; it is highly anomalous that a unit meander factor causes MACCS to trigger a run interrupt. Finally, runs were completed successfully when disabling the plume meander model (MNDMOD=OFF), independently of the approach for computing the Gaussian dispersion coefficients.

Regulatory Guide 1.145 meander model

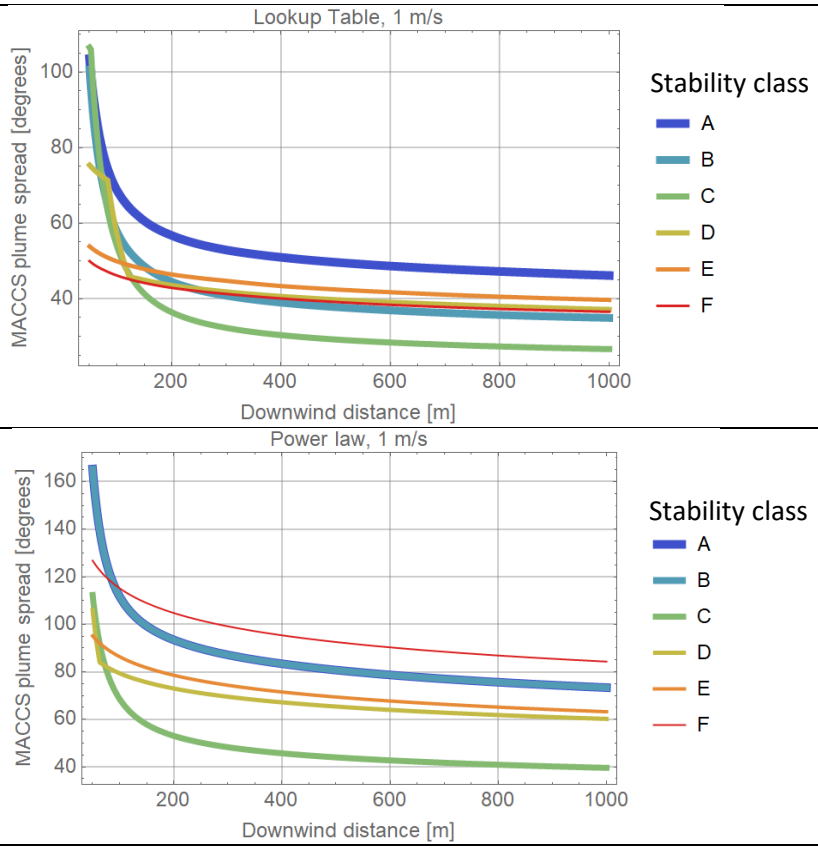

Figure 3-53. MACCS internal plume spread in degrees, based on ±2.15 $\sigma_y(x)$ boundaries, versus the downwind distance x, considering windspeed = 1 m/s. In the top plot, the dispersion coefficients were computed based on a lookup table, and in the bottom plot, based on power law functions.

3.8.4 Test Conclusions

The test revealed anomalies in the implementation of the broad-plume run stop trigger when plume meander models are enabled. A run stop is expected to be triggered when the plume spread (based on ±2.15 σ_y limits) exceeds 180° at 1000 m. When the Ramsdell and Fosmire meander model is enabled (MNDMOD=RAF) and Gaussian dispersion coefficients are based on power law functions (NUM_DIST=0), the run interrupt is not triggered at low windspeeds, despite plume spreads well exceeding 180° at x=1000 m (see Figure 3-50).

On the other hand, when the Regulatory Guide 1.145 meander model (MNDMOD=NEW) is enabled, or the original MACCS 4.0 meander model (MNDMOD=OLD) is enabled, the run interrupt is always triggered whenever the power law function (NUM_DIST=0) is used, although the plume spreads are well below 180° at x=1000 m (see Figure 3-53). Therefore, plume spread checks are not implemented consistently when plume meander models are enabled in conjunction with Gaussian dispersion coefficients computed using power law functions (NUM_DIST=0).

The test verified that lateral Gaussian dispersion coefficients output by MACCS included meander factors computed according to equations in the SNL nearfield report (Clayton, 2021).

For the Ramsdell and Fosmire meander model (MNDMOD=RAF), the test results indicate that the meander factor is significant at low windspeeds, causing plumes to exceed 180° at nearfield distances (x<1000 m). Concentrations along arcs exceeding 180° are added to the east (0° sector) and west (180° sector) sectors. Runs considering power law functions (NUM_DIST=0) and YSCALE=2.1 produced cases where the plume spread exceeded 360°. This caused anomalously high values of integrated sector-average normalized concentrations (χ/Q) for the 0° and 180° sectors (see Figure 3-52). These anomalously high values lack physical meaning.

Caution is recommended on the use or Ramsdell and Fosmire meander model at low windspeeds. The test indicates that the plume meander factor is significant. Very broad plumes can occur at nearfield distances for any stability class at low windspeeds. MACCS applies the narrow plume approximation to extreme locales well beyond the range of validity of the approximation to transform polar to Cartesian coordinates.

The meander factors were designed as empirical corrections to lateral and vertical Gaussian dispersion coordinates, to compute concentration of contaminants in air in Cartesian coordinates. Those factors were not designed in conjunction with the MACCS narrow plume approximation, especially when resulting plumes spread well beyond 180°. Very large spreads due to meander are expected to dilute air concentrations, but in the MACCS implementation those large spreads result in high concentrations in the east and west sectors. It is recommended to examine the physical meaning of those numerical plumes exceeding 180° and consider changing the broad-plume run stop trigger.

3.9 Test 3.9: Early Relocation Model

The objective of the test was to examine the Early Relocation Model, as described in Section 4.2.2 of the MACCS Theory Manual (Nosek & Bixler, 2021). The model considers a whole-body dose limit to trigger relocation. If the projected individual whole-body dose at a location exceeds a specified dose limit, individuals are relocated after a relocation time. MACCS outputs an adjusted dose corresponding to the exposure incurred up to that relocation time. Two dose limits are specified in MACCS, labeled as DOSNRM and DOSHOT, with two corresponding relocation times TIMNRM and TIMHOT. The relocation times are defined with respect to the plume arrival time to a particular location. The DOSHOT is a higher dose limit (i.e., DOSHOT>DOSNRM) used to invoke a faster relocation (i.e., TIMHOT<TIMNRM). Given the straightforward concepts, only the "normal" parameters DOSNRM and TIMNRM were varied in the current test. The specific objectives of the test were the following

- Verifying that people are relocated in a sector if the whole-body dose exceeds DOSNRM
- Verifying that the adjusted relocation dose considers exposure up to a time TIMNRM
- Defining the precise relocation dose criterion in a sector implemented in MACCS; for example,
    - Are people in a sector relocated if <u>any point</u> in the sector exceeds the dose limit?
    - Are people in a sector relocated if the <u>sector-average dose</u> exceeds the dose limit?

3.9.1 Test Input

The same inputs than Test 3.7 were used, with the following changes

ATMOS

- Radionuclides
    - CORINV = 10^{20} Bq for Cs-137, 0 for other radionuclides
- Dispersion
    - Scaling Factors
        - YSCALE = 1, 3.9 (lateral plume spread factor)
        - ZSCALE = 1

EARLY

- Model Basis
    - Duration of Early Phase
        - ENDEMP (s) = 6.048E5 seconds (= 7 days, duration of the emergency-phase period after the arrival of the first plume segment)
    - Normal Relocation
        - TIMNRM (s) = 0, 1, 10, 100, 1000, 10000, 50000, 86400, 100000 (relocation time after plume arrival)
        - DOSNRM (Sv) = 0.1, 1, 10, 100, 1E10
    - Hot Spot Relocation
        - TIMHOT (s) = 0
        - DOSHOT (Sv) = 1E10 (high limit to avoid relocation trigger by hot dose)
- Emergency Cohort One
    - Shielding and Exposure
        - CSFACT = SKPFAC = GSHFAC = 0
        - PROTIN = 1 (only inhalation dose pathway)

- BRRATE (m3/s) = 1E-4, breathing rate

3.9.2 Test Procedure

A set of MACCS runs were executed varying the dose limit DOSNRM (=0.1, 1, 10, 100, 10^{10} Sv) and the YSCALE factor (=1, 3.9), and keeping constant the relocation time TIMNRM = 0. Type 6 central doses and Type C sector average doses were compared to independently computed doses. MACCS compares doses on a sector to the dose limit DOSNRM, and if the doses exceed the dose limit, the sector is assumed subjected to relocation. For this set of runs, since TIMNRM = 0, relocated people are not exposed to contaminants and, accordingly, the MACCS dose for sectors with relocation was zero.

Inhalation doses were independently computed based on the integrated air concentration, $\chi(x, y, z = 0)$ from Eqs. (2-1) and (2-2), multiplied by the whole-body inhalation dose coefficient for Cs-137 (4.688×10^{-9} Sv/Bq from the input database) and the inhalation rate (BRRATE = 10^{-4} m^3/s). The sector-average concentration was determined as a line integral of $\chi(x, y, z = 0)$ computed along the arc passing through the sector center, divided by the arc length, and considering the MACCS narrow plume approximation to transform polar to Cartesian coordinates, Eqs. (3-11) and (3-12). The Type C sector average dose was computed by multiplying the sector average concentration by the inhalation dose coefficient and the inhalation rate.

Alternative approaches to compare sector doses to DOSNRM were examined. The approach more closely reproducing the MACCS outputs is described as follows. Projected inhalation doses were independently computed on the center and extremes of the sector arc. The maximum of those three doses was compared to the dose limit DOSNRM. If the maximum dose exceeded DOSNRM, it was assumed that the sector was subjected to relocation. In other words, in MACCS it is assumed that if <u>any</u> local dose in the sector arc exceeds DOSNRM, the whole sector is subjected to relocation.

Relocation boundaries were numerically computed for the cases examined. In case of no dry or wet deposition, for a given downwind distance x, the lateral distance y_L measured from the centerline at which the inhalation dose becomes equal to DOSNRM is computed as

$$y_L(x) = \sqrt{2}\,\sigma_y(x)\sqrt{\ln\left[\frac{Q\,\psi(x,z)\,DCI\,BR}{\sigma_y(x)\,DOSNRM\,\sqrt{2\,\pi}\,u}\right]} \qquad (3\text{-}24)$$

BR — inhalation rate (m^3/s), BR=10^{-4} m^3/s in the test problem
$DOSNRM$ — relocation dose limit (Sv)
DCI — inhalation dose coefficient, DCI=4.688×10^{-9} Sv/Bq for Cs-137 in the test problem
Q — total activity in the plume segment (Bq), Q=10^{20} Bq in the test problem
u — windspeed (m/s), u=2 m/s in the test problem
x — downwind distance (m)
z — vertical distance from the ground (m), z = 0 in the test problem
$\sigma_y(x)$ — lateral Gaussian dispersion coefficient at x (m)
$\psi(x,z)$ — see Eq. (2-2) (m^{-1})

Note that Eq. (3-24) produces a real number only if the argument of the logarithmic function is greater or equal than 1. If the argument is less than 1, then the inhalation dose is always below DOSNRM for any lateral y distance along a line of constant x. Using Eq. (3-24), and the MACCS narrow plume approximation to transform polar to Cartesian coordinates, Eqs. (3-11)

and (3-12), relocation boundaries were computed and compared to MACCS non-zero dose outputs in sector plots. It was verified that MACCS non-zero dose sectors are outside the relocation boundaries. A second set of MACCS runs was executed varying the relocation time after the plume arrival TIMNRM (=0, 1, 10, 100, 1000, 10^4, 86400, 10^5 seconds), while keeping the dose limit constant DOSNRM = 0.1 Sv and YSCALE = 3.9. It was verified that the Type C sector average doses linearly increase with the exposure time, up to a point where TIMNRM equals the plume duration time (PLUDUR = 86400).

3.9.3 Test Results

In the first set of runs, the dependence of results on the dose limit DOSNRM was examined. The relocation time TIMNRM was set to zero, and DOSNRM was varied. A couple of lateral spread cases were examined, YSCALE=1, 3.9. Figure 3-54 compares MACCS Type 6 centerline inhalation doses from the file Model1.out (outputs labeled L-ICRP60ED INH LIF) to independently computed doses, based on integrated concentrations in air at the ground level, multiplied by the whole-body inhalation dose coefficient for Cs-137 and the inhalation rate. The MACCS outputs and the independently computed inhalation doses are in excellent agreement. The horizontal dashed line is the dose limit in the MACCS run. MACCS output zero if the projected dose exceeded DOSNRM.

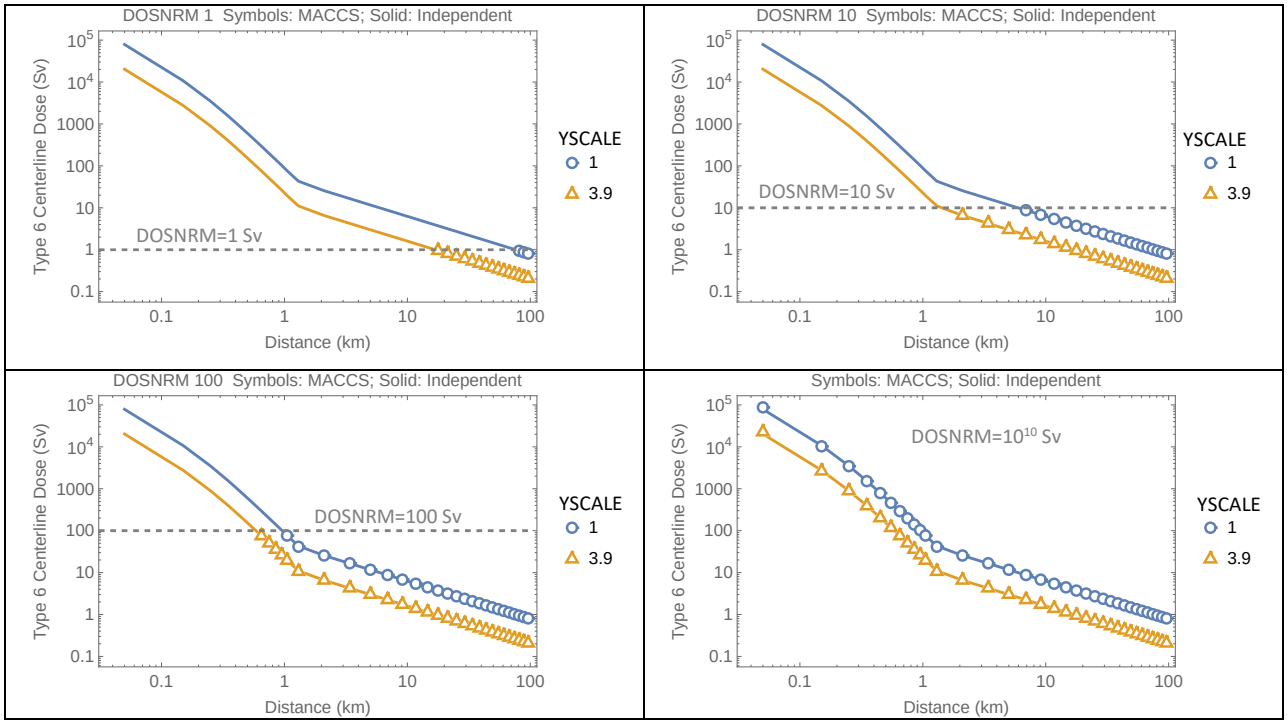

Figure 3-54. Type 6 centerline dose versus downwind distance for different dose limits DOSNRM (horizontal dashed lines). The symbols are MACCS outputs (centerline inhalation dose) and the solid curves are the independently computed centerline doses. TIMNRM = 0.

Figure 3-55 compares the Type C sector average dose MACCS outputs (symbols) to independently computed sector average inhalation doses (solid curves), with YSCALE=3.9 and TIMNRM=0. The legend indicates the sector angle; 0 radians corresponding to the east direction and $\pi/2$ radians (90°) to the north or centerline direction. The MACCS doses and the independent computations are in close agreement, except in sectors far from the center and at

far distances. This small variation has been noted in previous tests such as Test 3.5, and it is due to different numerical algorithms to compute averages, especially for sectors close to the 2.15 σ_y edges. In the runs with different values of DOSNRM, it was verified that the non-zero sector average doses are identical in the different runs independent of the value of DOSNRM. In the plots in Figure 3-55, the non-zero doses are well below the DOSNRM limit, indicating that the approach to setting the sector doses to zero in the relocated sectors in MACCS differs from a direct comparison of the sector average dose to DOSNRM. Instead, the relocation criterion in MACCS is based on comparison of the maximum dose sampled along the arc sector to DOSNRM. If any point in the sector arc exceeds DOSNRM, relocation is applied to the sector.

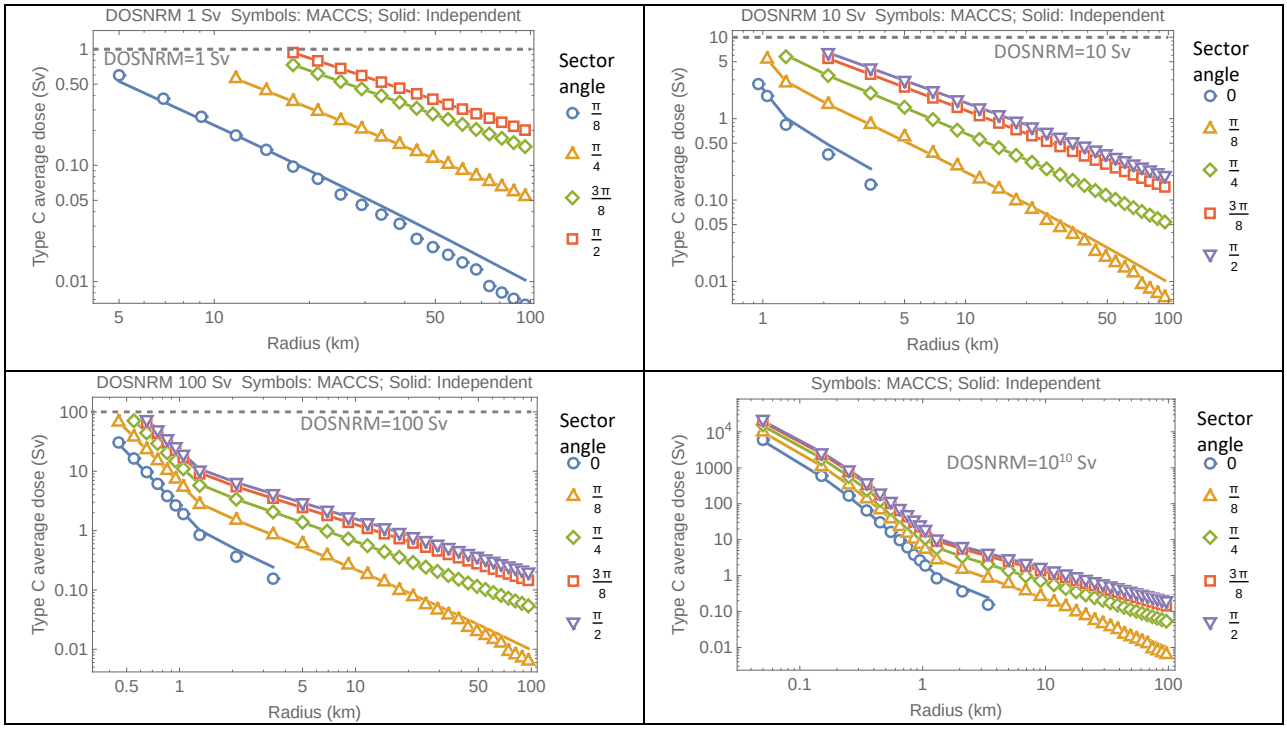

Figure 3-55. Type C sector average dose versus radius for different dose limits DOSNRM (horizontal dashed lines). The symbols are MACCS outputs and the solid curves are the independently computed sector average doses. YSCALE = 3.9 and TIMNRM = 0.

Figure 3-56 displays sector plots considering different values of DOSNRM. Figure 3-57 displays the same data as that in Figure 3-56, zoomed-in to a smaller region. The plots on the left are the MACCS Type C average dose outputs. The plots on the right include independently computed sector average inhalation doses. The dashed curves represent the ±2.15 σ_y boundaries and the solid curves enclose the relocation zone where local projected doses would exceed DOSNRM. The independent computations exhibited agreement with the MACCS outputs, with minor differences attributable to (i) roundup error, (ii) differences in dose computations for sectors close to the ±2.15 σ_y boundaries (also noted in Figure 3-55), and (iii) differences in Gaussian dispersion coefficients near the source due to alternative interpolation algorithms to compute the Gaussian dispersion coefficients.

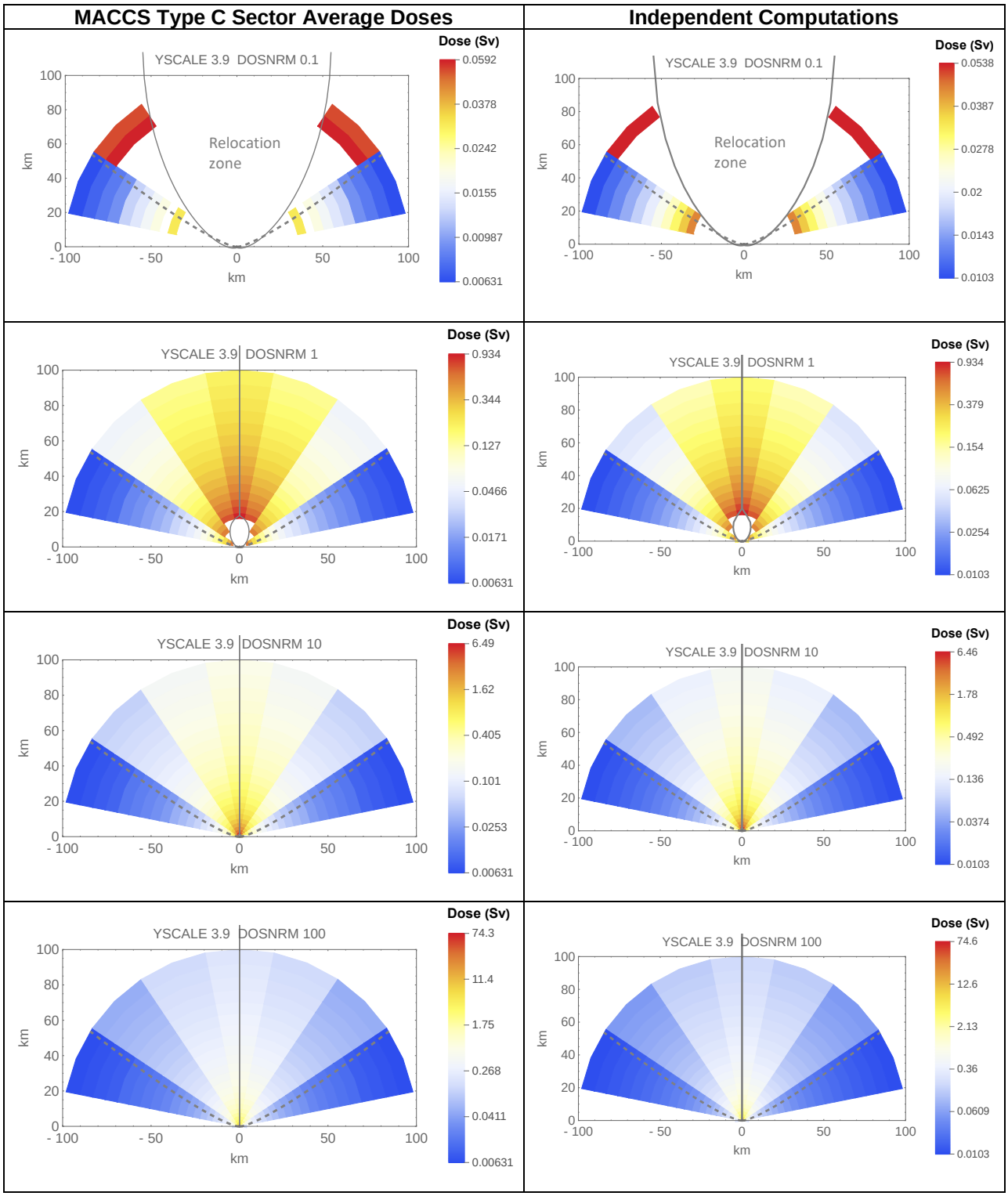

Figure 3-56. Sector plots of the Type C sector average dose for different dose limits (DOSNRM indicated in plot headers). Plots on the left are MACCS outputs and plots on the right are independent computations. YSCALE = 3.9.

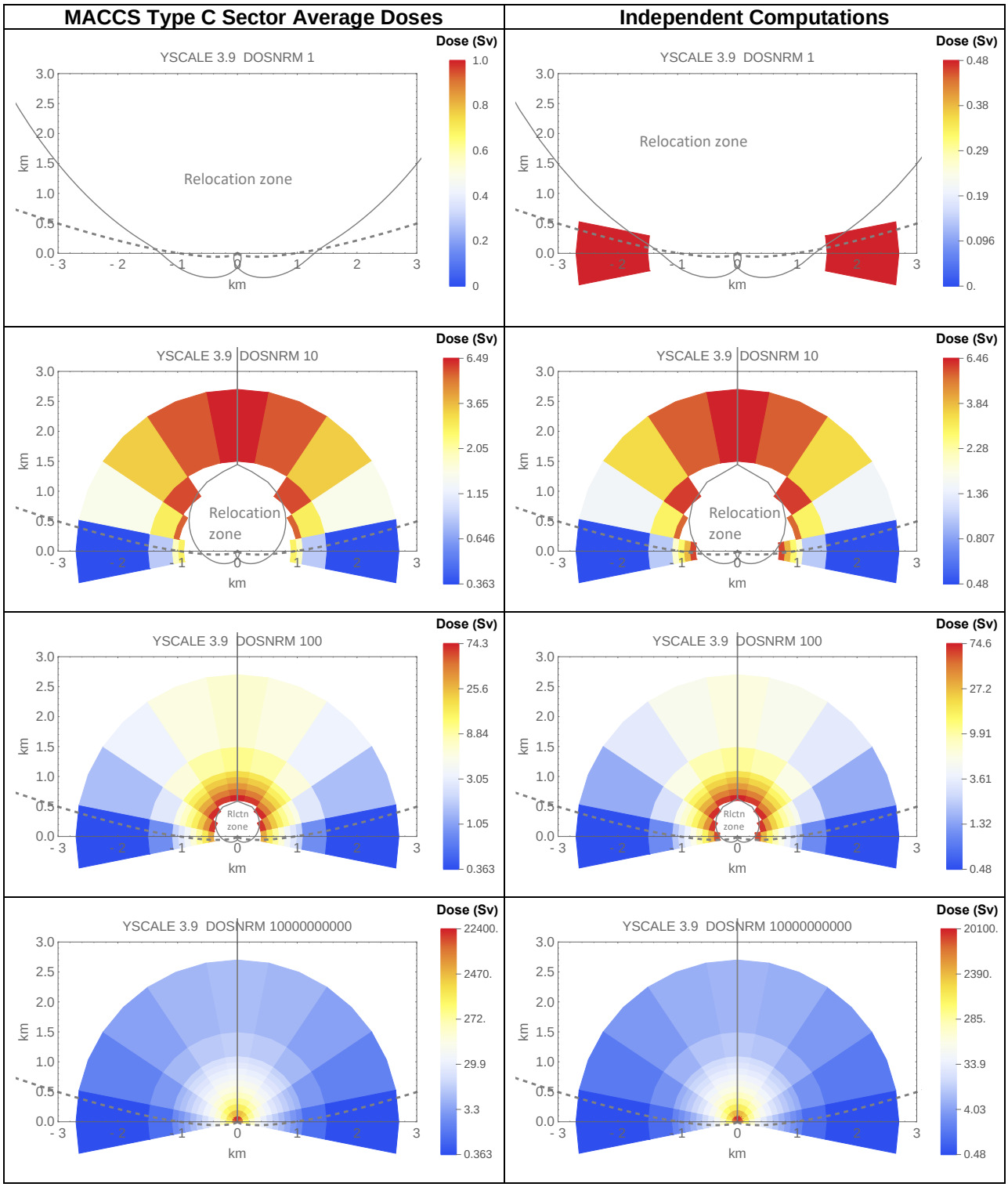

Figure 3-57. Sector plots of the Type C sector average dose for different dose limits (DOSNRM indicated in plot headers). Plots on the left are MACCS outputs and plots on the right are independent computations. YSCALE = 3.9.

Note the close agreement of the vertical color scales of the MACCS outputs (left plots) and the independently computed average inhalation doses (right plots) in Figure 3-56 and Figure 3-57. The low values of the color scales slightly differ, because the independent doses are greater than the MACCS outputs for sectors far from the source and close to the ±2.15 σ_y boundaries (related to differences noted in the plots in Figure 3-55). The top values of the color scales for the cases DOSNRM = 10 Sv and DOSNRM = 100 Sv are in excellent agreement. For the high dose limit case (DOSNRM = 10^{10} Sv), the maximal doses occur near the source. In this case, the independently computed Gaussian dispersion coefficients differ slightly from the MACCS coefficients near the source, and those differences are amplified in the integrated air concentrations, causing differences on the order of 10% in the inhalation dose. Such variation is entirely due to the different interpolation algorithms used to compute the Gaussian dispersion coefficients as a function of the downwind distance x.

The independent computations identified a few sectors with non-zero doses, which are output with zero values by MACCS due to relocation. This was due to the different algorithms yielding slightly higher dose in the independent computations for sectors near the ±2.15 σ_y boundaries. In the independent computations, such sectors were deemed outside the relocation zone, while MACCS identified those sectors within the relocation zone. MACCS slightly overestimates the area of the relocation zone compared to the independent computations. Nonetheless, it is concluded that the MACCS outputs and the independent computations are in excellent agreement, with minor differences due to different algorithms used in the verification computations.

A second set of runs was executed to examine the dependence of the results on TIMNRM. In the second set of runs YSCALE = 3.9, DOSNRM = 0.1 Sv, and TIMNRM was varied from 0 to 10^5 seconds. Figure 3-58 displays the Type 6 centerline dose (labeled L-ICRP60ED INH LIF in the Model1.out MACCS output file) versus the downwind distance. The MACCS outputs are the symbols and the independent computations, the solid curves. For the case DOSNRM = 0.1 Sv, the whole centerline is subjected to relocation (see Figure 3-56). The relocation time TIMNRM is an exposure time, and the centerline dose is linearly proportional to the relocation time up to TIMNRM = 86400 s, which is the plume duration in the runs (PLUDUR = 86400 s). After 86400 s, the exposure to the plume cloud is complete, the inhalation dose is maximal, and the inhalation dose does not further increase with increasing TIMNRM beyond 86400 s. As expected, the centerline doses for the cases TIMNRM = 86400 s and TIMNRM = 10^5 s are identical in the top plot of Figure 3-58. The lower plots of Figure 3-58 display the centerline dose versus TIMNRM for the downwind distance x = 9.1 km, in logarithmic and linear scales. These plots clearly show that the centerline dose is linearly related to TIMNRM and that a plateau is reached when TIMNRM is equal or greater than 86400 s. The MACCS results are expected, perfectly in agreement with the independent computations.

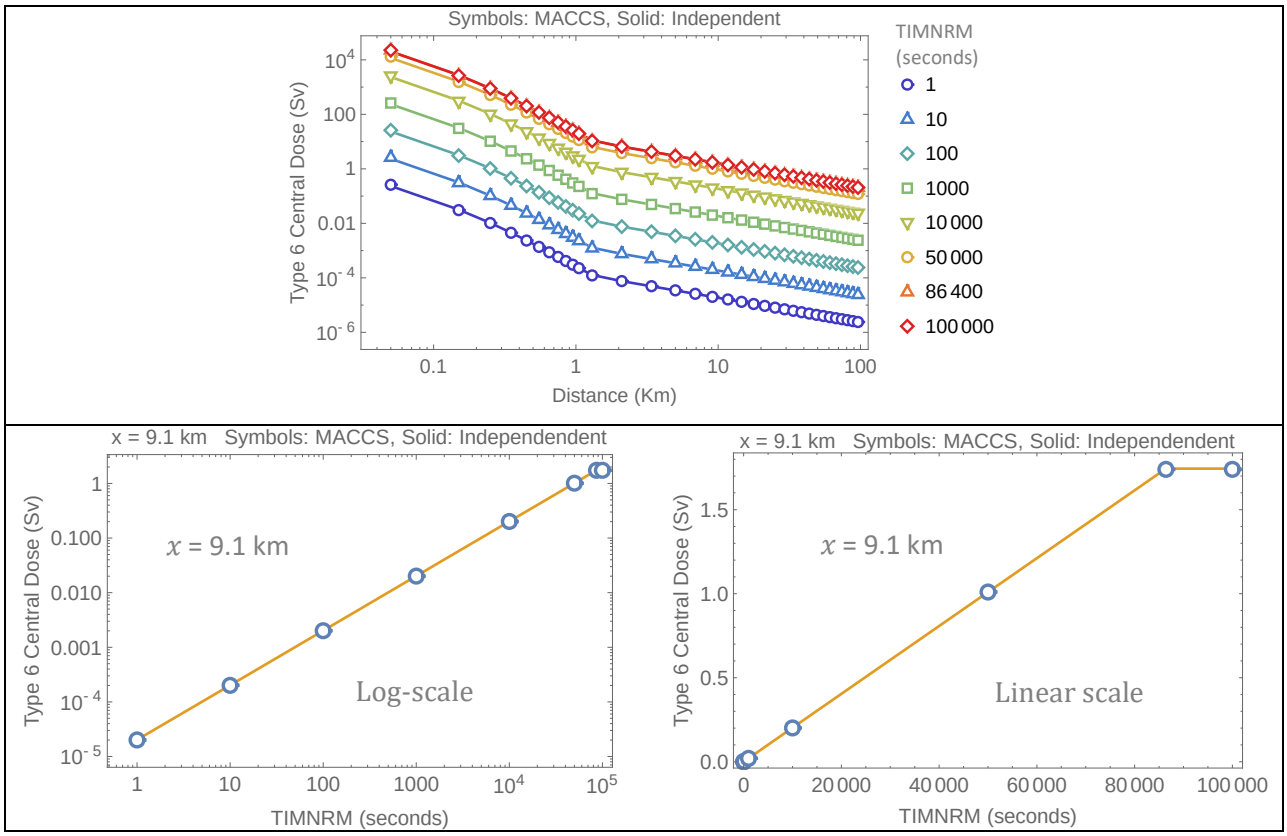

Figure 3-58. Type 6 centerline dose with different values of TIMNRM. The symbols are MACCS outputs and the solid curves are the independently computed centerline doses. DOSNRM = 0.1 Sv and YSCALE = 3.9.

The next set of results examine the dependence of the sector average dose on TIMNRM. Figure 3-59 displays sector plots of the sector average Type C dose for runs with different values of TIMNRM (indicated in the headers of the plots) and with DOSNRM=0.1 Sv. The case TIMNRM=0 clearly indicates the relocation zone as a white (0 dose) region. The non-zero dose sectors of the case TIMNRM=0 have identical doses in all runs, independently of the value of TIMNRM, because these sectors do not undergo relocation and are exposed to the full plume. The color of these sectors in the plots in Figure 3-59 changes because the color scale is different in each sector plot.

Doses are non-zero in the relocation zone for cases with exposure time TIMNRM>0. For cases with TIMNRM>0, the maximum and minimum doses lie within the relocation dose. The maximum and minimum doses are indicated in the color scale on the right of the sector plots. Note that the min-max values linearly change with the value of TIMNRM. This linear variation verifies that the sector-average dose is proportional to TIMNRM in the relocation zone. The MACCS results are expected, based on the description in the MACCS Theory Manual. No anomalous results were identified.

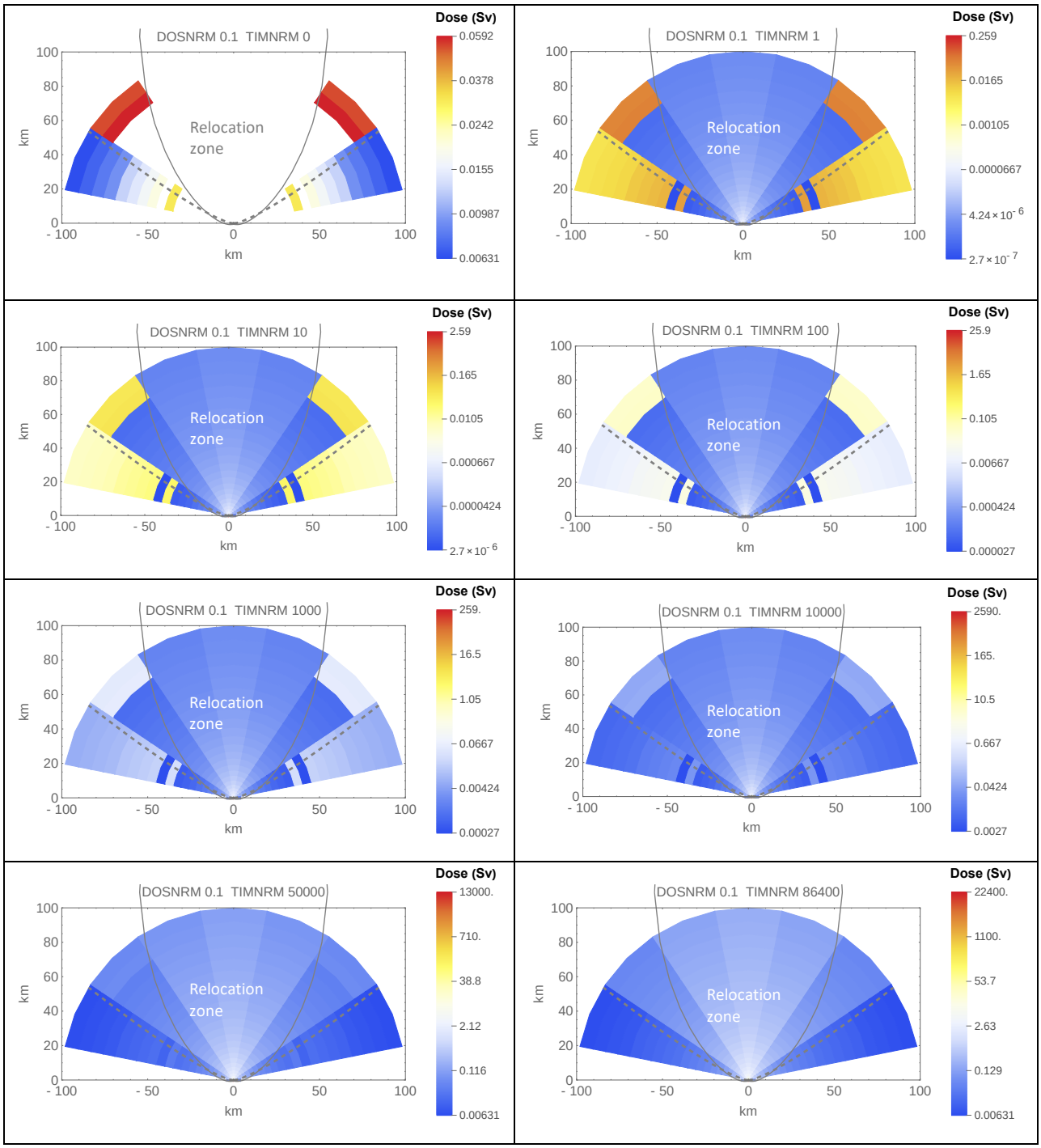

Figure 3-59. Sector plots of the Type C sector average dose for different relocation time (TIMNRM indicated in plot headers). DOSNRM = 0.1 Sv and YSCALE = 3.9.

3.9.4 Test Conclusions

No anomalies were identified in the test. MACCS outputs matched expected results consistent with the description in the MACCS Theory Manual.

The test revealed details of the implementation of the relocation dose limit criterion. MACCS applies relocation when the projected whole-body dose on any point on the sector arc exceeds the dose limit DOSNRM. Doses in the relocated sector are adjusted to account for partial exposure to a plume, up to an exposure time TIMNRM.

The testing focused on inhalation doses. The MACCS algorithms of the relocation concept are straightforward, and it is not envisioned that other dose pathways would introduce artefacts in the relocation algorithms.

3.10 Test 3.10: Comparison of Early Relocation Dose to FRMAC Protective Action Guides

The objective of this test is to compare dose computations of the EARLY MACCS module to early-phase individual dose projections defined by the Federal Radiological Monitoring and Assessment Center (FRMAC) (Blumenthal, et al., 2020), and implemented in the Turbo FRMAC (TF) software (Sandia National Laboratories, 2022). The objective of the test was to examine major differences in the computations of doses from multiple pathways (inhalation, cloudshine, inhalation of resuspension, groundshine), comparing the MACCS relocation dose limit DOSNRM to the FRMAC protective action guide (PAG), and examining introducing the FRMAC concept of derived response levels (DRL) in MACCS.

3.10.1 Test Input

The same inputs than in Test 0 were used, with the following changes

ATMOS

- Radionuclides
  - Radionuclides
    - CORINV (Bq) = 1E+20 for I-129 and 0 for other radionuclides
    - A long-lived radionuclide was selected to avoid decay complexity
- Deposition
  - Wet/Dry Depos Flags
    - DRYDEP = True for I
    - WETEP = False for I
  - Dry Deposition
    - VDEPOS (m/s) = 0.0034 for velocity 5
- Dispersion
  - Scaling Factors
    - YSCALE = ZSCALE = 1
- Release Description
  - Plume Parameters
    - PLUDUR (s) = 120
  - Particle Size Distribution
    - PSDIST = 1 for velocity 5, 0 for other velocities
    - All particles are of a single size, with a deposition velocity VDEPOS = 0.0034 m/s
  - Release Fractions
    - RELFRC = 1 for I, 0 for other elements
- Output Control
  - NUCOUT = 1-129

EARLY

- Model Basis
  - Duration of the Early Phase
    - ENDEMP (s) = 86400 (1 day)
  - Normal Relocation
    - DOSNRM (Sv) = 1E+10 (high dose limit to avoid relocation)
  - Emergency Phase Resuspension
    - RESCON (1/m) = 1E-5
    - RESHAF (s) = 8.56E5

- Emergency Cohort One
  - Shielding and Exposure
    - CSFACT = PROTIN = GSHFAC = 1
    - SKPFAC = 0
    - BRRATE (m^3/s) = 4.17E-4 (inhalation rate)
- Output Control
  - Centerline Dose (NUM6)
    - ORGNAM=L-ICRP60ED; PATHNM=INH LIF; ID1DIS6 =1; ID2DIS6=34
    - ORGNAM=L-ICRP60ED; PATHNM=CLD; ID1DIS6 =1; ID2DIS6=34
    - ORGNAM=L-ICRP60ED; PATHNM=GRD; ID1DIS6 =1; ID2DIS6=34
    - ORGNAM=L-ICRP60ED; PATHNM=RES LIF; ID1DIS6 =1; ID2DIS6=34
    - Settings adjusted to itemize the inhalation (INH LIF), cloudshine (CLD), groundshine (GRD), and inhalation of resuspension (RES LIF) doses

Turbo FRMAC inputs

The following default equation is used in Turbo FRMAC (TF) to compute the resuspension proportion, K_t, of contaminants as a function of time [Equation 2 of Appendix F, Supplement 2 of the FRMAC Assessment Manual (Blumenthal, et al., 2020)]

$$K_t = 10^{-5}\ \mathrm{m}^{-1}\ e^{-8.1\times10^{-7}\ \mathrm{s}^{-1}\ t} + 7\times10^{-9}\ \mathrm{m}^{-1}\ e^{-2.31\times10^{-8}\ \mathrm{s}^{-1}\ t} + 10^{-9}\ \mathrm{m}^{-1} \quad (3\text{-}25)$$

The variable t is the time measured in seconds. The TF inputs were adjusted to only keep the first term of Eq. (3-25); i.e.,

$$K_t = 10^{-5}\ \mathrm{m}^{-1}\ e^{-8.1\times10^{-7}\ \mathrm{s}^{-1}\ t} \quad (3\text{-}26)$$

In MACCS, the parameters of the resuspension function were adjusted to reproduce Eq. (3-26), by setting RESCON = 10^{-5} m^{-1} and RESHAF = ln(2)/(8.1×10^{-7} s^{-1}) = 8.56×10^{5} seconds.

The default inhalation rate in TF is 4.17×10^{-4} m^3/s to compute the inhalation dose. On the other hand, the default inhalation rate for dust resuspension is 2.56×10^{-4} m^3/s. The direct inhalation rate for the contaminant cloud is higher because individuals are assumed moving away from the release. By contrast, MACCS considers the same inhalation rate during the cloud passage and for dust resuspension, although it is possible to include independent adjustment factors through the shielding factors PROTIN and GSHFAC.

The main interface of TF for Public Protection and Derived Response Levels requires inputs in the Time Settings window. A screen capture of the Time Settings window is displayed in Figure 3-60, with the inputs to the test problem. A rationale for the inputs and the relationship to inputs of the MACCS simulation is described as follows. Integrated air concentrations and ground concentrations were extracted from MACCS runs considering ENDEPM = 86400 seconds (24 hours). The plume duration in the MACCS run (PLUDUR) was input as 120 seconds, and a long-lived radionuclide, I-129, was considered in the MACCS run. MACCS outputs integrated air concentrations and ground concentrations after the plume passage. The exposure time to those ground concentrations in the MACCS simulation was approximately 24 hours (minus negligible corrections to account for gradual buildup of ground concentration during the early 120-second plume passage). Accordingly, the TF Duration input was selected as 24 hours. TF allows the user to input two independent times, such as Start Time and Duration. The End Time is automatically computed by TF as End Time = Start Time + Duration. The enabled dose pathways were Plume Inhalation, Plume Submersion, Resuspension Inhalation, and Groundshine. The Start Time was set as 0; TF issues a warning when the Start

Time is different from zero with plume pathways (inhalation and submersion or cloudshine) enabled.

The TF Evaluation Time is denoted as t_n in the FRMAC Assessment Manual (Blumenthal, et al., 2020). The Evaluation Time represents the time at which the contaminant mixture in soil or air is measured or estimated. The Evaluation Time input was set as 0.033 hr, corresponding to 120 seconds of the plume duration. However, the TF dose outputs are independent of the t_n input. The Evaluation Time is used in TF to compute ground concentration Derived Response Level (DRL), by extrapolating back in time the decayed ground concentration to the Start Time. Those DRL outputs were not considered in the current test.

The deposition velocity was set equal to 0.0034 m/s (identical to VDEPOS). Weathering correction was disabled in TF.

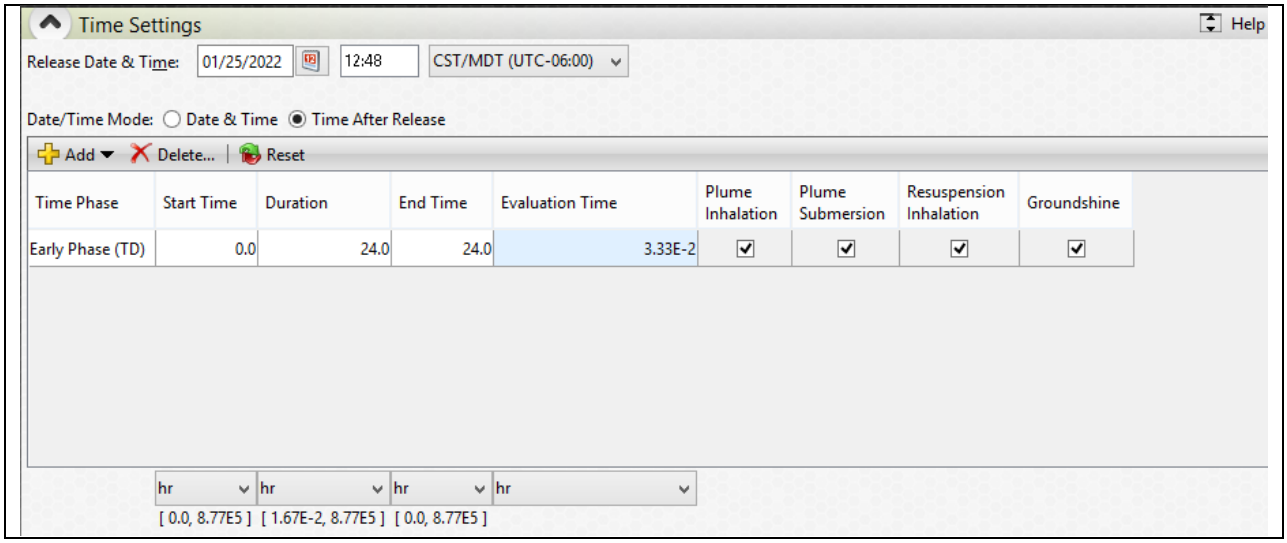

Figure 3-60. Time Settings inputs used in the TF computations.

3.10.2 Test Procedure

MACCS was executed with the defined inputs. The centerline doses (Type 6 outputs) for four pathways were extracted from the Model1.out file, associated with I-129 doses for inhalation, cloudshine, groundshine, and resuspension. The I-129 integrated air concentration at the ground level and the ground concentration were also extracted from Model1.out, corresponding to concentrations right after the plume passage at the different locations.

At any point, right after the passing of the radioactive cloud, the ground concentration equals the integrated air concentration at the ground level times the deposition velocity, Eq. (2-25). Because of this simple relationship, TF allows alternative pair of inputs at the detection time to compute the doses

- I-129 integrated air concentration and ground concentration; the deposition velocity is automatically computed

- I-129 integrated air concentration and the deposition velocity; the ground concentration is automatically computed

- I-129 ground concentration and the deposition velocity; the integrated air concentration is automatically computed

When the I-129 integrated air concentration and ground concentration were input, it was verified that the deposition velocity was 0.0034 m/s (VDEPOS in the MACCS run). Alternative inputs in the previous bullets produced the same doses. In the computations of the TF doses reported herein, the independent inputs were the I-129 integrated air concentration and the deposition velocity (VDEPOS=0.0034 m/s).

The I-129 integrated air concentrations were manually input to TF at the different downwind distances, and TF was run for every input concentration to compute itemized doses for the four pathways. The TF outputs for each downwind distance were captured in an Excel file and compared to the MACCS Type 6 centerline doses.

3.10.3 Test Results

The MACCS centerline Type 6 whole-body doses (symbols) and the TF dose outputs (solid curves) are compared in Figure 3-61. There is excellent agreement between the inhalation doses (legend INH). The dust resuspension inhalation dose (legend RES) is also in excellent agreement, considering that the MACCS inhalation rate is BRRATE = 4.17×10^{-4} m^3/s, and the TF inhalation rate for resuspension is 2.56×10^{-4} m^3/s. The MACCS and TF resuspension doses differ exactly by a factor 2.56×10^{-4} m^3/ 4.17×10^{-4} = 0.61, due to differences in the input inhalation rates. The cloudshine doses (legend CLD) are in reasonable agreement. The differences for distances near the source are due to the cloudshine factor, which is used in the MACCS computations, but not in the TF computations. Far from the source, the MACCS cloudshine factor approaches 1, and the MACCS and TF cloudshine doses become identical.

A very large difference between the I-129 groundshine doses (legend GRD) was identified, requiring additional investigation to identify causes. The TF groundshine dose is a factor of 1,200 greater than the MACCS groundshine dose. The lower plot in Figure 3-61 includes the groundshine dose, independently computed considering Eq. (3-1), and an exposure time equal to 24 hours − 60 seconds = 86340 seconds. The MACCS duration of the EARLY phase is ENDEMP = 24 hours, with respect to the plume arrival to a location. The subtraction of 60 seconds is to account for linear buildup of concentration in the ground, from zero to a maximal concentration at the time the radioactive cloud exits a location (the subtraction of 60 second is a marginal correction, which can be ignored). See Figure 3-3 of the MACCS Theory Manual (Nosek & Bixler, 2021) for a description of the exposure time, adjusted by linear buildup on the ground and radioactive decay. The radionuclide I-129 was selected due to its long-life, to ignore radioactive decay. The independently computed groundshine dose for the centerline, based on Eq. (3-1), agreed with the TF outputs. There was a difference of a factor equal to 0.82, which is an additional factor in the TF computations to account for surface roughness (which can be accounted in MACCS with the shielding factor GSHFAC). Otherwise, the independent computations for the centerline groundshine dose and the TF outputs were in excellent agreement. As previously stated, the MACCS groundshine dose was a factor of 1200 lower than the TF outputs.

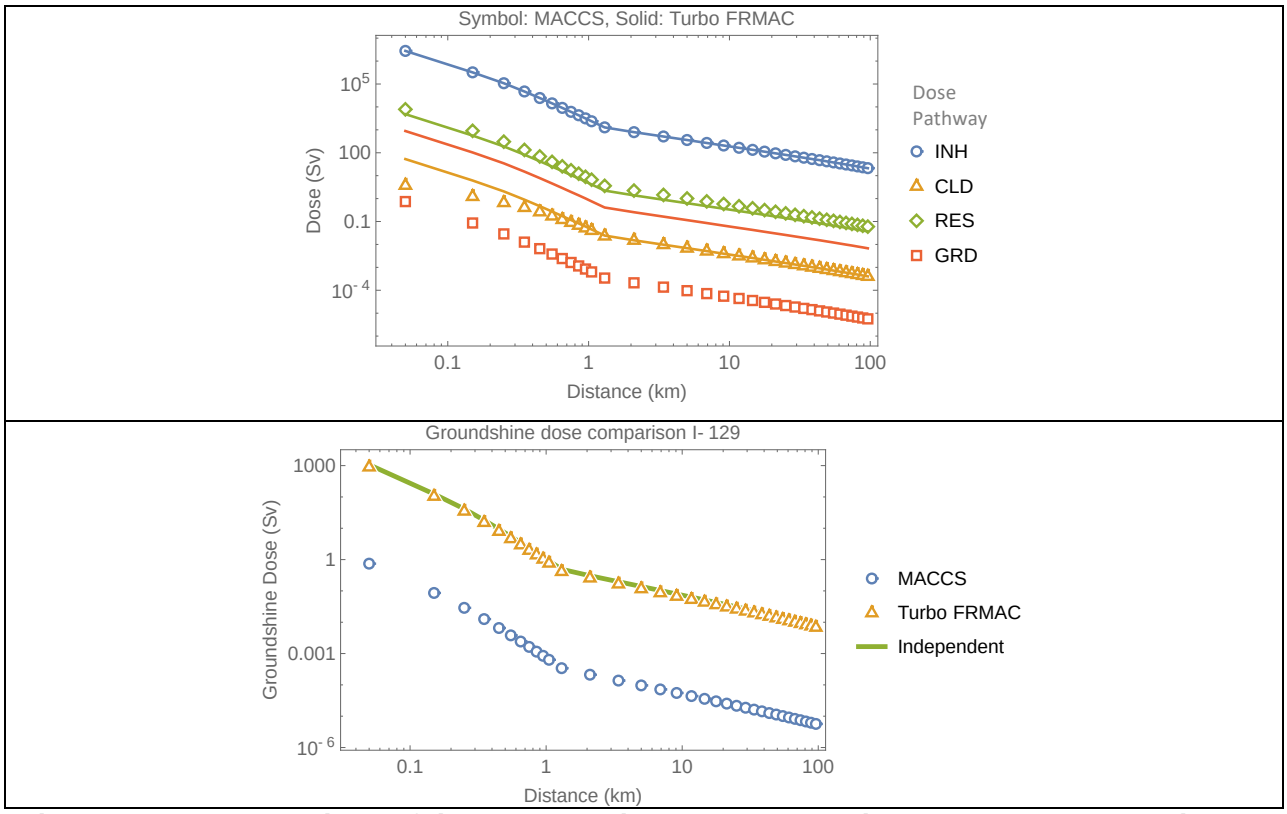

Figure 3-61. Comparison of doses output by MACCS to Turbo FRMAC outputs and to independent computations.

Additional MACCS runs were executed to further investigate causes behind the groundshine dose error. Single radionuclide runs were executed with I-124, I-125, I-129, and Cs-137 to compute the groundshine dose for different radionuclides. Type 6 groundshine centerline doses were independently computed and compared to the MACCS outputs. The plot in Figure 3-62 shows that the independent computations perfectly reproduced the MACCS Type 6 centerline doses, except for I-129. It appears that MACCS incorrectly retrieves the whole-body dose coefficient for I-129 for groundshine from the input database.

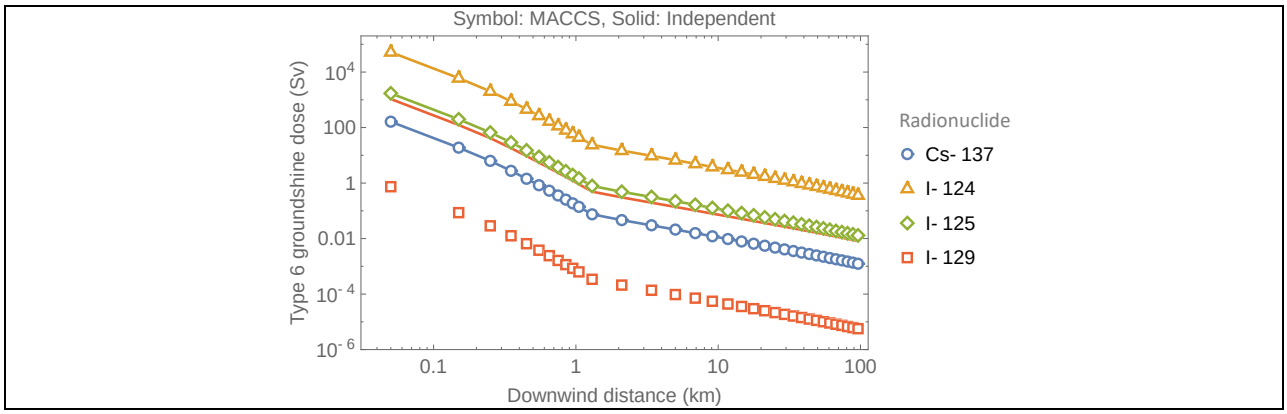

Figure 3-62. Comparison of Type 6 groundshine centerline doses output by MACCS to independent computations.

3.10.4 Comparison of Equations and Concepts in TF and MACCS

Comparison of Early Phase Period Equations in TF and MACCS

When inputs are made to align the models, the MACCS early phase doses agree with the TF total doses. An error in the MACCS groundshine dose for I-129 was identified, possibly related to a dose coefficient for whole-body dose incorrectly retrieved from the database of dose coefficients. This error was only exhibited in I-129. Groundshine doses computed for other radionuclides were in perfect agreement with expected doses according to Eq. (3-1).

It is concluded that equations for early phase doses in MACCS and the early phase TF are of similar structure. There are a few differences in the early phase dose equations:

- The MACCS cloudshine dose includes a cloudshine factor; the equivalent factor is 1 in the TF equation

- The groundshine and inhalation of resuspended dust pathways include corrections in MACCS to account for gradual buildup on the ground as a radioactive cloud moves above a location. TF includes simplified and conservative computations to simulate exposure to ground concentrations during the plume passage (details are provided in the section Commentary on the TF Derived Response Level)

- The groundshine dose in TF explicitly includes factor to account for surface roughness (ground roughness factor defaulted to 0.82 in TF). In MACCS, a roughness effect can be embedded in the shielding factor GSHFAC

- The function in TF to define resuspension as a function of time includes more terms than the corresponding resuspension function in MACCS

- TF includes an independent function to account for weathering with a weathering factor, WF, computed as [Equation 5 of Appendix F, Supplement 2 of the FRMAC Assessment Manual (Blumenthal, et al., 2020)]

$$WF_t = 0.4\, e^{-1.46\times10^{-8}\,\mathrm{s}^{-1}\,t} + 0.6\, e^{-4.44\times10^{-10}\,\mathrm{s}^{-1}\,t} \tag{3-27}$$

  The weathering factor is used in TF in the computation of doses from groundshine and resuspension inhalation pathways. The TF independent resuspension factor function is presented in Eq. (3-25). By contrast, in MACCS resuspension and weathering during the early phase is combined in a single exponentially decaying function of time (RESCON is the resuspension factor in MACCS and RESHAF is the half-life of the resuspension/weathering process) for the resuspension inhalation pathway. The groundshine pathway of the early phase does not include any weathering decrease in MACCS. In the CHRONC module, which includes an optional intermediate phase, MACCS considers independent functions for resuspension (input parameters RWCOEF and TRWHLF) and weathering (input parameters GWCOEF and TGWHLF); both functions are sums of exponentially decaying terms like the TF functions.

- TF considers two independent inhalation rates for the direct inhalation pathway and the dust resuspension inhalation pathway. In MACCS there is only one inhalation dose rate as input. A correction to the inhalation dose rate input in MACCS could be embedded in the shielding factor PROTIN or in the resuspension factor RESCON.

The differences in the Early Phase dose equations are relatively simple, and it would be straightforward to modify MACCS to reach full consistency with the TF Early Phase dose equations.

Comparison of Early Phase Exposure Periods in TF and MACCS

Early phase exposure periods are simulated differently in MACCS and in TF. Figure 3-63 displays default Time Settings inputs for TF computations of Public Protection and Derived Response Levels. The default computations include two early phase settings labeled TD (for total dose) and AD (for avoidable dose). Other periods are generated by TF default settings including a one-year, two-year, and fifty-year year periods. The dose and derived response level (DRL) equations for the TD and AD phases are identical. The TD and AD TF results (doses and DRLs) are identical if the corresponding inputs, including selected dose pathways, are identical. The TD phase is intended to include the plume passage and plume pathways (i.e., inhalation and submersion). The AD phase is intended to cover a period after plume passage. The TD and AD periods may overlap as in the default inputs in Figure 3-63. As previously stated, TF requires two time inputs to define the exposure time of the ground pathways, such as Start Time and Duration (End Time is automatically computed as End Time = Start Time + Duration). The Evaluation Time is an input to compute the derived response level for ground concentrations.

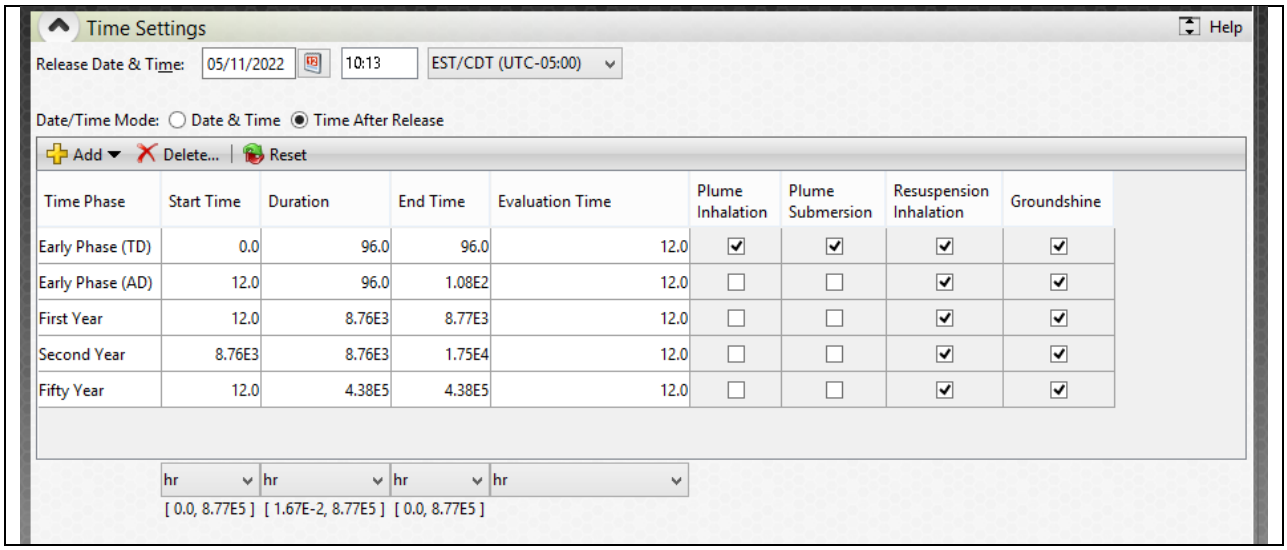

Figure 3-63. Default TF Time Settings inputs for Public Protection and Derived Response Level computations.

Figure 3-64 displays an example of inputs in the Radionuclide Mixture TF window used in the test problem. In the test problem, the only radionuclide in the mixture was I-129; however, TF allows to input concentrations of multiple radionuclides present in a contaminant mixture. As previously stated, the Evaluation Time, t_n, is the time immediately after plume passage. Concentrations input as radionuclide mixture to TF are concentrations measured at the time t_n. The check box on the right of Figure 3-64 indicates that TF allows to (i) input the integrated air concentration and the deposition velocity, (ii) input the ground concentration and the deposition velocity, or (iii) both concentrations (in this case the deposition velocity is computed as an output). TF assumes that the ground concentration is proportional to the integrated air concentration, with a proportionality constant equal to the deposition velocity. This assumption constrains the definition of the Evaluation Time t_n, because this proportionality is only valid if the air and ground concentrations are computed immediately after the plume passage. If the integrated air concentrations corresponded to a partial plume, the TF model does not include

tools to extrapolate to a full-plume integrated air concentration, and both air concentrations and ground concentrations would be underestimated. If the ground radionuclide concentration was measured long after the plume passage, the integrated air concentration of a highly decaying radionuclide computed by TF (as the ratio of the ground concentration and the deposition velocity) would be underestimated. Therefore, care should be exercised in providing consistent input concentrations to TF so that they correspond to concentrations immediately after the plume passage.

The default TD and AD phases can be compared to the early MACCS phase; however, there are differences. The MACCS early phase is intended to be a phase of long-enough duration to include the complete plume release. The plume segment release sequence in MACCS can be complex, with multiple independent plume segments overlapping or not in time and released over short or extended times. The buildup of radionuclide concentration is approximated in MACCS as linear buildup in time, from zero to a maximal concentration at the end of a plume segment. MACCS accounts for gradual buildup on the ground to compute doses from groundshine and inhalation of resuspension pathways. By contrast, the TF includes a factor interpreted as an extrapolation factor to estimate ground concentrations at the Start Time from ground concentration at the Evaluation Time. This correction factor is described later in detail, and it does not account for the gradual buildup process accounted for in MACCS. The TF Evaluation Time approximately corresponds to the MACCS plume duration (PLUDUR) for cases with a single plume and short plume duration, as in the problem examined in this test. Identifying an equivalent TF Evaluation Time is not straightforward for MACCS runs with multiple plume segments and especially with plumes of long duration with long temporal spacing between plume segments.

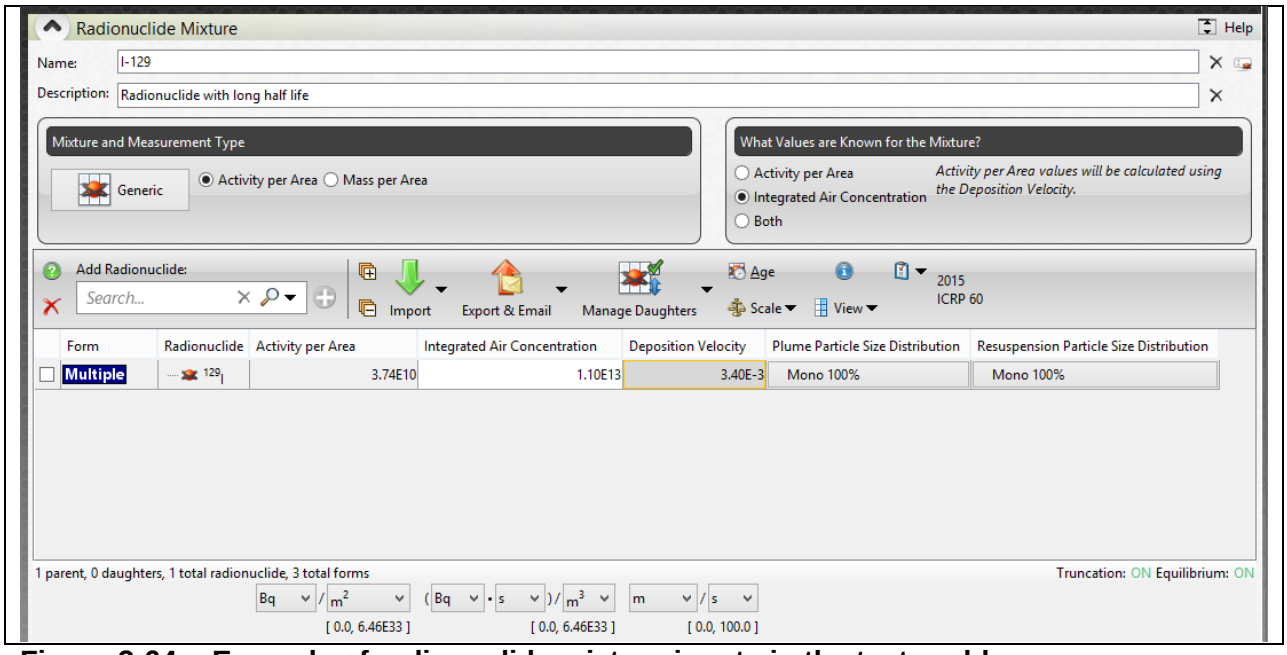

Figure 3-64. Example of radionuclide mixture inputs in the test problem.

In both TF and MACCS the inhalation and cloudshine doses are independent of the duration of the early phase, provided the duration of the early phase is longer that the plume duration. The duration of the early phase only affects the groundshine and resuspension dose. In MACCS, the time parameter ENDEMP defines the early period duration with respect to the arrival time of the leading edge of a plume to a location. The overhead plume duration in MACCS is a function of the time parameter PLUDUR (release time at the source), the windspeed, and changes of

windspeed. For the special case of constant windspeed, because of concentration on the ground is assumed in MACCS to linearly increase from 0 at the time of the plume arrival to a maximum concentration at the time the plume leaves a location, the effective exposure time to ground concentrations during the early period for runs with one plume segment equals ENDEMP − PLUDUR/2. Therefore, for scenarios with one plume segment with no plume delay, and constant windspeed, the following equivalences can be established for early phase dose computations to in MACCS to compare to TF TD early phase dose computations:

- Start Time = 0 (assuming no plume delay in MACCS)
- Duration = ENDEMP − PLUDUR/2 [b]
- Evaluation Time = PLUDUR [b]
- MACCS run should include inhalation, cloudshine, groundshine, and resuspension inhalation pathways

To approximate the TF AD early phase dose computations, similar equivalences can be adopted:

- Start Time = 0 (assuming no plume delay in MACCS)
- Duration = ENDEMP − PLUDUR/2 [b]
- Evaluation Time = PLUDUR [b]
- MACCS run should include only the groundshine and resuspension inhalation pathways

However, the MACCS early phase doses include contributions during the plume duration, which are not included in the TF AD early phase dose. This contribution may be a small component of the dose if the plume release time, PLUDUR, is small compared to the ENDEMP time. If the plume release time is significant, then MACCS dose estimates from ground pathways can be much higher than the TF AD doses estimates. To achieve closer agreement in general, MACCS should be modified to separate dose estimates during the plume passage and after the plume passage. In the absence of such capability, it is recommended to consider single plume segment scenarios with plumes of short duration. The shortest plume release time allowed in MACCS is 60 seconds.

As done in the test problem, to execute TF for the computation of doses comparable to the MACCS centerline doses (Type 6 outputs), the centerline concentrations output by MACCS (Type 0 concentrations, which are full concentrations in soil and air, after the plume passage) should be input to TF. The TF doses would slightly differ from the MACCS doses because the dose equations are not strictly identical, as previously highlighted. Similarly, Type D MACCS outputs, sector-average concentrations, could be input to TF for the computation of doses comparable to Type C sector-average doses. Note, however, that MACCS does not itemize the Type C doses per pathway (as MACCS does for Type 6 doses), and in this case, independent MACCS runs should be individually executed to isolate the different pathways.

Comparison of TF Protective Action Guide and MACCS Relocation Doses

The FRMAC protective action guide (PAG) dose can be basis for actions such as evacuation. MACCS includes a relocation strategy, triggered by comparison of the total dose to dose

[b]This equivalence is valid only in cases of constant windspeed. In general, the overhead plume duration and the time at which a plume passes a location are functions of changes in windspeed

thresholds DOSNRM and DOSHOT for the MACCS early phase, and through the dose threshold DSCRTI for the MACCS intermediate phase.

There FRMAC PAG concept is different than the MACCS relocation dose thresholds. The differences are discussed in the following paragraphs.

The individual dose computed by TF during the AD phase is the dose after the plume passage by ground pathways (i.e., groundshine and resuspension inhalation). This dose is referred to as avoidable dose (AD) because it could be avoided if people were relocated or evacuated. Protective actions would be triggered if the AD projected dose exceeds the PAG. The projected dose would be computed based on sampled radionuclide concentrations after the plume passage. If people were not evacuated beforehand, people would have received a dose from plume pathways (unavoidable dose).

The TF TD period includes plume pathways (i.e., inhalation and cloudshine) and ground pathways. The total dose is avoidable only in accidents with ample warning, allowing evacuation before initiation of release. Dose projections would be based on computer predictions before the initiation of radionuclide releases. Computer dose projections could be compared to the PAG to trigger protective actions.

Relocation in MACCS triggered by comparison of total doses to the DOSNRM dose threshold is an approach conceptually different than the FRMAC protective action strategy based on comparison of doses to the PAG. The MACCS relocation algorithm was examined in Test 0, considering the inhalation pathway. A summary of the MACCS relocation algorithm is provided in the following bullets

1. The dose for the early period is computed assuming people stay in place (full exposure dose)

2. The whole-body total dose is compared to the dose thresholds (DOSNRM and DOSHOT). If the total dose exceeds the thresholds, relocation is triggered

3. Relocation is assumed to occur instantaneously sometime after the plume arrival to a location (time defined by the parameters TIMNRM or TIMHOT); exposure to radionuclides after the evacuation is assumed nonexistent

As examined in Test 0, people could be exposed to a partial plume depending on the selection of the evacuation time parameter (TIMNRM or TIMHOT). The practical implementation in the field of such relocation approach is problematic. For example, when would information be gathered to compute the total dose in Step 1 to trigger relocation? If information was gathered after the plume passage based on field measurements, the dose would have been incurred and would not be avoidable. It is difficult to envision a field scenario where doses are dynamically computed based on field measurements, predicting future exposures to radionuclides, triggering relocation based on future predicted exposures, and still people avoiding and escaping part of the plume. The current MACCS model for computing the DOSNRM and DOSHOT dose projections is not consistent with a scenario where actual field measurements are used to compute a dose, and relocation is triggered after the incurred dose exceeds a threshold.

A scenario consistent with the MACCS relocation dose projection algorithm is the computation of doses based on computer predictions. Relocation is triggered by comparison of the predicted future doses to the threshold DOSNRM and DOSHOT. Relocation could take time to be executed, and doses could be incurred from partial exposure to a plume and exposure to

radionuclides on the ground. In this scenario, the MACCS relocation algorithm and the dose thresholds DOSNRM and DOSHOT might be comparable to the FRMAC PAG concept for the FRMAC Total Dose, TD, phase. People could be exposed to partial plumes and receive partial-exposure doses, depending on the efficiency of the relocation process (efficiency accounted for by the time delay parameters TIMNRM or TIMHOT), but relocation would be triggered by model predictions and not by field measurements.

The dose thresholds DOSNRM and DOSHOT do not correspond to the FRMAC PAG concept for the FRMAC Avoidable Dose, AD, phase. The MACCS dose thresholds include full exposure to the plume and ground pathways during the early period, while the FRMAC PAG for the AD phase only includes doses from ground pathways. The plume dose pathways could be manually disabled in MACCS by setting corresponding shielding factors equal to zero; however, MACCS doses include contributions from ground pathways during the plume passage. A modification to MACCS is required to exclude doses during the plume passage to implement a similar concept to the FRMAC PAG Avoidable Dose, AD, phase.

Commentary on the TF Derived Response Level

The FRMAC defines the derived response level (DRL) as an integrated concentration in Bq-s/m^3 units or surface concentration in Bq/m^2 units, intended as a threshold concentration for the consideration of protective actions. Comparing a field or predicted concentration of a reference radionuclide to the DRL is equivalent to comparing dose projections to the PAG. There is a DRL for integrated air concentration, DRL_A (in Bq-s/m^3 units), and a DRL for deposited contaminants on the ground, DRL_{Dp} (in Bq/m^2 units).

The DRL_A is an equivalent integrated air concentration for a reference radionuclide (e.g. Co-60). At a location where the single-radionuclide DRL_A is attained, the early dose from the radionuclide mixture and all pathways equals PAG. The dose includes plume and ground pathways in the TD phase, and ground pathways in the AD phase. The exposure time for the ground pathways is defined by the TD phase Duration input in TF, with exposure initiating at the start of the early phase (called Start Time in TF).

Similarly, DRL_{Dp} is an equivalent ground concentration for a reference radionuclide. For the TD Phase, at locations where this single-radionuclide DRL_{Dp} is attained, the dose from the complete radionuclide mixture and all pathways equals PAG. The exposure time for the ground pathways is defined by the TD phase Duration TF input (= End Time – Start Time). A similar DRL_{Dp} definition applies for the AD phase, but in this case the dose pathways are groundshine and resuspension inhalation; the exposure time is defined by the AD phase Duration TF input (= End Time – Start Time).

If the dose for the TD phase (including plume and ground pathways) or the dose of the AD phase (including only ground pathways) is symbolized as $MTDP$ (for mixture total dose parameter), the DRL_{Ai} for a reference radionuclide i (such as Co-60) is defined as

$$DRL_{Ai} = \frac{PAG}{MTDP}\, A_i \tag{3-28}$$

DRL_{Ai} — integrated activity derived response level for the reference radionuclide i (Bq-s/m^3 units)

A_i — integrated activity of the reference radionuclide i (Bq-s/m^3 units)

The DRL_{Dpi} is defined as

$$DRL_{Dpi} = \frac{PAG}{MTDP}\, Dp_i(t_n)\, WF(t_n) \tag{3-29}$$

DRL_{Dpi} — surface concentration derived response level of the reference radionuclide i (Bq/m^2 units)

$Dp_i(t_n)$ — surface concentration of the reference radionuclide i at the Evaluation Time t_n (Bq/m^2 units)

$WF(t_n)$ — weathering and decay factor fraction from the Start Time of the early phase to the time t_n

For the TD early phase, the $MTDP$ dose includes contributions from plume and ground pathways. The ground concentration $Dp_i(t_n)$ is measured at the Evaluation Time t_n. To account for higher concentrations at the Start Time of the TD early phase, a correction factor $WF(t_n)$ is included in Eq. (3-32). The dose

$$MTDP_{adj} = \frac{MTDP}{WF(t_n)} \quad (3\text{-}30)$$

is interpreted as an adjusted or corrected dose to include enhanced ground concentrations at the Start Time of the TD early phase. The correction is a conservative adjustment, because only the ground concentrations would be affected by decay and weathering, and not the integrated radionuclide air concentrations. The adjusted dose $MTDP_{adj}$ assumes that the proportion of the radionuclide mixture at the Start Time is the same than the proportion at the Evaluation Time. For the AD early phase, in general the Start Time of the period coincides with the Evaluation Time t_n, and $WF(t_n)$=1 for the AD early phase.

MACCS could be designed to output the DRL, DRL_{Ai} and DRL_{Dpi}, for a reference radionuclide such as Co-60. The DRL changes with the radionuclide mixture, and in principle, the DRL would vary from grid sector to grid sector, if the radionuclide proportion in the radionuclide mixture in air or on the ground changes. The DRL should be an auxiliary output of MACCS, and not used to trigger relocation in MACCS. As previously explained, the DRL is equivalent to the PAG. MACCS should continue using dose projections to trigger relocation, without invoking equivalent concentrations.

In the previous section, it was concluded that the FRMAC PAG is conceptually different to the MACCS dose thresholds DOSNRM and DOSHOT. To design MACCS to be consistent with the FRMAC recommendations, the PAG concept should be first introduced in MACCS, which will require considering TD and AD phases in the MACCS EARLY module, and disregarding plume dose contributions in the AD phase.

Adopting a definition DRL_{Dpi} as in Eq. (3-32) including a factor $WF(t_n)$ in MACCS is problematic for the TD phase. MACCS accounts for ground pathway contributions to the dose while the plume is passing; thus, there is no need in MACCS for a factor $WF(t_n)$ to correct doses at the Stat Time of the TD phase. Instead, it is recommended to drop the factor $WF(t_n)$ in Eq. (3-32), and interpret DRL_{Dpi} as DRL ground concentration at the Evaluation Time, right after the plume (or plume segments) have passed. In MACCS, DRL_{Dpi} at the Start Time of the TD phase is meaningless because concentrations are initially zero.

Summary of Recommended Changes in MACCS for Consistency with the FRMAC PAG and DRL Concepts

The MACCS early period computations require adjustments to ensure consistency with the FRMAC early phase PAG. Since EPA encourages emergency responders to use TF to implement the PAG (EPA, 2017) and because the TF radiological assessment methodologies are based on the consensus of an interagency working group (Sandia National Laboratories, 2022; Blumenthal, et al., 2020), it is reasonable for the MACCS algorithms and equations to be adjusted to match the TF.

The following changes to the MACCS EARLY module are recommended to reach consistency with the FRMAC early phase analysis approach.

- Define TD (total dose) and AD (avoidable dose) phases during the early phase. To evaluate the early PAG dose projections in MACCS as done in TF, it is recommended to apply the dose projection periods defined by the TF TD and AD phases to MACCS. In TF, the Start Time is the start of the dose projection period. To exclude doses during a

period that may be unavoidable, TF treats the Start Time as the period after the start of plume passage.

  - The TD phase Start Time is 0 hours
  - The TD phase default dose projection period is 4 days
  - The TD phase doses include plume and ground pathways
  - The AD phase default Start Time is 12 hours
  - The AD phase default dose projection period is 4 days
  - The AD phase dose includes ground pathways only
  - The TF default times are merely recommendations by the FRMAC. Those times can be adjusted to consider scenarios of plume releases during different timeframes, without contradicting the FRMAC definitions and approaches
  - MACCS has the advantage of scenario-specific information regarding plume release and arrival times. Instead of evaluating a single 4-day window for the AD dose projection period, MACCS should consider a sliding window over the course of the early phase. This approach can better evaluate the possibility that the dose rate may change as the event unfolds.

- Use the PAG dose projection as a threshold to trigger relocation. It is recommended to trigger relocation based on the AD phase dose. Relocation based on the TD phase dose implies accidents with ample warning before the release of radionuclides and use of predicted releases, concentrations, and doses to trigger such relocation (as opposed to using information during the release progression).

- Define an independent cohort to match TF computations. To evaluate PAG dose projections that is not affected by protective actions, it is recommended to create a phantom cohort independent from the population cohorts. The phantom cohort would implement separate shielding and exposure parameters for which users can provide values based on radiation protection assumptions. The phantom cohort should also have separate inputs for certain pathway parameters to match TF. Additional dose coefficients, possibly based on different standards, should also be considered to match TF. The use of plume submersion instead of cloudshine should also be considered. It is recommended to apply the following early phase changes.

  - Expand the resuspension function to include more exponential terms
  - Include an explicit weathering function in the EARLY module, and consistently apply for both groundshine and resuspension inhalation pathways. Currently in MACCS weathering and resuspension are combined in a single factor applied to the resuspension inhalation pathway; groundshine does not include any weathering adjustment
  - Include independent inputs for the breathing rates for direct inhalation and resuspension inhalation pathways
  - The TF default protection factors for inhalation and shielding are 1 (i.e., no protection)
  - The TF default surface roughness factor is 0.82. This should be included in the groundshine protection factor
  - The TF default breathing rate for direct inhalation is 4.17×10^{-4} m^3/s
  - The TF default breathing rate for resuspension inhalation is 2.56×10^{-4} m^3/s
  - The TF default weathering coefficients are as in Eq. (3-27)
  - The TF default values are merely recommendations by the FRMAC. Those values can be adjusted when better scenario-specific information is known without contradicting the FRMAC definitions and approaches

3.10.5 Test Conclusions

This test was a special test aimed at comparing dose computations and the relocation concepts to the FRMAC early phase dose projections and to the PAG concept.

A numerical test was designed to compare MACCS centerline doses to the TF total dose (TD) phase doses. The purpose of the test was examining in detail the TF early phase dose equations. When inputs are made to align the models, the MACCS early phase doses agreed with the TF total doses. An error in the MACCS groundshine dose for I-129 was identified, possibly related to a dose coefficient for whole-body dose incorrectly retrieved from the database of dose coefficients. This error was exhibited only for I-129 among the few isotopes examined. Groundshine doses computed for other few examined radionuclides were in perfect agreement with expected doses according to Eq. (3-1).

Independently on the adjustments to the input parameters, it was concluded that the MACCS equations for the early-phase dose are comparable to the TF early phase dose equations. MACCS would require limited modification to match TF early phase dose equations, including

- Setting the cloudshine factor equal to 1
- Additional exponential functions in the definition of the resuspension function
- A weathering function for the EARLY module

To align the MACCS EARLY module to the early phase TF concepts for public protection, additional changes to MACCS would be required including

- Defining total dose (TD) and avoidable dose (AD) phases during the early phase
- Computing AD doses that exclude contributions during the plume passage
- Adopting the PAG concept for the AD phase to trigger relocation (i.e., relocation would be triggered when the AD phase dose exceeds the PAG)

3.11 Test 3.11: Radial Evacuation Algorithm

The objective of the test was to examine the algorithm for computing doses under evacuation for a simple test problem. In the test problem, the evacuation zone is a circular zone of radius 5 km. It is assumed that as soon as people move beyond the 5 km radius, the dose for the evacuating cohort becomes zero. However, people already outside the 5 km radius receive a dose. Two cases were considered in the tests. In Case 1, it was assumed that evacuation initiates as soon as the plume arrives to the spatial grid sector (there is no period of normal activity nor a sheltering period, evacuation starts right away as soon as the plume arrives). In Case 2, evacuation was triggered by an alarm. The plume was delayed with respect to the alarm to give evacuees time to escape the plume.

The MACCS evacuation algorithm is described in Section 4.2 of the MACCS Theory Manual (Nosek & Bixler, 2021); however, some details are not described, and some assumptions regarding the computational approaches were adopted to design benchmarks. For that reason, the tests were considered successful if similar trends of dose estimates were reproduced by independent computations, although the MACCS doses and the independent dose computations may have differed slightly.

The MACCS algorithm accounts for the exposure time to a plume while people are in transit in a grid sector for the computation of inhalation, cloudshine, and skin dose. If there is any overlap of a plume with the evacuating cohort in a grid sector, in the verification computations it was assumed that the whole cohort is exposed to the corresponding grid segment air concentration (either mid-point concentrations for Type 6 centerline doses or sector-average concentrations for Typo C doses) during a time equal to the ratio of the grid sector length and the evacuation speed. For groundshine doses, the MACCS algorithms account for gradual concentration buildup on the ground (from zero concentration when the plume arrives to a maximum concentration when the whole plume leaves the sector). Some alternatives were examined to correct concentrations in a grid sector to account for partial exposure of the sector to the plume; the precise MACCS algorithm is not described in the MACCS Theory Manual. With respect to resuspension inhalation doses, MACCS considers a minimum exposure time of 8 hours. It appears that if the exposure time is less than 8 hours, the resuspension inhalation dose for evacuating people is set to zero.

3.11.1 Test Input

Case 1: Evacuation on Plume Arrival

The same inputs than Test 3.7 were used, with the following changes

Properties

- Evac/Rotation
    - Problem Model: Radial
    - Number of Cohorts: 1
        - Type: Circular (shape of the evacuation zone)
    - An initial run with Problem Model = None was executed to define reference doses for the no-evacuation case

ATMOS

- Radionuclides
    - CORINV = 10^{20} Bq for Cs-137, 0 for other radionuclides
- Deposition

    - Wet/Dry Depos Flags
        - DRYDEP = True for Cs
        - WETDEP = False for Cs
    - Dry Deposition
        - VDEPOS (m/s) = 0.1 for particle group 1, and 0 for other groups
- Dispersion
    - Scaling Factors
        - YSCALE = 1 (lateral plume spread factor)
        - ZSCALE = 1 (vertical plume spread factor)
- Release Description
    - Particle Size Distribution
        - PSDIST=1 for particle group 1, 0 for all other groups for Cs
- Weather
    - Constant or Boundary Conditions
        - BNDMXH (m) = 1000
        - IBDSTB (-) = 1 (atmospheric stability class A)
        - BNDRAN (mm/hr) = 0
        - BNDWND (m/s) = 2 (windspeed)

EARLY

- Model Basis
    - Duration of Early Phase
        - ENDEMP (s) = 6.048E5 seconds (= 7 days, duration of the emergency-phase period after the arrival of the first plume segment)
    - Normal Relocation
        - TIMNRM (s) = 0
        - DOSNRM (Sv) = 1E10 (high limit to avoid relocation trigger by normal dose)
    - Hot Spot Relocation
        - TIMHOT (s) = 0
        - DOSHOT (Sv) = 1E10 (high limit to avoid relocation trigger by hot dose)
    - Emergency Phase Resuspension
        - RESCON (1/m) = 1E-5 (resuspension factor)
        - RESHALF (s) = 1E10 (large value to minimize weathering)
- Emergency Cohort One
    - Phase Durations and Speeds
        - REFPNT = ARRIVAL (evacuation starts at the plume arrival)
        - TRAVELPOINT = CENTERPOINT (grid center to grid center)
        - DURBEG (s) = 0 (duration of initial evacuation phase)
        - DURMID (s) = 0 (duration of middle evacuation phase)
        - ESPEED (m/s) = Variable 1E-6 to 10 (evacuation speed)
        - ESPMUL (-) = 1 (evacuation speed adjustment factor in case of rain)
    - Sheltering and Evacuation Boundary
        - LASMOV = 15 (at this grid element the evacuating cohort is assumed to escape doses; doses are zero at this and farther grid elements from the source)
        - NUMEVA = 15 (size evacuation and sheltering region: from grid 1 to 15)
    - Shielding and Exposure

        - CSFACT = PROTIN = SKPFAC = GSHFAC = 1
        - BRRATE (m3/s) = 1E-4, breathing rate
    - Notification Delay
        - OALARM (s) = 0
- Output Control
    - Centerline Dose
        - NUM6 (-) 4 : number of outputs
        - ORGNAM = L-IRCP60ED, PATHNAM = INH LIF (inhalation),
        - ORGNAM = L-IRCP60ED, PATHNAM = CLD (cloudshine)
        - ORGNAM = L-IRCP60ED, PATHNAM = GRD (groundshine)
        - ORGNAM = L-IRCP60ED, PATHNAM = RES LIF (resuspension)
        - ORGNAM = A-SKIN, PATHNAM = TOT ACU (skin dose)
        - I1DIS6 (-) = 1, I1DIS6 (-) = 34, Report Options = NONE

Case 2: Evacuation Triggered by an Alarm

The same inputs than Case 1 were used, with the following changes

ATMOS

- Release Description
    - Plume Parameters
        - PDELAY (s) = 0 to 950 (delay of plume release)

EARLY

- Emergency Cohort One
    - Phase Durations and Speeds
        - REFPNT = ALARM (an alarm initiates evacuation)
        - TRAVELPOINT = CENTERPOINT (grid center to grid center)
        - DURBEG (s) = 0 (duration of initial evacuation phase)
        - DURMID (s) = 0 (duration of middle evacuation phase)
        - ESPEED (m/s) = 2 (evacuation speed = windspeed)
        - ESPMUL (-) = 1 (evacuation speed adjustment factor in case of rain)
    - Notification Delay
        - OALARM (s) = 0 (alarm time)

3.11.2 Test Procedure

Case 1: Evacuation on Plume Arrival

MACCS was executed varying the evacuation speed (ESPEED) from the smallest allowed speed of 10^{-6} m/s to 10 m/s. The goal was to consider evacuation speeds close to 0, which should yield results comparable to a no-evacuation case, and evacuation speeds less and greater than the windspeed. A no-evacuation run was executed to compute reference doses. These reference doses were scaled to account for the exposure time in a grid segment during evacuation, and to account for partial concentration buildup on the ground. The scaled doses were compared to MACCS Type 6 centerline doses.

To design independent benchmarks, the following equations were assumed. The precise equations and algorithms of the radial evacuation algorithm are not described in detail in the MACCS Theory Manual. Scaling factors for computing evacuation doses were defined based on

the relative evacuation speed with respect to the windspeed. If the windspeed is greater than the evacuation speed, $v_w > v_e$, (recall that evacuation starts when the plume arrives to sector i with midpoint r_i) the plume will travel a distance r_s to pass the evacuating cohort

$$r_s = r_i + \frac{v_e}{v_w - v_e} L_p \tag{3-31}$$

r_s — evacuation span of the cohort initiating evacuation in the grid sector i (m)
r_i — mid-point of start-evacuation sector i (m)
v_e — evacuation speed (m/s, ESPEED)
v_w — windspeed (m/s, BNDWND)
L_p — plume length (m, PLUDUR×BDNWND)

The symbol r_{LASMOV} represents the distance corresponding to the grid number LASMOV (=15 in the test problem, equal to a radial distance of 5 km). At this and farther distances from the source, MACCS algorithms assume that the evacuating cohort escapes dose consequences (doses are assumed zero). For inhalation, cloudshine, and skin doses, the dose of the evacuating cohort in grid sectors j between distances r_i and min(r_s, r_{LASMOV}) was computed as

$$d_{j,e} = d_j \frac{\Delta r_j / v_e}{\text{PLUDUR}} \tag{3-32}$$

$d_{j,e}$ — dose for sector j for the evacuation case (Sv)
d_j — dose for sector j for the no-evacuation case (Sv, reference dose)
Δr_i — length of the sector j
PLUDUR — plume duration

For grid sectors farther than r_s, the plume leaves the evacuating cohort behind and the inhalation, cloudshine, and skin doses in those sectors are zero. The doses in the sectors j are aggregated and assigned to the starting sector i.

If the evacuation speed, v_e, is greater than the windspeed, v_w, the cohort starting evacuation at sector i will travel a distance

$$r_s = r_i + \frac{v_w}{v_e - v_w} \Delta r_i \tag{3-33}$$

to fully pass the plume. In sectors at distances greater than r_s, the inhalation, cloudshine, and skin doses are zero because the plume is behind the evacuating cohort. Equation (3-32) was used to compute the evacuation doses in grid sectors j between distances r_i and min(r_s, r_{LASMOV}). Those doses were aggregated and assigned to the starting sector i.

Finally, if $v_e = v_w$, the plume is always overhead the evacuating cohort, and Eq. (3-32) was used to compute evacuation doses between sectors i and the LASMOV sector.

For groundshine and resuspension inhalation, the verification algorithm was more complicated, because MACCS assumes ground concentrations to increase linearly with time from 0 to a maximum concentration at the time the tail of the plume passes a location. If the windspeed is greater than the evacuation speed, $v_w > v_e$, the evacuating cohort is subjected to a dose in the complete evacuation path. The evacuation span, r_s, is defined as

$$r_s = \min\left(r_i + v_e \,\mathrm{ENDEMP},\ r_{\mathrm{LASMOV}}\right) \tag{3-34}$$

ENDEMP — duration of the emergency-phase period (EARLY period) measured from the arrival of the plume to the grid element i (=6.048×10^5 s in the test problem)

The front of the cohort (the "vanguard") starting evacuation at the grid segment i is exposed to a relative concentration on the ground when in segment j

$$c_v = \min\left(\frac{v_w - v_e}{v_e}\,\frac{r_j - r_i}{L_p}\,, 1\right) \tag{3-35}$$

c_v — fraction of the maximum ground concentration at the grid segment j (dimensionless) for the evacuating vanguard
L_p — plume length (=PLUDUR×BNDWND)

The relative concentration of the back of the evacuating cohort (the "rearguard") was computed as

$$c_r = \min\left(\frac{v_w - v_e}{v_e}\,\frac{r_j - r_i}{L_p} + \frac{\Delta r_i}{L_p}, 1\right) \tag{3-36}$$

c_v — fraction of the maximum ground concentration at the grid sector j (dimensionless) for the evacuating rearguard
Δr_i — length of the grid sector i (m)

The dose at the grid sector j (between r_i and r_s) for the evacuating cohort was computed as

$$d_{j,e} = d_j\,\frac{c_v + c_r}{2}\,\frac{\min\left(\Delta r_j / v_e\,, t_{\mathrm{full}}\right)}{t_{\mathrm{full}}} \tag{3-37}$$

$d_{j,e}$ — dose in sector j for the evacuating cohort (Sv)
d_j — dose in sector j for the no-evacuation case (Sv, reference dose)
t_{full} — effective exposure time to non-zero ground concentrations for the no-evacuation case (=ENDEMP – 0.5 PLUDUR)

If the evacuation speed exceeds the windspeed, $v_e > v_w$, the cohort initiating evacuation in the grid sector i passes the plume at a distance r_s, computed with Eq. (3-33). At farther distances from the source than r_s, the dose to the evacuating cohort is zero because the plume is behind. The evacuating vanguard is exposed to a zero contaminant concentration, because there is not enough time for contaminant concentration to buildup

$$c_v = 0 \tag{3-38}$$

The relative concentration at the rearguard, c_r, for this case was also computed using Eq. (3-36), and Eq. (3-37) was used to compute the evacuating dose for the grid sector j.

Finally, for the case $v_e = v_w$, the evacuating vanguard travels with the plume. It was assumed that when the vanguard is located at the grid sector j outer edge, the rearguard is located at the grid sector inner edge (sector closest to the source). The relative concentration at the

evacuating vanguard is zero, Eq. (3-38). At the evacuating rearguard, the relative concentration was computed as

$$c_r = \min(\Delta r_j / L_p, 1) \tag{3-39}$$

As in previous cases, the dose at the grid sector j (between r_i and r_s) for the evacuating cohort was computed using Eq. (3-37). In all cases, the doses for the j sectors were aggregated and assigned to the originating sector i.

For the resuspension inhalation case, Section 3.3.4 of the MACCS Theory Manual (Nosek & Bixler, 2021) states that resuspension is ignored during the plume passage. This statement is interpreted to mean that the dose is assumed zero at a grid sector if the plume is still flying overhead. Only when the end of a plume fully passed a grid sector, non-zero doses are computed according to Eqs. (3-34) to (3-37) for the case windspeed > evacuation speed. For the case windspeed ≤ evacuation speed, the end of the plume can never pass the evacuating cohort, and the dose must be assumed to be zero per the MACCS Theory Manual description. Only when the evacuation speed is very slow, the end of a plume can pass the evacuating cohort before the LASMOV grid sector within the ENDEMP exposure time. Non-zero doses for a sector i must be only computed in MACCS when

$$v_e < \frac{r_{\mathrm{LASMOV}} - r_i}{\mathrm{ENDEMP}} \tag{3-40}$$

In the test problem, considering r_{LASMOV} = 5 km and ENDEMP=6.048×10^5 s, the maximum evacuation speed (ESPEED) with non-zero resuspension evacuation doses is 8.3×10^{-3} m/s.

Again, it is highlighted that Eqs. (3-31) to (3-39) used in the verification computations were assumed from high-level descriptions in the MACCS Theory Manual. The precise equations and algorithms implemented in MACCS for the computation of evacuation doses are not described in detail. For that reason, differences in the independent verification computations with respect to the MACCS outputs are expected. Those differences are not necessarily indications of coding errors; they merely reflect a gap in the description of precise algorithms.

The verification computations considered runs varying the evacuation speed. Type 6 centerline doses for all dose pathways (inhalation, cloudshine, groundshine, resuspension, and skin dose) were extracted from the MACCS outputs. In addition, a run was executed disabling evacuation to define reference doses. The evacuation doses were computed using Eqs. (3-31) to (3-39) and compared to MACCS Type 6 centerline doses.

Case 2: Evacuation on Alarm

In the second case, it was assumed that evacuation was triggered by an alarm at time 0. The plume was delayed with respect to the alarm trigger, with different input delays in the MACCS runs. It was assumed that the windspeed and the evacuation speed were the same (2 m/s). People in sectors 2 to 15 initiate evacuation on the alarm and before the plume arrival, and thus would not be exposed to radioactivity. Doses in sectors 2 to 15 should therefore be zero, independently of the plume delay. People in sector 1 would be subject to a dose only if the plume delay is less than 50 s. In the test problem, the length of the grid sector closest to the source is 100 m. It would take 50 s = 100 m / (2 m/s) for full evacuation of grid sector 1. If the delay is more than 50 s, the grid sector 1 is evacuated before the release of radioactivity and the dose in sector 1 should also be zero. Those qualitative predictions were compared to MACCS Type 6 centerline doses.

3.11.3 Test Results

Case 1: Evacuation on Plume Arrival

Type 6 centerline doses output by MACCS are compared to independent computations based on Eqs. (3-31) to (3-39) in Figure 3-65. The agreement is reasonable, with the following observations:

- An identical algorithm was used in the verification computation of inhalation, skin dose, and cloudshine doses.
    - There is excellent agreement between the MACCS outputs and the independent computations for the inhalation and skin dose pathways, except for evacuation speed = 3 m/s.
    - Reasonable agreement was obtained between MACCS and independent cloudshine doses.
- An identical algorithm was used in the verification computation of groundshine and resuspension doses.
    - There was reasonable agreement between MACCS and independent groundshine doses, with greater differences for cases with the evacuation dose exceeding the windspeed.
    - The MACCS resuspension dose is non-zero only for the case with evacuation speed = 10^{-6} m/s. For other cases, the evacuation speed is greater than 8.3×10^{-3} m/s, which is the maximum expected speed with non-zero resuspension evacuation dose outputs by MACCS. MACCS assumes evacuation doses are zero while the plume is still flying over a grid sector with people in transit.
- For all dose pathways, the dose for the non-evacuation case (evacuation speed = 0) and the small evacuation speed case (evacuation speed = 10^{-6} m/s) are strictly identical, as expected.

Additional runs were executed enabling only the inhalation dose pathway (by setting CSFACT = SKPFAC = GSHFAC = 0 and PROTIN = 1). The Type C sector average dose was extracted from the Model1.out output file. The whole-body dose is labeled as L-ICRP60ED in Model1.out. The reference dose d_j in Eq. (3-32) was defined as the Type C inhalation dose, and an identical algorithm to the centerline dose was used to verify the Type C evacuation doses for the north sectors. MACCS outputs (symbols) are compared to the independent verification computations in Figure 3-66. The agreement is excellent except for the case ESPEED = 3 m/s, in similitude to the inhalation centerline dose results in Figure 3-65. Cloudshine, groundshine, resuspension, and skin deposition Type C doses were not individually examined, but it is expected that the verification algorithms adopted for the Type 6 centerline doses also work for the Type C sector-average doses.

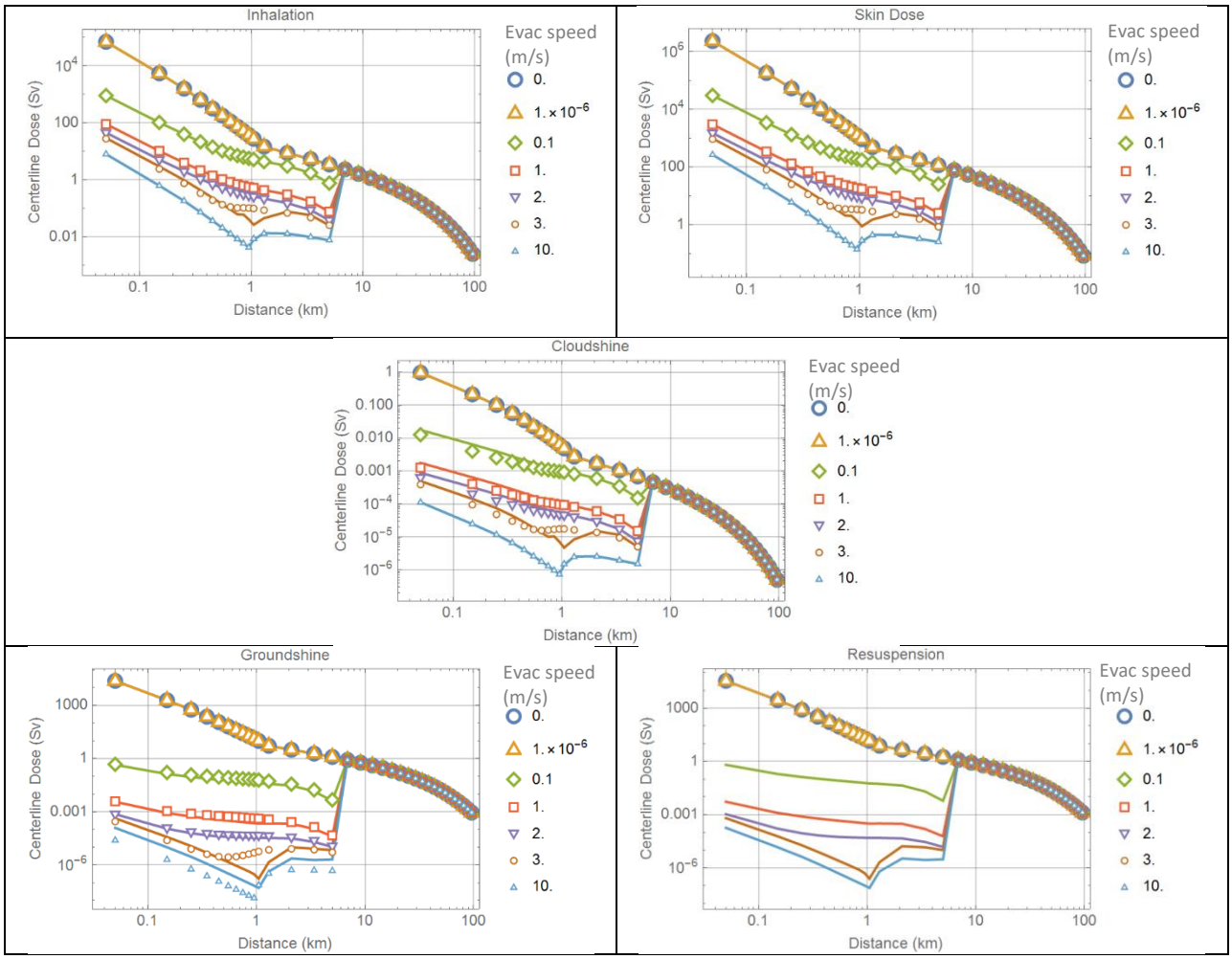

Figure 3-65. Comparison of Type 6 centerline doses output by MACCS (symbols) to independent computations (solid curves). The windspeed in all runs was 2 m/s.

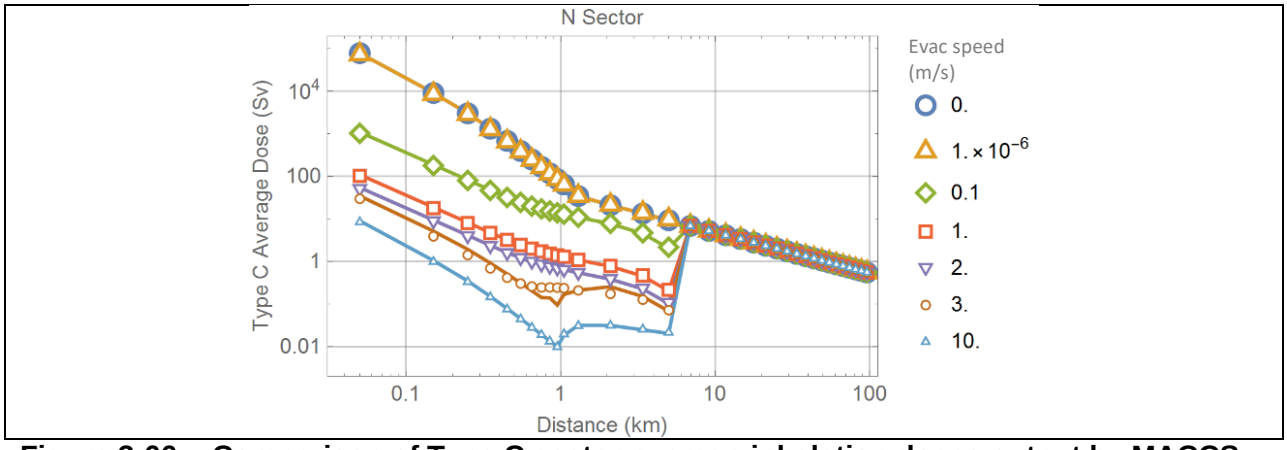

Figure 3-66. Comparison of Type C sector-average inhalation doses output by MACCS (symbols) to independent computations (solid curves). The doses are inhalation doses in the north (N) sectors.

With the special set of runs enabling only the inhalation dose pathway, an additional test was designed to check factors referred to a J and U factors in the MACCS Theory Manual [e.g., see Section 3.3.3 and Eq. (3-12) in (Nosek & Bixler, 2021)]. J is a factor to transform grid center concentrations to sector-average concentrations, used to compute sector-average doses if evacuation is disabled. If evacuation is enabled, the J factor is replaced by a U factor (=0.836). Under evacuation scenarios, MACCS adopts a simplification to constrain the lateral spread of a plume in the computation of doses: MACCS assumes that the lateral spread is limited to ±1.5 σ_y interval around the centerline (i.e., the concentration is assumed zero outside the ±1.5 σ_y interval). In grid sectors enclosed by the ±1.5 σ_y lateral interval, MACCS applies a factor U=0.836 to the grid-center concentration to approximate sector-average concentrations. The approach to constraining the lateral spread is referred to as the top-hat approximation [see Figure 3-2 in (Nosek & Bixler, 2021)].

The J or U factor was isolated by computing the ratio of Type C sector-average dose to the Type 6 centerline dose. The Type C dose to Type 6 dose ratio is displayed in Figure 3-67 for two runs: (i) no-evacuation run, and (ii) run with evacuation speed 10^{-6} m/s. For the case ESPEED= 10^{-6} m/s, the ratio approximately equals 0.836 up to a distance 5 km (radius delimiting the evacuation zone in the test run). At farther distances from the source, the ratio is equal to the J factor computed with the runs with evacuation disabled. Runs with other values of ESPEED yield similar results: the ratio is approximately 0.836 up to 5 km, and then it becomes identical to the J factor computed with outputs of the no-evacuation run. Those results are not included in Figure 3-67 to enhance the clarity.

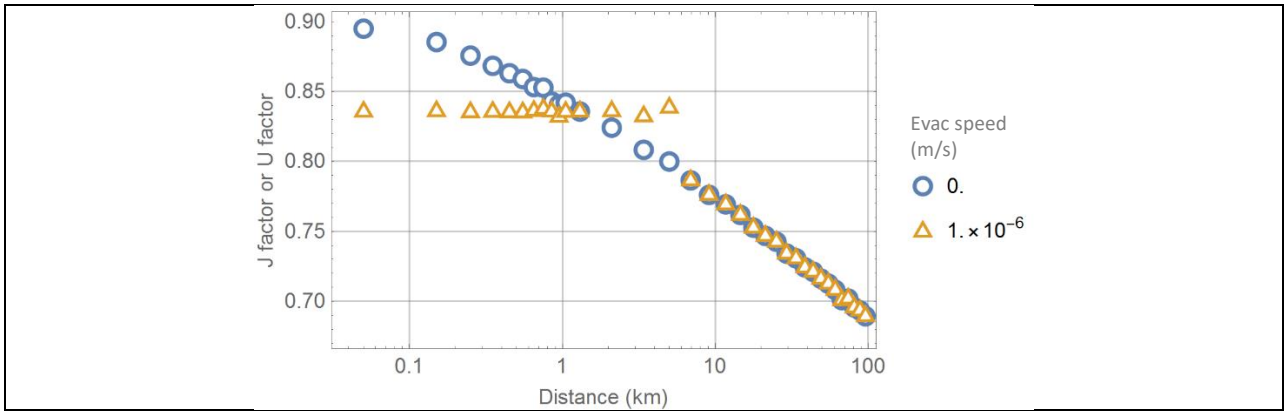

Figure 3-67. J or U factors computed with MACCS outputs as the ratio of Type C sector-average dose (north sectors) to Type 6 centerline dose. The runs considered only inhalation doses.

The top-hat approximation constraining the lateral spread is visualized in the Type C dose sector plots of Figure 3-68, considering all dose pathways. The plot on the left is the sector plot for the no-evacuation case. The plume spread over north (N), north-north east (NNE), and north-north west (NNW) sectors, with the NNE and NNW sectors enclosing the ±2.15 σ_y plume spread limits (dashed curves in Figure 3-68). The plot on the right is the sector plot for the case ESPEED = 10^{-6} m/s. Within the evacuation radius of 5 km, MACCS reports non-zero doses only in the N sectors; the centers of the NNE and NNW sectors are outside of the ±1.5 σ_y interval (black solid curves in Figure 3-68), and MACCS assumes that doses in those sectors are zero when evacuation is enabled. Although the evacuation speed 10^{-6} m/s is very small, the Type C sector-average doses are not identical to the no-evacuation case due to the top-hat approximation.

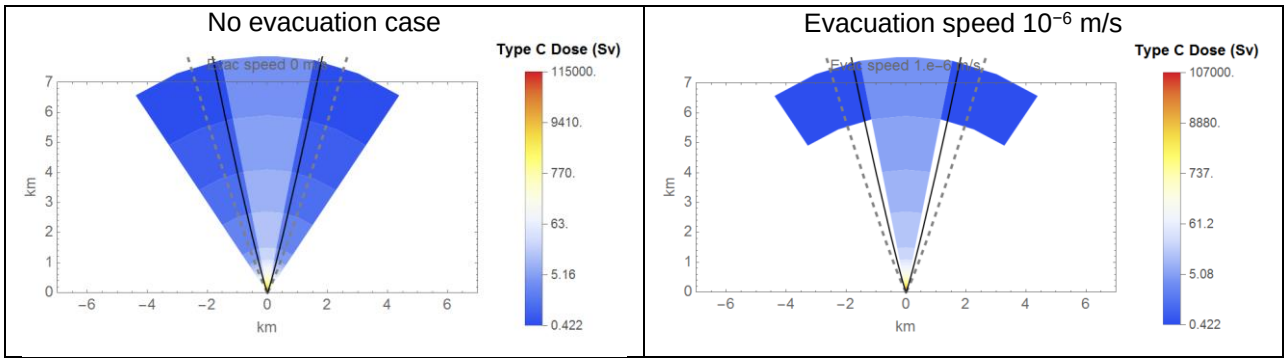

Figure 3-68. Sector plots of Type C whole-body doses output by MACCS. The dashed curves represent ± 2.15 σ_y lateral spread limits and the black solid curves the ± 1.5 σ_y limits of the top-hat approximation in case of evacuation.

The following test examined the computation of the population dose using the runs with all dose pathways enabled. Population doses were independently computed from the Type C sector average whole-body doses (all dose pathways) as the product of the Type C dose and the number of people in a sector, following the approach discussed in Test 3.2. The population doses were compared to Type 5 MACCS outputs. The MACCS Type 5 outputs are population doses aggregated over sectors spanning 360° rings. The comparison is presented in Figure 3-69, with MACCS outputs displayed in symbols and independent computations in solid curves, showing perfect agreement. It is noted that the population dose for the ESPEED=10^{-6} m/s case is less than the population dose of the no-evacuation case (legend 0 m/s in Figure 3-69), and such is a consequence of the top-hat approximation. For example in the plot to the right of Figure 3-68, the Type C doses in the NNE and NNW sectors are zero within the evacuation zone, and those sectors do not contribute to the population dose; but they do in the no-evacuation case. Therefore, the Type 5 population dose aggregated over rings for the no-evacuation case is greater than the corresponding Type 5 population dose of the 10^{-6} m/s evacuation speed case, as shown in Figure 3-69. The top-hat approximation was selected as a practical approach to limit the lateral spread of plumes, which may underestimate population doses, as visualized by comparing the case ESPEED=10^{-6} m/s population dose to the no-evacuation case (legend 0 m/s) in Figure 3-69.

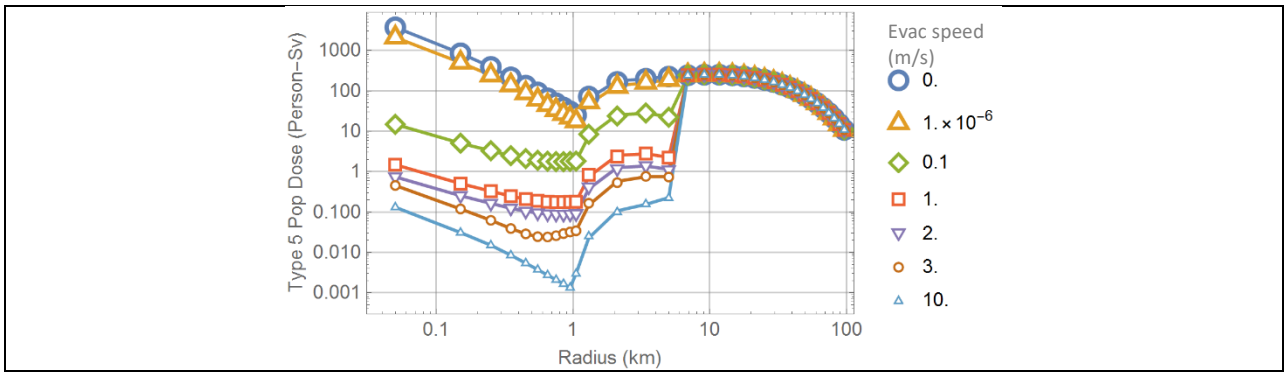

Figure 3-69. Comparison of Type 5 population doses output by MACCS (symbols) to independent computations (solid curves).

For the Case 1 (evacuation on plume arrival) it is concluded that MACCS outputs display expected trends. Differences with respect to the independent verification computations are due to the use of approximated algorithms (MACCS algorithms are not described in detail). It was noted that the resuspension evacuation doses are approximated as zero by MACCS, except for

cases with extremely small evacuation speeds. Although such result is consistent with the description in the MACCS Theory Manual, this result is highlighted for MACCS model developers to examine whether special treatment of the resuspension dose is justified, differing from the treatment of the groundshine dose and other dose pathways. The extremely small evacuation speeds that would yield non-zero resuspension doses are also highlighted; it is unclear whether model developers examined the magnitude of those speeds when designing simplifications to model resuspension dose during evacuation.

Case 2: Evacuation on Alarm

In the second case, it was assumed that evacuation was triggered by an alarm at time 0. The plume was delayed with respect to the alarm trigger, with input delays (PDELAY) in the MACCS runs ranging from 0 to 950 s. The windspeed (BNDWND) and the evacuation speed (ESPEED) were set to 2 m/s. Figure 3-70 displays the plume arrival time to locations downwind. The MACCS outputs (symbols) were extracted from Type 0 outputs in Model1.out, labeled as "Plume Arrival Time (s)." The solid lines are arrival times simply computed as distance/windspeed + plume delay. Figure 3-70 indicates that the plume arrival and plume delay align with intuitive definitions.

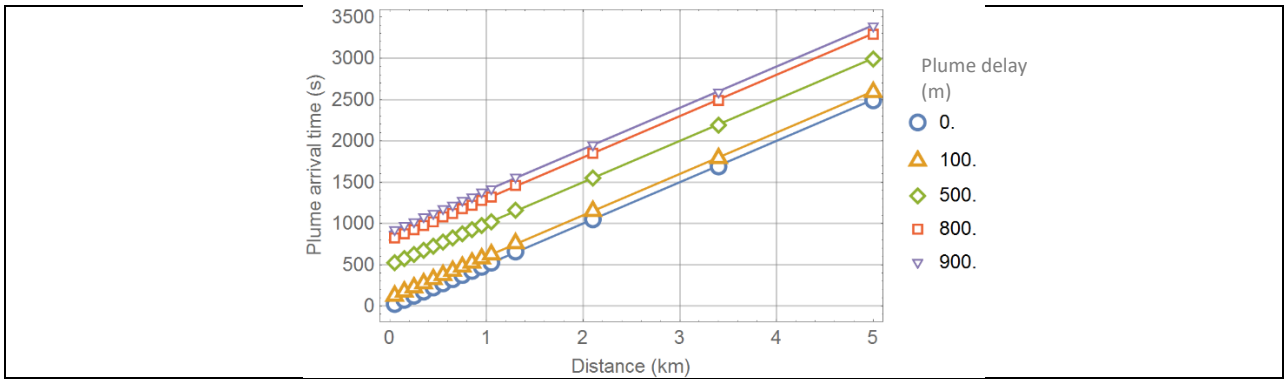

Figure 3-70. Plume arrival time versus downwind distance. MACCS outputs are displayed in symbols and independent computations in solid lines.

Centerline doses versus downwind distance output by MACCS are displayed in Figure 3-71. The legend NE labels results of the no-evacuation case, and other legends indicate the value of the plume delay in the run. The dose for the inhalation of resuspension pathway is not shown in the figure, because it was zero in the evacuation region. All centerline doses are zero in the grid sectors with centers between 2.1 km and 5 km. At farther distances from the source, the results are identical to results of the no-evacuation case, as expected. The run with plume delays of 950 s or longer output zero dose within the 5 km evacuation zone.

The results in Figure 3-71 are non-intuitive and could not be reproduced with independent computations. If the evacuation alarm is triggered at time zero, it is expected that people in sectors 2 to 15 would escape the plume would not experience and any dose, yet non-zero doses were output by MACCS in sectors 2 to 12 (grid centers 0.15 km to 1.3 km). Non-zero doses are expected in grid sector 1 (center 0.05 km) only when the plume delay is less than 50 s (the length of sector 1 is 100 m, which can be covered in 50 s if moving at a speed of 2 m/s). For delays longer than 50 s, the time is sufficient for people in sector 1 to escape the plume and avoid any dose; however, MACCS outputs non-zero doses in sector 1 for a range of delays, from 0 to 900 s. Presumably after 900 s, people in sector 1 would have advanced 1800 m, well outside the influence of the plume. It is unclear why MACCS outputs non-zero doses for sector 1. The results in Figure 3-71 are not transparent. Either the evacuation alarm

concept implemented in MACCS is different than interpreted in the test, or the implementation of the alarm concept in MACCS has errors.

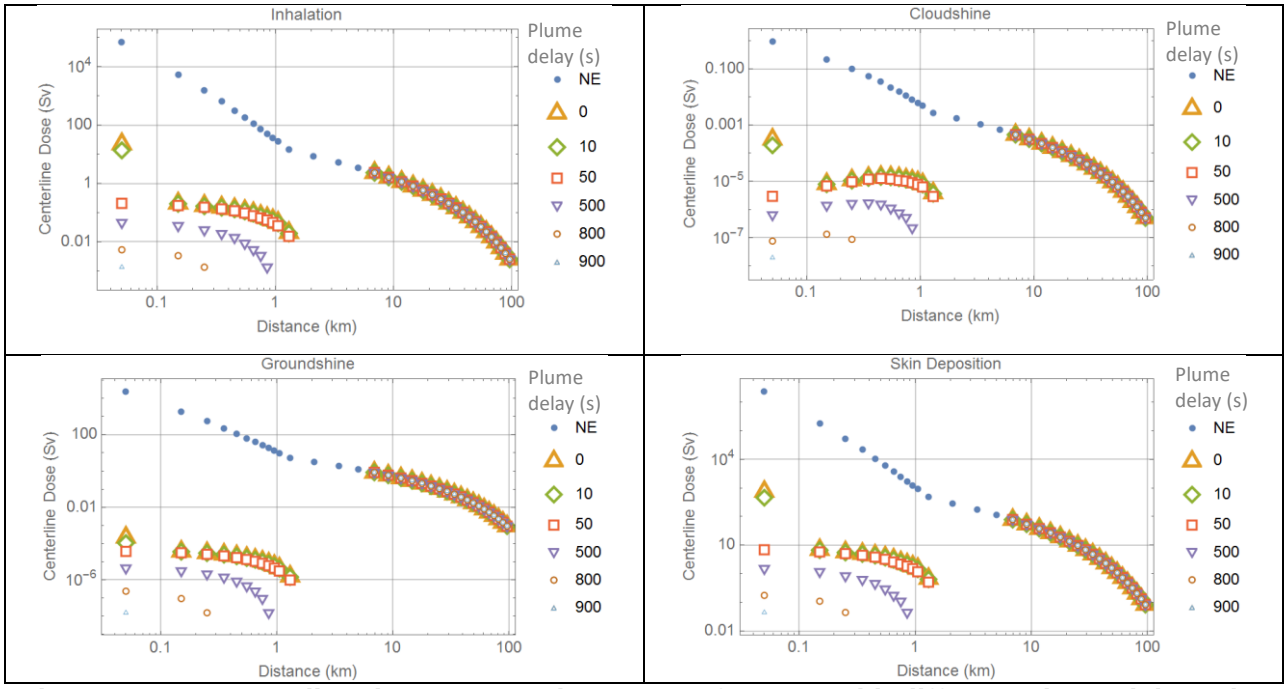

Figure 3-71. Centerline doses output by MACCS for runs with different plume delay. The legend NE indicates a run with no-evacuation.

3.11.4 Test Conclusions

The evacuation algorithm in MACCS was tested with simple cases: (1) radial evacuation after plume arrival or (2) radial evacuation triggered by an alarm. No deficiencies were identified in Case 1, although some MACCS results could not be accurately reproduced due to a lack of details in the MACCS documentation. Equations (3-31) to (3-40) used in the independent benchmarks were assumed equations; the actual evacuation equations implemented in MACCS are not described in the MACCS documentation.

MACCS outputs zero resuspension dose by design, except in cases with very low evacuation speeds. It is recommended that model developers revisit assumptions of the resuspension dose to verify that the model behaves as intended, especially since evacuation speeds that yield non-zero resuspension doses are extremely small.

For Case 2 (evacuation triggered by an alarm), the results are non-intuitive and difficult to rationalize. It is possible that there was a misunderstanding in the concept of the evacuation alarm trigger, but it is also possible that the implementation of the alarm trigger in MACCS is in error and should be corrected.

4 CHRONC MODULE

4.1 Test 4.1: Stochastic Health Effects from Groundshine

The objective of the test was examining the computation of the population dose and stochastic health effects from a groundshine dose pathway. The groundshine dose is computed as follows (based on equations 3-19 and 3-20 of the MACCS Theory Manual):

$$DG_k = \left(\sum_i DCG_{ik}\, GC_i \right) SFG\, \frac{1}{\mathrm{DRF}_\ell} \tag{4-1}$$

DG_k	—	groundshine dose to organ k in a sector (Sv)
DCG_{ik}	—	groundshine dose factor to organ k by radionuclide i (Sv-m^2/Bq)
GC_i	—	ground concentration of radionuclide i in a sector after the EARLY period (Bq/m^2)
SFG	—	groundshine shielding factor, specified by LGSHFAC
DRF_ℓ	—	dose reduction factor for decontamination level ℓ, specified by DSRFCT. Decontamination occurs when the dose exceeds a dose threshold DSCRLT over a period TMPACT

The groundshine dose factor DCG_{ik} is computed as

$$DCG_{ik} = DRCG_{ik} \int_{t_1}^{t_2} e^{-\lambda_i t}\, Gw(t)\, dt \tag{4-2}$$

$DRCG_{ik}$	—	groundshine dose rate coefficient to organ k by radionuclide i (Sv-m^2/Bq-s)
t_1	—	initial time for people to reside in a sector (s), t_1=ENDEMP=7 days in the test problem
t_2	—	exposure time end (s), t_2=EXPTIM + ENDEMP=50 years + 7 days in the test problem
λ_i	—	decay rate of radionuclide i (1/s)
$Gw(t)$	—	Gale's groundshine weathering function.

The dimensionless Gale's groundshine weathering function, $Gw(t)$, is a function defined as a sum of exponential decay functions, with time measured with respect to the end of the early phase (or end of the intermediate phase if such phase is enabled). The number of terms in the sum is specified by the parameter NGWTRM. The linear coefficients in the sum are specified by the parameter GWCOEF. Decay rates are specified via effective half-lives through the parameter TGWHLF with units of seconds. In the test problem, weathering was effectively disabled by setting TGWHLF = 10^{12} seconds ≈ 32,000 years, so that $Gw(t) \approx 1$.

4.1.1 Test Input

Identical inputs than Test 3.3 were used with the following changes:

General Properties

- SCOPE
  - Atmospheric Transport and Dispersion: Gaussian
  - Early Consequences

    - Late Consequences
- Food
    - No Food Model
- EARLY, Emergency Cohort One, Shielding and Exposure
    - CSFACT=0 (no cloudshine)
    - PROTIN=0 (no inhalation)
    - GSHFAC = 1 (groundshine pathway only for EARLY period)

Default inputs of the LNT Sample File were used for the CHRONC section, with the following changes:

- CHRONC Shielding and Exposure
    - LPROTIN = 0 (no inhalation pathway)
    - LGSHFAC = 1 (groundshine pathway only for CHRONC period)
- Weathering, Groundshine Weathering
    - NGWTRM = 2 (two exponential terms)
    - GWCOEF(1) = GWCOEF(2) = 0.5
    - TGWHLF(1) = TGWHLF(2) = 10^{12} seconds

Output Controls

Same outputs of Test 3.3 with the following addition

- Type 9 (NUM9) Population Dose Results
    - ORGNAM = L-ICRP60ED
    - IX1DS9 = 1 to 26 (inner radial interval)
    - IX1DS9 = 1 to 26 (outer radial interval)
    - Report Options = NONE

4.1.2 Test Procedure

A single run of the MACCS code was executed with the specified inputs. A python script was written to extract outputs from the file Model1.out. The results are printed in Model1.out in blocks, yielding the following outputs

- ATMOS Block
    - Type 0
- EARLY Block
    - Type 1, 3, 4, 5, 6, 8, A, C
    - Type D results are output in Summary.txt
- Combined Block: EARLY+CHRONC
    - Type 1, 3, 4, 5, 6, 8, A, C, D
- CHRONC Block
    - Type 1, 4, A, C
    - Type 6 results include only groundshine doses. Inhalation doses are not printed. The Type 6 doses are sector average doses for the central sector, and not centerline doses as the Type 6 EARLY module results.
    - Lone Type D results are not available, but combined EARLY+CHRONC Type D outputs are available in the Combined Block
    - Type 9 population dose results

The EARLY Type D ground concentrations (sector average concentrations) were extracted, and the groundshine dose was computed using Eq. (4-1), considering a long-term exposure equal

to 50 years (= EXPTIM). The results were compared to the CHRONC Type C sector average doses.

Using the CHRONC C Type C sector average doses, the population dose was computed using the method described in Test 3.2, and compared to the CHRONC Type 9 population dose. Similarly, the stochastic health effects were computed based on the CHRONC C Type C sector average dose, using the method described in Test 3.3, and compared to the Type 1 and Type 4 CHRONC outputs.

4.1.3 Test Results

Comparison of the CHRONC Type C sector average groundshine dose (north sector, centerline sector) to independent computations is presented in Figure 4-1.

The CHRONC Type 9 population dose (tracked in the output file Model1.out with the label "LONG-TERM GROUNDSHINE DOSE") was compared to the population dose independently computed based on the Type C individual groundshine dose (L-ICRP60ED) output by the CHRONC module and considering a uniform population density (POPDEN = 10 people/km^2). Independently computed population doses were aggregated over a 360° ring for comparison to the CHRONC Type 9 outputs. The results are presented in Figure 4-2.

Stochastic health effects, Type 1 and 4 outputs by the CHRONC module, were compared to independently computed health effects based on the Type C individual groundshine dose output by the CHRONC module (using the methods described in Test 3.3). The results are presented in Figure 4-3.

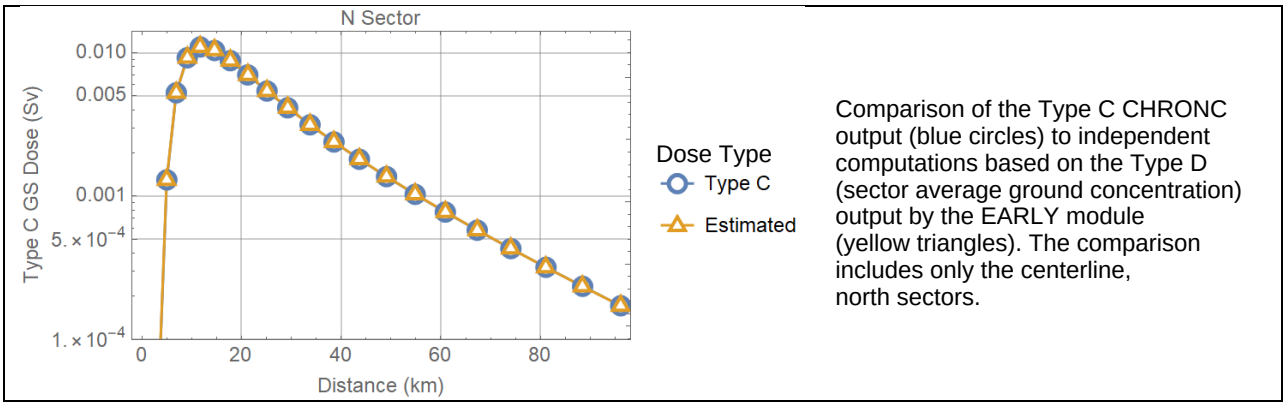

Figure 4-1. Type C groundshine dose (north sector) versus distance; comparison of MACCS outputs to independent computations.

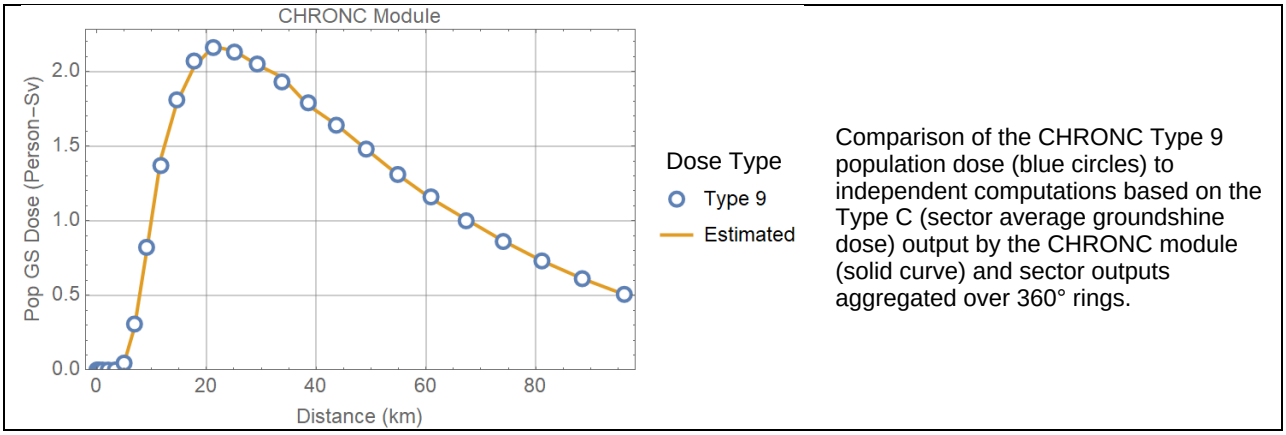

Figure 4-2. Type 9 population dose versus radial distance; comparison of MACCS outputs to independent computations.

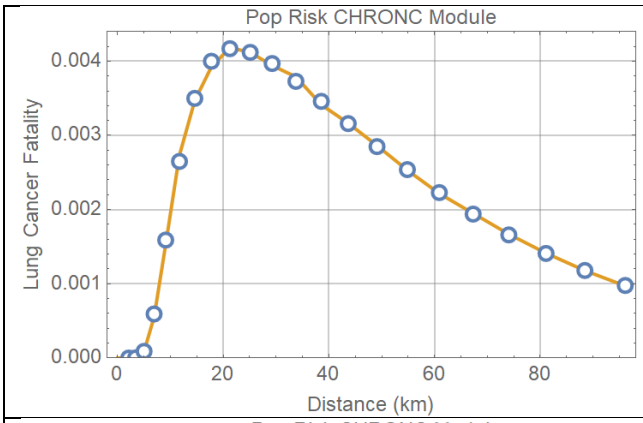

Comparison of the CHRONC Type 1 long-term lung cancer fatality (blue circles) to independent computations based on the Type C (sector average groundshine L-LUNGS dose) output by the CHRONC module (solid curve). The independent computations aggregate risk results over 360° rings.

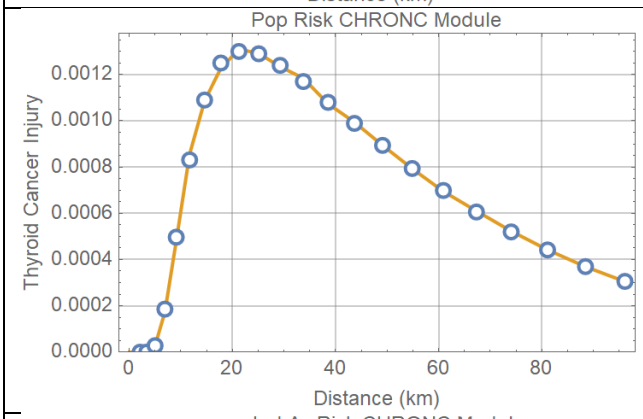

Comparison of the CHRONC Type 1 long-term non-fatal thyroid cancer (blue circles) to independent computations based on the Type C (sector average groundshine L-THYROID dose) output by the CHRONC module (solid curve). The independent computations aggregate risk results over 360° rings.

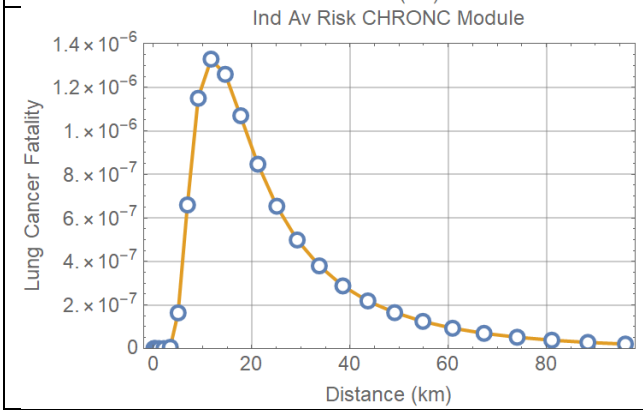

Comparison of the CHRONC Type 4 average individual long-term fatal lung cancer risk (blue circles) to independent computations based on the Type C (sector average groundshine L-LUNGS dose) output by the CHRONC module (solid curve). The independent computations aggregate risk results over 360° rings.

Figure 4-3. Type 1 and Type 4 health effects versus radial distance; comparison of MACCS outputs to independent computations.

4.1.4 Test Conclusions

MACCS successfully passed the designed tests.

4.2 Test 4.2: Stochastic Health Effects from Inhalation of Resuspension

The objective of the test was examining the computation of the population dose and stochastic health effects from an inhalation dose (inhalation of resuspension of radionuclides from the ground) pathway. The resuspension inhalation dose is computed as follows (based on equations 3-22 and 3-23 of the MACCS Theory Manual):

$$DR_k = \left(\sum_i DCR_{ik}\ GC_i \right) BR\ SFI\ \frac{1}{\mathrm{DRF}_\ell} \tag{4-3}$$

DR_k — inhalation dose to organ k in a sector due to resuspension of ground contamination (Sv)

DCR_{ik} — resuspension inhalation dose factor to organ k by radionuclide i for a given time period, defined in Eq. (4-4) below (Sv-s-m^{-1}/Bq-inhaled)

GC_i — ground concentration of radionuclide i in a sector after the EARLY period (Bq/m^2)

BR — breathing rate, specified by LBRRATE (m^3/s)

SFI — inhalation shielding factor, specified by LPROTIN

DRF_ℓ — dose reduction factor for decontamination level ℓ, specified by DSRFCT. Decontamination occurs when the dose exceeds a dose threshold DSCRLT over a period TMPACT

The resuspension inhalation dose factor DCR_{ik} is computed as

$$DCR_{ik} = DCI_{ik} \int_{t_1}^{t_2} e^{-\lambda_i t}\ Rw(t)\ dt \tag{4-4}$$

DCI_{ik} — inhalation dose coefficient to organ k by radionuclide i (Sv/Bq-inhaled)

t_1 — initial time for people to reside in a sector (s), t_1=ENDEMP=7 days in the test problem

t_2 — exposure time end (s), t_2=EXPTIM + ENDEMP=50 years + 7 days in the test problem

λ_i — decay rate of radionuclide i (1/s)

$Rw(t)$ — resuspension weathering function (m^{-1}).

The resuspension weathering function, $Rw(t)$, is a function defined as a sum of exponential decay functions, with time measured with respect to the end of the early phase (or end of the intermediate phase if such phase is enabled). The number of terms in the sum is specified by the parameter NRWTRM. The linear coefficients in the sum are specified by the parameter RWCOEF. Decay rates are specified via effective half-lives through the parameter TRWHLF with units of seconds. In the test problem, weathering was effectively disabled by setting TRWHLF = 10^{12} seconds ≈ 32,000 years, so that $Rw(t) \approx 1$.

4.2.1 Test Input

Identical inputs than Test 4.1 were used with the following changes.

General Properties

- EARLY, Emergency Cohort One, Shielding and Exposure
  - CSFACT = 0 (no cloudshine)
  - PROTIN = 1 (yes inhalation pathway)
  - BRRATE = 10^{-4} m^3/s (breathing rate for the EARLY period)
  - GSHFAC = 0 (no groundshine pathway)
- CHRONC Shielding and Exposure
  - LPROTIN = 1 (yes inhalation pathway)
  - LGSHFAC = 0 (no groundshine pathway)
- Weathering, Resuspension Weathering
  - NRWTRM = 3 (three exponential terms)
  - RWCOEF(1) = 0.5, RWCOEF(2) = RWCOEF(3) = 0.25
  - TRWHLF(1) = TRWHLF(2) = TRWHLF(3) = 10^{12} seconds
- Long Term Dose Criterion
  - DSCRLT (Sv) specified with different values in the different runs
- Decontamination Plan
  - LVLDEC = 2 (2 decontamination levels)
  - TIMDEC = 10^{-6} s (assumed almost instant decontamination, as soon as triggered)
  - DSRFCT(1) = 3, DSRFCT(2) = 15 (decontamination factors)

Output Controls

- The same outputs of Test 4.1 were used.

4.2.2 Test Procedure

This test was similar to Test 4.1, but focused on inhalation dose. The inhalation dose in the tests exceeded the threshold dose to trigger decontamination, DSCRLT. Therefore, in this test, the approach to computing the different decontamination levels was examined. Four runs of the MACCS code were executed with the following values of DSCRLT

- DSCRLT = 1 Sv
- DSCRLT = 5 Sv
- DSCRLT = 10 Sv
- DSCRLT = 100 Sv

In all runs, the long-term projection period for decontamination was TMPACT = 1.58×10^8 s = 5 years. The long-term projection period is used in MACCS to compute an individual dose and compare that dose to the threshold dose DSCRLT. If the individual dose exceeds DSCRLT, the different decontamination levels are applied [either DSRFCT(1) = 3 or DSRFCT(2) = 15] to bring the dose below the threshold. If the highest decontamination level is not enough to bring the individual dose below the threshold, then permanent interdiction is assumed: people are assumed mobilized away from all those sectors that cannot be brought below the target threshold dose. The test was aimed to verify the computational approach to implementing decontamination.

4.2.3 Test Results

Figure 4-4 compares the CHRONC Type C individual inhalation dose (circles) for the north sectors to independently computed inhalation doses (yellow, green, and red dashed curves).

The independently computed values were based on Type D ground concentrations (north sectors) output by the EARLY module, Eq. (4-3), and considering 50 years of exposure [EXPTIM=1.58×10^9 s]. The yellow curve considers no decontamination, the green curve considers a factor 3 decontamination [decontamination level 1, DSRFCT(1) = 3], and the red curve considers a factor 15 decontamination [decontamination level 1, DSRFCT(1) = 2].

The purple dots represent the inhalation dose after 5 years of exposure. They were computed as

$$D_5 = D_C \frac{\int_0^{5\ \mathrm{yr}} e^{-\lambda_{Cs-137} t}\ dt}{\int_0^{50\ \mathrm{yr}} e^{-\lambda_{Cs-137} t}\ dt} \approx 0.16\ D_C \qquad (4\text{-}5)$$

D_5 — 5-year projected inhalation dose (Sv)
D_C — Type C inhalation dose output by the CHRONC module (sector average dose)
λ_{Cs-137} — decay rate of Cs-137 (7.307×10^{-10} 1/s)

The results of the independent computations are in excellent agreement with the MACCS outputs. The purple dots lie all below the dose threshold, DSCRLT, indicated by a black horizontal dashed line, as expected. The dose threshold concept is correctly applied. The MACCS Type C dose outputs exhibit jumps consistent with the 5-yr projected dose, and it is zero at points where the 5-yr projected dose cannot be made less than DSCRLT after the highest decontamination level (triggering permanent interdiction).

The CHRONC Type 9 population dose (tracked in the output file Model1.out with the label “LONG-TERM RESUSPENSION DOSE”) was compared to the population dose independently computed based on the Type C individual inhalation dose (L-ICRP60ED) output by the CHRONC module and considering a uniform population density (POPDEN = 10 people/km^2). Independently computed population doses were aggregated over a 360° ring for comparison to the CHRONC Type 9 outputs. The results are presented in Figure 4-5. The symbols correspond to MACCS outputs, and the solid curves correspond to the independently computed population doses.

Figure 4-6 displays stochastic health effects, Type 1 and Type 4 outputs by the CHRONC module, compared to independent computations based on the Type C individual inhalation dose output by the CHRONC module. The computational approach is identical to the approach described in Test 3.3.

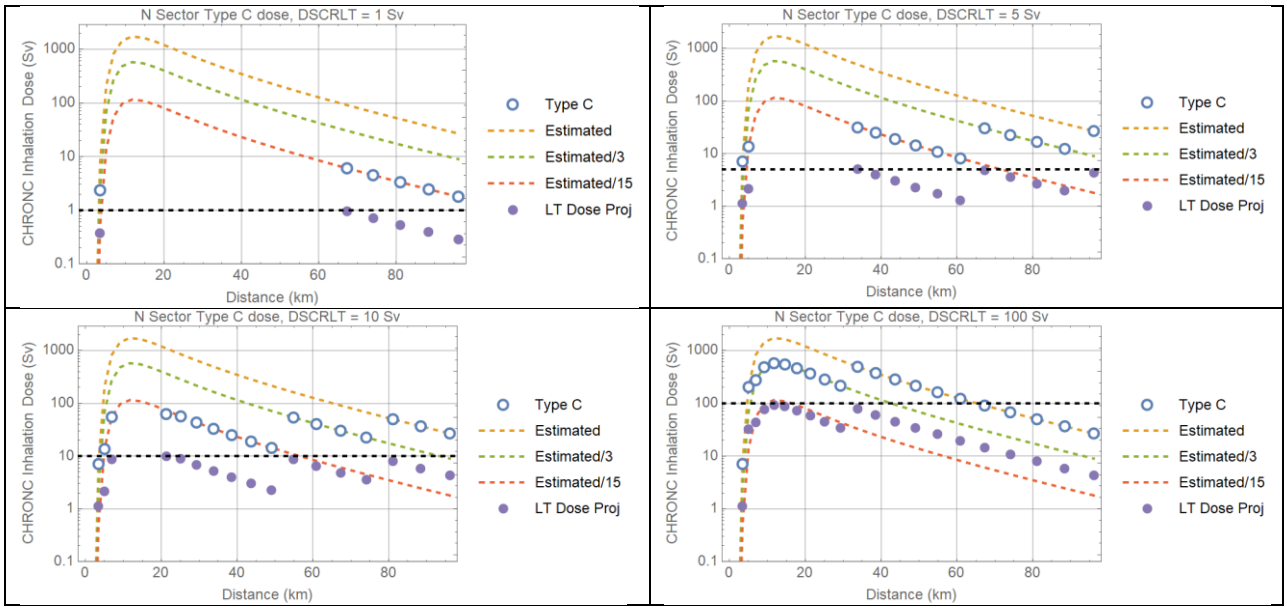

Figure 4-4. Type C inhalation dose versus radial distance; comparison of MACCS outputs (circles) and independent computations (dashed curves). Each plot displays a different case of threshold dose DSCRLT.

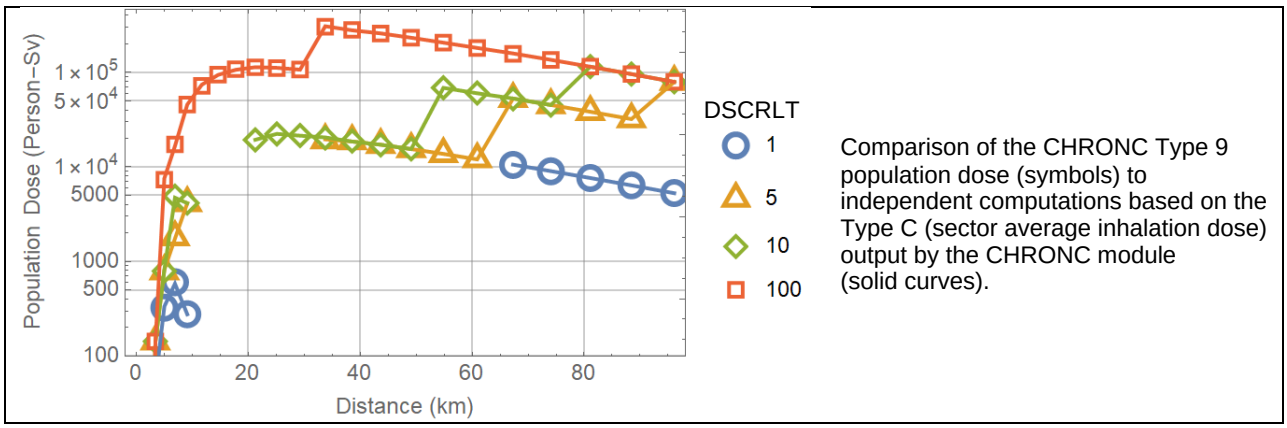

Figure 4-5. Type 9 population dose versus radial distance; comparison of MACCS outputs and independent computations.

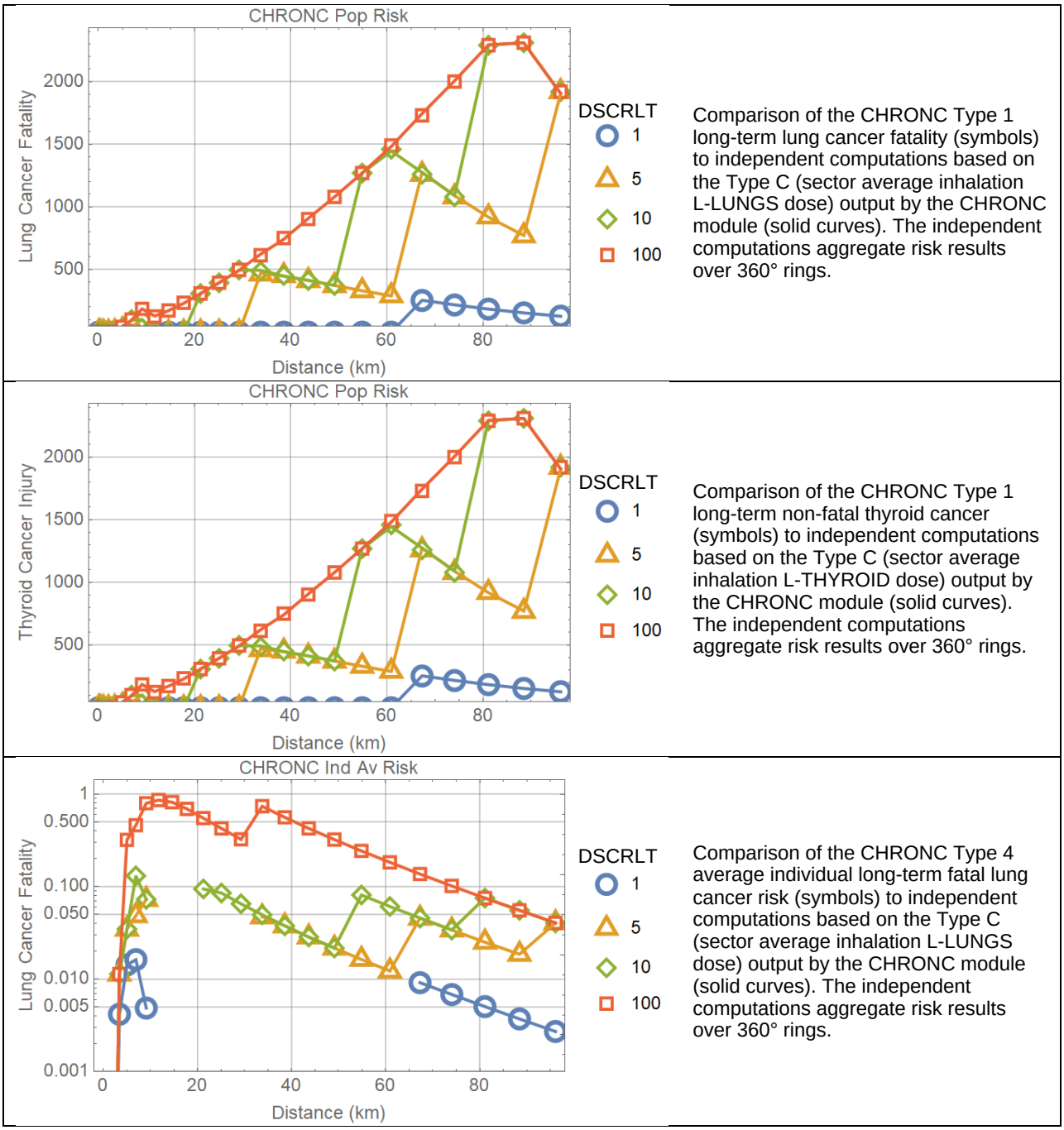

Figure 4-6. Type 1 and Type 4 outputs versus radial distance; comparison of MACCS outputs and independent computations.

4.2.4 Test Conclusions

MACCS successfully passed the designed tests.

5 CONCLUSIONS

Tests in this report examined and verified the implementation of numerical algorithms and functions of the MACCS code. The testing was organized in three main sections. Section 2 documents testing of the ATMOS module, Section 3 documents testing of the EARLY module, and Section 4 documents testing of the CHRONC module. Testing focused on equations to compute radionuclide concentrations in air and on the ground, doses from multiple pathways (groundshine, inhalation, cloudshine, and dose to the skin from plume passage), and health effects (injury due to passage of a radioactive plume and acute doses, and long-term cancer), based on examination of simple systems (e.g., constant wind speed and direction, one plume segment, one cohort, one single radionuclide, no mitigation actions, no evacuation, no relocation). Table 5-1 compares the scope of the testing to the table of contents of the MACCS Theory Manual. As demonstrated in the table, the testing covered a broad range of features and functions of the MACCS code, keeping in mind that the systems modeled in the test runs represented simple systems.

The tests were successful in the verification of equations and algorithms of the MACCS code as described in the MACCS Theory Manual (Nosek & Bixler, 2021). Minor differences of MACCS cloudshine dose outputs with respect to designed benchmarks, likely related to differences in interpolation methods for the computation of the cloudshine factor, which differences do not necessarily indicate deficiencies in the MACCS algorithms but the employment of practical approximations. In general, there was excellent agreement of the MACCS outputs with the designed benchmarks, keeping in mind that benchmarks did not include all details of the MACCS computations, and, thus, differences are expected in a few cases. The results provide confidence that the tested MACCS algorithms were properly implemented and consistent with descriptions in the MACCS Theory Manual, with few exceptions.

Testing with MACCS Version 4.0 revealed errors related to the treatment of broad plumes and computation of concentrations in off-center sectors. Those errors were addressed in MACCS Version 4.1, by applying limitations to the lateral spread of plumes (runs are aborted by MACCS if the lateral plume spread is too broad), enforcing practical limits to define off-center sectors with non-zero and zero concentrations, and greatly extending the domain of lookup tables to compute the cloudshine factor.

MACCS adopts a narrow plume (narrow angle) approximation to convert polar coordinates of the MACCS spatial grid to cartesian coordinates. This conversion is needed, for example, to use steady-state Gaussian plume functions and cloudshine factor functions defined in Cartesian coordinates. The narrow plume approximations become inaccurate in off-center sectors (e.g., north-north-east and north-east sectors if the wind is blowing north). Test 3.5 examined differences in results if accurate polar to Cartesian coordinate conversions were adopted. Given that MACCS Version 4.1 constrains the lateral spread of plumes to few sectors around the central sector, the tests suggest minor differences in both the sector average radionuclide concentrations and the sector average cloudshine doses with respect to simulations using a precise polar to Cartesian coordinate conversion. Although it would be desirable to remove approximations such as the narrow plume approximation to enhance the applicability of the MACCS models, the Test 3.5 suggests that the gain in precision would be modest if the lateral spread of plumes is kept constrained. Test 3.7 examined the implementation of the run interrupt to avoid broad plumes. MACCS runs are stopped if the spread of a plume [defined by ±2.15 $\sigma_y(x)$ limits] under atmospheric stability class A conditions exceeds an angular span of 180° at distances greater than or equal to 1000 m from the source. The angular span could exceed 180° at shorter distances than 1000 m without triggering a run interrupt. Test 3.8 identified that the broad plume run interrupt is inconsistently applied when plume meander is enabled,

especially when Gaussian dispersion coefficients are computed using power law functions. It is recommended that MACCS software developers address such inconsistencies.

Inconsistencies were identified in the implementation of the radial evacuation algorithm when evacuation is triggered by an alarm. Test 3.11 considered a simple case with evacuation triggered well before the release of radioactivity, and yet MACCS output non-zero doses for cohorts not exposed to any radioactivity carried or deposited by a plume.

The early relocation MACCS model was examined in Tests 0 and 3.10. The MACCS relocation algorithm first computes the projected dose assuming people stay in place and are exposed to a plume and to radioactivity deposited on the ground. If the projected dose exceeds a limit, then people are assumed to relocate and potentially avoid any exposure depending on the assumed relocation time. In Test 3.10 it was concluded that the MACCS relocation algorithm is not consistent with an approach relying on field measurements that trigger relocation only after those measurements were gathered and after people already experienced exposure to a plume and to deposited radioactivity. Test 3.10 included a comparison to early-phase dose projections of the Turbo FRMAC code. Dose projections of MACCS and Turbo FRMAC for the early phase are comparable; minor changes to the MACCS code could be implemented to attain full consistency in the dose equations. It was also concluded that the manner projected doses are used to define protective action guides in Turbo FRMAC is not consistent with the MACCS relocation algorithm. Recommendations were provided to align the MACCS relocation algorithm more closely to the Turbo FRMAC early-phase protective action guides.

Table 5-1. Comparison of the table of contents of the MACCS Theory Manual (Nosek & Bixler, 2021) to tests documented in this report.

MACCS Theory Manual Table of Contents	Test number addressing feature	Comments
2 Atmospheric Transport		
2.1 Introduction	NA	
2.2 Atmospheric Source Term		
2.2.1 Radionuclide Inventory Characteristics	Test 2.1	
2.2.2 Plume Segment Characteristics	Test 2.1	
2.3 Weather		
2.3.1 Weather Data	Indirect testing	During initial and exploratory testing, the input weather file was modified to set a simple weather pattern (constant wind speed, north direction, stability class D). The MACCS run successfully reflected features of the simple weather pattern. Documented tests in this report relied on an alternative approach to set a simple weather pattern, based on the constant or boundary weather inputs (METCOD=4).
2.3.2 Weather Modeling	Limited testing	All tests in this report used the option IPLUME=1 (no wind shift with rotation), with specified wind rose probabilities, WINROS, selected for wind blowing in the north direction only.
2.3.3 Weather Sequence Selection	Not tested	
2.3.4 Mixing Height Model	Not tested	When MAXHGT=DAY_ONLY, the mixing height is defaulted to the afternoon height. When MAXHGT=DAY_AND_NIGHT, the mixing height may increase from morning to afternoon values for a single plume segment (the height is not allowed to decrease). Variation in the mixing height should be a secondary (limited effects) process.
2.3.5 Boundary Weather	Limited testing	Most of the tests were implemented with constant

Table 5-1. Comparison of the table of contents of the MACCS Theory Manual (Nosek & Bixler, 2021) to tests documented in this report.

MACCS Theory Manual Table of Contents	Test number addressing feature	Comments
		weather inputs (METCOD=4). Tests 2.3 and 2.4 considered the user supplied weather, METCOD=4.
2.4 Atmospheric Release		
2.4.1 Wake Effects	Indirect testing, Test 2.1, 3.7, and 3.8	Wake effects are accounted for with selection of initial values of the Gaussian dispersion coefficients. Tests in this report mostly considered SIGYINIT=SIGZINIT=0.1 m, and it was verified that MACCS properly set the dispersion coefficient to those values at x=0.
2.4.2 Plume Rise	Test 2.7	Improved equations to compute plume rise were examined in Test 2.7.
2.5 Atmospheric Dispersion		
2.5.1 Gaussian Plume Equations	Tests 2.1, 2.5, 2.7, Test 3.5	
2.5.2 Dispersion Data	Tests 3.7 and 3.8	It was verified that dispersion coefficients input as lookup tables are properly used to compute the Gaussian dispersion coefficient as a function of x.
2.5.3 Dispersion Rate Models	Test 2.1, 2.6, Test 3.5, 3.7 and 3.8	The power law model was evaluated in Tests 2.1 and 3.5 and 3.8. The lookup table inputs were evaluated in Tests 3.7 and 3.8. Outputs considering lookup tables were compared to CDF outputs in Test 2.6. The Time-Based Option was not evaluated in the tests.
2.5.4 Virtual Source Calculation	Test 2.1, Test 3.5, 3.7 and 3.8	Test accounted for the location of the virtual source to set SIGYINIT=SIGZINIT=0.1 m x=0
2.5.5 Dispersion Scaling Factors	Test 2.1, Test 3.5, 3.7 and 3.8	The YSCALE and ZSCALE factors were heavily used in the tests in this report to examine the effect of different stability classes on the results
2.5.6 Plume Meander	Test 3.8	
2.6 Downwind Transport	Test 2.1, Test 3.11	The downwind plume movement was examined in Test 2.1. Test 3.11 includes downwind transport concepts.
2.7 Plume Depletion		
2.7.1 Radioactive Decay and Ingrowth	Test 2.1	Test 2.1 examined radioactive decay with the downwind plume movement
2.7.2 Dry Deposition	Test 2.5, Test 3.1	
2.7.3 Wet Deposition	Tests 2.2, 2.3, 2.4	
2.8 Centerline Air and Ground Concentrations	Tests 2.1, 2.2, 2.3, 2.4, 2.5, Test 3.5	
2.9 Atmospheric Transport Model Outputs	Test 2.1	
3 Dosimetry		
3.1 Dose Conversion	Test 2.1, Test 3.1, 3.10	The tests extracted information from the database of dose conversion factors, provided as input file to MACCS, and verified that those inputs were read by MACCS and used to compute individual acute and lifetime doses. Test 3.10 compares dose conversion to a third-party code, Turbo FRMAC
3.2 Off-Centerline Correction Factors	Test 2.1, Test 3.1	
3.3 Early Doses		
3.3.1 Cloudshine	Test 2.1, Test 3.1	
3.3.2 Groundshine	Test 3.1	
3.3.3 Direct Inhalation	Test 3.1	
3.3.4 Resuspension Inhalation	Test 3.10	

Table 5-1. Comparison of the table of contents of the MACCS Theory Manual (Nosek & Bixler, 2021) to tests documented in this report.

MACCS Theory Manual Table of Contents	Test number addressing feature	Comments
3.3.5 Skin Deposition	Test 3.1, 3.11	
3.4 Late Doses		
3.4.1 Groundshine	Test 4.1	
3.4.2 Resuspension Inhalation	Test 4.2	
3.4.3 Food Ingestion	Not tested	Independent extensive testing of the COMIDA module is documented elsewhere (Pensado & Speaker, 2020)
3.4.4 Drinking Water Ingestion	Not tested	
3.4.5 Decontamination Workers	Not tested	
3.5 Dosimetry Model Outputs	Test 2.1, Test 3.1, Tests 4.1, 4.2	
4 Protective Actions		
4.1 Cohort Data	Limited testing	The tests in this document considered a single cohort. The cohort shielding parameters (GSHFAC, PROTIN, CSFACT, or SKPFAC) were adjusted so that runs part of Test 3.1 would output groundshine, inhalation, cloudshine, or skin dose. The shielding parameters (LPROTIN, LGSHFAC) were adjusted so that runs part of Test 4.1 would output groundshine doses or inhalation doses from resuspension of contaminants on the ground. It was verified that MACCS properly responded to shielding inputs by the user.
4.2 Early Phase Protective Actions		
4.2.1 Evacuation and Sheltering Model	Test 3.11	
4.2.2 Early Relocation Model	Test 0, 3.10	
4.2.3 Potassium Iodide Ingestion Model	Test 3.6	
4.3 Intermediate Phase Protective Actions		
4.3.1 Intermediate Habitation Restrictions	Not tested	If the projected doses exceed the intermediate phase habitability dose criterion (DSCRTI), people in a grid element are assumed relocated for the duration of the intermediate phase and receive no-further dose before the long-term phase. Testing of a more complicated implementation, including decontamination when the dose exceeds a dose threshold DSCRLT is documented in Test 4.2.
4.4 Long-Term Phase Protective Actions		
4.4.1 Long-Term Habitation Restrictions	Test 4.2	The test accounted for effect of long-term habitation restrictions to explain dose versus distances exhibiting jumps.
4.4.2 Long-Term Farming Restrictions	Not tested	Independent extensive testing of the COMIDA module is documented elsewhere (Pensado & Speaker, 2020)
5 Socioeconomic Impact and Costs		
5.1 Early Phase Costs	Not tested	
5.2 Intermediate Phase Costs	Not tested	
5.3 Long-Term Phase Costs		
5.3.1 Costs in Nonfarm Areas	Not tested	
5.3.2 Costs in Farm Areas	Not tested	
5.4 Socioeconomic Impact and Cost Model Outputs	Not tested	
6 Radiogenic Health Effects		
6.1 Early Health Effects Models	Tests 3.3, 3.6	

Table 5-1. Comparison of the table of contents of the MACCS Theory Manual (Nosek & Bixler, 2021) to tests documented in this report.

MACCS Theory Manual Table of Contents	Test number addressing feature	Comments
6.2 Stochastic Health Effects Models		
6.2.1 Linear No-Threshold Dose Response	Test 3.3, Tests 4.1, 4.2	Tests assumed the linear no-threshold dose response model for the computation of health effects
6.2.2 Linear-Quadratic Dose Response	Not tested	
6.2.3 Annual-Threshold Dose Response	Not tested	
6.2.4 Piecewise-Linear Dose Response	Not tested	
6.3 Health Effect Model Outputs	Tests 3.3, 3.6, Tests 4.1, 4.2	

6 REFERENCES

Bixler, N., Walton, F., Eubanks, L., Haaker, R., & McFadden, K. (2017). *MELCOR Accident Consequence Code System (MACCS), User's Guide and Reference Manual.* Washington DC: US Nuclear Regulatory Commisssion. Retrieved from https://www.nrc.gov/docs/ML1704/ML17047A450.pdf

Blumenthal, D., Brunner, B., Cherniack, J., Beal, W., Cochran, L. D., Cleveland, G., . . . Hoover, S. (2020). *FRMAC Assessment Manual Volume 1 (Overview and Methods).* Albuquerque, New Mexico: Sandia National Laboratories. doi:https://doi.org/10.2172/1670254

Chang, R., Schaperow, J., Ghosh, T., Barr, J., Tinkler, C., & Stutzke, M. (2012). *State-of-the-Art Reactor Consequence Analyses (SOARCA) Report (NUREG-1935).* Washington DC: US Nuclear Regulatory Commission. Retrieved from https://www.nrc.gov/reading-rm/doc-collections/nuregs/staff/sr1935/index.html

Clayton, D. J. (2021). *Implementation of Additional Models into the MACCS Code for Nearfield Consequence Analysis.* Albuquerque NM: Sandia National Laboratories.

Demael, E., & Carissimo, B. (2008). Comparative Evaluation of an Eulerian CFD and Gaussian Plume Models Based on Prairie Grass Dispersion Experiment. *Journal of Applied Meteorology and Climatology, 47*, 888-900.

Eimutis, E. C., & Konicek, M. G. (1972). Derivations of Continuous Functions for the Lateral and Vertical Atmospheric Dispersion Coefficients. *Atmospheric Environment, 6*, 859-863.

EPA. (2017). *Protective Action Guides and Planning Guidance for Radiological Incidents.* Office of Radiation and Indoor Air, Radiation Protection Division. Washington DC: Environmental Protection Agency. Retrieved from https://www.epa.gov/sites/default/files/2017-01/documents/epa_pag_manual_final_revisions_01-11-2017_cover_disclaimer_8.pdf

Gifford, F. A. (1961). Use of routine meteorological observations for estimating atmospheric dispersion. *Nuclear Safety, 2*, 47-51.

Joseph, G. M., Hargreaves, D. M., & Lowndes, I. S. (2020). Reconciling Gaussian plume and Computational Fluid Dynamics models of particulate dispersion. *Atmospheric Enviornment: X, 5*, 100064. doi:https://doi.org/10.1016/j.aeaoa.2020.100064

Molenkamp, C. R., Bixler, N. E., Morrow, C. W., Ramsdell, J. V., & Mitchell, J. A. (2004). *Comparison of Average Transport and Dispersion Among a Gaussian, a Two-Dimensional, and a Three-Dimensional Model.* Lawrence Livermore National Laboratory. Washington DC: US Nuclear Regulatory Commission. Retrieved from https://www.nrc.gov/reading-rm/doc-collections/nuregs/contract/cr6853/index.html

Nosek, A. J., & Bixler, N. (2021). *MACCS Theory Manual.* Albuquerque NM: Sandia National Laboratories. Retrieved from https://maccs.sandia.gov/docs/MACCS_factsheets/MACCS Theory Manual Final_SAND2021-11535.pdf

Pasquill, F. (1961). The estimation of the dispersion of windborne material. *Meteor. Mag., 90*, 33-49.

Pensado, O., & Speaker, D. (2020). *Input Parameter Updates to the MACCS COMIDA2 Model.* Southwest Research Institute, Center for Nuclear Waste Regulatory Analyses. Washington DC: US Nuclear Regulatory Commission. Retrieved from https://www.nrc.gov/docs/ML2035/ML20350B615.pdf

Sandia National Laboratories. (2022). *Turbo FRMAC*. Retrieved February 18, 2022, from Nuclear Incident Response Program: https://nirp.sandia.gov/Software/TurboFRMAC/TurboFRMAC.aspx

SNL. (2015a). *History of MACCS.* Sandia National Laboratories. Washington DC: US Nuclear Regulatory Commission. Retrieved from https://www.nrc.gov/docs/ML1704/ML17047A451.pdf

SNL. (2015b). *History of WinMACCS.* Sandia National Laboratories. Washington DC: US Nuclear Regulatory Commission. Retrieved from https://www.nrc.gov/docs/ML1704/ML17047A452.pdf

SNL. (2017a). *State-of-the-Art Reactor Consequence Analyses (SOARCA) Project.* Sandia National Laboratories, Severe Accident Analysis Department. Washington DC: US Nuclear Regulatory Commission. Retrieved from https://www.nrc.gov/docs/ML1734/ML17340B209.pdf

SNL. (2017b). *MELCOR Accident Consequence Code System (MACCS) Software Quality Assurance Plan, Version 1.5.* Albuquerque NM: Sandia National Laboratories. Retrieved from https://www.nrc.gov/docs/ML1704/ML17047A458.pdf

SNL. (2019). *State-of-the-Art Reactor Consequence Analyses (SOARCA) Project, Sequoyah Integrated Deterministic and Uncertainty Analyses (NUREG/CR-7245).* Sandia National Laboratories, Severe Accident Analysis Department. Washington DC: US Nuclear Regulatory Commission. Retrieved from https://www.nrc.gov/reading-rm/doc-collections/nuregs/contract/cr7245/index.html

SNL. (2021). *MACCS: MELCOR Accident Consequence Code System*. (Sandia National Laboratories) Retrieved from MACCS: https://maccs.sandia.gov/default.aspx

Thoman, D. C., Brotherton, K. M., & Davis, W. (2009). *Benchmarking Upgraded HotSpot Dose Calculations Against MACCS2 Results.* Washington Safety Management Solutions LLC, 2009 EFCOG Safety Analysis Working Group. Washington DC: US Nuclear Regulatory Commission. Retrieved from https://www.nrc.gov/docs/ML1704/ML17047A449.pdf

Turner, D. B. (1970). *Workbook of Atmospheric Dispersion Estimates.* Research Triangle Park, North Carolina: US Environmental Protection Agency.

Wolfram Reseach. (2021). *Wolfram Mathematica*. (Wolfram Reseach) Retrieved from https://www.wolfram.com/mathematica/?source=nav